March 2018

The Molecular Basis of Caspase-9 Inactivation by PKA and c-Abl Kinases

Banyuhay Paningbatan Serrano

THE MOLECULAR BASIS OF CASPASE-9 INACTIVATION BY PKA AND C-ABL KINASES

A Dissertation Presented

by

BANYUHAY PANINGBATAN SERRANO

Submitted to the Graduate School of the
University of Massachusetts Amherst in partial fulfillment
of the requirements for the degree of

DOCTOR OF PHILOSOPHY

February 2018

Chemistry Department

THE MOLECULAR BASIS OF CASPASE-9 INACTIVATION

BY PKA AND C-ABL KINASES

A Dissertation Presented

by

BANYUHAY PANINGBATAN SERRANO

Approved as to style and content by:

_____
Jeanne A. Hardy, Chair

_____
Scott C. Garman, Member

_____
Michael J. Knapp, Member

_____
Peter Chien, Member

_____
Richard W. Vachet, Department Head
Chemistry Department

ACKNOWLEDGMENTS

I would like to express my deepest gratitude to the following people who helped me one way or another throughout my years in graduate school:

To Jeanne, for being an amazing mentor. It is truly an honor to have been trained and mentored by you. I am constantly amazed by your brilliance and your enthusiasm for science. Your confidence in me never wavered when I was suffering with self-doubt, and your optimism and persistence motivated me to look at that glass more often as half-full than half-empty. You found the perfect balance between challenging and encouraging me so that I become a better scientist. You are an inspiration to young female scientists. I have no doubt that you will continue to rock the science world and I am proud to be a part of your success.

To my Dissertation Committee members, Profs. Scott Garman, Mike Knapp and Peter Chien, for your masterful insights and suggestions that made my projects successful. I could not be more fortunate to be in the same room with these brilliant minds. Scott, I have always considered you as a mentor and I appreciate your constant encouragement, kind words and our mutual fondness for fonts. You always ask the most basic yet most difficult questions, which makes me take a step back and look at the science at a different angle. Mike, you have always been accommodating when I have naïve science questions, and you often look at my research at a different perspective. Peter, your scientific curiosity and excitement are infectious. The insights you've given on my projects pushed me to look beyond the data and into the bigger picture.

To our collaborators, Dr. Steve Eyles for the mass spec analysis, Prof. Dominique Alfandari for the cell-based experiments, and Prof. Jesse Rinehart (Yale) for the phosphoserine incorporation technology. Your expertise and assistance truly elevated my projects to another level.

To the members of the Hardy Lab, past and present, for simply being awesome beings. I had the best training from the senior members of the lab – Kristen, Sam, Elih, Muslum and Peng. You warmly welcomed me into the lab and imbibed in me a culture of hard work, perseverance

and excellence. Kevin, Scott, Maureen, Derek and Francesca, you guys are the perfect lab mates. You made lab life so much more enjoyable and pleasant, even during the most stressful of times. I am so proud of all of you and I am very thankful that I got to be a part of your success. I could not have survived grad school without your company, encouragement, support, and most of all, friendship.

To the amazing people in UMass with whom I made lasting friendships – Youngju, Oyuntuya, Molly, Carolyn, Heidi, Tiffany, Cola, Bo and Mo.

To my Filipino friends in Amherst – Tina, Kristine and Francis, Myles and JB, Kevin and Dolly, Bernard and Aileen, and their loving families, for providing a safe haven by reminding me of home.

To my friends back home, for the constant encouragement and pride.

To my extremely large family, your unrelenting love and support is what keeps me going every day. To my brothers and their families – Tong, Dake and Ninoy, for being constant reminders of what fun and happiness is. To Toshi, for the purest love and being my ultimate stress reliever.

To Ginggeng, my soul mate and my best friend. Words cannot express how thankful I am everyday that you are in my life. You make me feel like the luckiest person in the world because no one else has what we have. And as we always say, “On to the next adventure!”

Most importantly, to my parents, Nanay and Tatay, for your unconditional love and for being my utmost inspirations and heroes in life. I dedicate this work to you, for all the sacrifices that you’ve made in order for me to achieve my dreams. You raised me to be empowered and not be set by limits, but more importantly you also raised me to be kind. My greatest joy and pride is to have you as my parents.

ABSTRACT

THE MOLECULAR BASIS OF CASPASE-9 INACTIVATION

BY PKA AND C-ABL KINASES

FEBRUARY 2018

BANYUHAY PANINGBATAN SERRANO, B.S., UNIVERSITY OF THE PHILIPPINES

LOS BAÑOS

M.S., UNIVERSITY OF THE PHILIPPINES LOS BAÑOS

Ph.D., UNIVERSITY OF MASSACHUSETTS AMHERST

Directed by: Professor Jeanne A. Hardy

Caspases are the cysteine proteases that facilitate the fundamental pathway of programmed cell death or apoptosis. The activation and function of these powerful enzymes are tightly regulated to ensure the faithful execution of apoptosis and prevent untimely cell death. Many deadly human diseases such as cancer, neurodegeneration and autoimmune disorders have been associated with defective activation and faulty regulation of caspases. As such, caspases are considered as attractive drug targets, which when properly controlled, can lead to effective therapeutics for apoptosis-related diseases. Thus, comprehensive investigations of the structure, function and regulation of caspases are necessary to understand the complex mechanisms by which caspases are controlled in order to harness their potential for therapeutic purposes. This dissertation details the studies on the regulation of caspase-9 by phosphorylation mediated by the kinases PKA and c-Abl. Complementary approaches of biochemistry, structural biology and cell biology were utilized to elucidate the divergent mechanisms by which these kinases inhibit caspase-9 function. A critical residue was revealed to be a hotspot for inactivation upon PKA phosphorylation, utilizing two different mechanisms to silence caspase-9 activity. In addition, a novel site of phosphorylation by c-Abl that leads to inactivation was uncovered and is unique to caspase-9. These findings contribute to the growing information about caspases and kinases that will aid in the development of therapeutic strategies for apoptosis-related diseases.

TABLE OF CONTENTS

Page

Page

LIST OF TABLES

LIST OF FIGURES

CHAPTER I

INTRODUCTION

Apoptosis or programmed cell death is a conserved cellular pathway that serves as a mechanism for multicellular organisms to undergo normal development, achieve homeostasis and protect itself from cells that are in excess, not in use, damaged and/or potentially harmful to the organism. At the center of this pathway are enzymes called caspases that coordinate the intricate cascade of reactions to faithfully execute apoptosis. As specialized proteases, caspases display exquisite specificity towards their substrates, altering substrate structure and function in an irreversible manner. By inactivating or otherwise altering the function of a circumscribed number of key substrates, caspases can control cell fate. Ultimately, it is the activity of the powerful caspases that is responsible for the morphological changes that the cell undergoes during apoptotic cell death. Because caspases play a crucial role in inducing cell death, their expression and activation must be subject to tight regulation in order to maintain the balance between cell death and survival. The long list of diseases associated with caspase dysfunction indicates the severe consequences of their inappropriate activation and improper or lack of regulation in the apoptotic pathways. Thus, caspases are considered to be attractive drug targets which, when properly harnessed can lead to effective therapeutics for apoptosis-related diseases.

Apoptosis: Death for Survival

Apoptosis is central to the development and homeostasis of multicellular organisms. This irreversible pathway is sensitive to cellular signals that decide whether a cell must die or not. These death signals are then transduced via a series of biochemical reactions that commences in the activation of caspases that finally cleave specific intracellular protein substrates to start cellular destruction. Apoptosis is an active and deliberate kind of cell death, proceeding in an orderly and efficient manner. This tight and precise control manifests in its perhaps most distinct feature, which is the ability of cells undergoing apoptosis to avoid eliciting inflammatory

responses, keeping neighboring cells intact. Morphological changes following apoptosis include chromatin condensation, DNA fragmentation, cell shrinkage and membrane blebbing. The dying cell is then rapidly eliminated by phagocytosis without prompting inflammation in the surrounding areas.

The proper execution of apoptosis is critical to cellular and tissue homeostasis. Defects in its regulation have been implicated in a plethora of life-threatening diseases. Insufficient and suppressed apoptosis is considered a classic hallmark in many types of cancer, autoimmune disorders and persistent viral infections. In contrast, degenerative diseases that destroy cells such as Alzheimer's, Huntington's, as well as ischemia resulting from stroke and post-menopausal osteoporosis are known to exhibit an excessive degree of apoptosis. (reviews[1–4]). The ability to modulate cell death and survival is thus recognized for its immense therapeutic potential. In the past few decades key participants in the apoptotic pathways have been identified and extensively interrogated as potential targets for regulating apoptosis.

The Apoptotic Pathways

Depending on the nature of death signal that the cell receives, there are two pathways by which apoptosis can proceed - the extrinsic, or death receptor pathway, and the intrinsic, or mitochondrial pathway (Figure 1). The two pathways converge with the activation of the executioner caspases, which ultimately cut hundreds of their specific protein targets to amplify the cascade of cellular destruction.

In the extrinsic pathway, ligand binding of tumor necrosis factor (TNF) family such as Fas, and TNF-related apoptosis-inducing ligand (TRAIL) ligands causes these death receptors to cluster and recruit an adaptor protein Fas-associated death domain (FADD) and multiple procaspase-8 molecules, forming a death-inducing signaling complex (DISC). The DISC serves as a platform to increase the local concentration of procaspase-8 molecules, allowing its *trans*-processing and activation. Once active, caspase-8 cleaves and activates procaspases -3, -6 and -7 (reviews [5,6]).

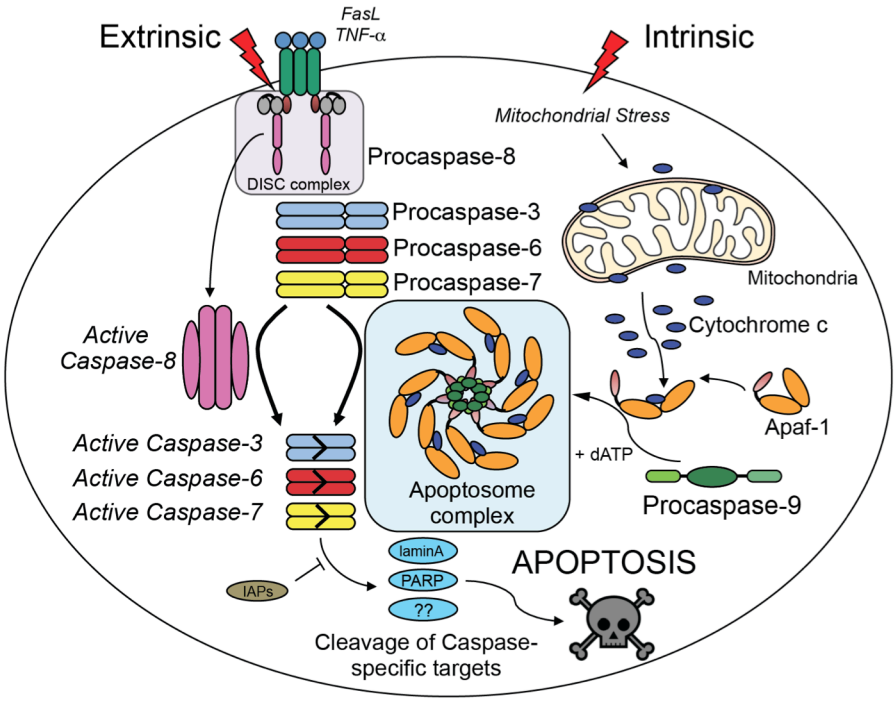

Figure 1.1. The Apoptotic pathways.
The extrinsic pathway is activated by death ligand-binding, such as FasL or TNF-α, while the intrinsic pathway is induced by mitochondrial stress such as DNA damage, hypoxia or build-up of reactive oxygen species. Upstream caspases or initiators, caspase-8 and/or caspase-9 mediate the extrinsic and intrinsic pathways, respectively. Both pathways converge with the activation of downstream or executioner caspases -3, -6 and -7, thereby committing the cell to its demolition.

The intrinsic or mitochondrial pathway is activated as a response to cellular stress such as DNA damage, toxins, hypoxia and activation of oncogenes, causing the outer mitochondrial membrane to be compromised. This allows cytochrome c to leak out of the mitochondria into the cytosol where it forms a heptameric complex with the apoptotic protease activation factor-1 (Apaf-1). This platform then recruits procaspase-9 molecules form the apoptosome assembly[7,8] where caspase-9 molecules are activated. Highly active caspase-9 then becomes incredibly efficient in cleaving and activating the executioner caspases,[9] which in turn amplify the downstream apoptotic signals. Although it seems that the two pathways are distinct from each other, crosstalk does occur, resulting in feedback loops between pathways, as well as serving as linkages that redirect caspases to participate in other signaling pathways.

Caspases: The Core of the Apoptotic Machinery

Caspases are considered to constitute the core of the apoptotic machinery. Depending on where they act in the apoptotic pathways, caspases are classified as either initiators, which operate upstream such as caspases -2, -8 and -9, or executioners such as caspases -3, -6 and -7, which facilitate downstream cleavage of hundreds of substrates in the apoptotic cascade[10,11] (Figure 1.1). Caspases are essentially molecular scissors that derive their name from the cysteine active site residue that they utilize in their chemistry and from their specificity to cleave after specific aspartate residues found within a defined recognition sequence. All caspases contain the catalytic dyad of a cysteine thiol and a neighboring histidine imidazole to perform hydrolysis of a target peptide bond (Figure 1.2A).

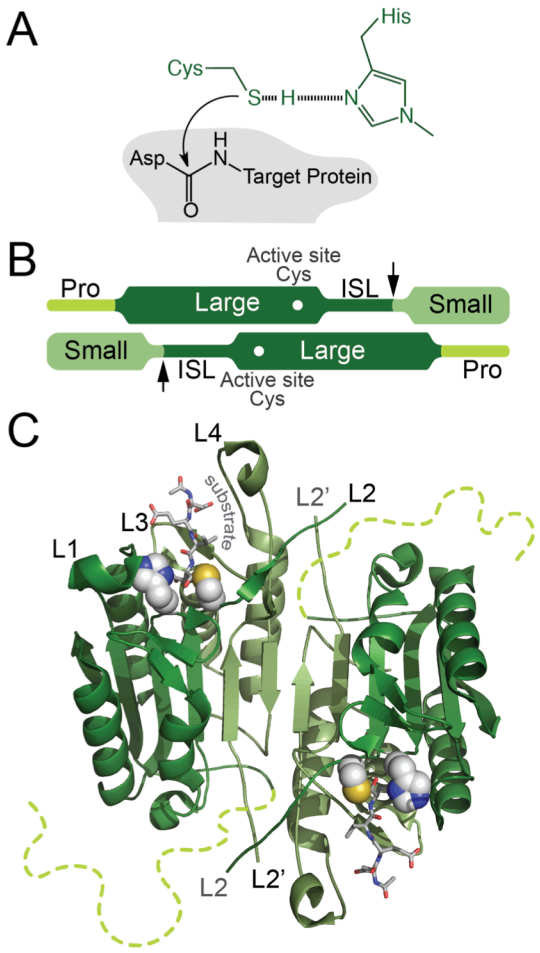

Figure 1.2. Chemistry and architecture of caspases.
(A) The His in the catalytic dyad promotes the nucleophilicity of Cys in the active site, which then performs a nucleophilic attack on the peptide backbone of the target protein substrate.
(B) Schematic representation of the structural domains of caspases. Caspases contain a core domain, which is composed of the large and small subunits connected by an intersubunit linker (ISL). At the N-terminus is a prodomain (Pro) preceding the core of the enzyme. The active site cysteine resides in the large subunit. All caspases have cleavage sites in the intersubunit linker. Most caspases, particularly executioners, have a cleavage site between the prodomain and the large subunit. Cleavage sites are indicated by arrows.
(C) Structure of a substrate-bound caspase dimer (PDB ID: 1F1J) showing the active site loops (L1, L2, L3, L4, from one monomer and L2' from the other monomer) and the Cys-His catalytic dyad (shown as spheres). The prodomain in all available crystal structures of caspases is mobile and has not been observed crystallographically, so was modeled in this figure as light green dashed lines.

Structurally, all caspases contain the highly homologous protease or core domain that is further subdivided into a large (17-20 kDa) and a small (10-12 kDa) subunit that are held together by an intersubunit linker (ISL) (Figure 1.2B). The N-terminus is a stretch of residues that comprise the prodomain (Pro), with the initiator caspases having longer and structured prodomains than the executioners. Initiator caspases such as caspase-8 and -9 are monomeric following synthesis on the ribosome, while executioners dimerize immediately upon ribosome release. Mature caspases exist as homodimers, having the two monomers aligned in a head-to-tail fashion (Fig. 1.2C). The two small subunits adjacent to one another make hydrophobic interactions that form the dimer interface. At the center of the structure is a sheet of 12 contiguous β-strands (six from each monomer) that are surrounded by several α-helices and a few short β-strands. The substrate-binding pocket that contains the active site is composed of four protruding, dynamic loops (L1, L2, L3, L4) sampling different conformations and are reorganized and stabilized upon substrate binding. A stabilizing element is the interaction of loops L4 and L2 from one half of the dimer with the N-terminus of the small subunit (loop L2') of the other half (Figure 1.2C). These loop interactions have been shown to be critical for caspase activity[12], and has been exploited to develop strategies to trap caspases into an inactive state that is incompetent to bind substrate.

The activity of caspases ultimately determines cell fate and any inopportune activation or inhibition is extremely detrimental to the cell. Because highly active caspases are lethal, they are synthesized and stored in their inactive zymogen forms (procaspases). The requirements for activation of executioner caspases are quite distinct from those of initiators. During zymogen activation, executioner caspases require cleavage at the intersubunit linker in order to be maximally active. These cleavage events are primarily carried out by initiator caspases, but could also be achieved by self-proteolysis. In contrast, initiator caspases are recruited to multimeric scaffolds such as the DISC (for caspase-8)[13], PIDDosome (for casp-2)[14] and the apoptosome (for

caspase-9)[7,15,16] for activation. Dimerization has also been shown to be paramount to caspase activity (reviews[17,18]).

Targeting caspases to either inhibit or activate them is an efficient way to prevent or accelerate cell death. Caspases are extremely selective proteases in the sense that they have strong preference to cut after specific aspartate residue in their substrates, but do not cut after all aspartates haphazardly. They are notably unlike other proteases that randomly cleave at any available site bearing a recognized amino acid. Caspases are signaling proteases and are not designed for degradation of substrates. They cut only at one or sometimes two sites. These specific substrate modifications lead to either have them gain or lose function. The most conserved region in the structure of caspases is the active site. The substrate-binding pocket has evolved to retain specific residues that stringently recognize an aspartate in the P1 position of the peptide, but this cleavage preference has been shown to extend to include glutamate and phosphoserine under specific circumstances[19–21]. The P4-P3-P2 residues must make complementary interactions with other residues in the catalytic pocket for tighter binding and cleavage. While the residues that compose the P1 pocket are highly conserved the P4, P3 and P2 pockets vary significantly between caspases.

The vast number and the range of protein substrates that undergo caspase cleavage, as well as the discrepancies between cleavage preferences *in vitro* and intracellularly prompted the idea that caspases possess exosites that serve as determinants of substrate recognition and processing (Figure 1.3A). Recently, caspase-7 was revealed to possess a lysine-rich exosite patch that facilitates faster cleavage of its substrate, poly(ADP ribose) polymerase 1 (PARP)[22]. In addition to exosites, data are emerging that caspases have allosteric sites (Figure 1.3B) that can act as switches when targeted by small molecules such as FICA and DICA in caspase-7[23], metal-binding such as zinc in caspase-6[24] and -9[25] and peptides as in the case of caspase-6[26]. Allosteric inhibitors generally function by trapping caspases into a conformational state that is incapable of binding substrate (Figure 1.3B). These exosites and allosteric sites are now acknowledged to be

excellent target regions, because while modifying the active site serves to efficiently and robustly inactivate caspases, it does not confer any specificity towards a particular caspase-substrate pair. Allosteric and exosite regions, especially those that are found to be unique to a specific caspase, could provide the needed specificity when directed for caspase inhibition or activation.

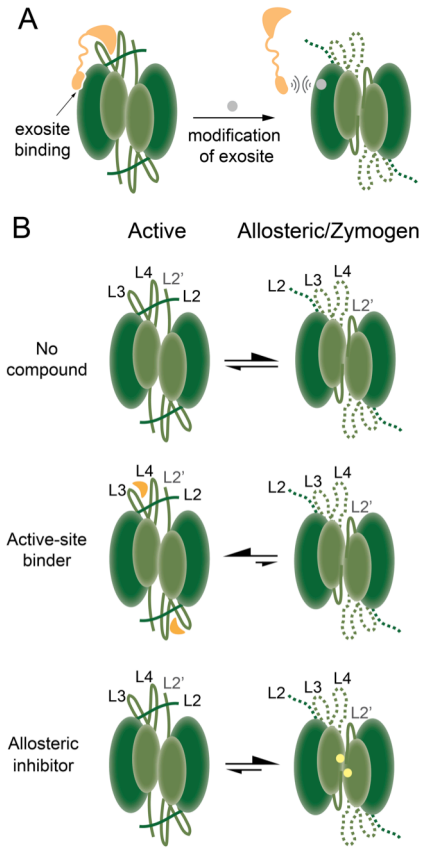

Figure 1.3. Exosites and allosteric regions control caspases function.
(A) Caspases possess exosites that aids in recognition and binding of a cognate substrate. Blocking the exosite results in either unproductive binding or no binding of the target substrate.
(B) In the absence of any inhibitor or substrate, caspases predominantly exist in the zymogen state (top). Binding of a compound to the active site reorganizes and orders the loop bundle, shifting the equilibrium in its active state (middle). An allosteric inhibitor (such as FICA and DICA for caspase-7) binding distal to the active site drives back the equilibrium to the zymogen state (bottom).

Natural Regulators of Caspase Activation and Function

The whole ensemble of apoptosis-related proteins must work in a precise and organized manner for apoptosis to function normally. As critical mediators of the apoptotic pathways, it is only fitting that caspase activity is tightly controlled. One can imagine the lethal or deleterious consequences when caspases are either missing/kept inactive or overexpressed/constitutively active. Knockout versions of mice that are deficient in specific caspases either result in perinatal lethality or have developmental defects (review[27]). A number of cancers[28,29] and neurodegenerative diseases[30,31] have been attributed to dysregulated activity and inappropriate expression of caspases. Fortunately, constant check-and-balance mechanisms have evolved to achieve timely activation and inhibition of caspases.

Upstream of the caspase activation cascade are Bcl-2 family proteins that are either pro- or anti-apoptotic (Figure 1.4). Many of the Bcl-2 family proteins are harbored inside the mitochondria and upon receiving an intracellular signal, these family members compete to enable the mitochondrial release of cytochrome c. Pro-apoptotic Bcl-2's (BAX and BAK) induce or facilitate release of cytochrome c while anti-apoptotic Bcl-2's do the opposite. IAPs (inhibitor of apoptosis proteins) are the first line of defense that keep caspase activation in check either by directly interacting with caspases or by facilitating ubiquitination and consequently proteasomal degradation of caspases (review[32]). Other cellular proteins identified to contribute to caspase regulation include heat shock proteins (Hsps) which have been observed to directly interact with caspases[33–35] (for review: [32,36,37]) and alternatively spliced caspase variants that generally act as dominant negatives[38]. In addition, adaptor proteins containing binding motifs compete for interaction with caspase activating scaffolds/complex, thereby regulating caspase activation.

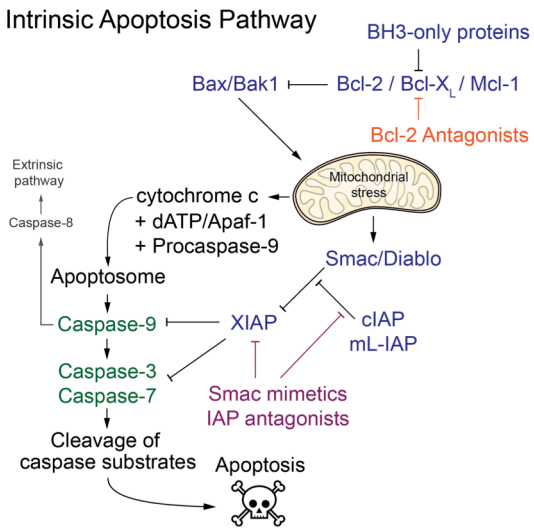

Figure 1.4. Pro- and anti-apoptotic proteins control the intrinsic pathway.

It is also now becoming clear that caspases have evolved to be sensitive to changes brought about by post-translational modifications (PTMs). Phosphorylation, nitrosylation, ubiquitination and oxidative modification of caspases have been linked to both suppression and induction of apoptosis (reviews[39,40]). Caspases are highly susceptible to modifications, and in most cases these reported PTMs result in dramatic alteration of their function. The ability of other proteins to modify the caspase structure and consequently transform its function is a promising avenue for co-regulation of caspases and cognate enzymes, and sensitive regions or sites arising from these PTMs can be exploited for precise control of caspase function.

Among the PTMs in caspases, phosphorylation is perhaps the most documented and well-explored. Although the apoptotic pathways do not directly involve kinases in the signaling cascade, activities of relevant kinases have been determinants of the cell's susceptibility to death. All apoptotic caspases harbor phosphorylation sites (Figure 1.5), and while numerous cell-based studies have identified the relevant caspase-kinase pairs and mapped their roles in the context of apoptosis, molecular details of the mechanisms of inhibition or activation that these phosphorylation events confer to caspases are still lacking. It is notable that these phosphorylation sites reside in different regions within the caspase structure, thus it is highly likely that these regions are potential allosteric sites and exosites that can be exploited to modulate the function of a specific caspase. An excellent model to interrogate the diverse mechanisms of caspase phosphoregulation is that of the initiator caspase-9, whose great extent of phosphorylation on all its domains could provide insights as to how phosphorylation precisely influences caspase structure, activation and function.

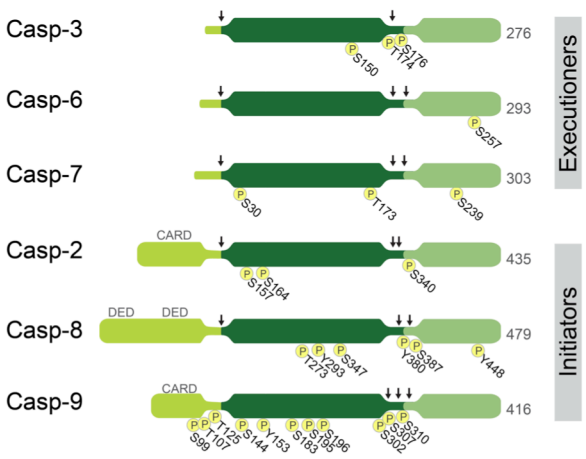

Figure 1.5. Reported phosphorylation sites in caspases.
Apoptotic caspases are phosphorylated at multiple sites in their structure. Cleavage sites at the linker and between the prodomain and large subunit are indicated by arrows.

The Initiator, Caspase-9

Caspase-9 is the initiator caspase that mediates the intrinsic apoptotic pathway. It is synthesized as a 46-kDa zymogen that has a long prodomain called the caspase recruitment domain (CARD) (res. 1-138) which, unlike in executioner caspases, does not get cleaved off during zymogen activation[8,16,41] due to its critical function of mediating caspase-9's recruitment to the apoptosome. The core of the enzyme is composed of the large subunit (res. 139-315) followed by a long linker (res. 316-330) and a small subunit (res. 331-416). The catalytic dyad of C287 and

H237 resides in the large subunit. There are three possible cleavage sites in the intersubunit linker- E306, D315 and D330 (Figure 1.6A). The majority of self-cleavage occurs at D315 with little observed cleavage at E306. D330 is a cleavage site for caspase-3, which is cleaved when the feedback loop present between caspase-3 and -9 is activated.

Although predominantly present as a monomer, the crystal structure of a CARD-deleted caspase-9 (ΔCARD casp-9) suggests that its active form is a dimer[42]. Interestingly, the structure (PDB ID:1JXQ) reveals that the two catalytic domains in the dimer have different conformations (Figure 1.6B). One active site is catalytically competent while the other is not, resting in what is called an "inactive" active site. Moreover, the loop bundle in this inactive catalytic site resembles the conformation of the loops assumed by the caspase-7 zymogen, hence it is incompetent to bind substrate in this arrangement. The presence of this catalytically incompetent active site

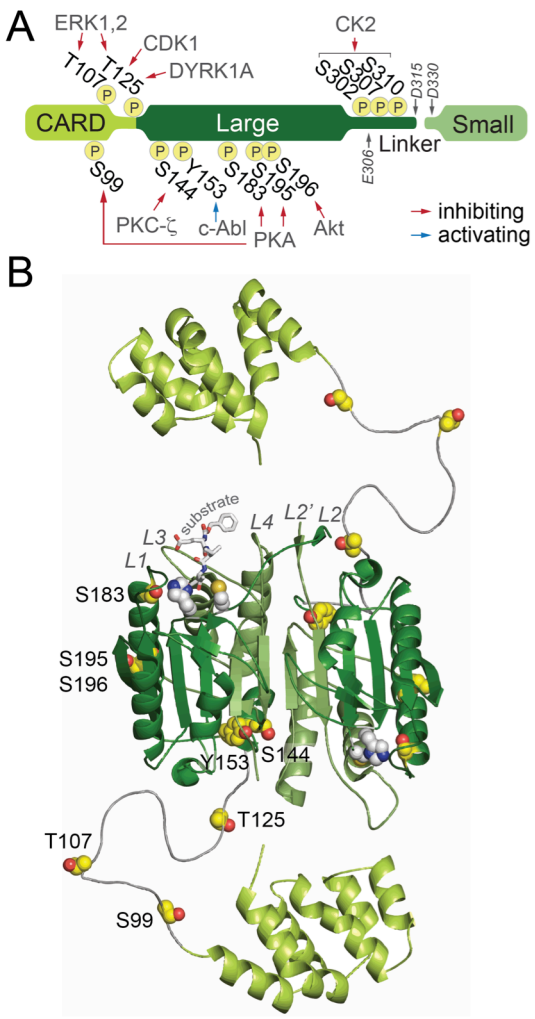

Figure 1.6. The caspase-9 structure.
(A) Domain organization of caspase-9 and location of reported phosphorylation sites within the caspase-9 structure, with cognate kinases indicated. (B) Structure of substrate-bound, dimeric, full-length caspase-9 showing the active site loops (L1, L2, L3, L4 and L2'), phosphorylation sites (in spheres) and the active site catalytic dyad (shown as sticks) which is competent in only one monomer. There is no existing structure of full-length caspase-9; this structure was modeled using available crystal structures of the CARD-deleted caspase-9 (PDB ID 1JXQ) and the complex between caspase-9 CARD and Apaf-1 CARD (PDB ID 3YGS). The region between the CARD and large subunit was modeled as grey coils, as it is not present in any available crystal structures of caspase-9.

was shown to be a result of alleviating steric clashes at the dimer interface should the site assume an active conformation, and not simply an artifact of crystal contacts[42].

Multiple Levels of Caspase-9 Activation

The activation of executioner caspases mainly lies in the intra-chain cleavage of the prodomain and the intersubunit linker. Thus their activation is a direct consequence of the action of initiator caspases. Unlike executioners wherein dimerization and cleavage renders them fully active, initiator caspases, particularly caspase-9, are activated in a different manner, primarily because there are no upstream proteases to cleave them. Caspase-9 does undergo self-processing, but this does not seem to convert caspase-9 into its fully active state[43,44]. In addition, caspase-9 activity seems to be influenced more by intra- and inter-domain interactions than by cleavage. This is supported by the observed increase in activity as protein domains are added stepwise to interact with the caspase-9 catalytic core, which is the simplest unit to generate caspase-9 constructs that possess maximal intrinsic (basal) activity. The presence of the CARD increases the activity of caspase-9 by ~20%, and is further enhanced five-fold in the presence of Apaf-1 CARD. The primary mode of caspase-9 activation is its recruitment to the apoptosome, in which it achieves its maximal activity, rendering it extremely efficient in cleaving downstream caspases and other substrates (Figure 1.7).

The apoptosome is a heptameric complex of Apaf-1, cytochrome c and d/ATP. Through homotypic interactions between Apaf-1 CARD and caspase-9 CARD, caspase-9 gets incorporated into the apoptosome where it undergoes auto-catalytic processing and activation. When bound to the apoptosome, caspase-9 activity is increased by 1000-fold, prompting the idea that caspase-9-bound apoptosome is the holoenzyme form of caspase-9. The fact that caspase-9 reaches its full activity in the apoptosome prompted many models of its activation (reviews[45,46]). The induced proximity model suggests that the apoptosome serves as a platform to increase the local concentration of procaspase-9 that results in trans-autoprocessing. However, this does not explain why cleaved/processed caspase-9 is not fully active. The observation that caspase-9 is

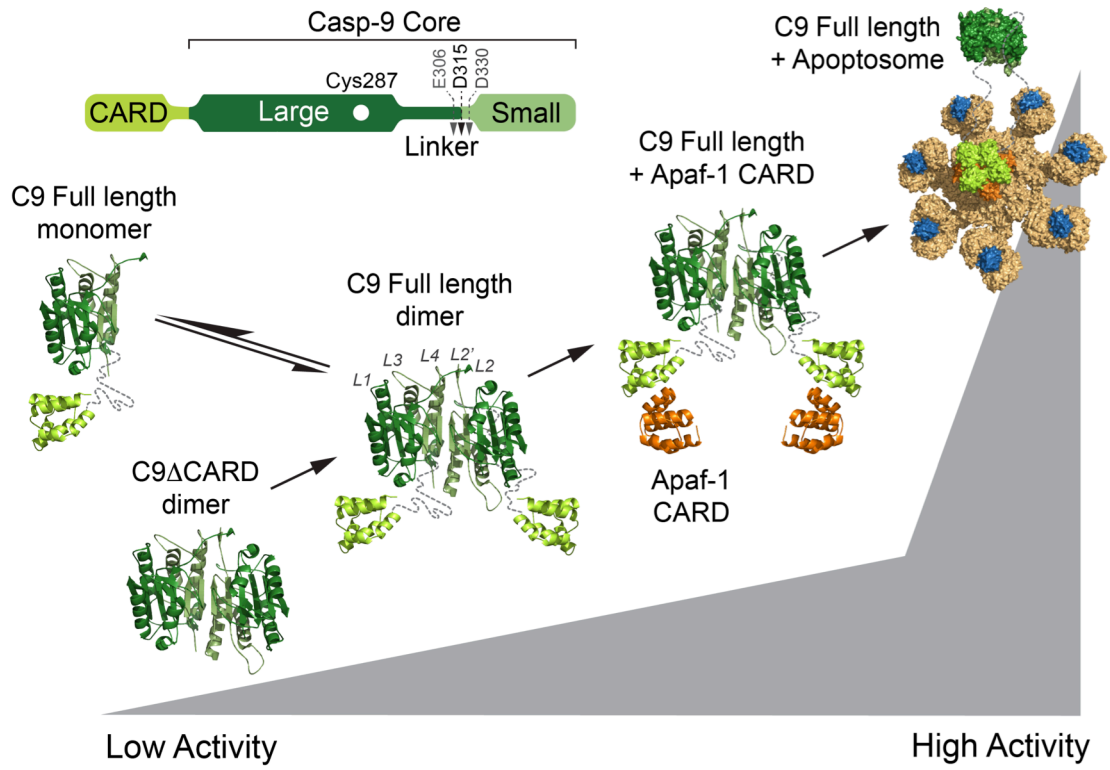

Figure 1.7. Levels of caspase-9 activation.
Caspase-9 is predominantly monomeric, but requires oligomerization, minimally dimerization, for activity. An increase in activity is facilitated by protein-protein interactions with Apaf-1 CARD. Caspase-9 achieves full activity by interacting with full-length Apaf-1, which together with cytochrome c, forms the apoptosome for caspase-9 binding. The structure of full-length caspase-9 was modeled using the CARD-deleted caspase-9 structure (PDB ID: 1JXQ) and caspase-9 CARD in complex with Apaf-1 CARD (PDB ID: 3YGS). The caspase-9 bound apoptosome was based on the structure reported by Cheng, et al, 2016[48])

predominantly monomeric but requires dimerization to be active led to the proximity-dimerization model: caspase-9's recruitment to the apoptosome leads to increase in local concentration and allows them to dimerize – and would also explain the ΔCARD caspase-9 crystal structure of being a catalytically active dimer. Another model is centered on the activating caspase-9 by induced conformational changes in its active site as it is bound to the apoptosome. These changes may possibly be brought about by interactions of the apoptosome to the dimerization interface of caspase-9 thereby stabilizing the active loops, or by facilitating different

oligomerization states of caspase-9. Recent near-atomic cryo-EM structures[47,48] and biochemical studies[49] on caspase-9-bound apoptosome have provided a clearer picture of how caspase-9 is poised to undergo activation in the apoptosome. Both models posit that proximity-driven dimerization and induced conformational changes in caspase-9 upon apoptosome binding are consistent with recent structures of the apoptosome.

While the canonical mode of caspase-9 activation lies in the apoptosome, caspase-9 has also been observed to undergo activation by alternative mechanisms that are independent of the apoptosome. This stems from observations that under certain cellular conditions such as viral infection[50] and lysosomal cell death[51], caspase-9 undergoes cleavage and activation without Apaf-1 or cytochrome c. Caspase-9 was also found to be present and activated in the "dependosome", a high-molecular weight complex composed of adaptor proteins (DRAL and TUCAN) and an E3 ubiquitin ligase (NEDD4)[52,53], in a manner analogous to that of the apoptosome.

Intracellular Regulation of Caspase-9

Disturbance in the normal activation of caspase-9 has been linked to a number of apoptosis-related diseases and thus caspase-9 is considered a therapeutic target. In certain cancers and viral infections, caspase-9 has been observed as either poorly expressed or has diminished activity. Very low or no expression levels of caspase-9 and caspase-7 are evident in colonic carcinoma cells[54] and caspase-9 expression was suggested to be a prognosticator of adverse carcinoma[55]. In testicular cancer cells, caspase-9 activation fails and confers greater resistance to apoptosis[56]. In degenerative diseases such as amyotrophic lateral sclerosis (ALS), caspase-9 was found to be highly abundant and active[57] in spinal cords of ALS subjects. Thus, due to the central role of caspase-9 in apoptosis, it is heavily regulated in the cell to guarantee its proper and timely activation.

The many layers by which caspase-9 can be activated allow for multiple levels of its regulation. This multi-level regulation ensures that caspase-9 function is modulated with high fidelity, even providing fail-safe mechanisms in case one mode of activation goes awry.

However, this also causes caspase-9 activation to be particularly susceptible to various intracellular imbalance or assaults in the apoptotic pathways. Nevertheless, from a therapeutic viewpoint, one advantage of this multi-level regulation of caspase-9 is that it provides several potential nodes for therapeutic intervention to specifically control caspase-9 function.

Caspase-9 endogenously experiences tight control by a number of mechanisms (Table 1.1). Mature caspase-9 is inhibited by XIAP by having its BIR3 domain interact with the small subunit of caspase-9 thereby preventing its dimerization[58]. An isoform caspase-9b that lacks the catalytic domain acts as a dominant negative factor and was found to interfere with caspase-9 CARD:Apaf-1 CARD binding [59]. Another CARD-containing protein that competes for Apaf-1 binding is TUCAN (tumor up-regulated CARD-containing antagonist of caspase-9), which is found to be overexpressed in many types of cancer including breast, gastric and colon cancer [60,61]. Zinc, which only recently has emerged as a relevant apoptotic regulator, has been reported to bind and inhibit caspase-9[62,63]. Caspase-9 also undergoes post-translational modifications. Nitrosation of the active site cysteine leads to its failure to self-activate[64–66]. Interestingly, ubiquitination of caspase-9 has opposing effects, depending on the polyubiquitin linkage. XIAP also acts as an E3 ubiquitin ligase, appending K47-linked ubiquitin chains that leads to proteasomal degradation of caspase-9. In contrast, the E3 ligase NEDD4 mediates K63-linked ubiquitination and this apparently leads to a more stable caspase-9 in the dependosome and results in its activation[52,53]. As previously mentioned, caspase-9 is extremely sensitive to phosphorylation, imparting another level of regulation which is the main focus of this dissertation.

Table 1.1. Natural regulators of caspase-9.

Regulation	Regulator	Result	Mechanism
Oligomerization	Self	Activation	Dimerization
	Apaf-1/cytochrome c	Activation	Holoapoptosome formation
Protein binding	XIAP	Inhibition	Prevents dimerization
	Caspase-9b isoform	Inhibition	Competes for Apaf-1 CARD binding
	TUCAN/CARD8	Inhibition	Competes for Apaf-1 CARD binding
Metals	Zinc	Inhibition	Binds to active site and allosteric site
Nitrosation	NO	Inhibition	Modifies active-site cysteine
Ubiquitination	XIAP	Inhibition	K48-linkage; leads to proteasomal degradation
	NEDD4	Activation	K63-linkage; stabilizes caspase-9 in the dependosome
Phosphorylation	Kinases	Inhibition (mostly)	Many/diverse

Phosphorylation of Caspase-9 Alters the Apoptotic Response

Caspase-9 is extensively phosphorylated. Eleven sites, spanning all domains, are reportedly phosphorylated by at least nine different kinases[67] (Figure 1.6A). The high degree of phosphorylation in caspase-9 highlights the various checkpoints that caspase-9 experiences during apoptosis as it is poised to undergo self-activation and perform cleavage of executioner caspases. Phosphorylation of caspase-9 has been implicated in insufficient apoptosis in Downs syndrome[68] and affects survival of breast and ovarian cancer cells[69]. The first report of its phosphorylation is by Akt[70] or protein kinase B (PKB), a serine-threonine kinase involved in apoptotic suppression. Since then, caspase-9 has been reported as a target of kinases that are involved in cell cycle (CDK1[69], CK2[71]), cellular stress (PKC-ζ[72], c-Abl[73], Akt[70]) and extracellular signals (ERK1,2[74] and DYRK1A[75]) . Cell-based studies on caspase-9 revealed that these kinases inhibit apoptosis by preventing caspase-9 from self-processing and activation[69,74,75], sometimes despite the release of cytochrome c[76].

The catalytic core of caspase-9 has the highest number of phosphorylation sites of all domains of caspase-9. The most studied phosphorylation site in caspase-9 is T125. This residue lies in the potentially flexible linker between the CARD and the large subunit. It is

phosphorylated by four different kinases (ERK 1 and 2 of the MAPK pathway, DYRK1A, CDK1) that have been implicated in cancer and tumorigenesis. In fact, phosphorylation of this residue has been found to be a hallmark of gastric carcinomas[77]. Akt/PKB, which was shown to phosphorylate S196 is involved in signaling pathways that respond to growth factors, thus is an important regulator of cell proliferation. Akt kinase transfected in HEK cells prevented caspase-3 from activating, thus suppressing cell death[70]. In cell extracts treated with okadaic acid, a phosphatase inhibitor, caspase-9 was reported to be phosphorylated at S144 by an atypical PKC isoform, PKCζ, upon inducing hyperosmotic shock using NaCl or sorbitol[72]. In this case, caspase-9 failed to undergo processing and apoptosis was restrained in HEK293 cells. In many types of cells elevated levels of cAMP have been found to confer resistance to apoptosis. The link between the cAMP elevation and apoptosis is the activation of cAMP-dependent protein kinase (PKA), which inhibits caspase-9 activation by phosphorylating it at three sites- S99, S183 and S195. However, it was reported that direct phosphorylation of these three sites is dispensable to caspase inhibition; instead it was suggested that PKA phosphorylates Apaf-1 and prevents it from oligomerizing and recruiting cytochrome c[78]. Intriguingly and in contrast to the inhibitory effect of kinases mentioned above, c-Abl is reported to promote caspase-9 processing at Y153 upon araC (DNA replication inhibitor)-induced apoptosis. Cells expressing a knockout of this site, Y153F, failed to undergo apoptosis even after araC treatment or exposure to UV radiation[73].

Divergent Mechanisms of Caspase-9 Control by Phosphorylation

It is clear that caspase-9 activity is particularly sensitive to phosphorylation, given the extent of its phosphorylation and the number of kinases that recognize it as a substrate. In the past decade, advancement in proteomics have identified phosphorylation sites in caspases-9 and in other caspases, but naturally, it has been difficult to perform wide-scale annotations under different cellular conditions. And while cell-based studies have been instrumental in determining the phenotypic consequence of either promotion or suppression of apoptosis upon

phosphorylation of caspase-9, to date there has been insufficient information on the molecular details to pinpoint the mechanism of phosphoregulation. Given the immense therapeutic potential of targeting caspase-9, knowing the precise molecular details of its phosphoregulation is absolutely essential if that mechanism is to be harnessed to specifically control caspase-9.

There are multiple aspects to caspase-9 phosphorylation that warrant deeper investigation. First, it is noteworthy that phosphorylation sites in caspase-9 are not clustered in one region, but rather are spread over different regions in caspase-9 structure (Figure 1.6B). All domains of caspase-9 - the CARD, catalytic core and intersubunit linker - are phosphorylated. Thus, phosphorylation of one site may confer a different mechanism of regulation to caspase-9, especially considering the fact that there are multiple levels to exert control within the caspase-9 activation cascade. We have recently observed a dual mechanism of inactivation of caspase-7 by the kinase PAK2, wherein phosphorylation at S30 prevents procaspase-7 binding to and processing by caspase-9, and phosphorylation at S239 in the mature form directly blocks substrate binding[79]. Second, given that there are multiple sites phosphorylated by a single kinase, it is important to discriminate which site directly imposes a functional effect on caspase-9 upon phosphorylation, and which are simply "bystander" or redundant residues. Such is the case for caspase-9 phosphorylation by PKA, ERK1,2 and CK2 (Figure 1.6A) where more than one site is phosphorylated by each kinase. Are all sites required to be phosphorylated to inactivate caspase-9, or does a single residue serve as a predominant phosphoregulator of caspase-9's catalytic activity? While the concept of "bystander" or "silent" phosphorylation is replete in kinase literature, non-observance of functional effects should be carefully interpreted. As caspase-9's activity is influenced by a variety of factors, the absence of a direct inhibition to the catalytic/proteolytic activity of caspase-9 upon phosphorylation does not necessarily mean that phosphorylation has no other influence on caspase-9 structure and function. Third, it is apparent from the great extent of phosphorylation in caspase-9 that phosphorylation is a major and critical regulator of its function. It is therefore fitting to ask whether there are more sites of

phosphorylation in caspase-9 that are yet to be uncovered, in what cellular context and how would it alter the apoptotic pathways. Finally, crosstalk between caspase-9 and its cognate kinases has not been thoroughly interrogated. Caspases and kinases are in constant molecular dialogue that allows for their co-regulation. Most caspases cleave the very kinase that phosphorylates them, resulting in either gain- or loss-of-function, or localization of the kinase into a different cellular compartment, thus tipping the balance between cell death and survival. Given that at least nine different kinases phosphorylate caspase-9, it is conceivable that this caspase-kinase interplay would play a more significant role in mediating the apoptotic response.

This dissertation focuses on addressing these molecular questions about caspase-9 phosphoregulation by employing sound and complementary studies of biochemistry, structural biology and cell biology. Specifically, Chapter II investigates the single-site, dual-mechanism of caspase-9 inhibition by PKA, a ubiquitous kinase that is involved in cellular signaling but whose aberrant expression and activity has been observed in many cancer cell types. Chapter III delves deeper into the hierarchical nature of caspase-9 activation by interrogating the physical interactions between the caspase-9 CARD and its catalytic domains that affects caspase-9 stability, and how phosphorylation by PKA perturbs these interactions. In Chapter IV we identify a novel site of phosphorylation in caspase-9 by c-Abl, a kinase that has both pro-apoptotic and anti-apoptotic/pro-survival roles, and elucidate the mechanism of inactivation.

References

1. Elmore, S. Apoptosis: a review of programmed cell death. *Toxicol. Pathol.* **35,** 495–516 (2007).
2. Wong, R. S. Y. Apoptosis in cancer: from pathogenesis to treatment. *J. Exp. Clin. Cancer Res.* **30,** 87 (2011).
3. Favaloro, B., Allocati, N., Graziano, V., Di Ilio, C. & De Laurenzi, V. Role of apoptosis in disease. *Aging (Albany. NY).* **4,** 330–49 (2012).
4. EGUCHI, K. Apoptosis in Autoimmune Diseases. *Intern. Med.* **40,** 275–284 (2001).
5. Li, J. & Yuan, J. Caspases in apoptosis and beyond. *Oncogene* **27,** 6194–206 (2008).
6. Hengartner, M. The biochemistry of apoptosis. *Nature* **407,** 770–6 (2000).
7. Zou, H., Li, Y., Liu, X. & Wang, X. An Apaf-1-cytochrome c multimeric complex is a functional apoptosome that activates procaspase-9. *J. Biol. Chem.* **274,** 11549–11556 (1999).
8. Rodriguez, J. & Lazebnik, Y. Caspase-9 and Apaf-1 form an active holoenzyme. *Genes Dev.* **13,** 3179–3184 (1999).
9. Slee, E. A. *et al.* Ordering the cytochrome c-initiated caspase cascade: Hierarchical activation of caspases-2, -3, -6, -7, -8 and -10 in a caspase-9-dependent manner. *Mol. Cell* **144,** 281–292 (1999).
10. Slee, E. A. *et al.* Ordering the cytochrome c-initiated caspase cascade: Hierarchical activation of caspases-2,-3,-6,-7,-8, and -10 in a caspase-9-dependent manner. *J. Cell Biol.* **144,** 281–292 (1999).
11. Fischer, U., Jänicke, R. U. & Schulze-Osthoff, K. Many cuts to ruin: a comprehensive update of caspase substrates. *Cell Death Differ.* **10,** 76–100 (2003).
12. Witkowski, W. A. & Hardy, J. A. L2' loop is critical for caspase-7 active site formation. *Protein Sci.* **18,** 1459–68 (2009).
13. Muzio, M. *et al.* FLICE, A Novel FADD-Homologous ICE/CED-3–like Protease, Is Recruited to the CD95 (Fas/APO-1) Death-Inducing Signaling Complex. *Cell* **85,** 817–827 (1996).
14. Tinel, A. & Tschopp, J. The PIDDosome, a Protein Complex Implicated in Activation of Caspase-2 in Response to Genotoxic Stress. *Science (80-.).* **304,** (2004).
15. Cain, K., Brown, D. G., Langlais, C. & Cohen, G. M. Caspase activation involves the formation of the apoptosome, a large (approximately 700 kDa) caspase-activating complex. *J. Biol. Chem.* **274,** 22686–92 (1999).
16. Bratton, S. B. *et al.* Recruitment, activation and retention of caspases-9 and -3 by Apaf-1 apoptosome and associated XIAP complexes. *EMBO J.* **20,** 998–1009 (2001).
17. Parrish, A. B., Freel, C. D. & Kornbluth, S. Cellular Mechanisms Controlling Caspase Activation and Function. *Cold Spring Harb Perspect Biol* **5,** 1–24 (2013).
18. MacKenzie, S. H. & Clark, A. C. Death by caspase dimerization. *Adv. Exp. Med. Biol.* **747,** 55–73 (2012).

19. Chęcińska, A., Giaccone, G., Rodriguez, J. A., Kruyt, F. A. E. & Jimenez, C. R. Comparative proteomics analysis of caspase-9-protein complexes in untreated and cytochrome c/dATP stimulated lysates of NSCLC cells. *J. Proteomics* **72,** 575–585 (2009).

20. Timmer, J. C. & Salvesen, G. S. Caspase substrates. *Cell Death Differ.* **14,** 66–72 (2007).

21. Seaman, J. E. *et al.* Cacidases: caspases can cleave after aspartate, glutamate and phosphoserine residues. *Cell Death Differ.* (2016). doi:10.1038/cdd.2016.62

22. Boucher, D., Blais, V. & Denault, J.-B. Caspase-7 uses an exosite to promote poly(ADP ribose) polymerase 1 proteolysis. *Proc. Natl. Acad. Sci. U. S. A.* **109,** 5669–74 (2012).

23. Hardy, J. A. & Wells, J. A. Dissecting an allosteric switch in caspase-7 using chemical and mutational probes. *J. Biol. Chem.* **284,** 26063–9 (2009).

24. Velázquez-Delgado, E. M. & Hardy, J. A. Zinc-mediated allosteric inhibition of caspase-6. *J. Biol. Chem.* **287,** 36000–11 (2012).

25. Huber, K. L. & Hardy, J. A. Mechanism of zinc-mediated inhibition of caspase-9. *Protein Sci.* **21,** 1056–65 (2012).

26. Stanger, K. *et al.* Allosteric peptides bind a caspase zymogen and mediate caspase tetramerization. *Nat. Chem. Biol.* **8,** 655–60 (2012).

27. McIlwain, D. R., Berger, T. & Mak, T. W. Caspase functions in cell death and disease. *Cold Spring Harb. Perspect. Biol.* **5,** 1–27 (2013).

28. Olsson, M. & Zhivotovsky, B. Caspases and cancer. *Cell Death Differ.* **18,** 1441–1449 (2011).

29. Ghavami, S. *et al.* Apoptosis and cancer: mutations within caspase genes. *J. Med. Genet.* **46,** 497–510 (2009).

30. Friedlander, R. M. Apoptosis and Caspases in Neurodegenerative Diseases. *N. Engl. J. Med.* **348,** 1365–1375 (2003).

31. Bredesen, D. E. Neurodegeneration in Alzheimer's disease: caspases and synaptic element interdependence. *Mol. Neurodegener.* **4,** 27 (2009).

32. LeBlanc, A. C. Natural cellular inhibitors of caspases. *Prog. Neuro-Psychopharmacology Biol. Psychiatry* **27,** 215–229 (2003).

33. Voss, O. H. *et al.* Binding of Caspase-3 Prodomain to Heat Shock Protein 27 Regulates Monocyte Apoptosis by Inhibiting Caspase-3 Proteolytic Activation. *J. Biol. Chem.* **282,** 25088–25099 (2007).

34. Green, D. R. *et al.* Heat-shock protein 70 inhibits apoptosis by preventing recruitment of procaspase-9 to the Apaf-1 apoptosome. *Nat. Cell Biol.* **2,** 469–475 (2000).

35. GARRIDO, C. *et al.* HSP27 inhibits cytochrome c-dependent activation of procaspase-9. *FASEB J.* **13,** 2061–2070 (1999).

36. Takayama, S., Reed, J. C. & Homma, S. Heat-shock proteins as regulators of apoptosis. *Oncogene* **22,** 9041–9047 (2003).

37. Lanneau, D. *et al.* Heat shock proteins: essential proteins for apoptosis regulation. *J. Cell. Mol. Med.* **12,** 743–761 (2008).

38. Schwerk, C. & Schulze-Osthoff, K. Regulation of Apoptosis by Alternative Pre-mRNA Splicing. *Mol. Cell* **19,** 1–13 (2005).

39. Zamaraev, A. V., Kopeina, G. S., Prokhorova, E. A., Zhivotovsky, B. & Lavrik, I. N. Post-translational Modification of Caspases: The Other Side of Apoptosis Regulation. *Trends Cell Biol.* **27,** 322–339 (2017).

40. Dagbay, K. *et al.* A multipronged approach for compiling a global map of allosteric regulation in the apoptotic caspases. *Methods Enzymol.* (2014). doi:10.1016/B978-0-12-417158-9.00009-1

41. Stennicke, H. R. *et al.* Caspase-9 Can Be Activated without Proteolytic Processing. *J. Biol. Chem.* **9,** 8359–8362 (1999).

42. Renatus, M., Stennicke, H. R., Scott, F. L., Liddington, R. C. & Salvesen, G. S. Dimer formation drives the activation of the cell death protease caspase-9. *Proc. Natl. Acad. Sci. U. S. A.* **98,** 14250–5 (2001).

43. McStay, G. P., Salvesen, G. S. & Green, D. R. Overlapping cleavage motif selectivity of caspases: implications for analysis of apoptotic pathways. *Cell Death Differ.* **15,** 322–31 (2008).

44. Stennicke, H. R. *et al.* Caspase-9 can be activated without proteolytic processing. *J. Biol. Chem.* **274,** 8359–62 (1999).

45. Shi, Y. Activation of Initiator Caspases : History, Hypotheses, and Perspectives. *J. Cancer Mol.* **1,** 9–18 (2005).

46. Shi, Y. Caspase activation: revisiting the induced proximity model. *Cell* **117,** 855–8 (2004).

47. Li, Y. *et al.* Mechanistic insights into caspase-9 activation by the structure of the apoptosome holoenzyme. *Proc. Natl. Acad. Sci. U. S. A.* **114,** 1542–1547 (2017).

48. Cheng, T. C., Hong, C., Akey, I. V., Yuan, S. & Akey, C. W. A near atomic structure of the active human apoptosome. *Elife* **5,** 1–28 (2016).

49. Wu, C.-C. *et al.* The Apaf-1 apoptosome induces formation of caspase-9 homo- and heterodimers with distinct activities. *Nat. Commun.* **7,** 13565 (2016).

50. Bitzer, M. *et al.* Caspase-8 and Apaf-1-independent Caspase-9 Activation in Sendai Virus-infected Cells. *J. Biol. Chem.* **277,** 29817–29824 (2002).

51. Gyrd-Hansen, M. *et al.* Apoptosome-Independent Activation of the Lysosomal Cell Death Pathway by Caspase-9. *Mol. Cell. Biol.* **26,** 7880–7891 (2006).

52. Mille, F. *et al.* The Patched dependence receptor triggers apoptosis through a DRAL–caspase-9 complex. *Nat. Cell Biol.* **11,** 739–746 (2009).

53. Fombonne, J. *et al.* Patched dependence receptor triggers apoptosis through ubiquitination of caspase-9. *Proc. Natl. Acad. Sci. U. S. A.* **109,** 10510–5 (2012).

54. Palmerini, F., Devilard, E., Jarry, A., Birg, F. & Xerri, L. Caspase-7 downregulation as an immunohistochemical marker of colonic carcinoma. *Hum. Pathol.* **32,** 461–7 (2001).

55. Sträter, J. *et al.* Expression and prognostic significance of APAF-1, caspase-8 and caspase-9 in stage II/III colon carcinoma: caspase-8 and caspase-9 is associated with poor prognosis. *Int. J. Cancer* **127,** 873–80 (2010).

56. Mueller, T. *et al.* Failure of Activation of Caspase-9 Induces a Higher Threshold for Apoptosis and Cisplatin Resistance in Testicular Cancer. *Cancer Res.* **63,** 513–521 (2003).

57. Inoue, H. *et al.* The crucial role of caspase-9 in the disease progression of a transgenic ALS mouse model. *EMBO J.* **22,** 6665–74 (2003).

58. Shiozaki, E. N. *et al.* Mechanism of XIAP-mediated inhibition of caspase-9. *Mol. Cell* **11,** 519–27 (2003).

59. Srinivasula, S. M. *et al.* Identification of an endogenous dominant-negative short isoform of caspase-9 that can regulate apoptosis. *Cancer Res.* **59,** 999–1002 (1999).

60. Pathan, N. *et al.* TUCAN, an antiapoptotic caspase-associated recruitment domain family protein overexpressed in cancer. *J. Biol. Chem.* **276,** 32220–9 (2001).

61. Yamamoto, M. *et al.* A Novel Isoform of TUCAN Is Overexpressed in Human Cancer Tissues and Suppresses Both Caspase-8– and Caspase-9–Mediated Apoptosis. *Cancer Res.* **65,** (2005).

62. Chimienti, F., Seve, M., Richard, S., Mathieu, J. & Favier, A. Role of cellular zinc in programmed cell death: temporal relationship between zinc depletion, activation of caspases, and cleavage of Sp family transcription factors. *Biochem. Pharmacol.* **62,** 51–62 (2001).

63. Huber, K. L. & Hardy, J. a. Mechanism of zinc-mediated inhibition of caspase-9. *Protein Sci.* **21,** 1056–65 (2012).

64. Kim, J.-E. & Tannenbaum, S. R. S-Nitrosation regulates the activation of endogenous procaspase-9 in HT-29 human colon carcinoma cells. *J. Biol. Chem.* **279,** 9758–64 (2004).

65. Mannick, J. B. *et al.* S-Nitrosylation of mitochondrial caspases. *J. Cell Biol.* **154,** 1111–6 (2001).

66. Mannick, J. B. Regulation of apoptosis by protein S-nitrosylation. *Amino Acids* **32,** 523–6 (2007).

67. Allan, L. A. & Clarke, P. R. Apoptosis and autophagy: Regulation of caspase-9 by phosphorylation. *FEBS J.* **276,** 6063–73 (2009).

68. Laguna, A. *et al.* The protein kinase DYRK1A regulates caspase-9-mediated apoptosis during retina development. *Dev. Cell* **15,** 841–53 (2008).

69. Allan, L. A. & Clarke, P. R. Phosphorylation of caspase-9 by CDK1/cyclin B1 protects mitotic cells against apoptosis. *Mol. Cell* **26,** 301–10 (2007).

70. Cardone, M. H. *et al.* Regulation of Cell Death Protease Caspase-9 by Phosphorylation. *Science (80-.).* **282,** 1318–1321 (1998).

71. McDonnell, M. A. *et al.* Phosphorylation of murine caspase-9 by the protein kinase casein kinase 2 regulates its cleavage by caspase-8. *J. Biol. Chem.* **283,** 20149–58 (2008).

72. Brady, S. C., Allan, L. A. & Clarke, P. R. Regulation of Caspase 9 through Phosphorylation by Protein Kinase C Zeta in Response to Hyperosmotic Stress. *Mol. Cell. Biol.* **25,** 10543–10555 (2005).

73. Raina, D. *et al.* c-Abl tyrosine kinase regulates caspase-9 autocleavage in the apoptotic response to DNA damage. *J. Biol. Chem.* **280,** 11147–51 (2005).

74. Allan, L. A. *et al.* Inhibition of caspase-9 through phosphorylation at Thr 125 by ERK MAPK. *Nat. Cell Biol.* **5,** 647–54 (2003).

75. Seifert, A., Allan, L. A. & Clarke, P. R. DYRK1A phosphorylates caspase 9 at an inhibitory site and is potently inhibited in human cells by harmine. *FEBS J.* **275,** 6268–80 (2008).

76. Tashker, J. S., Olson, M. & Kornbluth, S. Post–cytochrome c protection from apoptosis conferred by a MAPK pathway in Xenopus egg extracts. *Mol. Biol. Cell* **13,** 393–401 (2002).

77. Yoo, N., Lee, S. & Jeong, E. Expression of phosphorylated caspase-9 in gastric carcinomas. *APMIS* 354–359 (2007).

78. Martin, M. C. *et al.* Protein kinase A regulates caspase-9 activation by Apaf-1 downstream of cytochrome c. *J. Biol. Chem.* **280,** 15449–55 (2005).

79. Eron, S. J., Raghupathi, K. & Hardy, J. A. Dual Site Phosphorylation of Caspase-7 by PAK2 Blocks Apoptotic Activity by Two Distinct Mechanisms. *Structure* **0,** 1913–1918 (2016).

CHAPTER II

PHOSPHORYLATION BY PROTEIN KINASE A DISASSEMBLES THE CASPASE-9 CORE

Majority of this chapter is published: Serrano, B.P. and Hardy J.A. Phosphorylation by Protein Kinase A Disassembles the Caspase-9 Core. *Cell Death and Differentiation.* In press (2018).

Abstract

Caspases, the cysteine proteases which facilitate the faithful execution of apoptosis, are tightly regulated by a number of mechanisms including phosphorylation. In response to cAMP, PKA phosphorylates caspase-9 at three sites preventing caspase-9 activation and suppressing apoptosis progression. Phosphorylation of caspase-9 by PKA at the functionally relevant site S183 acts as an upstream block of the apoptotic cascade, directly inactivating caspase-9 by a two-stage mechanism. First, S183 phosphorylation prevents caspase-9 self-processing and directly blocks substrate binding. In addition, S183 phosphorylation breaks the fundamental interactions within the caspase-9 core, promoting disassembly of the large and small subunits. This occurs despite S183 being a surface residue distal from the interface between the large and small subunits. This phosphorylation-induced disassembly promotes the formation of ordered aggregates around 20 nm in diameter. Similar aggregates of caspase-9 have not been previously reported. This two-stage regulatory mechanism for caspase-9 has not been reported previously but may be conserved across the caspases.

Introduction

Caspases are specialized enzymes that coordinate the intricate cascade of reactions to faithfully execute apoptosis. Caspases irreversibly cleave protein substrates causing gain or loss of function, thereby committing the cell to its demise. Caspases display exquisite specificity towards substrates, generally preferring to cleave after an aspartate, glutamate[1,2] and in some cases phosphoserine[3]. Apoptotic caspases are classified as either initiators (caspase-2, -8 and -9) or executioners (caspase-3, -6 and -7). Uncontrolled activation of caspases is lethal, so caspases are synthesized and held as inactive zymogens (procaspases) prior to apoptosis induction. Activation generally relies on either recruitment to an activating scaffold (initiators) or cleavage at the intersubunit linker forming a mature caspase (executioners) (for review[4]). Most procaspases are homodimeric proteins that contain a highly homologous protease core, which can be cleaved into two large and two small subunits. While executioner caspases are constitutive dimers, initiator caspases exist in equilibrium between monomeric and dimeric states, with caspase-9 existing predominantly a monomer[5,6]. Upon activation, the highly dynamic loops comprising the active site undergo conformational rearrangements to bind and cleave substrates, thereby initiating cell death. Ultimately, caspase activity is intrinsic to apoptosis, so caspase expression and activation is tightly regulated. This is achieved by a number of mechanisms which exert control at various checkpoints in the cell. Improper regulation of caspases is associated with diseases ranging from cancer to neurodegeneration (for review[7–9]). Thus, caspases are considered attractive drug targets for apoptosis-associated diseases.

Phosphorylation is a central regulator of apoptosis (for review[10–12]). Although apoptosis is unlike other classic signaling pathways because it does not directly utilize kinases, the related activity of kinases can determine a cell's susceptibility to death. All apoptotic caspases are kinase substrates and caspases usually cleave the very kinases that phosphorylate them. Efforts to map kinase-caspase co-regulation and competition are ongoing (for review[10,12–14]), however, a more complex landscape of co-regulation becomes evident with the observation that some caspases

have multiple phosphorylation sites involving several kinases. Thus, although cell-based studies are fundamental in identifying cognate kinases and in determining the functional endpoint as either caspase inhibition or activation, biochemical and structural studies are essential in identifying critical residues and elucidating molecular details of diverse regulatory mechanisms arising from phosphorylation.

Among the apoptotic caspases, caspase-9 appears to be most sensitive to phosphorylation, which is mediated by a number of kinases activated in response to specific cellular signals (for review[15]). For example, in many cell types elevated cAMP levels have been found to confer protection from apoptosis[16–19] due to sustained Protein Kinase A (PKA) activity, which phosphorylates caspase-9 at three specific sites – S99, S183 and S195 – leading to failure of caspase-9 activation and eventual suppression of apoptosis[20]. Intriguingly, however, phosphorylation of these sites was reported to be dispensable in directly inhibiting caspase-9 and it was instead suggested that PKA acts on a more upstream substrate such as Apaf-1 to prevent caspase-9 activation. This observation seems to evoke silent or bystander phosphorylation in caspase-9, and while non-functional phosphorylation does occur in other proteins[21,22], the idea that PKA phosphorylates all three sites without any functional consequence seems to differ from what is known about the sensitivity of caspase activity to phosphorylation. Recent studies from our group[23,24] and others[25] have revealed that caspase activity is directly affected by phosphorylation both orthosterically and allosterically. In addition, the high conservation of phosphorylation sites across species[15] underscores the likelihood that phosphorylation yields functional effects, as functional phosphorylation sites evolve more slowly than non-functional sites[22]. Given the complexity of having three PKA phosphorylation sites, it is important to differentiate sites critical to inhibition from non-functional sites and is paramount for unraveling the dynamic control of caspase-9 activity by phosphorylation.

Here we identify S183 as the functionally relevant site that leads to direct inhibition of caspase-9 upon phosphorylation by PKA. Phosphorylation of the caspase-9 zymogen renders it incompetent to bind substrate, whereas phosphorylation of the mature form destabilizes the interactions within the caspase-9 core leading to its disassembly and formation of ordered aggregates. Understanding the multi-level mechanisms by which phosphorylation controls caspase-9 should provide new avenues to tap caspase-9's therapeutic potential in apoptosis-related disease.

Results

Phosphorylation of caspase-9 by PKA directly results in inhibition

All three reported sites of phosphorylation are located in the CARD (caspase activation and recruitment domain) plus large (CARD+Lg) region of caspase-9 (Figure 2.1A). S99 is in the highly flexible linker between the CARD and the large subunit. S183 sits just below Loop 1 (L1) in the vicinity of the substrate-binding groove and S195 is at the bottom of the α1 helix (Figure 1B). Building on the report that PKA directly phosphorylates caspase-9[20], we tested whether PKA activity affects caspase-9 function by assessing the ability of procaspase-9 to undergo self-processing in the presence of PKA and ATP. Procaspase-9 possesses a low level of basal activity[5,26,27] that allows *in trans* cleavage, under favorable conditions, to generate a mature, active caspase-9. Even in homogeneous preparations of wild-type (WT) procaspase-9, the intersubunit linker is rapidly cleaved, generating the CARD+Lg and small (Sm) subunits (Figure 2.2A). Addition of PKA with ATP greatly attenuated the rate of procaspase-9 self-cleavage (Figure 2.2A).

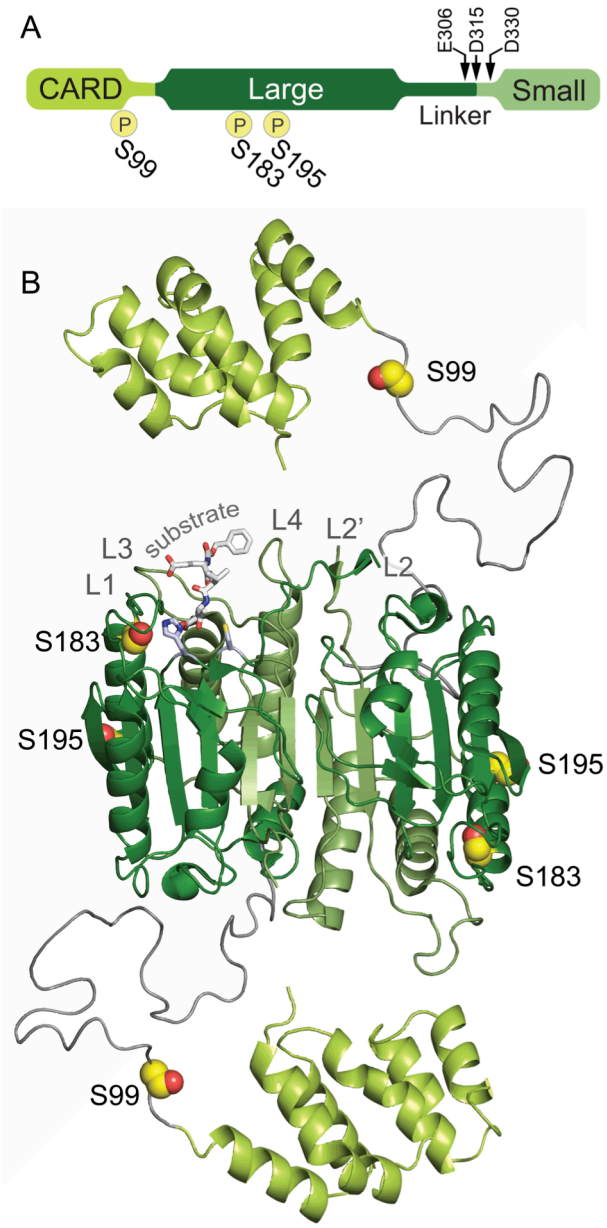

Figure 2.1. Sites of PKA phosphorylation in caspase-9.
(A) Domain architecture of caspase-9 showing the caspase activation and recruitment domain (CARD) (yellow green) and the protein core composed of the large (dark green) and small (light green) subunits connected by an intersubunit linker with three cleavage sites indicated by arrows: E306 (minor, self cleavage), D315 (major, self cleavage, and by caspase-8) and D330 (by caspase-3). The sites of PKA phosphorylation are indicated by .Ⓟ S99 is in the CARD while both S183 and S195 are in the large subunit.

(B) Structure of the caspase-9 dimer with phosphorylation sites (yellow spheres) noted. There is no structure of full-length caspase-9, so this model was built based on the CARD-deleted caspase-9 structure (aa 138-416; PDB ID: 1JXQ) and the caspase-9 CARD structure (aa 1-95; PDB ID: 3YGS) from a dimeric complex with Apaf-1 CARD. The region containing S99 is not present in either structure and is potentially highly disordered, so it was modeled as a dark gray coil. S99 is in the CARD; both S183 and S195 are located in the α1 helix.

To quantify the extent of inhibition, we assayed the activity of caspase-9 WT upon phosphorylation using the fluorogenic peptide substrate Ac-LEHD-AFC. Caspase-9 activity decreased two-fold when incubated with active PKA (Figure 2.2B), suggesting that PKA significantly inhibits caspase-9 function. *In vitro* phosphorylation using PKA and [γ-^{32}P]ATP showed phosphorylation of the CARD+Lg region of caspase-9 (Figure 2.2C) as expected, with a corresponding marked inhibition of caspase-9 activity (Figure 2.2D). This sensitivity of caspase-9 to phosphorylation is reversible. When treated with lambda protein phosphatase (λPP), we clearly observed the removal of phosphates from caspase-9 (Figure 2.2C). More importantly, caspase-9 activity was relieved of inhibition upon dephosphorylation (Figure 2.2D). This ability of caspase-9 being to be inactivated and reactivated by phosphorylation and dephosphorylation underscores the idea that this modification acts as a direct molecular regulator.

S183 is the critical residue leading to caspase-9 inactivation upon PKA phosphorylation

To pinpoint the single residue most responsible for inhibition, we generated unphosphorylatable alanine variants and correlated their phosphorylation states (Figure 2.2E) with caspase-9 inhibition (Figure 2.2F). All single alanine variants were phosphorylated only in the CARD+Lg region, and while S99A and S195A were highly inhibited by phosphorylation, S183A activity was less affected by phosphorylation. Among the double unphosphorylatable variants (S99A/S195A, S99A/S183A, S195A/S183A), only S99A/S195A, in which only S183 can be phosphorylated, displayed inhibition similar to phosphorylated WT.

Having all three sites unphosphorylatable (S99A/S183A/S195A) resulted in low levels of non-specific phosphorylation, especially with the appearance of a band corresponding to a phosphorylated small subunit (Figure 2.2E). This extra, non-specific phosphorylation had no substantial influence in caspase-9 activity, since only background levels of inhibition for the triple alanine mutant were observed. These results clearly suggest that S183 is the dominant site responsible for the inhibition due to PKA phosphorylation.

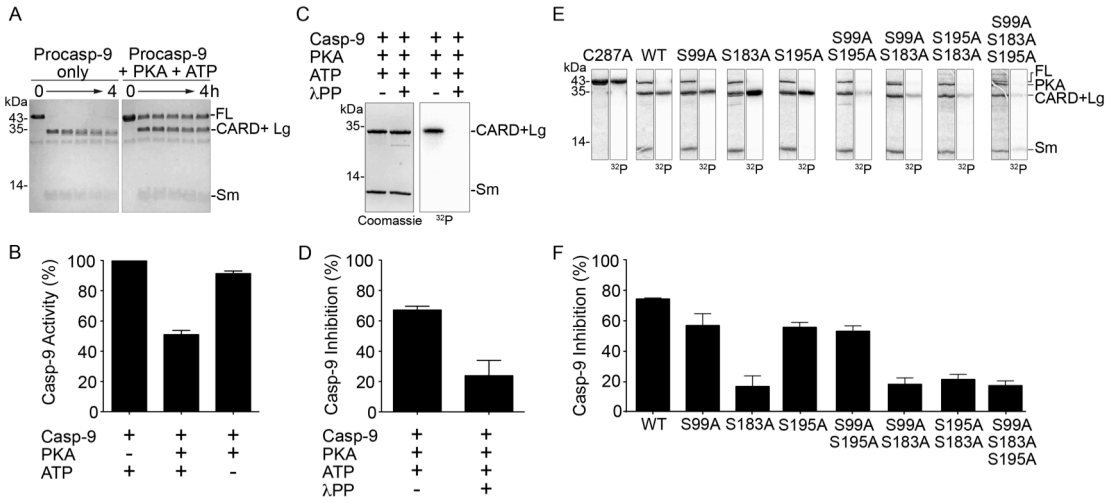

Figure 2.2. Phosphorylation of caspase-9 by PKA results in significant inhibition of caspase-9.
(A) Active PKA inhibits self-processing of procaspase-9. Full-length (FL) procaspase-9 WT rapidly undergoes self-cleavage to generate the CARD+Large (Lg) and Small (Sm) subunits as assessed by Coomassie-stained SDS-PAGE analysis. Addition of PKA and ATP to procaspase-9 slows the rate of self-cleavage, so that caspase-9 remains predominantly in the full-length, uncleaved form even after 4 h incubation.
(B) Addition of active PKA to cleaved caspase-9 WT results in a two-fold decrease in caspase activity after 2 h as measured by the hydrolysis of the fluorogenic caspase-9 substrate Ac-LEHD-AFC, suggesting that PKA treatment leads to inhibition. Percent caspase-9 activity is normalized against activity in the absence of PKA. Data shown are means (± SEM) of three independent trials on three separate days.
(C) Caspase-9 is phosphorylated by PKA only in the CARD+Lg region, as detected by autoradiography after *in vitro* phosphorylation using [γ-^{32}P] ATP for 4 h. There is no visible phosphorylation in the Sm subunit. PKA is phosphorylated during overexpression in bacteria[73], so it does not get efficiently labeled by [γ-^{32}P] ATP. Treatment of PKA-phosphorylated caspase-9 with λ protein phosphatase (λPP) results in dephosphorylation as manifested by loss of signal in the autoradiogram (labeled here and in the succeeding figures as ^{32}P).
(D) Phosphorylation of caspase-9 is reversible. Caspase-9 phosphorylated by PKA is inhibited. Treatment of phosphorylated caspase-9 with λ protein phosphatase (λPP) relieves the inhibition. Percent inhibition for phosphorylated caspase-9 (with both PKA and ATP present) was normalized against activity in the non-phosphorylated form (with PKA but no ATP present). Data shown are means (± SEM) of three independent trials on three separate days.
(E) Unphosphorylatable alanine variants (single, double and triple alanine substitutions at phosphorylated serines) and catalytic site-inactivated variant C287A were subjected to *in vitro* phosphorylation by PKA for 4 h. Double alanine variants show (observed by Coomassie-stained SDS-PAGE analysis in the first of each pair of panels) decreased levels of phosphorylation as the weaker intensity of the bands in the autoradiogram (second of each pair of panels). The triple alanine variant shows only weak, non-specific phosphorylation in the small subunit, indicating that all three sites S99, S183 and S195 are phosphorylated by PKA.
(F) Inhibition by phosphorylation of WT caspase-9 and alanine variants. Only when S183 is available to be phosphorylated (WT, S99A, S195A and S99A/A195A) does caspase-9 experience significant inhibition. All S183A variants are insensitive to PKA-mediated inhibition. The catalytic parameters of alanine variants are indicated in Table 1. Percent inhibition for phosphorylated caspase-9 (with both PKA and ATP present) was normalized against activity in the non-phosphorylated form (with PKA but no ATP present). Data shown are means (± SEM) of three independent trials on three separate days.

PhosphoS183 caspase-9 and the phosphomimetic S183E are completely inactive

Due to low levels of non-specific phosphorylation observed *in vitro*, we prepared versions of caspase-9 that are unambiguously phosphorylated at only one site. We used a genomically recoded *E. coli* method[28] to genetically encode site-specific phosphoserine incorporation during protein production. Three versions of caspase-9 that displayed phosphoserine only at S99, S183 or S195 (phosphoSer99, phosphoSerS183 and phosphoSerS195, respectively) were produced. All phosphocaspase-9 variants, as well as unphosphorylated WT caspase-9, were predominantly in the zymogen form (Figure 2.3A). WT caspase-9 and both phosphoSer99 and phosphoSer195 were able to self- process, while phosphoSer183 remained in its full-length/zymogen form (Figure 2.3A), suggesting that phosphoS183 limits caspase-9 activity. Consistent with the ability to self-process, phosphoS99 and phosphoS195 showed LEHDase activity, whereas phosphoS183 had no measurable activity (Figure 2.3B), clearly demonstrating that phosphorylation at S183 inactivates caspase-9.

Although the phosphocaspase variants are the biologically relevant forms, the yield of phosphoserine-incorporated caspase-9 was extremely low. To obtain sufficient quantities to enable thorough interrogation of the effects of phosphorylation on caspase-9 function and structure, we generated phosphomimetic variants in which glutamate was substituted for phosphoserine. Following expression, S99E was observed in the mature, cleaved form and was catalytically active, with a modest three-fold reduction of activity as compared to the WT (Figure 2.3C, 2.3D).

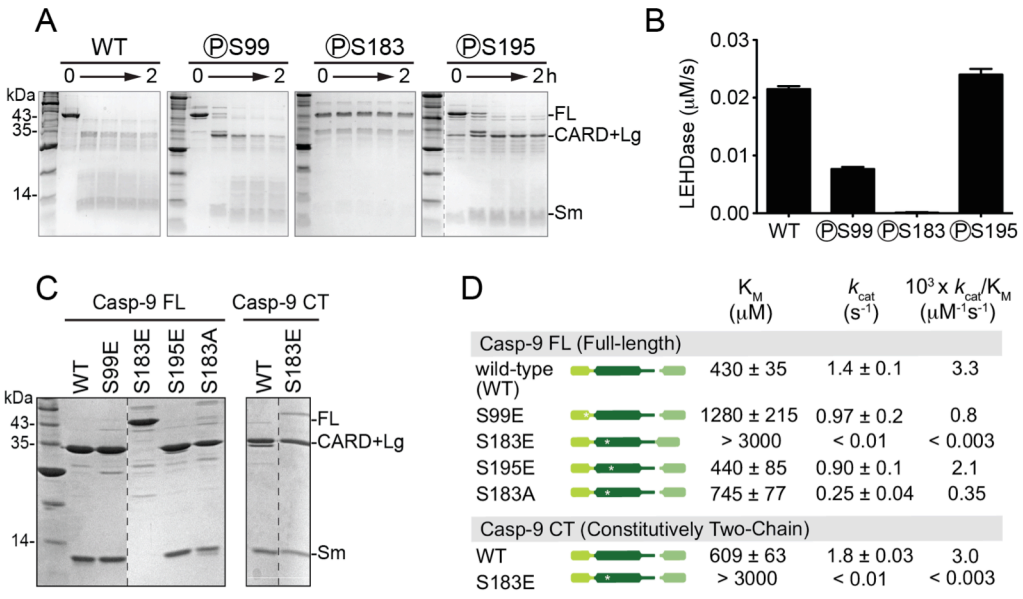

Figure 2.3. Caspase-9 phosphorylated at S183 and phosphomimetic S183E are inactive.
(A) Uncleaved zymogen versions of caspase-9 (WT and phosphocaspase, indicated with Ⓟ preceding the phosphoserine residue) purified from *E. coli* C321.ΔA which allows site-specific incorporation of phosphoserine, were subjected to self-cleavage for 2 h and assessed by Coomassie-stained SDS-PAGE analysis. Only caspase-9 specifically labeled at S183 (phosphoS183) did not self-process, indicating that its activity is inhibited. PhosphoS99 and S195 were able to self-process with kinetics similarly to WT caspase-9.
(B) LEHDase activities of phosphocaspase-9 variants. Activity was measured after 2 h to allow self-cleavage/activation of phosphocaspase-9. PhosphoS183 exhibited no LEHDase activity. Data shown are means (± SEM) of three independent trials on three separate days.
(C) Phosphomimetic S183E was expressed as full-length, uncleaved caspase-9, unlike WT and phosphomimetics S99E and S195E which were expressed in a mature, cleaved state following expression, as assessed by Coomassie-stained SDS-PAGE analysis. The constitutively two-chain (CT) version of caspase-9 is generated from the independent translation of the CARD+Lg and Sm subunits. CT WT and CT S183E are the cleaved forms of caspase-9.
(D) Catalytic parameters for caspase-9 phosphomimetic variants. Only the phosphomimetic S183E has a dramatic effect on caspase-9 activity in both full-length, uncleaved and CT versions. Data shown are means (± SEM) of three independent trials on three separate days.

S195E was also in the mature, cleaved state and had WT-like activity. In contrast, the S183E substitution adversely affected caspase-9 activity. In addition to retaining a zymogen form, it was also catalytically incompetent to turn over substrate (Figure 2.3C, 2.3D). The expression and activity profiles of the phosphomimetics were consistent with what we observed for the phosphocaspase counterparts, indicating that they are robust phosphomimetics.

While cleavage is not an absolute requirement for caspase-9 activation, we sought to test whether the loss of activity of S183E is due to its zymogen nature, or due to the intrinsic changes brought about by the phosphomimetic mutation. S183E expressed from a constitutively two-chain

(CT) construct, in which the CARD+Large region is translated independently from the small subunit, yields the mature, cleaved form (Figure 2.3C). Even in this mature version, CT S183E was still catalytically inactive (Figure 2.3D) with a 5-fold or greater increase in K_M and approximately 100-fold decrease in k_{cat}, suggesting that both substrate binding and catalytic ability are impacted. Overall, S183E shows a 1000-fold less efficient k_{cat}/K_M than WT caspase-9. S183A, which retains similar size and is uncharged like a serine residue, is active, albeit exhibiting a 10-fold lower catalytic efficiency than WT, primarily due to its decreased k_{cat} (Figure 2.3D). The triple alanine mutant S99A/S183A/S195A also shows only a 10-fold decrease in k_{cat}/K_M (Table 2.1). This suggests that phosphorylation or glutamate substitution, which results in a dramatic 1000-fold decrease in activity, is the major cause of inhibition, rather than simply generic sensitivity of the S183 site. These data strongly suggest that phosphorylation of S183 directly impairs substrate binding.

Table 2.1. Catalytic parameters[1] for caspase-9 alanine variants using substrate Ac-LEHD-AFC.

Caspase-9 variant	K_M (μM)	k_{cat} (s^{-1})	10^3 x k_{cat} / K_M ($\mu M^{-1}s^{-1}$)
S99A	768 ± 100	0.64 ± 0.04	0.83
S195A	681 ± 71	1.22 ± 0.05	1.8
S99A/S195A	469 ± 41	1.03 ± 0.03	2.2
S99A/S183A	1203 ± 100	1.16 ± 0.05	0.96
S195A/S183A	1318 ± 107	1.17 ± 0.05	0.89
S99A/S183A/S195A	726 ± 71	0.20 ± 0.01	0.26

[1] Values are mean (± SEM) of three trials done on three separate days.

Phosphorylation at S183 disorients a conserved S1 arginine leading to impaired substrate binding

S183 resides just below Loop 1 (L1) which, together with L3, L4, L2 and L2', form the active site loop bundle. L1 contains the highly conserved and critical R180. R180 plays two important roles. It directly binds substrate P1 residues and it orients R355, the most critical residue for substrate recognition, which makes bidentate interactions with substrate. The proper positioning of R180 is primarily due to an H-bond with the hydroxyl side chain of S183, with another set of H-bonds provided by their amide backbones (Figure 2.4A). These interactions ideally situate R180's guanidinium group to interact with the P1 aspartate in the substrate, keeping it in position for the active site residues to perform catalytic cleavage (Figure 2.4B).

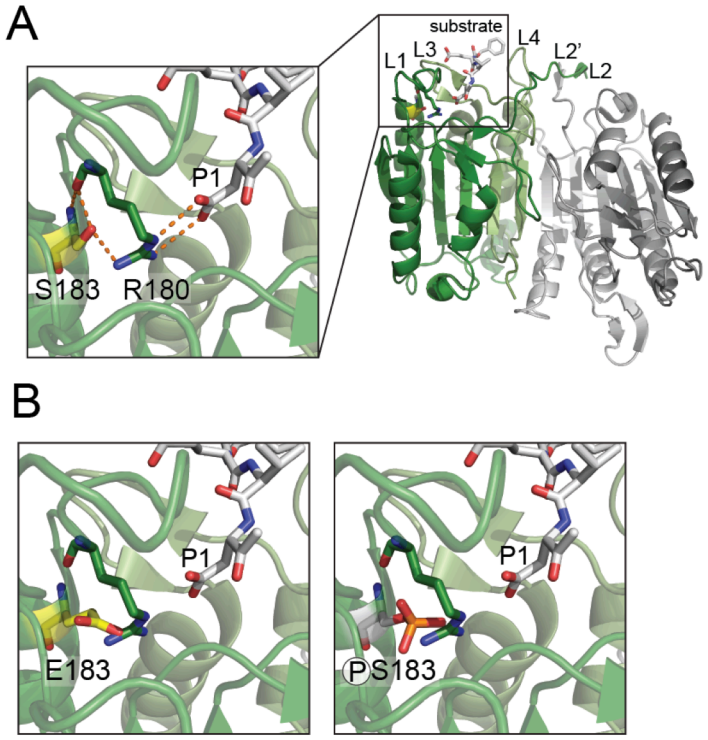

Figure 2.4. Model for caspase-9 inhibition by phosphomimetic S183E and phosphoS183.
(A) Structure of caspase-9 dimer (PDB ID IJXQ) highlighting the substrate-binding groove. Critical interactions between S183 (yellow sticks) and the conserved S1 subsite R180 (green sticks). R180 is an important residue that makes contacts with P1 aspartate in the substrate (light gray sticks).
(B) Models for inhibition of caspase-9 by S183E and phosphorylation at S183. Substitution at S183 by glutamate or phosphoserine are predicted to result in a steric clash with R180, thus disorienting the active site loops

The inability of S183E and phosphoS183 to bind substrate appears to stem from a steric clash between E183 or phosphoS183 and R180 (Figure 2.4B). The additional bulk and extra charge coming from these groups should cause R180 to become displaced from the S1 pocket, consequently disorienting the active site loop bundle, thus making caspase-9 incompetent to bind substrate. This model is consistent with the behavior of S183A which, although incapable of being an H-bond acceptor to R180, provides enough space to allow R180 attain the proper conformation to interact with the substrate, and thus exhibits activity, albeit a decreased one. This mechanism of inhibition of substrate binding is also consistent with the kinetic data for S183E (Figure 2.3D) and phosphoS183 (Figure 2.3B) in which both are completely inactive.

Phosphomimetic S183E impacts recognition by caspase-8

A hallmark of caspases is their involvement in complex cleavage cascades requiring that various caspases recognize and cleave other caspases. Caspase-9's canonical function is to cleave executioner caspases, but it is also cleaved and activated by caspase-8 (at D315) [29,30] and caspase-3 (at D330)[31–33]. We assessed the changes brought about by the phosphomimetic in the ability of other caspases to cleave caspase-9. For these experiments it is important that the intrinsic ability of S183E be understood. Whereas WT caspase-9 fully self-processes immediately, the full-length S183E phosphomimetic was completely devoid of self-processing activity (Figure 2.5A) so any processing can be attributed to caspases other than caspase-9.

S183E, like the full-length catalytically inactive variant C287A, was susceptible to cleavage by caspase-3 (Figure 2.5B, 2.5D) but remained completely inactive even after cleavage (Figure 2.5C), consistent with what was observed for CT S183E which was inactive in its mature form. Although caspase-8 was not as efficient as caspase-3 in cleaving caspase-9, it was striking that S183E remained mostly in its full-length form after incubation with caspase-8, suggesting that S183E transforms caspase-9 into a non-optimal substrate of caspase-8 (Figure 2.5D) and may represent another layer of regulation of caspase-9 by phosphorylation at S183. Phosphorylation of caspase substrates has been reported to alter their susceptibility to caspase cleavage (for

review[10]). This effect, whether promotion or protection against cleavage, is commonly observed when phosphorylation is directly adjacent to the caspase cleavage site. In this case, however, S183 and the cleavage site D315 in the linker are distal in sequence (Figure 2.1A). Thus it is possible that the long linker of caspase-9 (which is not ordered in any crystal structure) has a conformation bringing it in the vicinity of S183 where phosphorylation alters the ability of caspase-8 to cleave and activate caspase-9. Alternatively, S183E could be negatively influencing the interface between caspase-9 and caspase-8, perhaps by exploiting an allosteric mechanism or by disrupting a possible exosite on caspase-9 required for interaction with caspase-8.

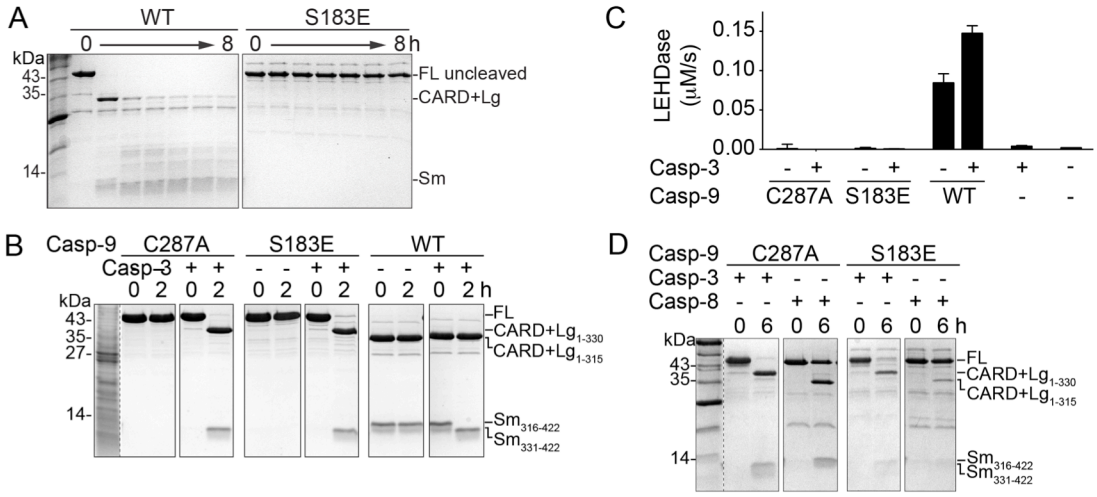

Figure 2.5. S183E impacts recognition by caspase-8.
(A) WT and S183E uncleaved zymogens were incubated for 8 h to allow self processing. S183E shows no self-processing activity as assessed by SDS-PAGE analysis.
(B) S183E is cleaved by caspase-3 at D330. The catalytic-site substituted C287A and S183E phosphomimetic are cleaved in a similar manner by caspase-3 at D330 as assessed by SDS-PAGE analysis. Since C287A and S183E are both catalytically inactive, the cleavage products (CARD+Lg and Sm) result from the activity of caspase-3. In contrast, WT caspase-9 can self-process, resulting in a small subunit spanning residues 316-422 ($Sm_{316-422}$) or can be cleaved by caspase-3, resulting in a small subunit spanning residues 331-422 ($Sm_{331-422}$).
(C) The catalytic-site inactivated variant C287A, the S183E phosphomimetic or WT caspase-9 were incubated for 2 h with caspase-3 to allow processing and then tested in an LEHDase activity assay. S183E does not gain activity even after cleavage by caspase-3. Data shown are means (± SEM) of three independent trials on three separate days.
(D) The catalytic-site inactivated variant C287A or the S183E phosphomimetic were incubated for 6 h with caspase-3 or caspase-8 to observe processing.. Whereas C287A is fully processed by both caspase-3 and caspase-8, S183E is only cleaved by caspase-3. S183E remains almost uncleaved after incubation with active casp-8, suggesting that S183E is a poor substrate for caspase-8.

CT S183E breaks the interaction between the large and small subunits

The catalytic core of a caspase-9 monomer is formed from the regions that become the large and small subunits after cleavage[5,34] (Figure 2.1B). The strong association between caspase large and small subunits is maintained by critical interactions that form and stabilize the core of both monomeric and dimeric caspase-9. In dimeric caspase-9, six β strands from each monomer associate edge-to-edge to form one contiguous 12-stranded β sheet across the dimer interface held together tightly by a series of hydrophobic residues on both the large and small subunits[5]. Although the subunits are expressed independently of each other in the CT version of WT caspase-9, they associate and assemble to form a properly folded protein composed of one small and one large subunit. This tight association between subunits usually manifests through their co-elution on an ion exchange gradient during protein purification, coupled with co-varying band intensities of the subunits visible in a Coomassie-stained denaturing gel. This behavior was observed for CT WT caspase-9, where peak fractions corresponded to the co-elution of the

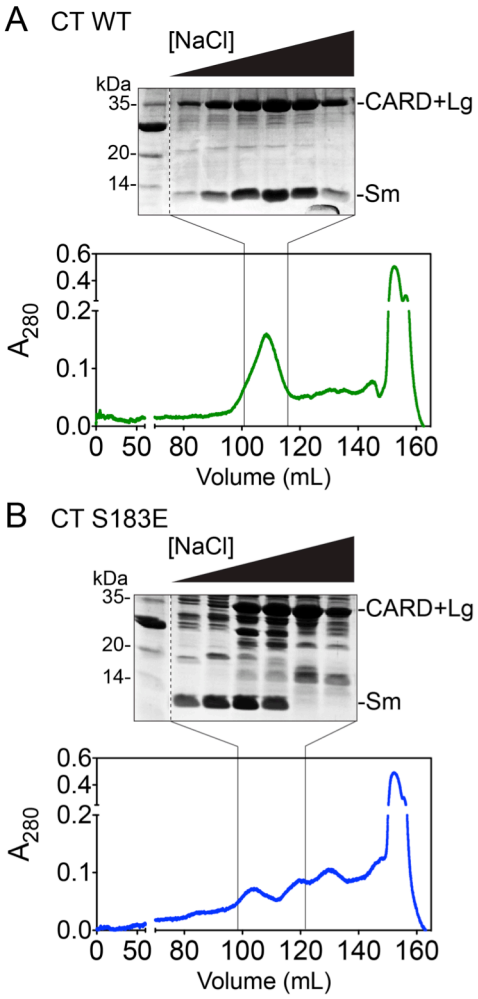

Figure 2.6. S183E breaks interactions within the core of caspase-9.
(A) Anion exchange chromatogram (bottom) and Coomassie-stained gel of peak fractions (top) for CT WT caspase-9. CARD+Lg and Sm subunits co-elute and corresponding band intensities co-vary along the salt gradient during an anion exchange column, suggesting tight interaction of the subunits in the caspase-9 core.
(B) Anion exchange chromatogram (bottom) and Coomassie-stained gel of peak fractions (top) for CT S183E. The independent elution of the Sm subunit from the CARD+Lg indicates dissociation of core subunits of S183E.

CARD+Lg and Sm subunits along a salt gradient and the subunit band intensities on a denaturing gel clearly co-varied (Figure 2.6A). This suggests that CT WT is well-behaved and properly folded, as supported by the data that it has the same catalytic efficiency as the FL WT (Figure 2.4D). In contrast, CT S183E CARD+Lg and Sm subunits eluted separately on an anion exchange column (Figure 2.6B). This separate elution of subunits implies that S183E breaks the interactions between the large and the small subunits, making the protein unstable. We also observed that traditional caspase purification schemes were not suitable to purify CT S183E, as we always obtained impure protein, thus CT S183E was purified from inclusion bodies and refolded (see Methods). In both approaches, purified CT S183E displayed no caspase activity, likely due to loss of or weakening of interactions between the large and small subunits of caspase-9.

Phosphorylation of S183 unfolds and disassembles the caspase-9 core

The fact that S183E decreased the interactions between the large and small subunits suggests that phosphorylation of S183 could have a similar effect. We used caspase-3 to cleave full-length (FL) versions of caspase-9 phosphomimetics to assess the impact of cleavage of a phosphorylated zymogen on stability of the caspase-9 core. Caspase-3 natively cleaves caspase-9 at D330; *in vitro* this occurs efficiently even at very low concentrations (Figure 2.7A). FL C287A and FL S183E showed distinct migration on a native gel (Figure 2.7B) with no significant aggregation nor any additional bands for each protein, suggesting that the protein samples retained their native, properly folded states. Upon cleavage by caspase-3, C287A's mobility only shifted slightly. In striking contrast, cleaved S183E exhibited a dramatic shift in mobility on a native gel (Figure 2.7D). Since protein mobility in native gels depends on the conformation as well as the charged state of a protein, this significantly altered mobility of cleaved S183E implies a shift in conformation to one distinct from a properly folded, cleaved caspase-9.

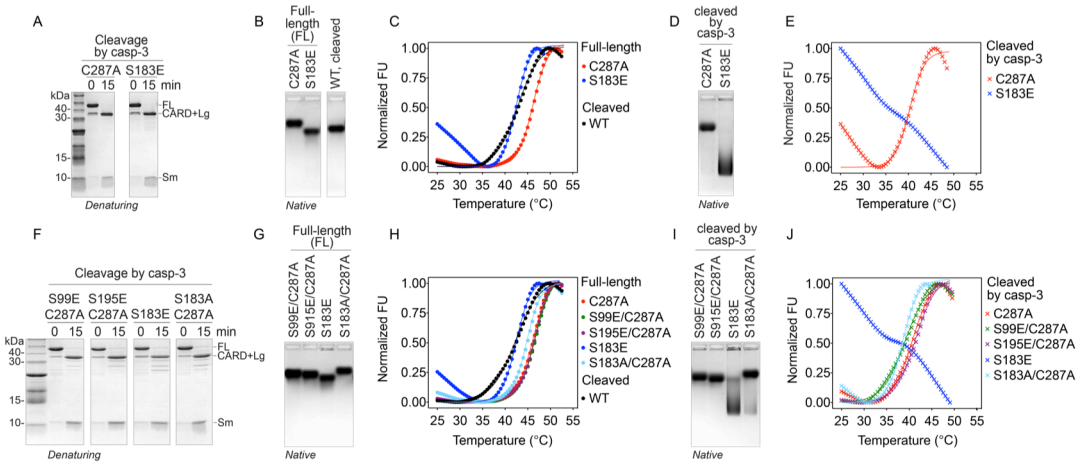

Figure 2.7. S183E is highly destabilized upon cleavage.
(A) Full-length (FL) S183E phosphomimetic and C287A catalytic site-inactivated variant are cleaved by caspase-3 (casp-3) in the same manner and with similar efficiencies as assessed by denaturing Coomassie-stained SDS-PAGE.
(B) FL C287A, FL S183E and cleaved WT caspase-9 showed similar, compact migration along the native (non-denaturing) Coomassie-stained agarose gels, indicative of properly-folded proteins.
(C) Thermal melting curves generated from differential scanning fluorimetry using SYPRO® orange. Both FL C287A and FL S183E showed typical melting transitions. FL S183E's stability is less than that of FL C287A and comparable to that of a cleaved WT caspase-9 (Table 2.2). Data shown are the mean of three independent trials. Fluorescence values were normalized against the lowest and highest values in each data set.
(D) Caspase-3-cleaved S183E exhibits a dramatic shift in mobility on a Coomassie-stained native agarose gel relative to casp-3-cleaved C287A caspase-9.
(E) Thermal melting curves of caspase-3-cleaved C287A and S183E. Caspase-3-cleaved C287A shows a melting transition similar to uncleaved C287A. No melting curve is observed for caspase-3-cleaved S183E. Data shown are means of three independent trials. Fluorescence values were normalized against the lowest and highest values in each data set.
(F) FL phosphomimetic variants and FL S183A were prepared in the background of the C287A mutation to prevent self-cleavage. All caspase-9 variants were cleaved by caspase-3 in the same manner as assessed by denaturing Coomassie-stained SDS-PAGE.
(G) Coomassie-stained native agarose gel of FL phosphomimetic variants and FL S183A. Compact migration on the native gel suggests these caspase-9 variants are properly folded.
(H) Thermal melting curves of full-length phosphomimetic variants and S183A. All variants displayed normal melting transitions. Data shown are means of three independent trials. Fluorescence values were normalized against the lowest and highest values in each data set.
(I) Cleavage by caspase-3 of phosphomimetic variants and S183A did not significantly alter mobilities on a Coomassie-stained native agarose gel. Only caspase-3-cleaved S183E showed a significant shift in mobility, indicating a substantial change in the folded state of the protein.
(J) Thermal melting curves of caspase-3-cleaved phosphomimetic variants and S183A. All variants displayed normal melting transitions, except for casp-3-cleaved S183E. Data shown are means of three independent trials. Fluorescence values were normalized against the lowest and highest values in each data set.

The stability of S183E before and after cleavage was assessed by a thermal shift assay by differential scanning fluorimetry (DSF). Both FL C287A and FL S183E exhibited typical melting curves, indicating that they are properly folded (Figure 2.7C). It is notable, however, that the FL S183E is less stable than FL C287A (Table 2.2). After cleavage by caspase-3, no drastic changes in the melting transitions of C287A were observed, however, cleaved S183E was severely destabilized and no melting transition was observed (Figure 2.7E). The magnitude of the initial fluorescence was also very high, suggesting that cleaved S183E was already in an unfolded or molten globule state at the start of the thermal denaturation.

Table 2.2. Melting temperatures[2] (T_m) obtained from thermal shift assay of caspase-9 full-length and caspase-3-cleaved variants.

Caspase-9 variant	T_m (˚C)	
	Full-length (FL)	Cleaved by caspase-3
C287A	46.2 ± 0.1	40.6 ± 0.5
S183E	42.5 ± 0.2	no fit
S99E/C287A	46.7 ± 0.6	39.0 ± 0.3
S195E/C287A	46.5 ± 0.2	41.4 ± 0.2
S183A/C287A	44.7 ± 0.1	38.6 ± 0.2
WT (cleaved)	42.5 ± 0.3	not done

[2] Values are mean (± SEM) of three trials done on three separate days.

We likewise tested whether the corresponding phosphomimetics of the two other sites (S99 and S195) would impart instability to caspase-9 upon cleavage by caspase-3. We also sampled S183A to discriminate the effect of a stringent (glutamate) from a conservative (alanine) modification on stability. The phosphomimetics and S183A were constructed in the background of C287A to remove the ability to self-process. Caspase-9 S99E/C287A, S195E/C287A and S183A/C287A (Figure 2.7F) all showed properties of properly-folded proteins as demonstrated by their distinct migration on a native gel (Figure 2.7G) and by exhibiting typical protein melting

curves (Figure 2.7H, Table 2.2). Upon cleavage by caspase-3, none of the three variants showed dramatic shifts in either gel mobility (Figure 2.7I) or melting transitions (Figure 2.7J). Strikingly, amongst all the caspase-9 variants, a dramatic mobility shift and unusual melting curve were again only observed for cleaved S183E. Moreover, phosphorylation at S183 by PKA recapitulated what we observed for cleaved S183E. Using S183A and S99A/S195A to direct phosphorylation to S99/S195 or S183, respectively, we found that only when S183 is phosphorylated by PKA is the mobility shift similar to cleaved S183E (Figure 2.8). This demonstrates that phosphorylation at S183 destabilizes the caspase-9 monomer, and subsequent cleavage at the linker causes the core subunits to dissociate, rendering caspase-9 non-functional.

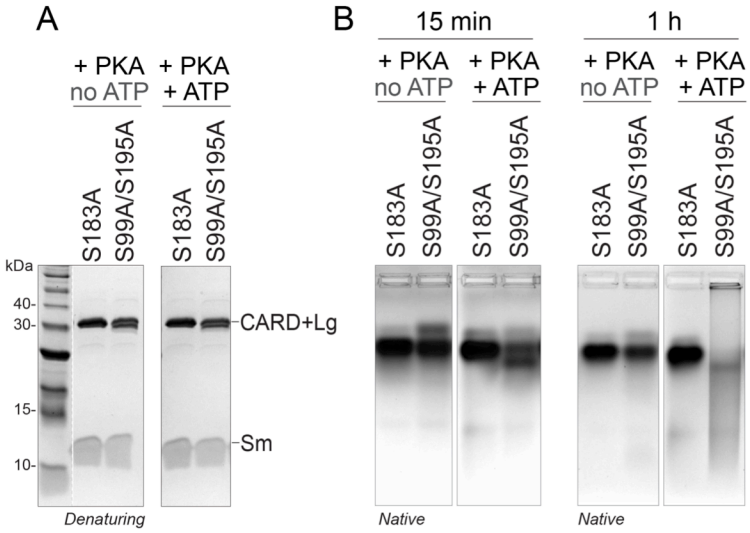

Figure 2.8. Phosphorylation of caspase-9 by PKA at S183 results in destabilization similar to caspase-9 S183E.
(A) Mature, cleaved forms of caspase-9 unphosphorylatable alanine variants were incubated with PKA and ATP to direct phosphorylation specifically at S99 and S195 or at S183. No impact on mobility was observed upon Coomassie-stained denaturing SDS PAGE.
(B) Mobility shifts of unphosphorylated (no ATP) and phosphorylated (+ ATP) S183A or S99A/S195A caspase-9 following non-denaturing native agarose gel electrophoresis after 15 min or 1 h of phosphorylation. After 1 h of phosphorylation, S99A/S195A (conditions promoting S183 phosphorylation) exhibited a drastic shift in migration, similar to what was observed in cleaved S183E, indicating that S183 phosphorylation destabilizes caspase-9 leading to a shift in the conformation.

Caspase-3-cleaved S183E caspase-9 forms ordered aggregates

Destabilized and partially unfolded globular proteins are known to have an increased propensity to aggregate *in vitro*[35]. We reasoned that the unfolded nature of S183E following cleavage could potentially render caspase-9 prone to aggregation. The tendency of cleaved S183E to form aggregates was assessed by monitoring Thioflavin T (ThT) fluorescence *in vitro*. A large increase in ThT fluorescence was observed for cleaved S183E (Figure 2.9A). In contrast, there was little to no increase in fluorescence observed for FL S183E, and cleaved or FL C287A. Cleaved S183E was found exclusively in the insoluble fraction, while most of cleaved C287A remained in the soluble fraction (Figure 2.9B). This magnitude of increase in ThT fluorescence, as well as the rapid kinetics of aggregate formation, strongly indicate that cleaved S183E forms aggregates which assume a regularity in structure, particularly an assembly or stacking of β-sheets, since amorphous or early aggregates are not known to bind ThT[36,37].

The size and morphology of the aggregates were visualized by transmission electron microscopy (TEM). The shape of the aggregates varied from circular to elongated clusters that also ranged in size from 10-40 nm (round) and 40-80 nm (elongated) (Figure 2.9C, Figure 2.10). At 400,000x magnification, the microscope was able to resolve individual units that are approximately 2-5 nm in diameter, which corresponds to the diameter of caspase-9 monomers, which are 2.5 nm in diameter. Moreover, it appears that the aggregates were assembled from proteins arranged adjacent to one another. Although not sufficient to form fibrils, this arrangement appears to confer enough structural regularity to form ordered aggregates that bind ThT.

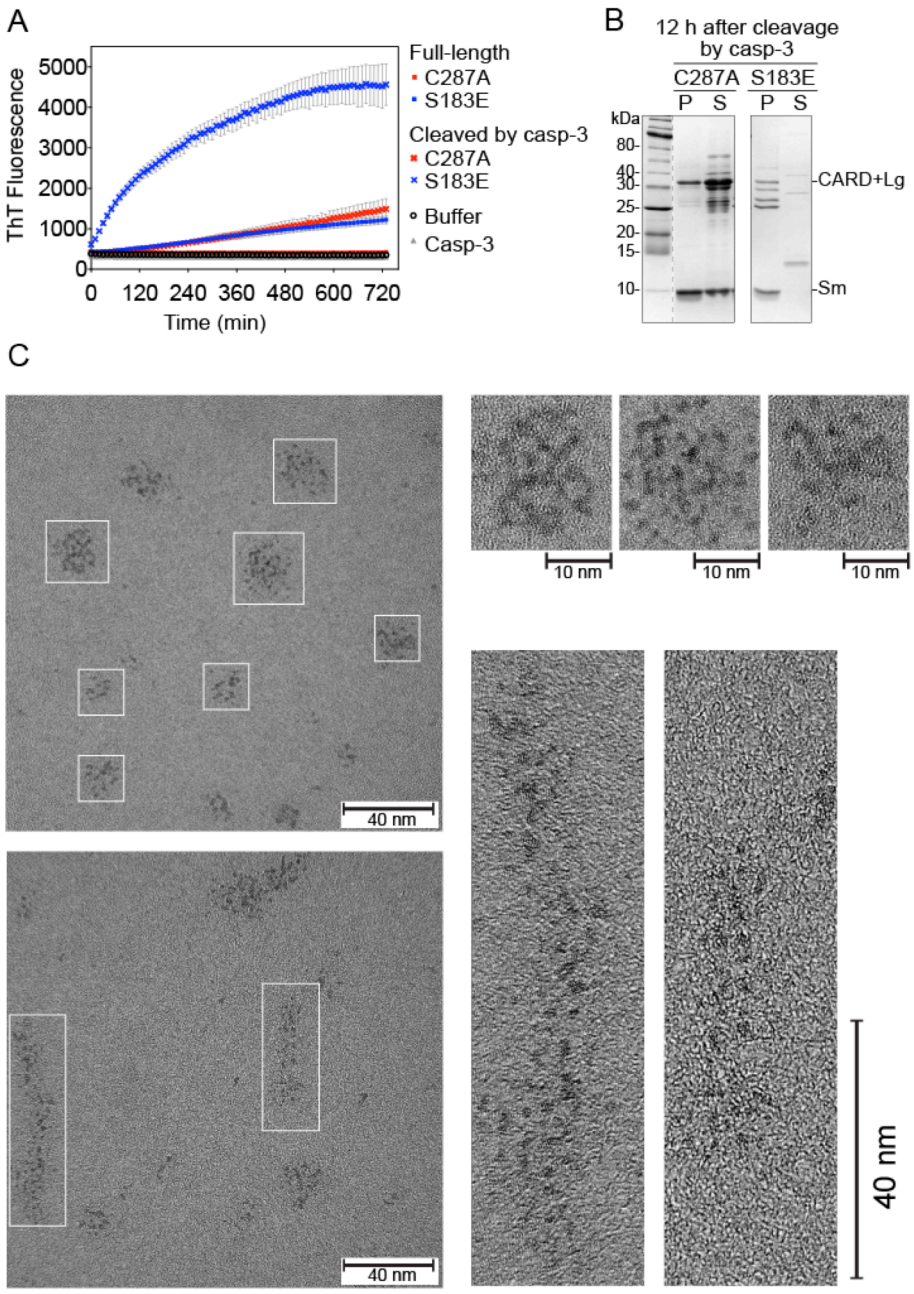

Figure 2.9. Cleaved S183E forms ordered aggregates.
(A) *In situ* ThT fluorescence monitored for 12 h. Only caspase-3-cleaved S183E showed significant increase in ThT fluorescence, suggesting that it forms higher order oligomers or aggregates. Very little increase in ThT fluorescence was observed for FL S183E or cleaved C287A. Data shown are means (± SEM) of three independent trials done on three different days.
(B) SDS-PAGE analysis by Coomassie staining of the pellet (P) and supernatant (S) fractions of FL caspase-9 C287A or S183E after 12 h of cleavage by caspase-3. The caspase-9 CARD+Lg and Sm subunits fractionated mostly into the soluble supernatant for cleaved C287A, while for cleaved S183E, the subunits are found exclusively in the insoluble/ pellet fraction.
(C) TEM images of aggregates of cleaved S183E. Individual units (e.g. caspase-9 monomers) appear to form ordered aggregates (enlarged images). The scale bar is 40 nm wide and 10 nm for selected enlarged images; all images are magnified 400 000x.

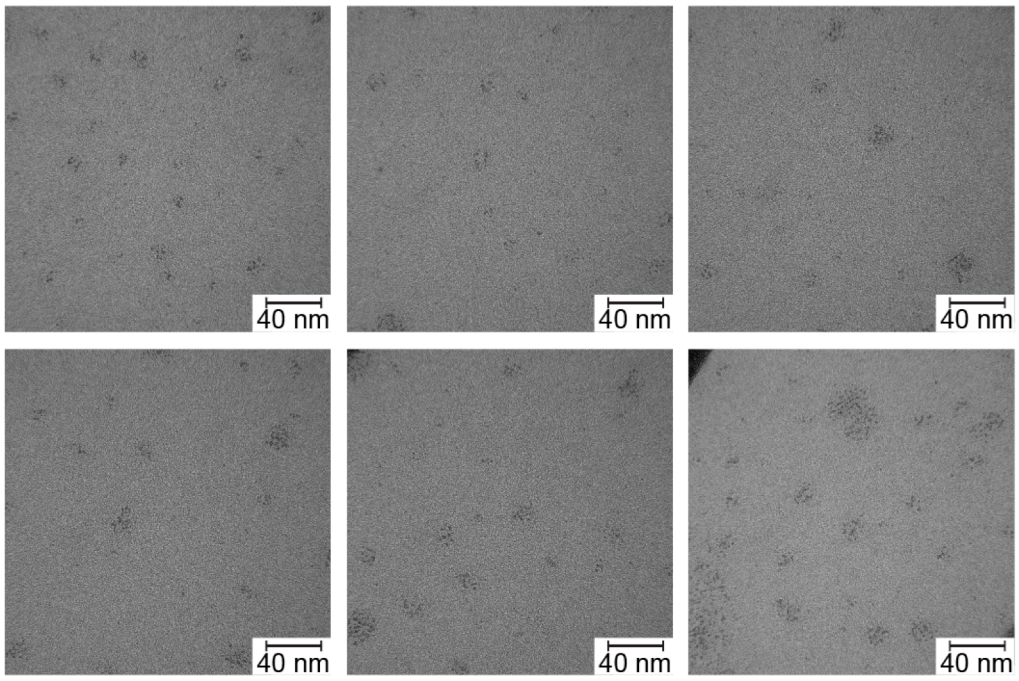

Figure 2.10. TEM images of negatively stained aggregates of cleaved S183E.

Sample TEM images collected from various grids. The scale bar is 40 nm wide; all images are magnified 400,000x.

Cell-Based Studies to Interrogate Phosphorylation of Caspase-9 Intracellularly

Our *in vitro* phosphorylation results clearly demonstrated that phosphorylation of S183 leads to dramatic inhibition of caspase-9 activity. We recognized the importance of showing the biological relevance of S183 phosphorylation. An ideal experiment would be to knock-out endogenous caspase-9 in cells and individually introduce wild-type (WT) caspase-9 and the unphosphorylatable variants S183A, S99A/S195A, and S99A/S183A/S195A. Upon expression, endogenous PKA would be activated by treatment with a cAMP analog or an activator of adenylate cyclase to induce the synthesis of cAMP. The phosphorylation states of each variant can be assessed by immunoblot against phosphoserine after immunopull-down with a caspase-9 antibody. The LEHDase activities of cell lysates can then be measured and correlated to the phosphorylation state of caspase-9.

While it appears that these experiments are straightforward, it is quite important to take note that the caspase-9 variants do not have WT-like activities (Figure 2.3D, Table 2.1). In fact, the activities of S183A and the triple mutant S99A/S183A/S195A is decreased to only ~10% of the WT enzyme. Thus the maximum enzyme activity that can be measured from cells transfected with S183A or the triple mutant will almost be close to background. In addition, the extent of in-cellular phosphorylation must also be taken into consideration, since only a certain fraction of the caspase-9 pool is usually phosphorylated (refer to Chapter IV, Figure 4.13B). These factors must be carefully considered, otherwise interpreting the results will be quite confounding and conclusions derived from those interpretations will be misleading. Nevertheless, we decided to pursue these cell-based experiments to support and strengthen our model that S183 phosphorylation in caspase-9 is functionally and biologically relevant.

Instead of knocking out caspase-9 in cells, we used a caspase-9-deficient cell line, Jurkat JMR. This particular Jurkat clone was resistant to etoposide-induced cell death, which was found to be a consequence of the absence of caspase-9[67,68]. We confirmed from immunoblot using an anti-caspase-9 antibody that JMR does not express any endogenous caspase-9 (Figure 2.11), and was a good cell line to transfect with caspase-9 variants.

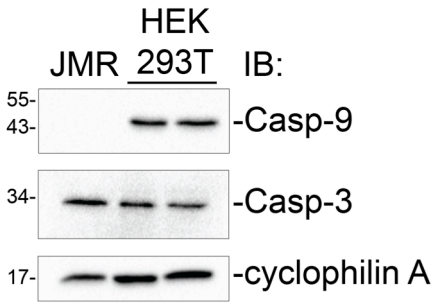

Figure 2.11. Jurkat JMR cells are deficient in casp-9.
Immunoblot of lysates of Jurkat JMR cells show that JMR cells are casp-9- deficient. As controls, HEK293T cells were used to verify the antibody against caspase-9 and caspase-3. Caspase-3 is present in both JMR and HEK293T.

Prior to transfection, it is imperative to ensure that PKA is present and can be activated in JMR. JMR cells were treated either with a common cell-permeable cAMP analog, 8-BrcAMP, or with Forskolin, which is an activator of adenylate cyclase that synthesizes cAMP. In order to check that PKA is specifically activated, cells were pre-treated with a PKA-specific inhibitor, H89[69]. Immunoblot against the catalytic domain of PKA shows that PKA is expressed in JMR (Figure 2.12). More importantly, JMR was

amenable to PKA activation by treatment with Forskolin. Using an antibody that specifically recognizes phosphorylation of PKA substrates with a defined consensus sequence, it was observed that Forskolin strongly induced the phosphorylation of these substrates compared with 8-BrcAMP. Phosphorylation of PKA substrates was diminished when cells were pre-treated with H89, a PKA inhibitor, indicating that phosphorylation was specific PKA activation in JMR cells.

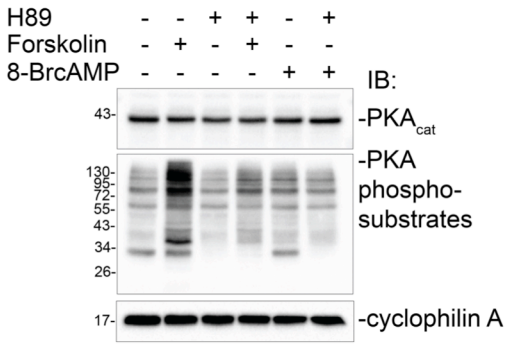

Figure 2.12. PKA is activated by Forskolin and inhibited by H89.
JMR cells were treated with Forskolin (30 µM for 20 min) or 8-BrcAMP (1 mM, 30 min). For PKA inhibition, cells were initially treated with H89 (20 µM, 20 min) prior to Forskolin or 8-BrcAMP treatment.

JMR cells were transfected to transiently express WT caspase-9 and the catalytic site-inactive variant C287A. Low transfection efficiencies were observed (Figure 2.13A), which were not unusual for Jurkat cell lines. However, it appears that the expression of WT caspase-9 was toxic to JMR cells. After 48 h of transfection, cells began to form unusually large clumps and exhibited morphologies of dying cells (Figure 2.13B). This was confirmed by Trypan Blue staining of dead cells. After 48 h, only about 40% of cells in WT-transfected JMR cells were alive (Figure 2.13C). It is then highly likely that transfection of any active variant of caspase-9 into JMR cells would also be toxic. This would be a reasonable outcome, since JMR cells which were previously caspase-9-deficient could be more sensitive to caspase-9 activity especially when overexpressed. While others have managed to introduce WT caspase-9 into JMR cells to generate a stable caspase-9-expressing cell line[68], our efforts were not as successful. Thus, even by scaling-up both transfection and cell culture to have enough material to work with, it would be extremely difficult to interpret whether any change in caspase-9 activity in PKA-active and PKA-inactive cells is due to its phosphorylation, since JMR with WT caspase-9 would have already induced apoptosis prior to PKA activation.

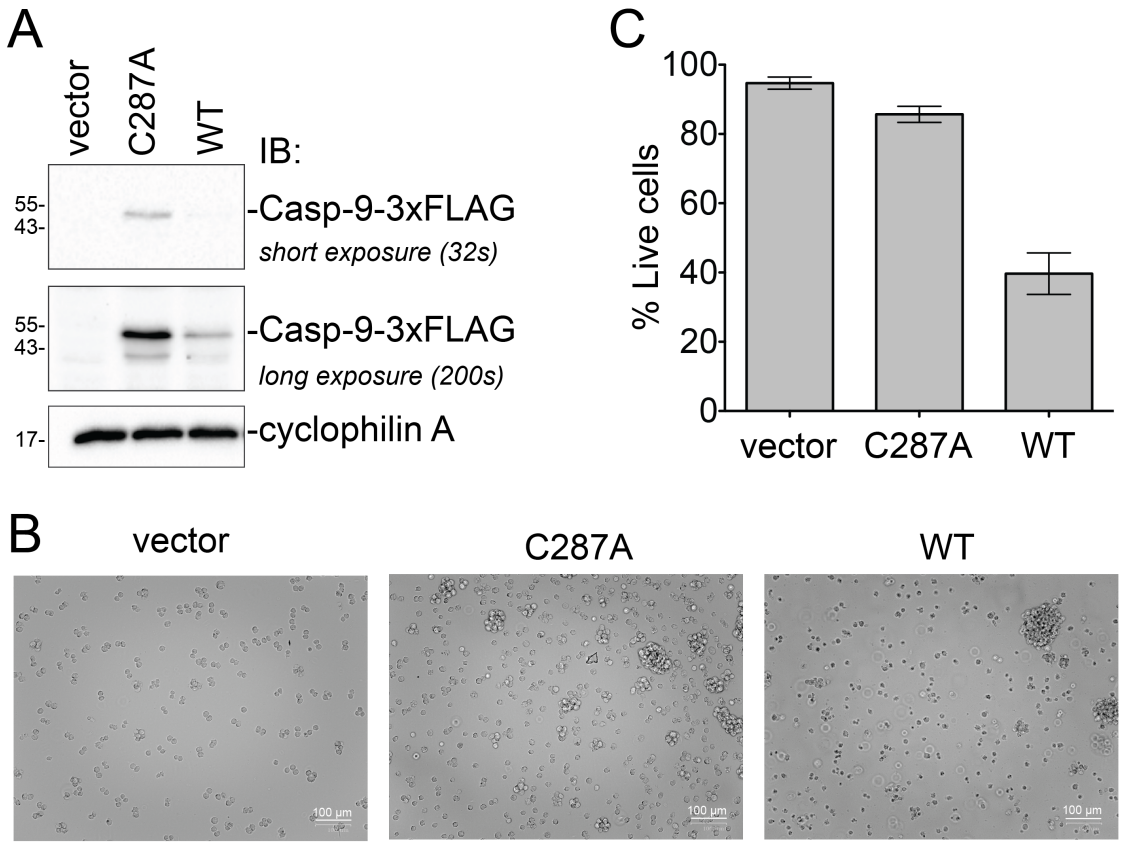

Figure 2.13. Transfection of active, wild-type (WT) caspase-9 leads to cell death in JMR cells.
Jurkat JMR cells were transfected with vector only or 3x-FLAG-tagged caspase-9 variants (catalytic site-inactivated C287A or wild type). 48 h post transfection, cells were counted, washed with PBS, and lysed.
(A) Caspase-9 C287A is moderately expressed in Jurkat JMR, whereas active WT caspase-9 is weakly expressed.
(B) Cell morphology of vector-, C287A- and WT caspase-9-transfected Jurkat JMR. Cells transfected with WT caspase-9 exhibit morphology of unhealthy and dying cells. Cells were visualized using ZOE fluorescent imager (BioRad) in bright-field mode.
(C) Relative amount of live/healthy JMR cells 48h after transfection. % live cells was measured by Trypan Blue staining and counted using the TC20 automated cell counter (BioRad).

These results underscore the challenges in conducting and interpreting caspase functional assays in cells, particularly when one intends to assign a loss-of-function property to a mutation or modification of a specific residue. Besides having necessary controls, it is critical to have prior knowledge of the intrinsic properties, specifically activity, of any caspase variant that will be introduced in the cell.

Discussion

Phosphorylation is recognized as one of the global regulators of caspase function, but the molecular basis of how this modification mediates caspase structure and function, especially of caspase-9, is vastly understudied. Our results demonstrate that phosphorylation of caspase-9 by PKA at S183 is sufficient to directly inactivate caspase-9 activity and hence block the apoptotic cascade. This result agrees well with the data in the report that initially identified the three sites of PKA-mediated phosphorylation[20] however our new data on the kinetic activity of the S183 substitution variants (Table 1) substantially impacts the conclusions made in the earlier work. The prior report[20] measured DEVDase activity in cell extracts that had been depleted of caspase-9, supplemented with either WT caspase-9 or the unphosphorylatable S99A/S183A/S195A variant by *in vitro* translation and finally activated to apoptosis with cytochrome c. We surmise that the prior work was not based on transfection due to the fact that transfection of active caspase-9 is toxic (Figure 2.13), which prevented our exploration of the function of caspase-9 in a whole-cell context. In the *in vitro* translation assays, they found that DEVDase activity in cell extracts supplemented with either WT or the S99A/S183A/S195A variant were sensitive to the presence of PKA, leading to the conclusion that PKA does not directly act on caspase-9[20]. Caspase-9 shows strong LEHDase activity, but very weak DEVDase activity[38]. The major DEVDases activated by cytochrome c addition in HeLa cell extracts are caspase-3 and caspase-7, so the earlier assay[20] measured the downstream activity of caspase-3 and -7 but did not directly assess the activity of caspase-9. The implicit assumption in the experiment was that caspase-3 and -7 are activated by the added WT or S99A/S183A/S195A caspase-9, however the intrinsic activity of S99A/S183A/S195A caspase-9 was not reported. In our work, we have shown that the intrinsic activity of S99A/S183A/S195A (Table 2.1) is decreased to only ~10% of WT caspase-9 activity. Due to the inherent differences in the catalytic activity of WT and S99A/S183A/S195A caspase-9, if caspase-9 had been responsible for activating the measured DEVDase activity, then the activity in the cell extracts supplemented with S99A/S183A/S195A should have been only ~10% of the

WT levels. That was not the case. The S99A/S183A/S195A DEVDase activity in the absence of PKA was 84% of that of WT caspase-9. This strongly suggests that the DEVDase activity was not due solely to activation by caspase-9, but was probably due to activation of caspase-3 and -7 by another factor, likely caspase-8. Thus the interpretation that PKA was not acting directly on caspase-9 is confounded by the assumption that S99A/S183A/S195A is fully active. Our kinetic data on the intrinsic activity of S99A/S183A/S195A allows an updated interpretation of the prior data, which is consistent with direct inactivation of caspase-9 by PKA.

The hierarchical nature of caspase-9 activation allows phosphorylation to exert multiple levels of regulation during the life cycle of caspase-9. It is conceivable that caspase-9 phosphorylated at S183 would still be recruited to the apoptosome since CARD:CARD interactions are not likely disrupted, however this phosphorylated form of caspase-9 is inherently non-activatable. It appears that phosphorylation at S183 should not favor a conformation in either the zymogen or cleaved form that would allow caspase-9 to bind substrate, even if it were docked as part of the apoptosome, the ultimate caspase-9 activating platform. Thus, phosphorylation at S183 acts as a block in the initiation phase of the caspase activation cascade, by rendering caspase-9 incapable of cleaving executioner caspases. S183 resides within the vicinity of the active site. Other caspases such as caspase-6 and caspase-7 are similarly phosphorylated at sites neighboring the active site loops which results in inhibition by preventing these loops to assume an active conformation[23–25]. This mechanism likewise appears to be pertinent to phosphorylation of caspase-9 at S183, thus this orthosteric nature of inhibition emerges as a common theme among phosphorylated caspases.

It is evident from our *in vitro* experiments that the two other sites, S99 and S195 are phosphorylated by PKA, yet the phosphorylated versions and their corresponding phosphomimetics showed little or no influence in any of the caspase-9 activities we interrogated. One possibility is that these are simply "functionally neutral" sites that have persisted through evolution since they do not confer any disadvantage associated with their phosphorylation[21,22].

Another possibility is that their phosphorylation may influence caspase-9 on a different level than directly affecting its catalytic activity. Given that S99 resides within the CARD, phosphorylation may impact either caspase-9's recruitment or its conformational activation in the apoptosome. S195 is highly exposed on the surface of helix α1, and phosphorylation might mediate protein-protein interactions with other caspase-9 substrates. These possible mechanisms warrant further studies to uncover other levels of caspase-9 phosphoregulation.

Crosstalk usually occupies the regulatory landscape involving caspases and cognate kinases (for review[10]). This caspase-kinase interplay is essential in keeping the balance between cell death and survival. Typically, caspases cleave their cognate kinase, either freeing up regulatory elements and relieving the inhibited state, or rendering the kinase inactive (for review[10]). In our *in vitro* phosphorylation assays, we observed no cleavage of PKA by caspase-9. Should there be an interplay in a cellular context, a caspase cleavage site within PKA and homotypic binding motifs present in both enzymes are requisites. However, sequence analysis predicted no caspase-9 cleavage sites in PKA, which could indicate that the interplay is heavily weighted towards that of caspase-9 phosphorylation and its subsequent inhibition. Moreover, the observation that the phosphomimetic S183E greatly attenuates its cleavage by caspase-8 (Figure 4D) suggests that once phosphorylated, caspase-9 could no longer be alternatively activated by the extrinsic pathway. Thus it appears that the impacts of phosphorylation by PKA prevails over several modes of caspase-9 activation. PKA is overexpressed in many cancers (for review[39–41]) and phosphorylation of caspase-9 to prevent its full-scale activation could be one of the mechanisms by which unregulated PKA could promote tumorigenesis, proliferation and transformation.

S183 appears to be a hotspot for inactivation upon phosphorylation, utilizing divergent mechanisms to limit caspase-9 activity. In addition to directly blocking substrate binding, our results have uncovered that S183 phosphorylation breaks the critical interactions within the caspase-9 core causing it to change conformation. This dramatic transition is fascinating since

S183 is not situated at the interface of the large and small subunits, hence this dissociation seems most likely to stem from conformational strains translated from one region to another within the caspase-9 core. We believe this to be the first report of such a mechanism for inactivation by phosphorylation. Moreover, this phosphorylation-induced destabilization appears to affect the mature (cleaved) form of caspase-9 more severely than the zymogen, likely due to covalently-induced proximity.

On one hand, we could view this in the context of caspase-9 activation in the apoptosome where an S183-phosphorylated caspase-9 would remain non-activatable and would likely disengage from the apoptosome because it is no longer structurally and functionally intact after maturation. On the other hand, it is possible that caspase-9 can enter a different pathway that allows it to assume altered conformations that could potentially confer different functions to caspase-9 beyond its known role in activation of executioner caspases. Unfolding mechanisms have been observed to serve as direct regulators of signaling pathways, wherein unfolding facilitates remodeling of the active site or binding interfaces, allow disorder-to-order transitions and vice-versa, or interconvertion between tertiary and quaternary structures (for review[42,43]). Here we observed that unfolded, phosphorylated caspase-9 serves as a precursor to forming ordered aggregates.

Accumulation of unfolded protein is a hallmark of protein aggregation diseases such as Alzheimer's, Huntington's and amyotrophic lateral sclerosis (ALS) (for review[44,45]) and a common feature of toxic aggregation is phosphorylation (for review[46]). Phosphorylation of Tau, amyloid-β and α-synuclein has been associated with accelerated misfolding, aggregation and toxicity[47–49], and while it may be reminiscent of what we observed with the phosphorylation-induced unfolding of caspase-9, to date no disease of such type has been attributed to caspase-9 aggregation. Hence, it seems that evolution has allowed this unfolding and aggregation mechanism of caspase-9 to persist because it does not appear to be deleterious to the cell, potentially due to low caspase-9 titers intracellularly. Whereas amyloid-like aggregates and fibrils

are usually associated with and causative of diseases, functional aggregates have also been identified to be exploited in many species[35,50] to play a number of valuable roles. Cell death and inflammation pathways are known to utilize functional aggregates or higher-order structures to amplify and propagate signals, increase local concentration, facilitate recruitment or even direct subcellular localization[51–57]. Other cell death-related proteins known to assemble into higher-order structures *in vivo* include caspase-1[58], apoptosis-associated speck-like protein containing CARD (ASC)[59], and Bax and Bak[60]. Thus the idea of a caspase-9 functional aggregate in the cell is not unprecedented, and it is worthwhile to note that we observed caspase-9 aggregation under conditions that are close to physiological. Nevertheless, whether these aggregates actually form *in vivo* and what their functional roles are in the cell remain to be explored. One could only speculate that at least for S183-phosphorylated caspase-9, these aggregates may prevent apoptosis, yielding either protective or, more likely, proliferative effects. Regardless, this is the first report of caspase-9 forming higher-order structures in the absence of any other protein or recruitment platform. PKA recognition sites are present in the sequences of other caspases including caspase-3, -6, -7, -8, and -10, although PKA-mediated regulation of these caspases has not been reported. Given the high structural homology among caspases, it is likely that other caspases may also form similar ordered aggregates in response to phosphorylation.

The mechanisms by which phosphorylation modulates protein structure and function are diverse and heterogeneous; each of these mechanisms is tailored and engaged to effectively regulate specific signaling pathways. Phosphoregulation stems from altering protein conformations and modulating protein-protein interactions. Conformational changes range from small or local to those that translate into larger structural rearrangements, resulting in activation or inhibition of a protein. Typical of these phosphorylation-induced perturbations are disorder-to-order transitions and vice versa that have been reported to be common functional and stability switches[61–64]. Phosphorylation also imparts change in specificity, often creating new sites for recognition such as protease cleavage[14], metal/cofactor binding and priming sites during

sequential activation or binding (for review[65,66]). In addition to inducing shifts in conformational states of proteins, phosphorylation greatly influences protein-protein interactions, and is often responsible for transitions between oligomeric states and complexes of proteins. In the case of caspase-9, a unique two-stage mechanism of caspase phosphoregulation is revealed. First, phosphorylation directly blocks substrate binding and inactivates caspase-9. In addition, phosphorylation at a site distal from the small:large subunit interface, dissociates the two constitutively interacting chains, thereby promoting the disassembly of the caspase core leading to inhibition. Whether this unfolding/disassembly mechanism is coupled to the assembly of higher order caspase-9 complex or aggregates in the cell, the nature and structure of these aggregates, and their functional or biological relevance in protection from or causation of disease remain to be examined.

Materials and Methods

DNA constructs and *E. coli* strains

The caspase-9 (C9) full-length wild-type (C9FL) expression construct consists of the full-length, C-terminal His_{6x}-tagged human caspase-9 gene (amino acids 1-416 plus the six terminal Histidines) in pET23b[27] (gift of Guy Salvesen). The caspase-9 constitutively two-chain (C9 CT) expression construct consists of a synthetic gene (Genscript, Piscataway NJ) in pET21b that encodes *E. coli* codon-optimized human caspase-9 that is built for separate expression of the caspase-9 large subunit (amino acids 1- 315) independently from the small subunit (amino acids 316-416 + His_{6x}) which was under the control of a second ribosome binding site. Caspase-9 variants encoding amino acid substitutions were generated using the QuikChange site-directed mutagenesis method (Stratagene/Agilent, Santa Clara CA). The caspase-3 wild type expression construct consists of the full-length, C-terminal His_{6x}-tagged human caspase-3 gene (amino acids 1-279 plus six terminal His) in pET23b[70] (gift of Guy Salvesen). The gene for the catalytic subunit of PKA in pET15b[71] was expressed from a construct supplied by Susan Taylor (Addgene

plasmid # 14921). The SepOTSλ (phosphoserine orthogonal translation system) plasmid, pBAD-GST-AmpR vector, and the fully recoded *E. coli* strain C321.ΔA[28] were gifts from Jesse Rinehart (Yale University).

Expression and Purification of Proteins

Purification of soluble caspase-9 proteins. Caspase-9 variants (except C9 CT S99A/S183A/S195A) were transformed into BL21(DE3) strain of *E. coli*. The cultures were grown in 2xYT media with 100 µg/mL of ampicillin at 37˚C with vigorous shaking until they reached an optical density (OD_{600}) between 1-1.2. The temperature was lowered to 15˚C and protein expression was induced by adding 1 mM of IPTG (Anatrace, Maumee OH). Protein expression was allowed to proceed for 3 h (except for C9 FL WT zymogen which was expressed for only 30 min, C9FL S183A, C9FL S99A/S183A and C9FL S195A/S183A which were expressed for 16 h) and cells were harvested by centrifugation at 4 700 x g for 10 min at 4˚C. Cell pellets were stored at -80˚C, freeze-thawed and lysed in a microfluidizer (Microfluidics, Inc., Westwood MA) in lysis buffer (50 mM sodium phosphate pH 7.0, 300 mM NaCl and 2 mM imidazole). Cell lysates were centrifuged at 30 600 x g for 50 min at 4˚C to remove cellular debris. The supernatant was filtered through 0.45 µm PVDF (EMD Millipore, Billerica MA) filter and loaded unto a 5-mL HiTrap Ni-affinity column (GE Healthcare, Pittsburgh PA). Proteins were eluted using a linear gradient of 2-100 mM imidazole in lysis buffer. Protein fractions were analyzed by SDS PAGE and fractions containing caspase-9 were pooled and diluted 8x with a buffer containing 20 mM Tris pH 8.5 and 5 mM DTT (buffer A) and loaded onto a HiTrap Q-column (GE Healthcare). Proteins were eluted by a linear gradient from 0-275 mM of NaCl in buffer A. Caspase-9 eluted in buffer A at 180 mM NaCl. Peak fractions were analyzed by SDS PAGE for purity and were stored in -80˚C until use.

Purification of caspase-9 from inclusion bodies. Caspase-9 variants C9 CT S99A/S183A/S195A and C9 CT S183E were transformed into BL21(DE3) strain of *E. coli*. The

cultures were grown in 2xYT media with 100 µg/mL of ampicillin at 37˚C with vigorous shaking until they reached OD_{600}=0.8. The temperature was lowered to 30˚C and protein expression was induced by addition of 1 mM IPTG. Protein expression was allowed to proceed for 3 h and cells were harvested by centrifugation at 4 700 x g for 10 min at 4˚C. Cells were freeze-thawed and lysed in a microfluidizer in a buffer containing 10 mM Tris pH 8.0 and 1 mM EDTA. The lysate was centrifuged at 27000 x g for 1h at 4˚C. Inclusion bodies were purified from the pellet by was washing 3x with buffer containing 100 mM Tris pH 8.0, 1 mM EDTA, 500 mM NaCl, 2% Triton-X and 1M urea, centrifuging at 17 000 x g for 15 min between washes. The pellet was then washed 3x with 100 mM Tris pH 8.0 and 1 mM EDTA to remove urea and performing the same centrifugation between washes. The pellet was then resuspended in minimal volume of 6M guanidine chloride with 20 mM β-mercaptoethanol and placed in a rotating platform for 1 hour. The mixture was centrifuged at 20 000 x g for 20 min at 4˚C. Supernatant containing denatured caspase-9 was added dropwise to a refolding buffer containing 100 mM Tris pH 8.0, 10% sucrose, 0.1% CHAPS, 150 mM NaCl and 10 mM β-mercaptoethanol. Refolding was allowed to proceed by dialyzing the solution against 10 mM Tris pH 8.0, 0.1 mM EDTA and 10 mM β-mercaptoethanol. The dialysate was centrifuged at 20 000 x g for 10 min at 4˚C to remove aggregates and the supernatant was filtered through a 0.45 µm PVDF membrane and loaded onto a 5-mL HiTrap Q-column. The column was developed by a linear gradient from 0-250 mM NaCl. Refolded caspase-9 eluted in a buffer containing 20 mM Tris pH 8.0, 200 mM NaCl and 5 mM β-mercaptoethanol. Fractions were analyzed by SDS PAGE for purity and were stored in -80˚C until use.

Purification of caspase-3 protein. The gene for full-length wild-type Caspase-3 in pET23b was transformed into BL21(DE3) *E. coli*. Cultures were grown in 2xYT media with 100 µg/mL Ampicillin at 37˚C with shaking until OD_{600}=0.8. Protein expression was induced by addition of 1 mM IPTG at 30˚C for 3 h and cells were harvested by centrifugation at 4 700 x g for

10 min at 4˚C. Cells were freeze-thawed, lysed in a microfluidizer in a lysis buffer containing 50 mM sodium phosphate pH 8.0, 300 mM NaCl and 2 mM imidazole, and centrifuged at 30 600 x g for 50 min at 4˚C to remove cellular debris. The supernatant was loaded onto a 5-mL HiTrap Ni-affinity column, washed with 50 mM imidazole and proteins were eluted with 250 mM imidazole in lysis buffer. The eluted protein fraction was diluted six-fold with 20 mM Tris pH 8.0 with 2 mM DTT (buffer A) and loaded onto a HiTrap Q-column. Proteins were eluted by a linear gradient from 0-500 mM of NaCl in buffer A. Caspase-3 eluted in buffer A with 250 mM NaCl. Peak fractions were analyzed by SDS PAGE for purity and were stored in -80˚C until use.

Purification of PKA catalytic subunit. PKA in pET15b was transformed into the BL21(DE3) strain of *E. coli*. Cultures were grown in 2xYT media with 100 µg/mL of ampicillin at 37˚C with vigorous shaking until OD_{600}=0.6. Protein expression was induced by addition of 0.5 mM IPTG at 16˚C for 12 hours. Cells were harvested by centrifugation at 4 700 x g for 10 min at 4˚C. PKA was purified as reported[72] with modifications. Cells were resuspended in lysis buffer (50 mM KH_2PO_4 pH 8.0 and 20 mM Tris-HCl), lysed by microfluidizer and centrifuged at 30 600 x g for 45 min at 4˚C to remove cellular debris. The supernatant was loaded onto a 5-mL HiTrap Ni-affinity column and the column was washed with 50 mM imidazole in lysis buffer. Proteins were eluted with 500 mM imidazole in lysis buffer, diluted 6x with a buffer containing 50 mM KH_2PO_4 pH 7.15, 20 mM KCl and 1 mM DTT and loaded onto a 5-mL HiTrap Q-column. The column was developed by a linear gradient from 20-250 mM KCl. PKA eluted in a buffer of 50 mM KH_2PO_4 pH 7.15, 150 mM KCl and 1 mM DTT. Fractions were analyzed by SDS-PAGE to determine purity (Fig. S4) and were stored in -80˚C until further use.

***In vitro* phosphorylation and dephosphorylation of caspase-9**

Autophosphorylation of PKA. PKA was incubated in kinase buffer (50 mM Tris-HCl pH 7.5, 10 mM $MgCl_2$, 0.1 mM EDTA and 0.01% Brij 35) with 250 µM ATP at 30˚C for 30 min.

Phosphorylation of caspase-9. Caspase-9 was added to the autophosphorylated PKA reaction and supplemented with 250 µM [γ-^{32}P]ATP (10 µCi/µL, Perkin Elmer) and incubated for

30 min to 4 h at 32˚C. Reactions were stopped by adding SDS-PAGE loading dye and boiling for 10 min.

Dephosphorylation of caspase-9. Lambda protein phosphatase (NEB) was used to dephosphorylate caspase-9. 100 U of phosphatase were used for every 10 µM of phosphate attached to caspase-9. The reaction was allowed to proceed for 1 h at 30˚C. The reaction was stopped by addition of SDS-PAGE loading dye and boiling for 10 min. Removal of phosphates was confirmed by loss of band intensity in the phosphorimage. Phosphorylation levels were quantified from an ATP standard curve on the same phosphorimage (Figure 2.14). Bands were imaged using Typhoon FLA 7000 (GE Healthcare) and quantified using ImageQuant TL software (GE Healthcare).

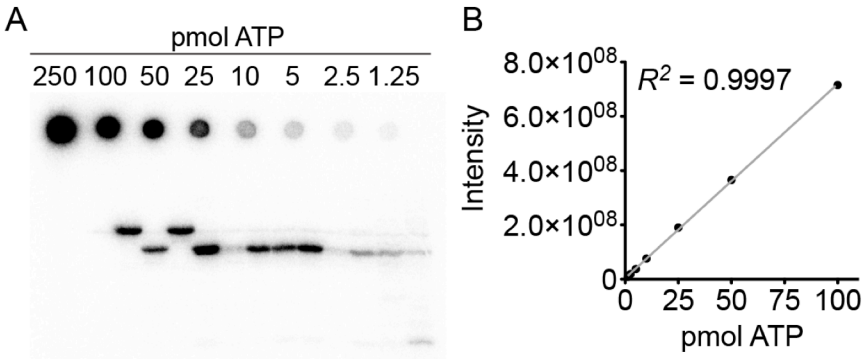

Figure 2.14. ATP standard curve to determine phosphorylation levels.

(A) [γ-^{32}P] ATP standard samples were prepared by serial dilution. 1 µL was spotted and exposed on the same phosphorimage as the phosphorylated caspase-9 samples.

(B) Standard curve constructed from intensities of [γ-^{32}P] ATP standards. Band and spot intensities were quantified using ImageQuant software.

Assay for caspase-9 activity

Caspase-9 was diluted in caspase-9 activity assay buffer (100 mM MES pH 6.5, 10% PEG 8 000, 5 mM DTT) to a final concentration of 800 nM. A substrate titration was performed in the range of 0 - 3 mM fluorogenic substrate Ac-LEHD-AFC (Ex 365/Em 495) (Enzo Life Sciences). Enzyme concentrations were determined by labeling the active-site using a quantitative

inhibitor z-VAD-FMK. The rate of LEHD cleavage was measured with a fluorescence plate reader (SpectraMax M5, Molecular Devices, Sunnyvale CA).

Caspase-9 cleavage assays

Caspase-3 (30 nM) or caspase-8 (300 nM) was diluted in their respective activity buffers (caspase-3: 20 mM HEPES pH 7.5, 150 NaCl 5 mM $CaCl_2$, 10% PEG 400 and 2 mM DTT; caspase-8: 10 mM PIPES pH 7.2, 100 mM NaCl, 1 mM EDTA, 0.05% CHAPS, 10% sucrose and 2 mM DTT). Caspase-9 (3 µM) (catalytic site-inactive variant C287A or FL S183E) was added and the cleavage reactions were incubated at 37˚C for times indicated. For self-cleavage of caspase-9, 3 µM of caspase-9 zymogen (FL uncleaved WT caspase-9) was diluted in caspase-9 minimal activity buffer (100 mM MES, 20% PEG 400 and 5 mM DTT) and incubated at 37˚C at each time point indicated. For cleavage of FL caspase-9 C287A phosphomimetics and FL S183E by caspase-3 for native gel electrophoresis and thermal shift assays, 500 nM of caspase-3 was prepared in 50 mM Tris-Cl pH 7.5, 150 mM NaCl and 2 mM DTT (cleavage buffer). Caspase-9 was then added to a final concentration of 50 µM and cleavage was allowed to proceed for 15 min at 37˚C. Reactions were stopped by adding SDS-PAGE loading dye and boiling for 10 min. Cleavage of the full-length caspase-9 band was analyzed by SDS-PAGE and densitometry using ImageLab™ (BioRad). For cleavage of FL caspase-9 as parallel samples for the ThT fluorescence assay, 75 µM of caspase-9 FL C287A or FL S183E was incubated with caspase-3 (500 nM) in caspase-3 cleavage buffer at 37˚C for 15 min. The cleavage reactions were transferred to a 96-well black plate and further incubated at 30˚C for 12 h, after which the samples were centrifuged at 18 000 x g to pellet the aggregates. The pellet was dissolved in 2% SDS and both the pellet and supernatant fractions were analyzed by SDS PAGE.

Construction, expression and purification of site-specific phosphocaspase-9

C9FL + His_{6x} (1-422) was subcloned into NdeI and HindIII sites of pBAD-GST-AmpR vector to generate the plasmid C9F-pBAD. Codons that code for S99 (TCG), S183 (TCC) and S195 (TCC) were replaced by TAG using a QuikChange mutagenesis approach to generate

phosphocaspase-9 expression plasmids (C9pBAD-SepC9). Site-specific phosphoincorporation was performed as reported by Pirman, et al[28]. Briefly, recoded *E. coli* (r*Ecoli*) C321.ΔA were co-transformed with the C9pBAD-SepC9 and SepOTSλ plasmids. Cultures were grown in LB media supplemented with 2 mM *O*-phospho-*L*-serine (Sigma) pH 7.5, 100 µg/mL Ampicillin and 25 µg/mL Kanamycin at 30˚C with shaking until an OD_{600} = 0.8. The temperature was lowered to 18˚C and protein expression was induced by 0.4% *L*-arabinose (Acros Organics, NJ) and 1 mM IPTG for 20 h. Cells were harvested by centrifugation at 4 700 x g for 10 min at 4˚C. Cells were lysed and caspase-9 proteins were purified as described above, except for the addition of glycerol (5%), phosphatase inhibitors NaF (20 mM) and β-glycerophosphate (2 mM) in all purification buffers, as well as the use of a MonoQ 5/50 GL column (GE Healthcare) for the final ion exchange purification using a gradient of 0-300 mM NaCl. Yields of the phosphoserine-incorporated caspase-9 were extraordinarily low: approximately 0.05-0.10 mg from 12L of expression.

Native agarose gel electrophoresis

Caspase-9 (full-length and caspase-3-cleaved versions of phosphomimetics and alanine variants) (20 µg) was mixed with 2x native gel sample buffer and loaded onto a 0.8% agarose gel (prepared using 25 mM Tris-Cl pH 8.5 and 192 mM glycine). The gel was run for 90 min at 60 V. Protein bands were stained with Coomassie dye, imaged and analyzed using ImageLab™ (BioRad).

Thermal shift assay by differential scanning fluorimetry

The thermal stability of caspase-9 variants in 10 µM in 50 mM Tris-Cl pH 7.5, 150 mM NaCl and 2 mM DTT was analyzed in the presence of SYPRO® Orange (ThermoFisher) (0.5x final concentration) using a CFX Connect Real-Time PCR detection system (BioRad). Measurements were performed in a 96-well plate in 50 µL reactions. The fluorescence intensity

was monitored by increasing the temperature in 0.5˚C increments from 25 to 95˚C. Thermal melting points (T_m) were determined by curve fitting analysis using Prism (GraphPad) software.

***In situ* ThT Fluorescence Assay**

Caspase-9 samples (FL and caspase-3-cleaved C287A and S183E versions of caspase-9) (75 μM) were mixed with Thioflavin T (ThT, Sigma) to a final concentration of 10 μM and incubated at 30°C in black 96-well plates that were sealed to prevent evaporation. The total reaction volume was 100 μL. The ThT fluorescence (Ex 450/Em 485) intensity of each sample was recorded every 10 min using a SpectraMax M5 plate reader over the course of 12 h.

Transmission Electron Microscopy

A 50 μL sample of caspase-3-cleaved S183E (75 μM) was incubated at 30˚C for 12 h in parallel with the ThT fluorescence samples. After 12 h, the sample was centrifuged for 10 min at 18 000 x g and the pellet was washed twice and resuspended in 25 μL nanopure water. A 3 μL sample of a three-fold diluted suspension was embedded on an ultra thin carbon film supported by a lacey carbon film on a 400-mesh copper grid (Ted Pella, Inc.) for 5 min. The grid was blotted to remove excess sample and was washed twice with nanopure water. The grid was then incubated upside-down on a drop of 2% uranyl acetate for 30 s, washed with water to remove excess stain and dried overnight for negative stain EM analysis. A JEOL JEM-2200 FS EFTEM (Energy Filtered Transmission Electron Microscope) operating at 200 kV was used to obtain micrographs at 200 000x to 400 000x magnification (UMass Amherst Electron Microscopy Center). In order to enhance contrast all images were zero-loss filtered using an energy slit width of 20 eV.

Mammalian Cell Culture, Transfection and Preparation of Extracts

Jurkat JMR cells (gift of Douglas Green, St Jude Children's Research Hospital) were grown in RPMI media supplemented with 10% fetal bovine serum, 2 mM glutamine and 1 mM HEPES. Cells were incubated at 37°C in a humidified atmosphere maintained at 5% CO_2. Cells were transiently transfected with either empty vector (p3xFLAG-CMV-14 (Sigma)) or caspase-9

(C9 WT-3xFLAG or C9 C287A-3xFLAG) using the DNA-In Jurkat transfection reagent (MTI-Global Stem) according to manufacturer instructions. A ratio of 5µg DNA : 10 µL reagent per well of a 6-well plate was observed to be optimal. Fresh media was supplemented after 24 h to support cell growth.

After 48 h of expression, transfected cells were washed with 1x PBS and lysed for 20 min with 1x Lysis buffer containing 50 mM Tris pH 7.5, 150 mM NaCl, 1% Triton-X100 and supplemented with 1x Halt™ protease and phosphatase inhibitor cocktail (Thermo Scientific). Lysates were clarified by centrifugation for 30 min at 16,100 x g at 4˚C.

Activation of PKA in Jurkat JMR

JMR cultures grown to ~90% confluency were treated with 30 µM Forskolin (CST) for 20 min, or with 1 mM 8-BrcAMP (8-Bromoadenosine 3',5'-cyclic monophosphate sodium salt) (Sigma) for 30 min. For untreated cells, DMSO was added in place of the compounds. To determine the selective inhibition of endogenous PKA, JMR cells were initially treated with 20 µM H89 (*N*-[2-[[3-(4-Bromophenyl)-2-propenyl]amino]ethyl]-5-isoquinoline-sulfonamide dihydrochloride) (CST) for 20 min prior to Forskolin or 8-BrcAMP treatment.

Immunoblotting

Total lysates were loaded onto a 12 % SDS-PAGE and electroblotted to a PVDF membrane. Lysates were probed with antibodies against the following: caspase-9 (rabbit, Cell Signaling Technologies, CST), caspase-3 (rabbit, CST) and cyclophilin A (rabbit, CST) which served as a loading control. PKA activation was assessed by immunoblot using antibody against PKA (rabbit, CST) and an antibody against phosphorylated forms of PKA substrates with arginine at position -3 (mouse, CST). All primary antibodies were used at 1:1000 dilution. The following HRP-conjugated secondary antibodies (dilution 1:50.000) were used (all from Jackson Immunoresearch): goat anti-mouse IgG and goat anti-rabbit IgG. Bands were were detected by enhanced chemiluminescence and visualized in ChemiDoc XRS+ (BioRad).

Acknowledgments

This work was supported by the National Institutes of Health (GM 080532) to JH. BS was supported in part by the UMass Chemistry-Biology Interface Training Program (National Research Service Award T32 GM 08515 from the National Institutes of Health). We thank the following individuals for their generosity and helpful advice and expertise: Jesse Rinehart (Yale University) for generously providing the *E. coli* strain C321.ΔA, the pBAD-GST-AmpR and SepOTSλ plasmids and for advice and helpful discussions about phosphoprotein synthesis; Alex Ribbe, Director of the UMass Electron Microscopy facility for the collection of EM images; Tyler Marcinko for his assistance with both negative staining of protein samples and ThT assay; Scott Eron for providing caspase-8 proteins as samples for caspase cleavage assays, and Douglas Green (St. Jude Children's Research Hospital) for providing Jurkat JMR cells.

References

1. Srinivasula, S. M. *et al.* A conserved XIAP-interaction motif in caspase-9 and Smac/DIABLO regulates caspase activity and apoptosis. *Nature* **410,** 112–116 (2001).
2. Chęcińska, A., Giaccone, G., Rodriguez, J. A., Kruyt, F. A. E. & Jimenez, C. R. Comparative proteomics analysis of caspase-9-protein complexes in untreated and cytochrome c/dATP stimulated lysates of NSCLC cells. *J. Proteomics* **72,** 575–585 (2009).
3. Seaman, J. E. *et al.* Cacidases: caspases can cleave after aspartate, glutamate and phosphoserine residues. *Cell Death Differ.* (2016). doi:10.1038/cdd.2016.62
4. Pop, C. & Salvesen, G. S. Human caspases: activation, specificity, and regulation. *J. Biol. Chem.* **284,** 21777–81 (2009).
5. Renatus, M., Stennicke, H. R., Scott, F. L., Liddington, R. C. & Salvesen, G. S. Dimer formation drives the activation of the cell death protease caspase-9. *Proc. Natl. Acad. Sci. U. S. A.* **98,** 14250–5 (2001).
6. Shiozaki, E. N. *et al.* Mechanism of XIAP-mediated inhibition of caspase-9. *Mol. Cell* **11,** 519–27 (2003).
7. McIlwain, D. R., Berger, T. & Mak, T. W. Caspase functions in cell death and disease. *Cold Spring Harb. Perspect. Biol.* **5,** 1–27 (2013).
8. Friedlander, R. M. Apoptosis and Caspases in Neurodegenerative Diseases. *N. Engl. J. Med.* **348,** 1365–1375 (2003).

9. Howley, B. & Fearnhead, H. O. Caspases as therapeutic targets. *J. Cell. Mol. Med.* **12,** 1502–1516 (2008).

10. Kurokawa, M. & Kornbluth, S. Caspases and kinases in a death grip. *Cell* **138,** 838–54 (2009).

11. Franklin, R. A. & McCubrey, J. A. Kinases: positive and negative regulators of apoptosis. *Leukemia* **14,** 2019–2034 (2000).

12. López-Otín, C. & Hunter, T. The regulatory crosstalk between kinases and proteases in cancer. *Nat. Rev. Cancer* **10,** 278–92 (2010).

13. Parrish, A. B., Freel, C. D. & Kornbluth, S. Cellular Mechanisms Controlling Caspase Activation and Function. *Cold Spring Harb Perspect Biol* **5,** 1–24 (2013).

14. Dix, M. M. *et al.* Functional interplay between caspase cleavage and phosphorylation sculpts the apoptotic proteome. *Cell* **150,** 426–40 (2012).

15. Allan, L. A. & Clarke, P. R. Apoptosis and autophagy: Regulation of caspase-9 by phosphorylation. *FEBS J.* **276,** 6063–73 (2009).

16. Rossi, A. G. *et al.* Agents That Elevate cAMP Inhibit Human Neutrophil Apoptosis. *Biochem. Biophys. Res. Commun.* **217,** 892–899 (1995).

17. Martin, M. C., Dransfield, I., Haslett, C. & Rossi, A. G. Cyclic AMP regulation of neutrophil apoptosis occurs via a novel protein kinase A-independent signaling pathway. *J. Biol. Chem.* **276,** 45041–50 (2001).

18. Orlov, S. N. *et al.* Activation of cAMP signaling transiently inhibits apoptosis in vascular smooth muscle cells in a site upstream of caspase-3. *Cell Death Differ.* **6,** 661–672 (1999).

19. Insel, P. A., Zhang, L., Murray, F., Yokouchi, H. & Zambon, A. C. Cyclic AMP is both a pro-apoptotic and anti-apoptotic second messenger. *Acta Physiol.* **204,** 277–287 (2012).

20. Martin, M. C. *et al.* Protein kinase A regulates caspase-9 activation by Apaf-1 downstream of cytochrome c. *J. Biol. Chem.* **280,** 15449–55 (2005).

21. Lienhard, G. E. Non-functional phosphorylations? *Trends in Biochemical Sciences* **33,** 351–352 (2008).

22. Landry, C. R., Levy, E. D. & Michnick, S. W. Weak functional constraints on phosphoproteomes. *Trends Genet.* **25,** 193–197 (2009).

23. Velázquez-Delgado, E. M. & Hardy, J. A. Phosphorylation regulates assembly of the caspase-6 substrate-binding groove. *Structure* **20,** 742–51 (2012).

24. Eron, S. J., Raghupathi, K. & Hardy, J. A. Dual Site Phosphorylation of Caspase-7 by PAK2 Blocks Apoptotic Activity by Two Distinct Mechanisms. *Structure* **0,** 1913–1918 (2016).

25. Cao, Q. *et al.* Inhibitory mechanism of caspase-6 phosphorylation revealed by crystal structures, molecular dynamics simulations, and biochemical assays. *J. Biol. Chem.* **287,** 15371–9 (2012).

26. Boatright, K. M. *et al.* A Unified Model for Apical Caspase Activation. *Mol. Cell* **11,** 529–541 (2003).

27. Stennicke, H. R. *et al.* Caspase-9 Can Be Activated without Proteolytic Processing. *J. Biol. Chem.* **9,** 8359–8362 (1999).

28. Pirman, N. L. *et al.* A flexible codon in genomically recoded Escherichia coli permits programmable protein phosphorylation. *Nat. Commun.* **6,** 8130 (2015).

29. McDonnell, M. A., Wang, D., Khan, S. M., Vander Heiden, M. G. & Kelekar, A. Caspase-9 is activated in a cytochrome c-independent manner early during TNF α -induced apoptosis in murine cells. *Cell Death Differ.* **10,** 1005–1015 (2003).

30. Gyrd-Hansen, M. *et al.* Apoptosome-Independent Activation of the Lysosomal Cell Death Pathway by Caspase-9. *Mol. Cell. Biol.* **26,** 7880–7891 (2006).

31. Fujita, E., Egashira, J., Urase, K., Kuida, K. & Momoi, T. Caspase-9 processing by caspase-3 via a feedback amplification loop in vivo. *Cell Death Differ.* **8,** 335–344 (2001).

32. Slee, E. A. *et al.* Ordering the cytochrome c-initiated caspase cascade: Hierarchical activation of caspases-2,-3,-6,-7,-8, and -10 in a caspase-9-dependent manner. *J. Cell Biol.* **144,** 281–292 (1999).

33. Srinivasula, S. M., Ahmad, M., Fernandes-Alnemri, T. & Alnemri, E. S. Autoactivation of Procaspase-9 by Apaf-1-Mediated Oligomerization. *Mol. Cell* **1,** 949–957 (1998).

34. Fuentes-Prior, P. & Salvesen, G. S. The protein structures that shape caspase activity, specificity, activation and inhibition. *Biochem. J.* **384,** 201–32 (2004).

35. Chiti, F. & Dobson, C. M. Protein Misfolding, Functional Amyloid, and Human Disease. *Annu. Rev. Biochem.* **75,** 333–366 (2006).

36. Biancalana, M. & Koide, S. Molecular mechanism of Thioflavin-T binding to amyloid fibrils. *Biochim Biophys Acta* **1804,** 1405–12 (2010).

37. Groenning, M. Binding mode of Thioflavin T and other molecular probes in the context of amyloid fibrils-current status. *J. Chem. Biol.* **3,** 1–18 (2010).

38. McStay, G. P., Salvesen, G. S. & Green, D. R. Overlapping cleavage motif selectivity of caspases: implications for analysis of apoptotic pathways. *Cell Death Differ.* **15,** 322–331 (2008).

39. Caretta, A. & Mucignat-Caretta, C. Protein kinase a in cancer. *Cancers (Basel).* **3,** 913–26 (2011).

40. Sapio, L. *et al.* Targeting protein kinase A in cancer therapy: an update. *EXCLI J.* **13,** 843–55 (2014).

41. Nesterova, M. V. & Cho-Chung, Y. S. in *Apoptosis, Cell Signaling, and Human Diseases* 3–30 (Humana Press, 2006). doi:10.1007/978-1-59745-199-4_1

42. Mitrea, D. M. & Kriwacki, R. W. Regulated unfolding of proteins in signaling. *FEBS Lett.* **587,** 1081–1088 (2013).

43. Schultz, J. E. & Natarajan, J. Regulated unfolding: a basic principle of intraprotein signaling in modular proteins. *Trends Biochem. Sci.* **38,** 538–545 (2013).

44. Ross, C. A. & Poirier, M. A. Protein aggregation and neurodegenerative disease. *Nat. Med.* **10,** S10–S17 (2004).

45. Aguzzi, A. & O'Connor, T. Protein aggregation diseases: pathogenicity and therapeutic perspectives. *Nat. Rev. Drug Discov.* **9,** 237–248 (2010).

46. Tenreiro, S., Eckermann, K. & Outeiro, T. F. Protein phosphorylation in neurodegeneration: friend or foe? *Front. Mol. Neurosci.* **7,** 42 (2014).

47. Kumar, S. & Walter, J. Phosphorylation of amyloid beta peptides- A trigger for formation of toxic aggregates in Alzheimer's disease. *Aging (Albany. NY).* **3,** 803–812 (2011).

48. Sato, H., Kato, T. & Arawaka, S. The role of Ser129 phosphorylation of α-synuclein in neurodegeneration of Parkinson's disease: a review of in vivo models. *Rev. Neurosci.* **24,** 115–123 (2013).

49. Samuel, F. *et al.* Effects of Serine 129 Phosphorylation on α-Synuclein Aggregation, Membrane Association, and Internalization. *J. Biol. Chem.* **291,** 4374–85 (2016).

50. Fowler, D. M., Koulov, A. V, Balch, W. E. & Kelly, J. W. Functional amyloid – from bacteria to humans. doi:10.1016/j.tibs.2007.03.003

51. Lin, S.-C., Lo, Y.-C. & Wu, H. Helical assembly in the MyD88-IRAK4-IRAK2 complex in TLR/IL-1R signalling. *Nature* **465,** 885–90 (2010).

52. Qiao, Q. *et al.* Structural Architecture of the CARMA1/Bcl10/MALT1 Signalosome: Nucleation-Induced Filamentous Assembly. *Mol. Cell* **51,** 766–779 (2013).

53. Siegel, R. M. *et al.* Death-effector filaments: novel cytoplasmic structures that recruit caspases and trigger apoptosis. *J. Cell Biol.* **141,** 1243–53 (1998).

54. Li, J. *et al.* The RIP1/RIP3 Necrosome Forms a Functional Amyloid Signaling Complex Required for Programmed Necrosis. *Cell* **150,** 339–350 (2012).

55. Hou, F. *et al.* MAVS Forms Functional Prion-like Aggregates to Activate and Propagate Antiviral Innate Immune Response. *Cell* **146,** 448–461 (2011).

56. Berson, J. F., Harper, D. C., Tenza, D., Raposo, G. & Marks, M. S. Pmel17 initiates premelanosome morphogenesis within multivesicular bodies. *Mol. Biol. Cell* **12,** 3451–64 (2001).

57. Fowler, D. M. *et al.* Functional Amyloid Formation within Mammalian Tissue. doi:10.1371/journal.pbio.0040006

58. Lu, A. *et al.* Molecular basis of caspase-1 polymerization and its inhibition by a new capping mechanism. *Nat. Struct. Mol. Biol.* **23,** 1–12 (2016).

59. Masumoto, J. *et al.* ASC, a Novel 22-kDa Protein, Aggregates during Apoptosis of Human Promyelocytic Leukemia HL-60 Cells. *J. Biol. Chem.* **274,** 33835–33838 (1999).

60. Westphal, D., Kluck, R. M. & Dewson, G. Building blocks of the apoptotic pore: how Bax and Bak are activated and oligomerize during apoptosis. *Cell Death Differ.* **21,** 196–205 (2014).

61. Metcalfe, E. E., Traaseth, N. J. & Veglia, G. Serine 16 phosphorylation induces an order-to-disorder transition in monomeric phospholamban. *Biochemistry* **44,** 4386–4396 (2005).

62. Bah, A. *et al.* Folding of an intrinsically disordered protein by phosphorylation as a regulatory switch. *Nature* **519,** 106–109 (2014).

63. Garza, A. M. S., Khan, S. H. & Kumar, R. Site-Specific Phosphorylation Induces Functionally Active Conformation in the Intrinsically Disordered N-Terminal Activation Function (AF1) Domain of the Glucocorticoid Receptor. *Mol. Cell. Biol.* **30,** 220–230 (2010).

64. Steinmetz, M. O. *et al.* Phosphorylation disrupts the central helix in Op18/stathmin and suppresses binding to tubulin. *EMBO Rep.* **2,** 505–510 (2001).

65. Cohen, P. The regulation of protein function by multisite phosphorylation – a 25 year update. *Trends Biochem. Sci.* **25,** 596–601 (2000).

66. Salazar, C. & Höfer, T. Multisite protein phosphorylation - from molecular mechanisms to kinetic models. *FEBS J.* **276,** 3177–3198 (2009).

67. Samraj, A. K., Sohn, D., Schulze-Osthoff, K. & Schmitz, I. Loss of caspase-9 reveals its essential role for caspase-2 activation and mitochondrial membrane depolarization. *Mol. Biol. Cell* **18,** 84–93 (2007).

68. Samraj, A. K., Keil, E., Ueffing, N., Schulze-Osthoff, K. & Schmitz, I. Loss of caspase-9 provides genetic evidence for the type I/II concept of CD95-mediated apoptosis. *J. Biol. Chem.* **281,** 29652–9 (2006).

69. Chijiwa, T. *et al.* Inhibition of Forskolin-induced Neurite Outgrowth and Protein Phosphorylation by a Newly Synthesized Selective Inhibitor of Cyclic AMP-dependent Protein Kinase, N-[2-(p-Bromocinnamylamino)ethyl]- 54soquinolinesulfonamide (H-89), of PC12D Pheochromocytoma Cells*. *J. Biol. Chem.* **265,** 5267–5 (1990).

70. Zhou, Q. *et al.* Target Protease Specificity of the Viral Serpin CrmA: ANALYSIS OF FIVE CASPASES. *J. Biol. Chem.* **272,** 7797–7800 (1997).

71. Narayana, N., Cox, S., Shaltiel, S., Taylor, S. S. & Xuong, N. Crystal structure of a polyhistidine-tagged recombinant catalytic subunit of cAMP-dependent protein kinase complexed with the peptide inhibitor PKI(5-24) and adenosine. *Biochemistry* **36,** 4438–48 (1997).

72. Slice, L. W. & Taylor, S. S. Expression of the Catalytic Subunit of CAMP-dependent Protein Kinase in. *J. Biol. Chem.* **264,** 20940–20946 (1989).

73. Yonemoto, W., McGlone, M. L., Grant, B. & Taylor, S. S. Autophosphorylation of the catalytic subunit of cAMP-dependent protein kinase in Escherichia coli. *Protein Eng.* **10,** 915–25 (1997).

CHAPTER III

CASPASE-9 CARD:CORE DOMAIN INTERACTIONS REQUIRE A PROPERLY-FORMED ACTIVE SITE

This chapter appeared in Kristen L. Huber's Ph.D. Dissertation "Regulation of Caspase-9 by Natural and Synthetic Inhibitors" (2012), but has since been revised to include additional data and interpretation of results. The majority of this chapter is under revision: Huber, K.L.*, Serrano, B.P.* and Hardy, J.A. Caspase-9 CARD:Core Domains Interactions Require a Properly-formed Active Site. *Biochem J.* (2018).

*These authors shared equally in this work.

Abstract

Caspase-9 is a critical factor in the initiation of apoptosis, and as a result is tightly regulated by a number of mechanisms. Caspase-9 contains a Caspase Activation and Recruitment Domain (CARD), which enables caspase-9 to form a tight interaction with the apoptosome, a heptameric activating platform. The caspase-9 CARD has been thought to be principally involved in recruitment to the apoptosome, but its roles outside this interaction have yet to be uncovered. In this work we show that the CARD is involved in physical interactions with the catalytic core of caspase-9 in the absence of the apoptosome; this interaction requires a properly formed caspase-9 active site. The active sites of caspases are composed of four extremely mobile loops. When the active-site loops are not properly ordered, the CARD and core domains of caspase-9 do not interact and behave independently, like loosely tethered beads. When the active site loop bundle is properly ordered, the CARD domain interacts with the catalytic core, forming a single folding unit. Together these findings provide mechanistic insight into a new level of caspase-9 regulation.

Introduction

Apoptosis or programmed cell death is a fundamental cellular process that is paramount to cellular regeneration and tissue homeostasis in multicellular organisms. Unlike other cell death pathways, apoptosis efficiently dismantles the cell without adverse effects on neighboring cells or its environment. Its faithful execution is essential in avoiding a number of catastrophic disease states and is also critical in organismal development, hence apoptosis is tightly regulated. Caspases (cysteine aspartate proteases) are special proteases dedicated to properly carry out the apoptotic pathways. Initiator caspases (caspase-2, -8 and -9) function upstream of the apoptotic pathways while executioners (caspase-3, -6 and -7) mediate downstream reactions. Because highly active caspases are lethal, they are synthesized and held as inactive zymogens (procaspases) to avoid untimely activation of apoptosis. Apoptotic pathways are triggered upon receipt of a death signal, either through ligand binding (extrinsic pathway) or mitochondrial assault (intrinsic pathway). Initiator caspases are then recruited to a multi-complex activating scaffold to undergo activation. These active initiators in turn cleave and activate downstream executioners, thereby initiating the series of proteolytic reactions, which ultimately culminates in cell death. Because the caspase activation cascade signals the commitment of the cell to its demise, the activation of these suicidal enzymes is tightly controlled.

Caspase-9 is a critical initiator of the intrinsic pathway, and is responsible for activating downstream executioners caspases -3, -6 and -7. Defects in the intrinsic pathway are characteristic of diseases ranging from autoimmune disorders to cancer. In these diseases, activation of caspase-9 is particularly critical [1–3], however, because of caspase-9's upstream role in the intrinsic pathway, its regulation is quite distinct from that of the executioner caspases. Caspase-9 also has structural and functional characteristics that are distinct from other caspases. Like all caspases, the caspase-9 structure contains the highly homologous catalytic core, composed of the large and the small subunit connected by an intersubunit linker (Figure 1). While cleavage at the linker converts most caspases to their active form, caspase-9 is somewhat active

even prior to cleavage of the intersubunit linker [4]. Caspase-9 is also predominantly monomeric in solution, unlike other caspases, which are constitutively dimeric. In addition, the catalytic core of caspase-9 is preceded by a long prodomain called the Caspase Activation Recruitment Domain (CARD). A six-helix bundle with protein binding motifs, the caspase-9 CARD facilitates protein-protein interaction with the CARD in apoptotic protease activation factor 1 (Apaf-1), anchoring caspase-9 to its activation platform, the apoptosome [5–7]. Caspase-9's interaction with the apoptosome is one of the most significant unique features of this caspase.

The apoptosome platform is formed when an intracellular stress signal leads to release of cytochrome c from the mitochondria. Cytochrome c is then available to bind to Apaf-1, initiating a conformational change resulting in a dATP-dependent Apaf-1 heptamerization into the apoptosome. The apoptosome then recruits and activates caspase-9 (Figure 1.7). The molecular details of caspase-9 activation by the apoptosome have not been fully elucidated, but binding to the apoptosome increases caspase-9's activity by approximately 2000-fold[4]. Intriguingly, even in the absence of the apoptosome, the presence of individual domains influence caspase-9 activity. Caspase-9 is 20% more active when caspase-9's catalytic core remains covalently linked to the CARD domain, as in full-length caspase-9, than when it is proteolytically removed to form the ΔCARD version of caspase-9 [8] (Figure 1). The authors who made this observation suggested that increased tangling of CARD domains leads to an increase in the dimeric fraction of full-length caspase-9 over ΔCARD caspase-9, which accounts for this difference in activity. Addition of the isolated Apaf-1 CARD further enhances caspase-9 activity by five-fold, *in vitro* [8]. The greatest increase in activity, though, occurs when full-length caspase-9, including both the CARD and core domains, binds to the apoptosome through caspase-9 CARD: Apaf-1 CARD interactions.

Early models of the apoptosome activation of caspase-9 argued that the increased activity is due to a change in the oligomeric state of the enzyme via increasing the local concentration of monomeric caspase-9. Recruitment of additional molecules of caspase-9 was hypothesized to participate as partners in dimerization [9] or facilitate dimerization amongst the apoptosome-bound

monomers [10]. This model is supported by the evidence that enhanced activity is associated with dimerized caspase-9 molecules [11]. Alternative views of the activation mechanism invoke induced conformational changes in which the apoptosome binds to the dimerization interface of caspase-9 and stabilizes the active site region leading to a catalytically competent conformation [12]. This conformational change model is supported by the evidence from high-resolution cryoelectron microscopy (cryo-EM) which shows that caspase-9 is potentially monomeric in the highly active state, bound to the apoptosome[9]. Recent near atomic resolution cryo-EM structures of the human apoptosome show that a catalytic core of a caspase-9 monomer is bound to the apoptosome hub, independent of potential caspase-9 dimers undergoing activation [13,14]. Additional studies of caspase-9's activation mechanism have also suggested that cleavage of its intersubunit linker initiates dissociation from the apoptosome thus regulating the time of apoptosome activity [15].

While it is clear that caspase-9 is recruited to the apoptosome through CARD:CARD interactions, it is not clear what prompts the release of caspase-9 from the apoptosome or how the caspase-9 CARD influences caspase-9 function when not bound to the apoptosome. This becomes more relevant with the observation that caspase-9 activation can be achieved without apoptosome formation through different pathways [16–18]. If the caspase-9 CARD were predominantly involved in tethering caspase-9 to the apoptosome, then in the absence of the apoptosome removal of CARD should not decrease activity significantly. On the contrary, a significant decrease in caspase-9 catalytic efficiency is observed when the CARD is removed. This suggests that the CARD plays another role in function and regulation of caspase-9. The most direct hypothesis is that the caspase-9 CARD interacts this the core domain directly, influencing the structure and thus the function of the enzyme. The goal of this work is to probe and uncover the nature of any existing CARD:caspase-9-core interactions.

Results

The Influence of CARD on the Oligomeric State of Caspase-9

The catalytic core of caspase-9 (ΔCARD) has a lower catalytic efficiency than the full-length version of the enzyme, but the fundamental structural and physical basis of these differences are not known. We interrogated the effect of the presence of the CARD on the specific biophysical properties of caspase-9 to understand why the presence of the CARD domain has a synergistic effect on function. To ensure that the caspase-9 ΔCARD and full-length reagents used for this study were comparable to the studies that show CARD's ability to enhance caspase-9 activity, we independently measured the catalytic properties of various caspase-9 constructs. Consistent with previous reports[4,8], the ΔCARD variant of caspase-9 has a decreased catalytic efficiency relative to the full-length version (Table 3.1). Therefore the difference in activity observed between the two caspase-9 variants is most likely due to the presence or absence of the CARD.

Table 3.1. Catalytic parameters[3] for caspase-9 variants using substrate Ac-LEHD-AFC.

Caspase-9 variant	K_M (μM)	k_{cat} (s^{-1})	10^3 x k_{cat} / K_M (s^{-1} μM^{-1})
Caspase-9 Full-length (C9FL)	430 ± 35	1.4 ± 0.1	3.3
Caspase-9 ΔCARD	992 ± 34	0.3 ± 0.002	0.3

[3]Values are mean (± SEM) of three trials done on three separate days.

Caspase-9 is predominantly monomeric in solution, but when subjected to size exclusion chromatography, proteolytic activity correlated with the small fraction of dimeric caspase-9 and not with monomeric caspase-9, suggesting that dimerization is required for caspase-9 activity[8,11]. Thus, one potential reason for the increase in the activity of full-length caspase-9 could be due to an increase in the ratio of dimeric caspase-9 when the CARD is attached, as has been suggested previously[8]. To assess this, full-length and ΔCARD versions of caspase-9 were subjected to size

exclusion chromatography (SEC) to determine the oligomeric state of each enzyme. Both full length and ΔCARD caspase-9 were predominantly monomeric in solution and no oligomeric fraction could be observed in the chromatogram (Figure 3.1). Caspase-9 can be forced into a dimeric state by binding of a covalent active-site inhibitor z-VAD-FMK. The full-length and ΔCARD caspase-9 were both capable of completely converting to their respective dimeric states in the presence z-VAD-FMK (Figure 3.1).

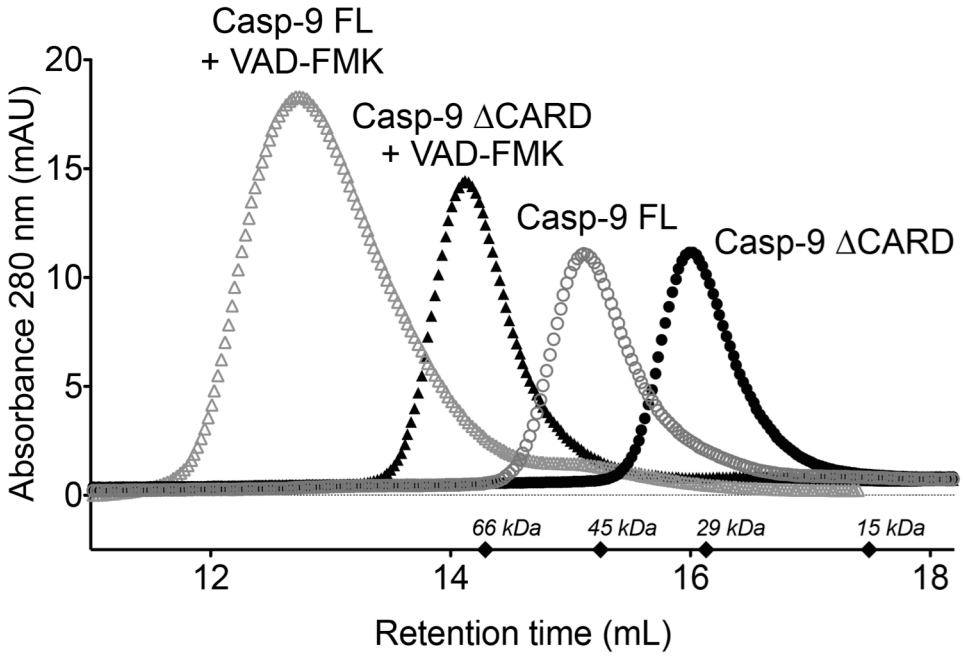

Figure 3.1. CARD does not influence caspase-9 oligomerization.
Size exclusion chromatography of full-length caspase-9 (Casp-9 FL) and caspase-9 ΔCARD (Casp-9 ΔCARD) in the presence and absence of active site ligand z-VAD-FMK. Both Casp-9 FL and Casp-9 ΔCARD are capable of dimerization induced by z-VAD-FMK. The molecular weights for the standards are marked as diamonds.

Table 3.2. Molecular weights of caspase-9 variants from Size Exclusion Chomatography.

Caspase-9 variant	Molecular Weight (kDa)	
	Observed	Expected[4]
Casp-9 ΔCARD	30	29.0
Casp-9 ΔCARD + VAD-FMK	71	58.0
Casp-9 Full-length (FL)	45	47.2
Casp-9 Full-length + VAD-FMK	136	94.4

[4]Expected / Theoretical molecular weights were calculated from the protein sequence of caspase-9 variants using ExPASy ProtParam tool[19].

We observed that the molecular weight of the dimeric full-length caspase-9 was larger than expected (136 kDa vs. 94 kDa expected) (Table 3.2), which could be due to either a significant change in the hydrodynamic radius of dimeric full length caspase-9 or an enhanced interaction with the negatively charged matrix in the column, as we have observed with caspase-6[20]. Nevertheless, these results suggest that the CARD does not appear to have a great influence on the oligomeric state of the enzyme and thus cannot be the cause of the increased activity observed in the presence of the CARD.

The Presence of CARD Influences Stability of Caspase-9

Another potential reason for the increased activity of full-length caspase-9 could be that the presence of the CARD affects the protein's stability. To assess this, both full-length and ΔCARD caspase-9 in monomeric and dimeric forms were analyzed for changes in thermal stability by circular dichroism (CD) spectroscopy. Full-length caspase-9, which was cleaved at the intersubunit linker between the large and small subunits, and included the CARD domain, showed a three-state unfolding curve (Figure 3.2A). The first melting transition occurred at 48 ± 2˚C while a second occurred at 62 ± 2˚C. To determine the domain of the full-length enzyme that unfolds at each melting transition, the catalytic core and CARD domains were expressed independently and interrogated in a similar fashion. The catalytic core of the enzyme (ΔCARD), which was also cleaved at the intersubunit linker, corresponded to the first melting transition at 49 ± 1˚C (Figure 3.2B) while the second transition corresponded to that of CARD only with a melting temperature of 61 ± 2˚C (Figure 3.2C). These results suggest that when caspase-9 is in its cleaved monomeric state, the presence of CARD does not affect the overall thermal stability of the caspase-9 catalytic core and the two domains (CARD and core) of the enzyme unfold independently.

Although caspase-9 exists in equilibrium between monomer and dimer, it is predominantly monomeric in solution (Figure. 3.1). To assess whether the oligomeric state of caspase-9 influences its stability, thermal denaturation studies were similarly performed on the

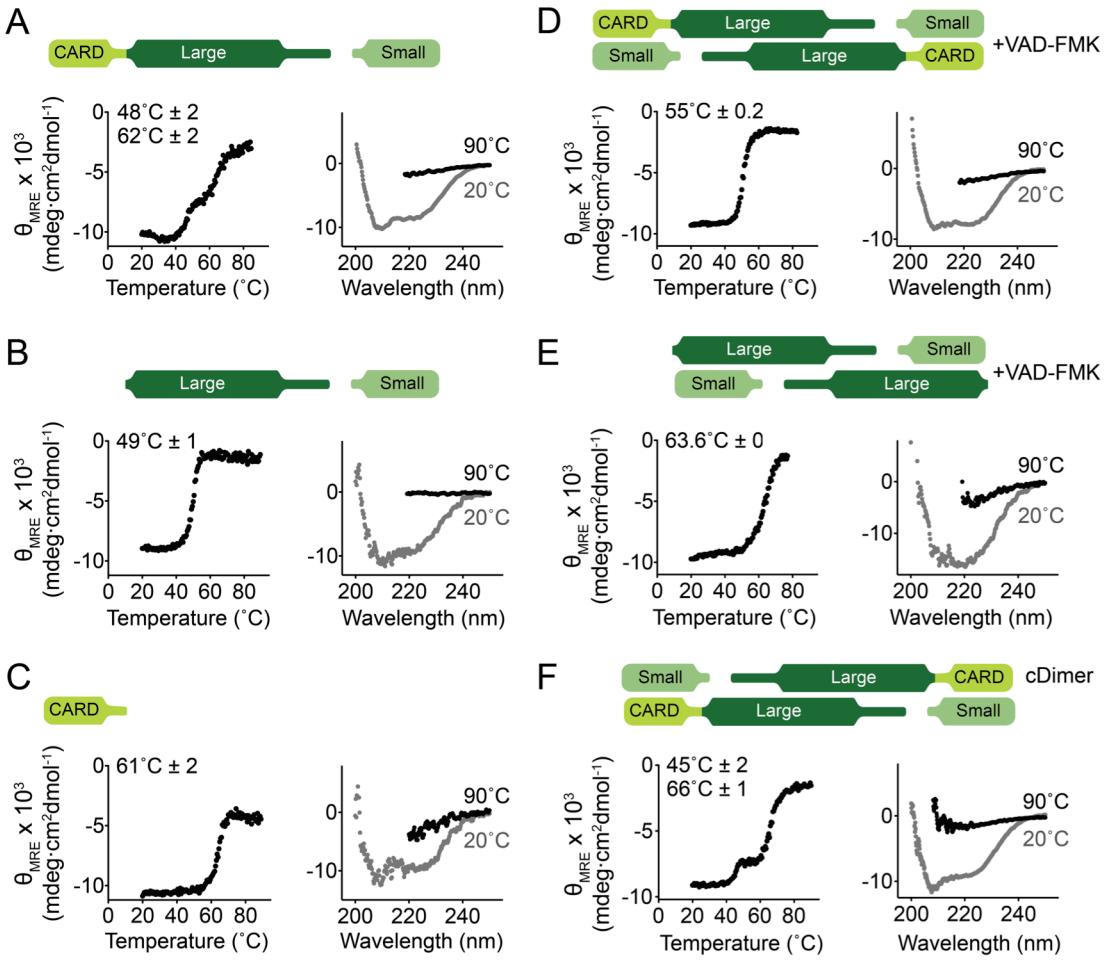

Figure 3.2. Monomeric and dimeric states of caspase-9 have different unfolding properties.
Thermal denaturation profiles (left) and circular dichroism spectra (right) of various forms of caspase-9 (top schematics).
(A) Two melting transitions are observed in the cleaved full-length, monomeric, caspase-9.
(B) and (C) Thermal denaturation profile of caspase-9 core and CARD, respectively, showing that the first melting transition in full-length, monomeric caspase-9 (A) is due to the unfolding of the core, while the second is due to that of the CARD.
(D) Full-length, cleaved caspase-9 is dimeric in the presence of an active site ligand z-VAD-FMK. Upon thermal denaturation, caspase-9 at this state exhibits a single melting transition, likely due either to dimerization, or the presence of an ordered active site, or both.
(E) Dimeric, cleaved caspase-9 ΔCARD with bound z-VAD-FMK is highly stabilized by 14˚C compared to monomeric, cleaved ΔCARD (B).
(F) Constitutive dimer (cDimer) full-length caspase-9 cleaved at the intersubunit linker exhibits two melting transitions, suggesting independent unfolding of CARD and core domains.

cleaved full-length and ΔCARD versions of caspase-9 when the enzyme is in a dimeric state with an active site ligand (z-VAD-FMK) bound (Figures 3.2D and 3.2E). Both versions of caspase-9 showed an increase in thermal stability. Caspase-9 ΔCARD had a 14˚C increase in thermal stability in the presence of active site ligand (Figure 3E), which is similar to the increase in stability observed when caspase-7 binds active site ligand[21]. Full-length caspase-9 (Figure 3.2D) showed only a 6˚C increase in thermal stability in the presence of active site ligand, more similar to the 3˚C increase in stability observed for caspase-6 upon ligand binding[22]. Strikingly, in the presence of substrate, the three-state unfolding (two melting transitions) of the full-length caspase-9 was no longer observed (Figure 3.2A vs. 3.2D). It appears that binding a ligand to the active site of caspase-9, which induces dimerization and ordering of the active site loop bundle, also transitions caspase-9 to a two-state unfolding mechanism (single melting transition). In addition, full-length caspase-9 is completely unfolded at 90˚C as observed in the circular dichroism spectrum (Figure 3.2A, 3.2D). These data suggest that in the cleaved, dimeric and active-site bound state, the catalytic core and the CARD of caspase-9 unfold cooperatively.

To discriminate the influence of substrate-binding from dimerization on the observed cooperative unfolding, thermal denaturation was performed on a caspase-9 variant that exists as a constitutive dimer (cDimer) (Figure 3.2F). This dimeric version of caspase-9[23] was constructed by substituting residues in the dimer interface with those present in caspase-3, which is constitutively dimeric. Full-length, unbound dimeric caspase-9, which was cleaved at the intersubunit linker exhibited three-state unfolding (Figure 3.2F), suggesting that substrate binding was responsible for the observed changes in unfolding properties. Thus, the single melting transition observed when cleaved, full-length caspase-9 in the dimeric, active-site bound state (Figure 3.2D) indicates that substrate binding-induced dimerization either results in the complete unfolding of CARD, or causes the catalytic core and CARD to unfold as one cooperative unit. Comparison of the circular dichroism spectra of the full-length, cleaved caspase-9 in monomeric and dimeric states (Figure 3.3) show that there is no significant change overall in the secondary

structure content. The CARD is composed of six helices[24]; if the CARD became unfolded in the presence of substrate or upon dimerization, we would expect to see a significant loss in the CD signal. Secondary structure content analyses from the CD spectra revealed that there is ~5 % loss in helical content when full-length caspase-9 binds an active site ligand to induce dimerization (Figure 3.3, FL monomer vs FL + VAD-FMK). The similarity in the CD spectra with and without active site ligand suggests that the CARD remains folded and that the caspase-9 catalytic core and CARD must be unfolding as a single cooperative unit. This observation suggests that a physical interaction between the CARD and core domains occurs, which causes the two domains to unfold as a single unit.

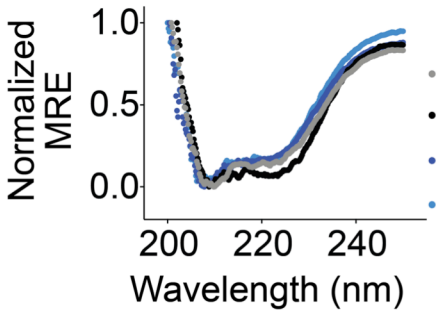

	Estimated helix content	$\frac{\theta_{208}}{\theta_{222}}$
C9 FL monomer	24.4%	1.17
C9 FL + VAD-FMK	23.2%	1.03
C9 FL cDimer	25.9%	1.23
C9 FL cDimer C287A	24.6%	1.15

Figure 3.3. Comparison of CD spectra of caspase-9 full length (C9 FL) in monomeric and dimeric states.
The secondary structure of caspase-9 with (+ VAD-FMK) and without (FL monomer, cDimer and cDimer C287A) an active site ligand bound was assessed by CD. C9 FL cDimer is a constitutive dimer variant of caspase-9. There is no significant change in the helical content of caspase-9 upon dimerization and substrate binding. Estimation of helix content was performed using BeStSel structure prediction and fold recognition software (http://bestsel.elte.hu/index.php)[57].

An Ordered Active Site Supports CARD:Core Interactions

Caspase-9 has been shown to possess catalytic function even as an uncleaved zymogen[4] possibly due to its increased intersubunit linker length. Caspase-9 possesses a longer L2 loop, allowing L2' some flexibility to assume a productive conformation which enables caspase-9 to support a properly formed active site even without linker cleavage[25]. Therefore, the uncleaved/zymogen form of caspase-9 can be utilized to interrogate whether the interaction

observed between the CARD and the catalytic core of caspase-9 is due to changes in the active site conformation. Analysis of the full-length monomeric caspase-9 in the uncleaved state (catalytic site-inactivated variant C287A), resulted in a two-state unfolding mechanism (Figure 3.4A) similar to that observed for the cleaved, dimeric and active site-bound state (Figure 3.2D). The monomeric, uncleaved caspase-9 zymogen appears to support the interaction of the core and CARD domains because they unfold as a single unit. To further test this mechanism, we cleaved the same caspase-9 zymogen construct with caspase-3. Cleavage of the intersubunit linker by caspase-3 disrupted the interaction of the CARD and catalytic core domains as observed by the independent three-state unfolding properties (Figure 3.4B), which is similar to that of the cleaved wild-type monomeric caspase-9. The presence of an intact linker also appears to support CARD:core interactions in constitutively dimeric (cDimer) full-length caspase-9 zymogen (C287A). This version of caspase-9 had a two-state unfolding mechanism (Figure 3.4C), similar to that of a full-length, dimeric caspase-9 with a bound active site ligand (Figure 3.2D). Together, these data suggest that the CARD domain and the catalytic core of caspase-9 do not physically

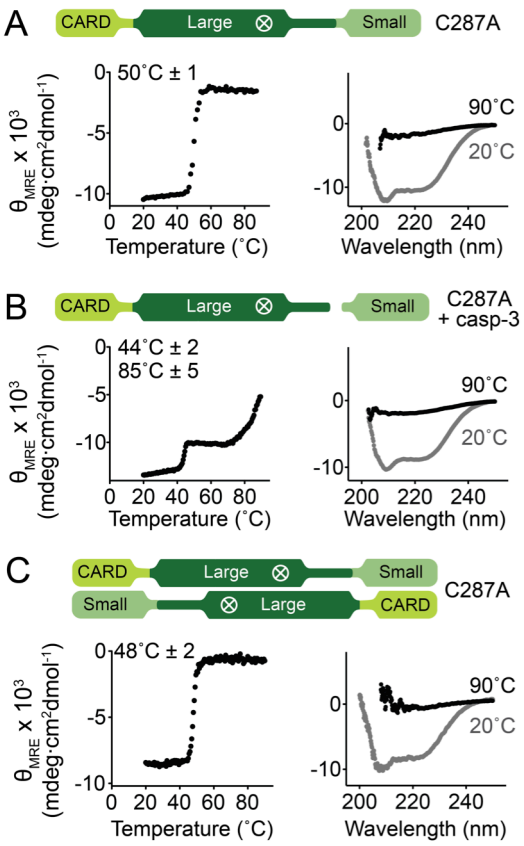

Figure 3.4. The CARD and core of caspase-9 unfold as a single unit when the intersubunit linker is intact.
Thermal denaturation profiles (left) and circular dichroism spectra (right) of various forms of caspase-9.
(A) Monomeric, zymogen (uncleaved) caspase-9 (catalytic site-inactivated C287A) exhibited a single melting transition, which suggests cooperative unfolding of CARD and core of caspase-9.
(B) Cleavage of the linker of (A) by caspase-3 results in independent unfolding, as manifested by two separate melting transitions.
(C) Zymogen (catalytic site-inactivated C287A), uncleaved caspase-9 in a constitutive dimeric state (cDimer) shows a single melting transition.

interact and unfold independently in monomeric or in dimeric caspase-9 that has a disordered active site resulting from cleavage of the intersubunit linker. In contrast, these domains physically interact and unfold cooperatively, as a single unit, when the active site region assumes an ordered conformation as supported by either an intact linker in both monomeric and dimeric states, or by binding of a substrate to the active site.

Characterizing the Site of Interaction Between Caspase-9 Catalytic Core and CARD

The ΔCARD caspase-9 variant is less active than full-length caspase-9 (Table 3.1), suggesting that the presence of the CARD could increase the catalytic activity of the caspase-9 core. Indeed, an increase of caspase-9 activity was observed when CARD was incubated with ΔCARD (Figure 3.5A). This increase in activity was not simply due to molecular crowding since adding BSA in place of CARD did not amount to any significant change in activity. However, this enhancement did not reflect the full activity of full-length caspase-9, suggesting that a covalent tether between CARD and the catalytic core of caspase-9 is necessary for CARD's impact on enzymatic activity. Since the linker between the CARD and core domains is essential to mediate the increase in the activity of caspase-9, we reasoned that perhaps there were either specific interactions with the tether and the adjacent domains or a length-dependence to the interaction. To test this, a five amino acid Ser-Gly

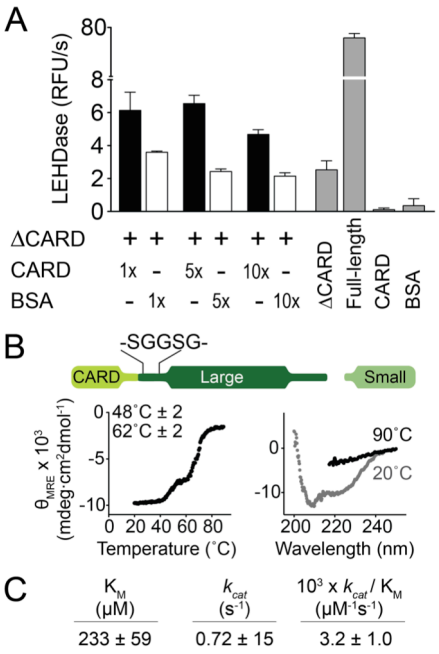

Figure 3.5. Linker between CARD and core supports CARD:core interaction.
(A) *In trans* activity assay of ΔCARD caspase-9 with CARD. The presence of CARD enhances caspase-9 activity, but does not recapitulate the full activity of a full-length caspase-9. Error bars are SD from three independent trials done on three separate days.
(B) Thermal denaturation analysis (left) and CD (right) f Ser-Gly linker extension variant of caspase-9 showing the same melting transitions as that of full-length, cleaved WT caspase-9.
(C) Ser-Gly linker extension variant exhibits the same kinetic behaviors as WT caspase-9.

extension was inserted within the linker between CARD and the large subunit of caspase-9's catalytic core (Figure 3.5B). This variant behaves like the native full-length form of caspase-9 in both thermal stability (Figure 3.5B) and catalytic efficiency (Figure 3.5C), suggesting that a longer and potentially more flexible linker does not negatively impact the function of caspase-9.

The cooperative unfolding observed between the CARD domain and the catalytic core of dimeric caspase-9 implies a physical interaction between the two domains. To characterize this, the interaction between the isolated CARD and catalytic core domains *in trans* was interrogated (Figure 3.5). The catalytic core (ΔCARD) in its monomeric or dimeric form (ΔCARD+VAD-FMK) was incubated with the CARD and analyzed for an interaction between the two domains by native gel electrophoresis (Figure 3.6A). An interaction between the two domains would result in a band migrating with the molecular weight of the full-length enzyme during native gel analysis. However, no visible shift in band migration was observed that would correspond to complex formation between CARD and ΔCARD, which suggests either no interaction between the domains, or very weak and transient interactions, or that the conditions for native gel electrophoresis did not promote CARD:core interactions. Ni-affinity isolation assay was then performed (Figure 3.6B) in which His-tagged ΔCARD in different states (cleaved with VAD-FMK-bound, cleaved with no ligand bound, or uncleaved with no ligand bound (C287A)) was incubated with CARD (no His6x tag). Only ΔCARD with bound VAD-FMK was able to isolate the CARD after elution out of the Ni beads, suggesting complex formation between the catalytic core and the CARD (Figure 3.6B). In addition, fluorescent polarization/anisotropy binding experiments showed that while FITC-labeled CARD also binds to monomeric, cleaved ΔCARD caspase-9, tighter binding was observed with dimeric ΔCARD caspase-9 bound with an active site ligand (+ VAD-FMK) (Figure 3.6C). Together these data are consistent with those observed from thermal denaturation studies, where an ordered active site appears to promote CARD:core interactions.

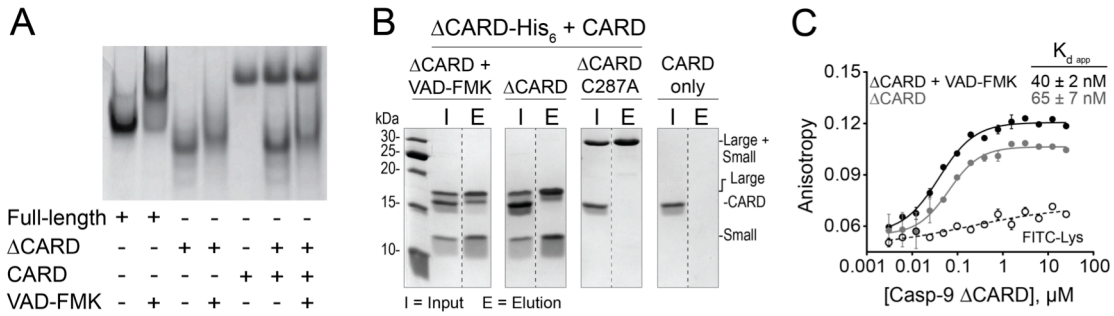

Figure 3.6. Characterizing CARD-core interaction.
(A) Native gel electrophoresis showed no visible obility shift to indicate interaction between CARD and caspase-9 core (unbound/monomeric and z-VAD-FMK-bound/dimeric).
(B) His-tagged, dimeric, VAD-FMK-bound ΔCARD was able to pull down untagged CARD by Ni-NTA affinity assay, suggesting interaction between CARD and catalytic core of caspase-9.
(C) Fluorescence anisotropy shows binding of FITC-labeled CARD to both monomeric and dimeric (+VAD-FMK) ΔCARD. Error bars are SD from three trials done on three separate days.

Given the observation that the CARD and core domain physically interact, we undertook a program designed to uncover sites where substitution of the native amino acids by alternatively charged amino acids might disrupt interactions between the CARD and core domain. To generate candidate sites for interaction and mutations, we performed docking studies between reported crystal structures of the CARD (PDB ID: 3YGS)[24] and the dimeric form of the caspase-9 catalytic core (PDB ID: 1JXQ)[11] using the RosettaDock server[26]. The top docking models were those that avoided interactions of CARD residues involved in the caspase-9 CARD/Apaf-1 CARD complex and avoiding unfavorable (e.g. steric) interactions between caspase-9 CARD and core. Two models fit these criteria (Figure 3.7), both showing putative electrostatic interactions between the CARD and the core. Model 1 predicted the interaction between negatively charged residues in α4 helix of the core with arginines of the H1 helix of CARD (Figure 3.7A). Model 2 predicted homotypic helix to loop interactions: helices α1 and α4 in the core interacting with L1-2 (loop between helix H1 and H2) and a small kink in H4 of the CARD (Figure 3.7B).

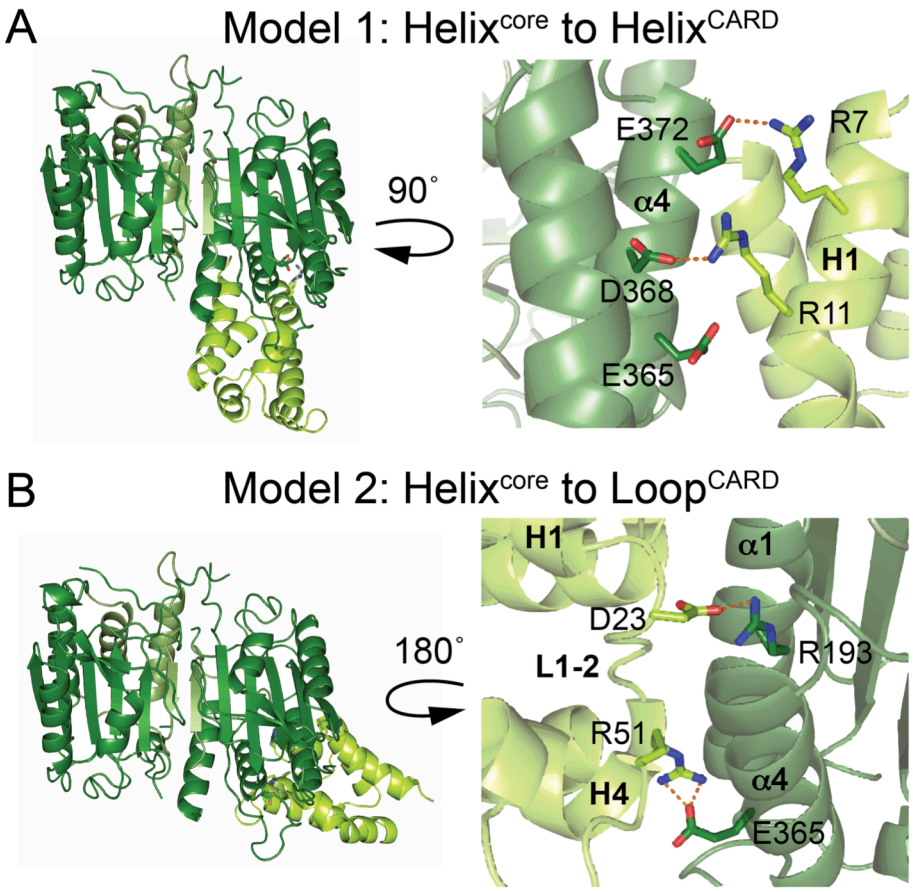

Figure 3.7. Representative docking models of possible sites of CARD-core interactions. Docking analysis between reported crystal structures of the caspase-9 core domain (PDB ID: 1JXQ) and caspase-9 CARD (PDB ID: 3YGS) generated top two models depicting (A) helix to helix and (B) loop to helix interactions of caspase-9 core with the CARD domain. Both models should not interrupt Apaf-1 CARD- caspase-9 CARD interactions and were chosen for substitution studies that may potentially disrupt the CARD-core interactions. Docking studies were performed using the RosettaDock server.

Single and combination charge swapping variations based on the docking models were introduced in the CARD and core in an attempt to disrupt the interaction between the two domains and thus decrease the catalytic efficiency of the caspase-9 variants. We expected that mutations that disrupted the interaction between the CARD and core domain would decrease the catalytic efficiency of the variant versions of caspase-9 and would be comparable to the catalytic activity of ΔCARD (Table 3.1). Upon analysis of the charge swap effects on the catalytic efficiency of caspase-9, a two-fold decrease in catalytic efficiency was observed for variant R7E

(Table 3.3) which would support Model 2, the helix-to-helix binding mode of CARD to the caspase-9 core. A similar effect was observed by the single site variant R11E which further supports a helix-to-helix binding model of CARD and the catalytic core of caspase-9. However the double site variant of R7E/R11E did not show an enhancement of this effect (Table 3.3). This could indicate that R7 and R11E are included in the activating affect of CARD; however, the combination of both these variants is not strong enough to completely eliminate the activation property of CARD, as the catalytic efficiency of the ΔCARD version (Table 3.1) of the enzyme was not recapitulated.

Table 3.3. Catalytic parameters[5] for caspase-9 charge-swap variants.

Caspase-9 variant	Region of Mutation	K_M (μM)	k_{cat} (s^{-1})	10^3 x k_{cat} / K_M ($\mu M^{-1}s^{-1}$)
Wild-type	none	430 ± 35	1.4 ± 0.1	3.3
R7E	CARD (H1)	693 ± 55	0.76 ± 0.2	1.1
R11E	CARD (H1)	477 ± 19	0.73 ± 0.06	1.5
R7E/R11E	CARD (H1)	469 ± 216	0.6 ± 0.2	1.3
D23R	CARD (L1-2)	337 ± 103	0.78 ± 0.2	2.3
R51E	CARD (H4)	197 ± 56	0.85 ± 0.2	4.3
E365R	Core (α4)	429 ± 67	1.2 ± 0.2	2.8

[5]Values are means (± SEM) of three trials done on three separate days.

Phosphomimetic S183E Breaks CARD:core Interactions

The propensity of the CARD:core interactions to exist when caspase-9 is in a conformation with an ordered active site suggests that any modification in caspase-9 that would lead to a disordered active site loop bundle would disrupt these interactions. One particular caspase-9 variant that we have shown to inactivate caspase-9 by that precise mechanism is the phosphomimetic S183E (Chapter II). S183E was observed to have a profound effect on caspase-9 function[27]. S183E prevents substrate binding by displacing a specific arginine residue (R180) in the S1 specificity pocket (Figure 2.4), resulting in the active site loop bundle to become

disoriented. After overexpression S183E remains uncleaved and exhibits no LEHDase activity (Figure 2.3C, 2.3D). Since S183E is in its monomeric and uncleaved form, we expected its stability to be comparable to that of the zymogen, catalytic-site inactivated caspase-9 C287A, and predicted it would exhibit only one melting transition upon thermal denaturation (Figure 3.4A). However, S183E underwent two melting transitions (Figure 3.8A), corresponding to the unfolding of the core (43˚C) and the CARD domain (64˚C). The S183E thermal denaturation profile suggests that the interaction between the CARD and core domain has been disrupted by the S183E substitution, leading the two domains to unfold independently. Importantly, the melting temperature of the core is unchanged from WT caspase-9 suggesting that the core is intact when the S183E variant is in the uncleaved zymogen conformation. The striking observation that the CARD:core interactions were eliminated upon modification of the S183 site,

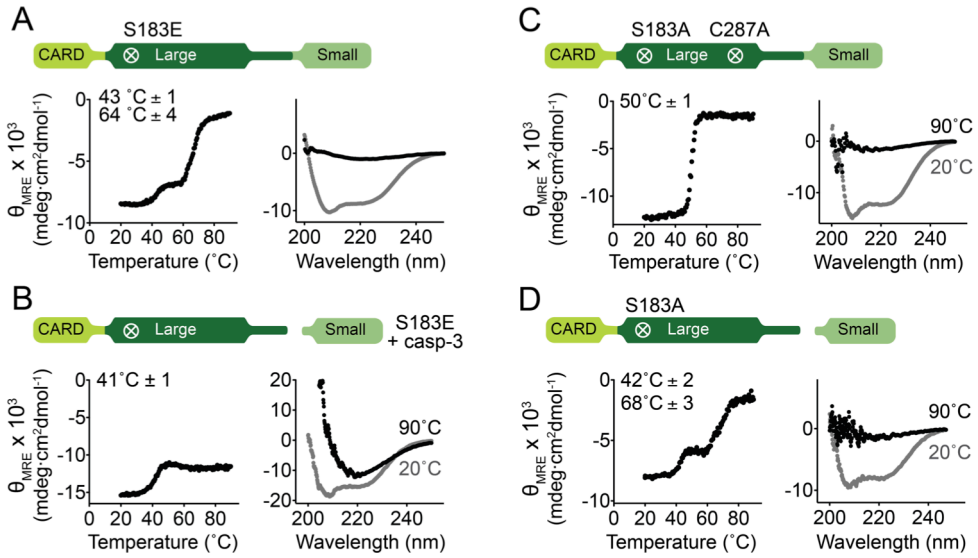

Figure 3.8. Phosphomimetic S183E disrupts CARD:core interactions.
Thermal denaturation curves (left) and CD spectra (right) of caspase-9 S183 substitution variants.
(A) Full-length, monomeric, uncleaved S183E exhibits three-state unfolding (two melting transitions), unlike other full-length uncleaved caspase-9 variants, suggesting that S183E breaks CARD:core interactions because the two domains unfold independently.
(B) Cleavage of S183E by caspase-3 leads to destabilization and formation of aggregates.
(C) Full-length, monomeric, uncleaved S183A (catalytic-site inactivated C287A) shows a single melting transition, indicating an intact CARD:core interaction.
(D) Full-length, monomeric, cleaved S183A behaves similarly to full-length, monomeric, cleaved caspase-9 that exhibits three-state unfolding.

suggests that S183 must sit at the binding interface between the caspase-9 core and its CARD. However, our results from interrogating the effect of S183 phosphorylation on caspase-9 structure (Chapter II) point to a different mechanism in which S183E imparts conformational instability to caspase-9 in the cleaved state. All zymogen/uncleaved caspase-9 variants we interrogated were observed to have similar thermal stabilities, whether by CD (Figure 3.4A, 3.4C, 3.10A, 3.10C) or by DSF (Table 2.2), while S183E was observed to be less stable. This most likely contributes to the unusual three-state unfolding of S183E upon thermal denaturation – its unstable conformation cannot fully support CARD:core interactions. Moreover, cleaving S183E with caspase-3 to generate a fully mature caspase-9 led to its aggregation, which was evident in both its thermal denaturation curve that showed a decrease in thermal stability of the core (41˚C in cleaved S183E vs. 48˚C in WT caspase-9), and CD spectrum at 90˚C (Figure 3.8B), which was typical of an unfolded protein. These results are consistent with our observations that the core of S183E is becomes extremely unstable upon linker cleavage, and ultimately leads to the formation of ordered aggregates (Figure 2.7, 2.9). In addition, the CARD:core interactions appear to remain intact in the alanine variant S183A. Full-length, monomeric S183A showed a single melting transition in its uncleaved state (Figure 3.8C), suggesting cooperative unfolding of domains, and two melting transitions in its cleaved state (Figure 3.8D), indicating independent unfolding of CARD and core domains. Thus, although S183 did not emerge as a critical site of CARD:core interactions, our model of caspase-9 inactivation by S183E by disorienting the active site loops is in agreement with our hypothesis that a properly formed active site is crucial for the interaction between caspase-9 core and its CARD domain.

Phosphorylation has been shown to be a robust mechanism to disrupt binding interfaces[28–30]. Three reported phosphorylation sites - S99[31], T107 and T125[32,33] - reside in the potentially highly flexible region between the CARD and the large subunit (Figure 1.6A, 1.6B). Given that the linker which tethers the CARD to the catalytic core seems to be required for increased catalytic activity (Figure 3.5C), it is conceivable that phosphorylation at this region

could impact interactions between the CARD and core. We examined whether the phosphomimetic versions of these residues would break the CARD:core interactions by conducting the same thermal denaturation studies on both cleaved and zymogen/uncleaved forms. Both S99E and T125E in monomeric, uncleaved form showed cooperative unfolding of domains, exhibiting a single melting transition (Figure 3.9A, 3.9C), suggesting that the interaction between CARD and core is still present and was not interrupted by these mutations. Cleavage at the linker resulted in independent unfolding of the CARD and core domains (Figure 3.9B, 3.9D). These results suggest that S99 and T125 sites are not within the binding interface of the CARD and catalytic core.

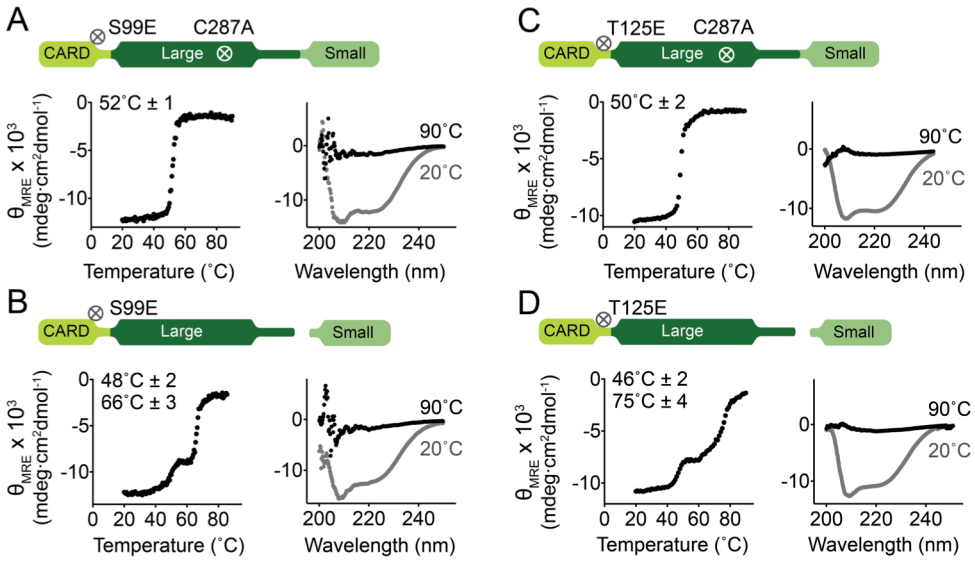

Figure 3.9. Phosphomimetic variants S99E and T125E retain CARD:core interactions.
Thermal denaturation curves (left) and CD spectra (right) of caspase-9 CARD phosphomimetic variants.
(A) and (C) Full-length, monomeric, uncleaved (constructed in the background of C287A) S99E (A) and T125E (C) exhibit two-state unfolding (single melting transition), suggesting intact CARD:core interactions.
(B) and (D) Full-length, monomeric, cleaved S99E and T125E behaves similarly to full-length, monomeric, cleaved caspase-9 that exhibits three-state unfolding.

Discussion

Full control of the caspases involved in apoptosis, inflammation and neurodegeneration requires detailed understanding of the functions and regulatory mechanisms for each individual caspases. Caspase-9 has a particularly unique activation mechanism including changes in its conformational and oligomeric states and association with the apoptosome activation platform. Furthermore, the presence of individual domains such as the caspase-9 CARD (in *cis*) or the Apaf-1 CARD (in *trans*) have the ability to increase caspase-9 basal activity[8]. Altering enzymatic activities by additional domains have been observed in other proteins including PAS (Per-Arnt-Sim) Kinase[34], Dnmt1 DNA methyltransferase[35], and ADAMTS-4 (A disintegrin and metalloproteinase with thrombospondin motifs 4)[36], suggesting that this property may be of widespread significance. Therefore studying the individual activation effects of a particular domain provides further insights towards how caspase-9 becomes activated on the apoptosome.

Here we investigated the mechanism by which the caspase-9 CARD domain influences caspase-9 activity. We have demonstrated that the oligomeric state of both full-length and CARD-deleted (ΔCARD) caspase-9 are similar, thus the increase in caspase-9 activity in the presence of the CARD is not due to a shift the oligomeric state as had been previously suggested[11]. We also observed that the mere presence of CARD is not responsible for the increased enzymatic activity but requires specific interactions between the CARD and core domain, particularly with the active site. We have observed that caspase-9 CARD:core interaction is controlled by the folded state of the active site (Figure 3.11). Specifically, the CARD and catalytic core domains of caspase-9 unfold independently and do not physically interact in either monomeric or dimeric states of the cleaved enzyme because the active site is unable to form a properly ordered substrate-binding groove and is therefore unable to support the interactions between the CARD and caspase-9 core. In the dimeric state with a ligand bound to the active site, these domains unfold cooperatively, as a single folding unit, indicating a physical interaction

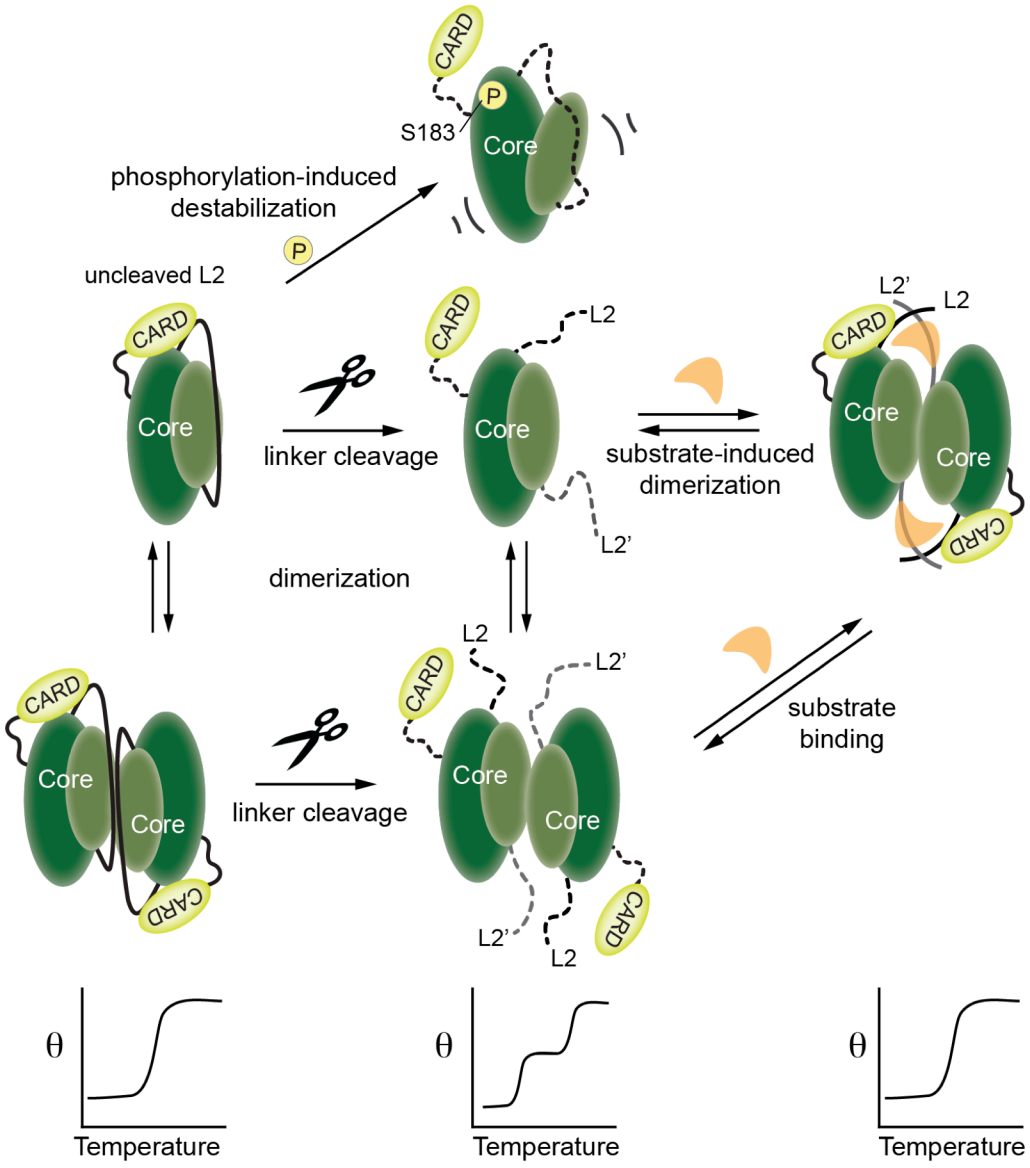

Figure 3.10. Model for caspase-9 conformational states in the presence of CARD domain. Relevant conformations of caspase-9 are shown as cartoons in the upper panels. Caspase-9 in both its uncleaved, monomeric state and cleaved, dimeric state assumes a conformation wherein an ordered active site supports the interaction of CARD with the core of the protein, allowing cooperative unfolding of the two domains as depicted in the lower panels. The enzyme assumes a different conformation when this interaction is abolished either by transitioning to a cleaved monomeric or cleaved dimeric states where the active site is disordered, or by introducing a mutation in the core (as in S183E) that leads to its destabilization and disorder of active site loops.

between the CARD and core domain when the cleaved enzyme dimerizes and has a properly ordered active site that is capable of binding CARD.

The substrate-binding groove is ordered in dimeric, cleaved caspases (-1, -3, -6, -7, -8 and -9) with a bound substrate. Notably a similar ordered conformation can be formed in uncleaved zymogen of caspase-9, due to linkage effects which allow the intersubunit linker to buttress the L3 and L4 loops in an ordered conformation[11,37] (Figure 3.10). This manifests in the cooperative unfolding of CARD and the catalytic core of caspase-9 observed in the zymogen/uncleaved form of full-length caspase-9, whether monomeric or dimeric, when the intact intersubunit linker can properly order the active site even prior to cleavage. Intriguingly, this CARD-core domain interaction is disrupted either by cleavage of the intersubunit linker by self-processing or by caspase-3, or by a mutation in the core such as S183E, all of which prevent the active site from assuming an ordered conformation. Thus, the CARD appears to be interacting with the caspase-9 core in any version of caspase-9 presenting a properly formed substrate-binding groove.

Our attempt to pinpoint the binding interface between the CARD and catalytic core of caspase-9 showed that single charge swap mutations on the surface of the protein distal from the active site were not strong enough or properly positioned to disrupt the activating affect of CARD. A more extensive alanine scanning mutagenesis study or charge repulsion analysis around the substrate-binding groove could further define the region of interaction between the CARD and core domains mediated by the active-site region of the enzyme. Once the binding interface is defined, its role in the caspase-9 activation cascade can be further interrogated, and may serve as a potential junction to control caspase-9's intrinsic activity.

The primary role of the CARD is to facilitate recruitment and subsequent activation of caspase-9 in the apoptosome. Prior to our work there has been no data to suggest that there are existing interactions between the CARD and the catalytic core of caspase-9. The role of these interactions in the context of the caspase-9 activation via the apoptosome remains to be explored,

but seems to be consistent with the induced conformational changes model[12], wherein binding to the apoptosome stabilizes the active site region leading to its activation. Recent cryo-EM structures of caspase-9-bound apoptosome show that a catalytic core of caspase-9 is bound to the apoptosome hub[14,38], and mechanistic studies have also shown that the catalytic core is able to interact with the nucleotide binding domain of Apaf-1 in the apoptosome[39]. Our results complement these observations in the sense that there are regions in the catalytic core that engage in stabilizing interactions with other proteins (in this case, the caspase-9 CARD), possibly influencing capase-9 activity. Given our observations that CARD:core interactions influence caspase-9 stability, it is possible that these interactions exist to stabilize caspase-9 prior to its recruitment to the apoptosome. One can envision caspase-9 utilizing the same binding interface in the CARD to interact with the catalytic core in the zymogen state when it is free from the apoptosome. Once the apoptosome is formed, the caspase-9 CARD:core interaction gives way to caspase-9 CARD:Apaf-1 CARD binding, allowing caspase-9 to be finally recruited and activated in the apoptosome. Moreover, in light of observations that caspase-9 is activated independent of the apoptosome to facilitate alternative pathways (both apoptotic and non-apoptotic)[17,18,40], the presence of CARD:core interactions could also serve as a mechanism to retain, modulate or even enhance caspase-9 activity as it functions outside the apoptosome. Other human caspases (caspase-1, -2, -4/-5, -12) also possess a CARD (review[41]). Among these caspases, caspase-2 is most similar to caspase-9. It would be interesting to examine whether caspase-2 CARD is also able to form these interactions with the catalytic core, which would suggest natural prevalence of these interdomain interactions in caspases and not limited to caspase-9. This could also be a relevant theme in caspase-2 activation. Although caspase-2 has been shown to be activated via proximity-induced oligomerization via the PIDDosome[42], genetic experiments have challenged this mode of activation, since caspase-2 was observed to be activated in the absence of this activating scaffold[43,44]. Alternative modes of caspase-2 activation have since been proposed depending on the type of cellular death signals (review[45]); in these cases it is tempting to

speculate that CARD:core interactions may play a role in regulating caspase-2 function, should they be present. Interdomain interactions have been demonstrated to be critical in controlling the different conformational states and in regulating the catalytic activity of several proteins including the deubiquitinating enzyme USP4[46], phenylalanine hydroxylase[47] and ERAP-1 (endoplasmic reticulum aminopeptidase-1)[48].

Prior works on other caspases have suggested that regulation may be dependent on the most unique regions within the caspase structure, the prodomain and intersubunit linker. It is well established that the cleavage of the intersubunit linker primarily acts as an activation switch in executioner caspases (and in some initiator caspases such as caspase-8). However, it seems that there is no consensus as to the function of prodomain in executioner caspases. For example, while the prodomains of caspase-3 and caspase-7 have been shown to be dispensable for activity *in vitro*, it appears that *in vivo*, having an intact prodomain keeps the enzyme in its inactive state until cleaved by another downstream caspase[49,50]. The caspase-3 prodomain has been also shown to bind Hsp27 in monocytes, leading to inhibition of its proteolytic activation[51]. In caspase-6, an intact prodomain was reported to inhibit self-cleavage at the linker region *in vivo*[52] and both the prodomain and linker are predicted to be highly disordered protein-binding regions[53] that dramatically affect the stability of caspase-6[20]. In the case of caspase-9 it appears that the cleaved state of the intersubunit linker and the interactions between the CARD (prodomain) and the catalytic core is essential for the appropriate function that is unique to caspase-9.

Materials and Methods

Caspase-9 Expression and Purification

The caspase-9 full-length gene (human sequence) construct, encoding amino acids 1-416, in pET23b (Addgene plasmid 11829 [4]) was transformed into the BL21 (DE3) T7 Express strain of *E. coli* (NEB) and purified in a manner similar to that previously reported [54]. The cultures were grown in 2xYT media supplemented with ampicillin (100 mg/L, Sigma-Aldrich) at 37˚C until

they reached an optical density (OD) at 600 nm of 1.2. The temperature was reduced to 15˚C and cells were induced with 1 mM IPTG (Anatrace) to express soluble 6xHis-tagged full-length protein. Cells were harvested after 3 h to obtain single-site processing at Asp315. Cell pellets stored at -20˚C were freeze-thawed and lysed in a microfluidizer (Microfluidics, Inc.) in 50 mM sodium phosphate pH 8.0, 300 mM NaCl, and 2 mM imidazole. Lysed cells were centrifuged at 37,000 x g to remove cellular debris. The filtered supernatant was loaded onto a 5-mL HiTrap Ni-affinity column (GE Healthcare). The column was washed with a buffer containing 50 mM sodium phosphate pH 8.0, 300 mM NaCl, and 2 mM imidazole until 280 nm absorbance returned to baseline. The protein was eluted using a linear imidazole gradient of 2 to100 mM over the course of 270 mL. The eluted fractions containing protein of the expected molecular weight and composition were diluted 10-fold into a buffer composed of 20 mM Tris pH 8.5, 10 mM DTT to reduce the salt concentration. This protein sample was loaded onto a 5-mL Macro-Prep High Q column (Bio-Rad Laboratories, Inc.). The column was developed with a linear NaCl gradient and eluted in 20 mM Tris pH 8.5, 100 mM NaCl, and 10 mM DTT buffer. The eluted protein was stored in -80˚C in the above buffer conditions. Purified caspase-9 was analyzed by SDS-PAGE and ESI-MS to confirm mass and purity. Caspase-9 variants, C287A, R7E, R11E, D23E, R51E E365R, R7E/R11E, S183E, S183A, C287A/S183A, S99E, C287A/S99E, T125E, C287A/T125E and the Ser-Gly linker extension, were constructed by site-directed mutagenesis method in the full-length expression construct, and were purified by the same method (except for S183E, S183A, C287A/S183A, S99E, C287A/S99E, T125E, C287A/T125E) as described here for the wild-type protein.

Caspase-9 S183E, S183A, C287A/S183A, S99E, C287A/S99E, T125E, C287A/T125E were purified using the same method except 50 mM NaH_2PO_4 pH 7.0, 300 mM NaCl and 2 mM imidazole buffer was used to lyse the bacterial cells and wash the HiTrap Ni column. A linear imidazole gradient from 2 mM to 100 mM was used to elute the protein. All proteins were further purified by anion exchange chromatography as described above.

Caspase-9 ΔCARD was expressed from a two-plasmid expression system. Two separate constructs, one encoding the large subunit, residues 140-305, and the other encoding the small subunit, residues 331-416, each in the pRSET plasmid, were separately transformed into the BL21 (DE3) T7 Express strain of *E. coli* (NEB). The recombinant large and small subunits were individually expressed as inclusion bodies for subsequent reconstitution. Cultures were grown in 2xYT media supplemented with ampicillin (100 mg/L, Sigma-Aldrich) at 37°C until they reached an optical density at 600 nm of 0.6. Protein expression was induced with 0.2 mM IPTG. Cells were harvested after 3 hrs at 37˚C. Cell pellets stored at -20˚C were freeze-thawed and lysed in a microfluidizer (Microfluidics, Inc.) in 10 mM Tris pH 8.0 and 1 mM EDTA. Inclusion body pellets were washed twice in 100 mM Tris pH 8.0, 1 mM EDTA, 0.5 M NaCl, 2% Triton, and 1M urea, twice in 100 mM Tris pH 8.0, 1 mM EDTA and finally resuspended in 6 M guanidine hydrochloride. Caspase-9 large and small subunit proteins in guanidine hydrochloride were combined in a ratio of 1:2, large:small subunits, and rapidly diluted dropwise into refolding buffer composed of 100 mM Tris pH 8.0, 10% sucrose, 0.1% CHAPS, 0.15 M NaCl, and 10 mM DTT, allowed to stir for one hour at room temperature and then dialyzed four times against 10 mM Tris pH 8.5, 10 mM DTT, and 0.1mM EDTA buffer at 4˚C. Typically 5 mL of mixed caspase large and small subunits was diluted to 80 mL in refolding buffer and dialyzed against 5 L of dialysis buffer. The first and last dialysis steps were allowed to proceed for 4 hours at 4˚C while the second dialysis proceeded overnight at 4˚C. The dialyzed protein was centrifuged for 15 minutes at 16,500 x g to remove precipitate and then purified using a HiTrap Q HP ion exchange column (GE Healthcare) with a linear gradient from 0 to 250 mM NaCl in 20 mM Tris buffer pH 8.5, with 10 mM DTT. Protein eluted in 20 mM Tris pH 8.5, 100 mM NaCl, and 10 mM DTT buffer was stored in -80˚C. The identity of the purified caspase-9 ΔCARD was analyzed by SDS-PAGE and ESI-MS to confirm mass and purity. The ΔCARD-His6x construct was generated by deleting the CARD (res1-138) from the caspase-9 full-length construct by deletion mutagenesis. ΔCARD-His6x was purified using the same method as wild-type caspase-9.

Oligomeric-State Determination

Caspase-9 wild-type, full-length and ΔCARD variant protein samples in 20 mM Tris pH 8.5, 110 mM NaCl, and 5 mM DTT were incubated alone (monomer) or with covalent inhibitor z-VAD-FMK (carbobenzoxy-Val-Ala-Asp-fluoromethylketone, Enzo Life Sciences) (dimer) for 2 hours at room temperature. The oligomeric state of the caspase-9 samples was determined via gel filtration. 100 μL of 0.5 mg/mL protein sample was loaded onto a Superdex 200 10/300 GL (GE Healthcare) gel-filtration column. Apo and z-VAD-FMK-incubated protein samples were eluted with 20 mM Tris pH 8.0, 100 mM NaCl, and 2 mM DTT. Eluted peaks were analyzed by SDS-PAGE to identify the eluted protein. Four different molecular weight standards from the gel-filtration calibration kit LMW (GE Healthcare) were run in the same conditions and a standard plot was generated to determine whether the peaks were caspase-9 monomer or dimer.

CARD Expression and Purification

The CARD only construct (amino acids 1-138) in pET23b was made by QuikChange mutagenesis (Stratagene) using the oligonucleotide primer 5`-CCCAGACCAGTGGACATT-GGTTCTGGAGGATTCGGTGATCACCACCACCACCACCACTAAGTCGGTGCTCTTGAG AGTTTGAGGGGAAATGCAGATTTGG-3`and its reverse compliment on the caspase-9 full-length gene (Addgene plasmid 11829). These oligo-nucleotide primers insert a 6xHis-tag and a stop codon after the last amino acid of the CARD domain (Asp138), leaving the remaining portion of the caspase-9 gene in the plasmid. A separate CARD construct was made to insert a human rhinovirus-3C (HRV) protease cleavage site (LEVLFQGP) before the 6xHis-tag using the primers 5'-CTCGGGCTGGAAGTGCTGTTCCAGGGTCCGCACCACCACCACCACCACT-AAGCCG-3' (forward) and 5'-ATCACCGAATCCTCCAGAACCAATGTCC-3' (reverse). Each construct was transformed into BL21 (DE3) T7 Express strain of *E. coli*. The cultures were grown in 2xYT media supplemented with ampicillin (100 mg/L, Sigma-Aldrich) at 37˚C until they reached an optical density at 600 nm of 0.6. The temperature was reduced to 15˚C and cells were induced with 1 mM IPTG (Anatrace) to express soluble 6xHis-tagged full-length protein.

Cells were harvested after 18 hrs. Cell pellets stored at -20˚C were freeze-thawed and lysed in a microfluidizer (Microfluidics, Inc.) in 50 mM sodium phosphate pH 8.0, 300 mM NaCl, and 2 mM imidazole. Lysed cells were centrifuged at 37,000 x g to remove cellular debris. The filtered supernatant was loaded onto a 5-mL HiTrap Ni-affinity column (GE Healthcare). The column was washed with a buffer containing 50 mM sodium phosphate pH 8.0, 300 mM NaCl, 2 mM imidazole until 280 nm absorbance returned to baseline. The column was washed with 50 mM phosphate pH 8.0, 300 mM NaCl, 50 mM imidazole and the protein was eluted with 50 mM phosphate pH 8.0, 300 mM NaCl, 250 mM imidazole. The eluted fraction was diluted 10-fold into a buffer containing 20 mM Tris pH 8.0 and 2 mM DTT to reduce the salt concentration. This protein sample was loaded onto a 5 mL Macro-Prep High Q column (Bio-Rad Laboratories, Inc.). The column was developed with a linear NaCl gradient. Protein eluted in 20 mM Tris pH 8.0, 2 mM DTT, and 130 mM NaCl. Eluted protein was analyzed by SDS-PAGE to assess purity and stored in -80˚C. For cleavage of the His6x-tag, eluted fractions from the Ni-NTA column was diluted 2x with 50 mM Tris pH 7.5, 150 mM NaCl, 1 mM EDTA and 1 mM DTT. 100 μg of hrv3C protease was added per 1 μg of CARD-6xHis and the reaction was incubated for 16h at 4˚C with gentle mixing. The cleavage reaction was filtered through 0.45 μm PVDF. Filtered protein solution was diluted 6x with Buffer A and loaded onto a HiTrap Q column (GE Healthcare). The column was developed with a linear NaCl gradient. Caspase-9 CARD (no His tag) eluted in 20 mM Tris pH 8.0, 130 mM NaCl and 2 mM DTT. Full cleavage was assessed by running samples on a 16% SDS-PAGE gel.

Thermal Stability and Secondary Structure Analysis by Circular Dichroism

All caspase-9 variants (except for S183E , S183A, C287A/S183A, S99E, C287A/S99E, T125E, C287A/T125E) and the CARD protein were buffer exchanged via dialysis against 100 mM sodium phosphate pH 7.0, 110 mM NaCl, and 5 mM TCEP and diluted to 7 μM. The samples were split in half and incubated in the presence or absence of four molar equivalents of active site ligand VAD-FMK for 3 hours at room temperature. To ensure complete binding of the

active site ligand to the protein, remaining enzymatic activity was assayed using 300 μM substrate, LEHD-AFC (N-acetyl-Leu-Glu-His-Asp-7-amino-4-fluorocoumarin), (Enzo Life Sciences). Once full inhibition was achieved, samples were buffer-exchanged six times with 100 mM phosphate buffer pH 7.0, 100 mM NaCl and 5 mM TCEP using an Amicon Ultracell 3K concentrator (Millipore) to remove unbound inhibitor. For S183E, S183A, C287A/S183A, S99E, C287A/S99E, T125E, C287A/T125E variants of caspase-9, prior to thermal denaturation by CD, the proteins were buffer exchanged with 100 mM phosphate buffer pH 7.5, 110 mM NaCl and 5 mM TCEP using a NAP^{TM}-5 Column (GE Healthcare). For cleavage of the unprocessed caspase-9 C287A and S183E variants, 7 μM protein sample was incubated with 3% active caspase-3 protein for two hours at room temperature. Full processing of caspase-9 C287A and S183E by caspase-3 was determined by SDS-PAGE analysis.

Thermal denaturation of caspase-9 variants and CARD was monitored by loss of CD signal at 222 nm over a range of 20–90°C. The circular dichroism spectra were monitored from 250-190 nm. Both were performed on a J-720 or J-1150 CD spectrometer (Jasco) with a Peltier controller. Data were collected four separate times on different days from different batches of purified proteins. Curves were fit with Origin Software (OriginLab) using sigmoid fit to determine the melting temperature.

Caspase-3 Expression and Purification

Caspase-3 full-length gene (human sequence) in pET23b (Addgene plasmid 11821 [55]) was transformed into BL21 (DE3) T7 Express strain of E. coli and protein expression was induced with 1 mM IPTG at 30°C for 3 hours [56]. The protein was purified as described previously for caspase-3 [21]. The eluted protein was stored in -80°C in the buffer in which they eluted. The identity of purified caspase-3 was assessed by SDS-PAGE and ESI-MS to confirm mass and purity.

Native Gel Electrophoresis and Ni-NTA Affinity Isolation Assay to Determine *in trans* Interactions

For native gel electrophoresis to diagnose an interaction between caspase-9 ΔCARD and caspase-9 CARD *in trans*, full-length caspase-9, caspase-9 ΔCARD and the CARD domain only were dialyzed twice against 100 mM phosphate pH 7.0 and 2 mM DTT for 90 minutes to rid of excess salt. Samples were incubated either alone or combined with CARD to achieve a 1:1 ratio of caspase-9 ΔCARD plus CARD. Each protein sample was diluted to a final concentration of 10 μM in the dialysis buffer. To induce dimerization samples were incubated with 5-fold excess z-VAD-FMK. All samples were allowed to incubate at room temperature for one hour. All samples were mixed with glycerol loading dye and fractionated on a 10% Tris/Glycine pH 8.3 polyacrylamide gel. The oligomeric state of the mixed caspase-9 ΔCARD and CARD samples were identified by comparison to the apo (monomer) and z-VAD-FMK-bound (dimer) of both the caspase-9 full-length and caspase-9 ΔCARD protein in addition to the CARD only sample.

For Ni-NTA affinity isolation assay of caspase-9 ΔCARD-His6x (ΔCARD, ΔCARD C287A, ΔCARD+VAD-FMK) with CARD *in trans*, samples were diluted to 10 μM in binding buffer (50 mM phosphate pH 8.0, 100 mM NaCl) with 5 mM DTT. To induce dimerization, 20 μM ΔCARD was incubated with 5-fold excess z-VAD-FMK for 1 h at RT. Complete inhibition was assessed by assaying caspase-9 activity using 300 μM LEHD-AFC. Excess z-VAD-FMK was removed by buffer exchanging 5x with binding buffer using Amicon Ultra centrifugal filter 10K MWCO (Millipore). Samples were incubated either alone or with CARD to achieve a 1:2 ratio of caspase-9 ΔCARD-His6x plus CARD (no His tag). 100 μL of protein sample was added to a tube containing 35 μL of HisPur Ni-NTA magnetic beads (ThermoFisher) that were washed three times in water and twice in binding buffer without DTT. Ni-NTA beads plus caspase-9 ΔCARD-His6x and CARD samples were incubated for 3 hours at 4°C with mixing using an end-to-end rotator. Supernatant (unbound fraction) was aspirated and the beads were washed three times with binding buffer to remove any unbound or weakly bound protein (wash fraction).

Protein elution was then carried out by incubating the Ni-NTA beads with 50 µL elution buffer (binding buffer + 250 mM imidazole) for 30 minutes at room temperature. The supernatant (elution fraction) was collected and all fractions were subjected to SDS-PAGE analysis.

Fluorescence Anisotropy

Fluorescence anisotropy was monitored using a SpectraMax M5 plate reader (Molecular Devices, Inc.) with a fixed excitation wavelength set to 485 nm and an emission wavelength set to 525 nm. Caspase-9 CARD (without the His tag) was labeled with fluorescein isothiocyanate (FITC) isomer 1 (Sigma) in labeling buffer containing 0.1 M sodium bicarbonate pH 9.0, 100 mM NaCl for 2h at RT. Unreacted FITC was removed by buffer exchange using a NAP5 column equilibrated in 50 mM Tris (pH 7.5) and 150 mM NaCl. A fixed concentration of FITC-labeled CARD (25 nM) was titrated into a serially diluted caspase-9 ΔCARD (3 nM – 25 µM). The final volume of each binding reaction is 100 µL. All measurements were taken at 25˚C after a 1.5 h incubation at RT.

Activity Assays

For kinetic measurements of caspase activity, 800 nM caspase-9 full-length protein was diluted in 100 mM MES pH 6.5, 10% PEG 8,000 and 5 mM DTT. Each sample was subjected to a substrate titration, performed in the range of 0-300 µM fluorogenic substrate, Ac-LEHD-AFC, (Ex 365/Em 495) which was added to initiate the reaction. Assays were performed in duplicates at 37°C in 100 µL volumes in 96-well microplate format using a Molecular Devices Spectramax M5 spectrophotometer. Initial velocities versus substrate concentration were fit to a rectangular hyperbola using GraphPad Prism (Graphpad Software) to determine kinetic parameters K_M and k_{cat}. Enzyme concentrations were determined by active site titration with quantitative inhibitor z-VAD-FMK. Active site titrations were incubated over a period of 3 hours in 100 mM MES pH 6.5, 10% PEG 8,000, and 5 mM DTT. Optimal labeling was observed when protein was added to z-VAD-FMK solvated in DMSO in 96-well V-bottom plates, sealed with tape, and incubated at room temperature in a final volume of 200 µL. 90 µL aliquots were transferred to black-well

plates in duplicate and assayed with 300 μM substrate. The protein concentration was determined to be the lowest concentration at which full inhibition was observed.

To test the ability of CARD to activate caspase-9 ΔCARD *in trans*, 10 μM of ΔCARD was incubated with CARD at different ratios (1x, 5x and 10x CARD) in minimal activity assay buffer (100 mM MES pH 6.5, 20% PEG 400 and 5 mM DTT) for 1h at RT. Control reactions were made using BSA in place of CARD. Samples were diluted to a final concentration of 800 nM ΔCARD using minimal activity assay buffer and LEHDase activity was measured over the course of 10 min in 100 μL volumes using a Spectramax M5 fluorescence plate reader.

Acknowledgments

This work was supported by the National Institutes of Health (GM 080532) to JH. KH and BS were supported in part by the UMass Chemistry-Biology Interface Training Program (National Research Service Award T32 GM 08515 from the National Institutes of Health). We thank Scott Eron for providing the caspase-9 constitutive dimer proteins.

Author Contributions

KH designed and performed most of the experiments, analyzed and interpreted data and wrote the initial manuscript. BS designed and performed additional experiments, analyzed and interpreted data and revised the manuscript in its final form. JH conceptualized and directed the research project, secured funding, analyzed and interpreted data, wrote and edited parts of the manuscript.

References

1. Zhai, D. *et al.* Vaccinia virus protein F1L is a caspase-9 inhibitor. *J. Biol. Chem.* **285,** 5569–80 (2010).
2. Öztaş, P. *et al.* Caspase-9 expression is increased in endothelial cells of active Behçet's disease patients. *Int. J. Dermatol.* **46,** 172–176 (2007).
3. Sekimura, A. *et al.* Expression of Smac/DIABLO is a novel prognostic marker in lung cancer. *Oncol. Rep.* **11,** 797–802 (2004).

4. Stennicke, H. R. *et al.* Caspase-9 can be activated without proteolytic processing. *J. Biol. Chem.* **274,** 8359–62 (1999).

5. Rodriguez, J. & Lazebnik, Y. Caspase-9 and Apaf-1 form an active holoenzyme. *Genes Dev.* **13,** 3179–3184 (1999).

6. Zou, H., Li, Y., Liu, X. & Wang, X. An Apaf-1-cytochrome c multimeric complex is a functional apoptosome that activates procaspase-9. *J. Biol. Chem.* **274,** 11549–11556 (1999).

7. Pop, C., Timmer, J., Sperandio, S. & Salvesen, G. S. The apoptosome activates caspase-9 by dimerization. *Mol. Cell* **22,** 269–75 (2006).

8. Shiozaki, E. N., Chai, J. & Shi, Y. Oligomerization and activation of caspase-9, induced by Apaf-1 CARD. *Proc. Natl. Acad. Sci. U. S. A.* **99,** 4197–202 (2002).

9. Acehan, D. *et al.* Three-Dimensional Structure of the Apoptosome : Implications for Assembly, Procaspase-9 Binding, and Activation. *Mol. Cell* **9,** 423–432 (2002).

10. Salvesen, G. & Dixit, V. Caspase activation: the induced-proximity model. *Proc. Natl. Acad. Sci. U. S. A.* **96,** 10964–10967 (1999).

11. Renatus, M., Stennicke, H. R., Scott, F. L., Liddington, R. C. & Salvesen, G. S. Dimer formation drives the activation of the cell death protease caspase-9. *Proc. Natl. Acad. Sci. U. S. A.* **98,** 14250–5 (2001).

12. Shi, Y. Caspase activation: revisiting the induced proximity model. *Cell* **117,** 855–8 (2004).

13. Yuan, S. *et al.* The Holo-Apoptosome: Activation of Procaspase-9 and Interactions with Caspase-3. *Structure* **19,** 1084–1096 (2011).

14. Cheng, T. C., Hong, C., Akey, I. V., Yuan, S. & Akey, C. W. A near atomic structure of the active human apoptosome. *Elife* **5,** 1–28 (2016).

15. Malladi, S., Challa-Malladi, M., Fearnhead, H. O. & Bratton, S. B. The Apaf-1-procaspase-9 apoptosome complex functions as a proteolytic-based molecular timer. *EMBO J.* **28,** 1916–25 (2009).

16. Manns, J. *et al.* Triggering of a novel intrinsic apoptosis pathway by the kinase inhibitor staurosporine: activation of caspase-9 in the absence of Apaf-1. *FASEB J.* **25,** 3250–61 (2011).

17. Gyrd-Hansen, M. *et al.* Apoptosome-Independent Activation of the Lysosomal Cell Death Pathway by Caspase-9. *Mol. Cell. Biol.* **26,** 7880–7891 (2006).

18. Mille, F. *et al.* The Patched dependence receptor triggers apoptosis through a DRAL–caspase-9 complex. *Nat. Cell Biol.* **11,** 739–746 (2009).

19. Gasteiger, E. *et al.* in *The Proteomics Protocols Handbook* (ed. John M. Walker) 571–607 (Humana Press Inc, 2005).

20. Vaidya, S., Velázquez-Delgado, E. M., Abbruzzese, G. & Hardy, J. A. Substrate-induced conformational changes occur in all cleaved forms of caspase-6. *J. Mol. Biol.* **406,** 75–91 (2011).

21. Witkowski, W. A. & Hardy, J. A. L2' loop is critical for caspase-7 active site formation. *Protein Sci.* **18,** 1459–68 (2009).

22. Vaidya, S. & Hardy, J. A. Caspase-6 Latent State Stability Relies on Helical Propensity. *Biochemistry* **50,** 3282–3287 (2011).

23. Chao, Y. *et al.* Engineering a dimeric caspase-9: a re-evaluation of the induced proximity model for caspase activation. *PLoS Biol.* **3,** e183 (2005).

24. Qin, H. *et al.* Structural basis of procaspase-9 recruitment by the apoptotic protease-activating factor 1. *Nature* **399,** 549–57 (1999).

25. Shi, Y. Mechanisms of Caspase Activation and Inhibition during Apoptosis Caspases are central components of the machinery. *Mol. Cell* **9,** 459–470 (2002).

26. Lyskov, S. & Gray, J. J. The RosettaDock server for local protein-protein docking. *Nucleic Acids Res.* **36,** W233–W238 (2008).

27. Serrano, B. P. & Hardy, J. A. Phosphorylation by Protein Kinase A Disassembles the Caspase-9 Core. *Cell Death Differ.* (2017). *In press*

28. Nishi, H., Fong, J. H., Chang, C., Teichmann, S. A. & Panchenko, A. R. Regulation of protein–protein binding by coupling between phosphorylation and intrinsic disorder: analysis of human protein complexes. *Mol. Biosyst.* **9,** 1620 (2013).

29. Nishi, H., Hashimoto, K. & Panchenko, A. R. Phosphorylation in Protein-Protein Binding: Effect on Stability and Function. *Structure* **19,** 1807–1815 (2011).

30. Nishi, H., Shaytan, A. & Panchenko, A. R. Physicochemical mechanisms of protein regulation by phosphorylation. *Front. Genet.* **5,** 270 (2014).

31. Martin, M. C. *et al.* Protein kinase A regulates caspase-9 activation by Apaf-1 downstream of cytochrome c. *J. Biol. Chem.* **280,** 15449–55 (2005).

32. Allan, L. A. *et al.* Inhibition of caspase-9 through phosphorylation at Thr 125 by ERK MAPK. *Nat. Cell Biol.* **5,** 647–54 (2003).

33. Seifert, A., Allan, L. A. & Clarke, P. R. DYRK1A phosphorylates caspase 9 at an inhibitory site and is potently inhibited in human cells by harmine. *FEBS J.* **275,** 6268–80 (2008).

34. Rutter, J., Michnoff, C. H., Harper, S. M., Gardner, K. H. & McKnight, S. L. PAS kinase: an evolutionarily conserved PAS domain-regulated serine/threonine kinase. *Proc. Natl. Acad. Sci. U. S. A.* **98,** 8991–6 (2001).

35. Fatemi, M., Hermann, A., Pradhan, S. & Jeltsch, A. The activity of the murine DNA methyltransferase Dnmt1 is controlled by interaction of the catalytic domain with the N-terminal part of the enzyme leading to an allosteric activation of the enzyme after binding to methylated DNA. *J. Mol. Biol.* **309,** 1189–1199 (2001).

36. Kashiwagi, M. *et al.* Altered proteolytic activities of ADAMTS-4 expressed by C-terminal processing. *J. Biol. Chem.* **279,** 10109–19 (2004).

37. Twiddy, D. & Cain, K. Caspase-9 cleavage, do you need it? *Biochem. J.* **405,** e1-2 (2007).

38. Yuan, S., Yu, X., Asara, J. & Heuser, J. The holo-apoptosome: activation of procaspase-9 and interactions with caspase-3. *Structure* **19,** 1084–1096 (2011).

39. Wu, C.-C. *et al.* The Apaf-1 apoptosome induces formation of caspase-9 homo- and heterodimers with distinct activities. *Nat. Commun.* **7,** 13565 (2016).

40. Murray, T. V. A. *et al.* A non-apoptotic role for caspase-9 in muscle differentiation. *J. Cell Sci.* **121,** 3786–93 (2008).

41. Park, H. H. *et al.* The death domain superfamily in intracellular signaling of apoptosis and inflammation. *Annu. Rev. Immunol.* **25,** 561–86 (2007).

42. Tinel, A. & Tschopp, J. The PIDDosome, a Protein Complex Implicated in Activation of Caspase-2 in Response to Genotoxic Stress. *Science (80-.).* **304,** (2004).

43. Manzl, C. *et al.* PIDDosome-independent tumor suppression by Caspase-2. *Cell Death Differ.* **19,** 1722–1732 (2012).

44. Kim, I. R. *et al.* DNA damage- and stress-induced apoptosis occurs independently of PIDD. *Apoptosis* **14,** 1039–1049 (2009).

45. Fava, L. L., Bock, F. J., Geley, S. & Villunger, A. Caspase-2 at a glance. *J. Cell Sci.* **125,** (2013).

46. Clerici, M., Luna-Vargas, M. P. A., Faesen, A. C. & Sixma, T. K. The DUSP–Ubl domain of USP4 enhances its catalytic efficiency by promoting ubiquitin exchange. *Nat. Commun.* **5,** (2014).

47. Kobe, B. *et al.* Structural basis of autoregulation of phenylalanine hydroxylase. *Nat. Struct. Biol.* **6,** 442–448 (1999).

48. Stamogiannos, A. *et al.* Critical Role of Interdomain Interactions in the Conformational Change and Catalytic Mechanism of Endoplasmic Reticulum Aminopeptidase 1. *Biochemistry* **56,** 1546–1558 (2017).

49. Meergans, T., Hildebrandt, A.-K., Horak, D., Haenisch, C. & Wendel, A. The short prodomain influences caspase-3 activation in HeLa cells. *Biochem. J* **349,** 135–140 (2000).

50. Denault, J.-B. & Salvesen, G. S. Human caspase-7 activity and regulation by its N-terminal peptide. *J. Biol. Chem.* **278,** 34042–50 (2003).

51. Voss, O. H. *et al.* Binding of caspase-3 prodomain to heat shock protein 27 regulates monocyte apoptosis by inhibiting caspase-3 proteolytic activation. *J. Biol. Chem.* **282,** 25088–99 (2007).

52. Klaiman, G., Champagne, N. & LeBlanc, A. C. Self-activation of Caspase-6 in vitro and in vivo: Caspase-6 activation does not induce cell death in HEK293T cells. *Biochim. Biophys. Acta - Mol. Cell Res.* **1793,** 592–601 (2009).

53. Dagbay, K. B. & Hardy, J. A. Multiple proteolytic events in caspase-6 self-activation impact conformations of discrete structural regions. *Proc. Natl. Acad. Sci. U. S. A.* 201704640 (2017). doi:10.1073/pnas.1704640114

54. Huber, K. L. & Hardy, J. a. Mechanism of zinc-mediated inhibition of caspase-9. *Protein Sci.* **21,** 1056–65 (2012).

55. Zhou, Q. *et al.* Target Protease Specificity of the Viral Serpin CrmA: ANALYSIS OF FIVE CASPASES. *J. Biol. Chem.* **272,** 7797–7800 (1997).

56. Stennicke, H. R. & Salvesen, G. S. Caspases: Preparation and Characterization. *Methods* **17,** 313–319 (1999).

57. Micsonai, A. *et al.* Accurate secondary structure prediction and fold recognition for circular dichroism spectroscopy. *Proc. Natl. Acad. Sci. U. S. A.* **112,** E3095-103 (2015).

CHAPTER IV

ACTIVE-SITE ADJACENT PHOSPHORYLATION AT TYR-397 BY c-ABL KINASE INACTIVATES CASPASE-9

Majority of this chapter is published: Serrano, B.P., Szydlo, H.S., Alfandari, D.R. and Hardy J.A. Active-Site Adjacent Phosphorylation at Tyr-397 by c-Abl Kinase Inactivates Caspase-9. *J. Biol. Chem*. 292:21352-21365 (2017).

Abstract

Caspase-9 is an initiator caspase and plays a central role in activating apoptotic cell death. Control of caspase-9 and all caspases is tightly regulated by a series of phosphorylation events enacted by a number of different kinases. Caspase-9 is the most heavily phosphorylated of all caspases, and is is thus perhaps the most tightly regulated of all caspases. Phosphorylation of caspase-9 by the non-receptor tyrosine kinase c-Abl, at Y153 reportedly leads to caspase-9 activation. All other phosphorylation events on caspases have been shown to block proteolytic function by a number of mechanisms, so we undertook a project to understand the molecular mechanism of caspase-9 activation by phosphorylation. Surprisingly, we observed no evidence for Y153 phosphorylation under any of the conditions studied, perhaps suggesting that Y153 is not directly phosphorylated by c-Abl, but by another similarly activated kinase. Instead we identified a new site of c-Abl phosphorylation, Y397, which is adjacent to the caspase-9 active site, but as a member of the second shell, not a residue that directly contacts substrate. Our data indicate that Y397 is the dominant site of c-Abl phosphorylation both *in vitro* and upon c-Abl activation in cells. Phosphorylation at the Y397 site inhibits caspase-9 activity. It appears that the bulk of the added phosphate moiety directly blocks substrate binding. c-Abl is known to play both proapoptotic and prosurvival roles; these data on c-Abl regulation of caspase-9 suggest that c-Abl functions in a prosurvival mode.

Introduction

Cells undergo constant turnover to maintain normal tissue function and homeostasis. This is achieved by a delicate and dynamic balance of cellular networks involving cell proliferation and cell death signaling pathways. Apoptosis or programmed cell death is an essential pathway that proceeds via a series of biochemical reactions that ultimately result in the controlled dismantling of cellular components without adverse damage to neighboring cells. Tight regulation of apoptosis is fundamental to attain cellular homeostasis. Defects in regulation of apoptotic pathways have been implicated in many diseases that are in nature both proliferative, such as cancer, and degenerative, like Alzheimer's and Huntington's. As such, elements involved in apoptotic signaling are recognized as attractive drug targets for the development of therapeutics for apoptosis-related diseases.

Caspases are specialized proteases that mediate the faithful execution of apoptosis. Caspases cleave protein substrates causing either activation or inhibition which eventually commits the cell to death. Caspases are extremely specific towards substrates, generally preferring to cleave after an aspartate[1] or glutamate[2], and in some cases a phosphoserine[3]. Depending on where they act in the apoptotic pathways, caspases are classified as either upstream initiators (caspase-2, -8 and -9) or downstream executioners (caspase-3, -6 and -7). Because caspase activity inherently induces apoptosis, caspases are synthesized and held as inactive zymogens (procaspases). Procaspases contain an N-terminal prodomain region and the highly homologous caspase core, consisting of a large and a small subunit joined together by an intersubunit linker. Most procaspases exist predominantly as homodimeric proteins. Upon apoptosis induction, initiator caspases are recruited to complex protein scaffolds that promote activation, while executioner caspases depend on initiator caspases to cleave the intersubunit linker which consequently converts the inactive procaspase into a mature, active form. Once assembled into an active form, the highly dynamic loops that compose the active site assume a conformation that allows substrate binding and catalytic cleavage, thereby initiating a cascade of

reactions that eventually lead to the cell's demise. Caspases exert such dominant impact on apoptosis, that any inopportune caspase activation is deleterious to the cell. Thus, caspase expression and activation are tightly regulated by various mechanisms at different checkpoints in the cell.

Phosphorylation is recognized to be a critical mediator of apoptosis (reviews[4,5]). Caspases form a subset of kinase substrates whose functions are directly affected by phosphorylation (review[6]). The initiator caspase-9 (caspase-9), for example, appears to be extremely sensitive to phosphorylation, having the largest number of phosphorylation sites reported of any caspase (Figure 4.1A; reviews[6–8]). This suggests that phosphorylation is a strong regulator of caspase-9 function. This is perhaps because phosphorylation can impact caspase-9 on multiple levels, as caspase-9 achieves activation in many ways – from cleavage to dimerization to protein-protein interactions to the formation of the apoptosome. Phosphorylation sites are present in all domains of caspase-9 (Figure 4.1A) and are targeted by kinases that are involved in cell cycle[9,10], cellular stress[11–13] and extracellular signals[14,15].

In general, phosphorylation of caspases results in apoptotic suppression, which is a direct consequence of caspase inhibition. Intriguingly, of all the reported sites of phosphorylation in caspase-9, Y153 is the only site reported to activate caspase-9[12]. All other sites of phosphorylation reportedly have led to inactivation (review[16]). Y153 in caspase-9 is reported to be phosphorylated by the non-receptor tyrosine kinase c-Abl. c-Abl is activated in response to various extrinsic and intrinsic signals, which causes it to possess both pro- and anti-apoptotic roles (review[17]). c-Abl generally recognizes the sequence I/V/L-Y-X-X-P and phosphorylates a large number of functionally diverse substrates, in part due to its ability to shuttle between the cytosol and the nucleus. Interestingly, this nucleocytoplasmic shuttling of c-Abl dictates whether its activation would promote either cell death or survival. For example, oncogenic forms of c-Abl exhibit strictly cytoplasmic localization and constitutive activity, while nuclear c-Abl activated by cellular stress such as DNA damage promotes apoptosis. This pro-apoptotic function of c-Abl has

been attributed to its phosphorylation of caspase-9 resulting in self-processing and subsequent activation of caspase-3[12]. We were intrigued by this functional effect of c-Abl on caspase-9, especially since all other sites were reported to be inhibiting upon phosphorylation. For this reason we undertook a study of the mechanism of caspase-9 activation by Y153 phosphorylation. During this study we also identified a new site of phosphorylation.

In the last decade a number of cell-based studies identified sites of phosphorylation in caspase-9 (review[16]). Many excellent proteome-wide studies have annotated sites of phosphorylation in caspase-9 and other caspases. Given the multitude of different cellular contexts, it has naturally been impossible to perform these large-scale, proteome-wide studies under all relevant cellular conditions. Thus, although a number of sites have been identified it is likely that many other sites of phosphorylation by particular kinases have not yet been identified. Here we report a novel site of phosphorylation in caspase-9 by c-Abl. An active-site adjacent residue Y397 is phosphorylated by c-Abl both *in vitro* and intracellularly, leading to caspase-9 inhibition.

Results

Caspase-9 is composed of the caspase activation and recruitment domain (CARD) and the core which consists of the large and the small subunit. The reported phosphorylation site Y153 resides in the caspase-9 large subunit (Figure 4.1A, 4.1B). In the dimeric, substrate-bound structure of caspase-9, the hydroxyl group of Y153 forms an H-bond with D350 in the L2' loop. This interaction seems to support the position of L2' as it correspondingly interacts with L2 and L4 in the other half of the dimer to form the substrate binding groove and catalytic site (Figure 4.1C). Thus it is conceivable that phosphorylation of Y153 would impact caspase-9 activity. Phosphorylation of caspases typically leads to inhibition (review[6]), yet it has been reported that upon DNA damage, Y153 phosphorylation by c-Abl results in self-processing and promotes caspase-9 cleavage of caspase-3[12].

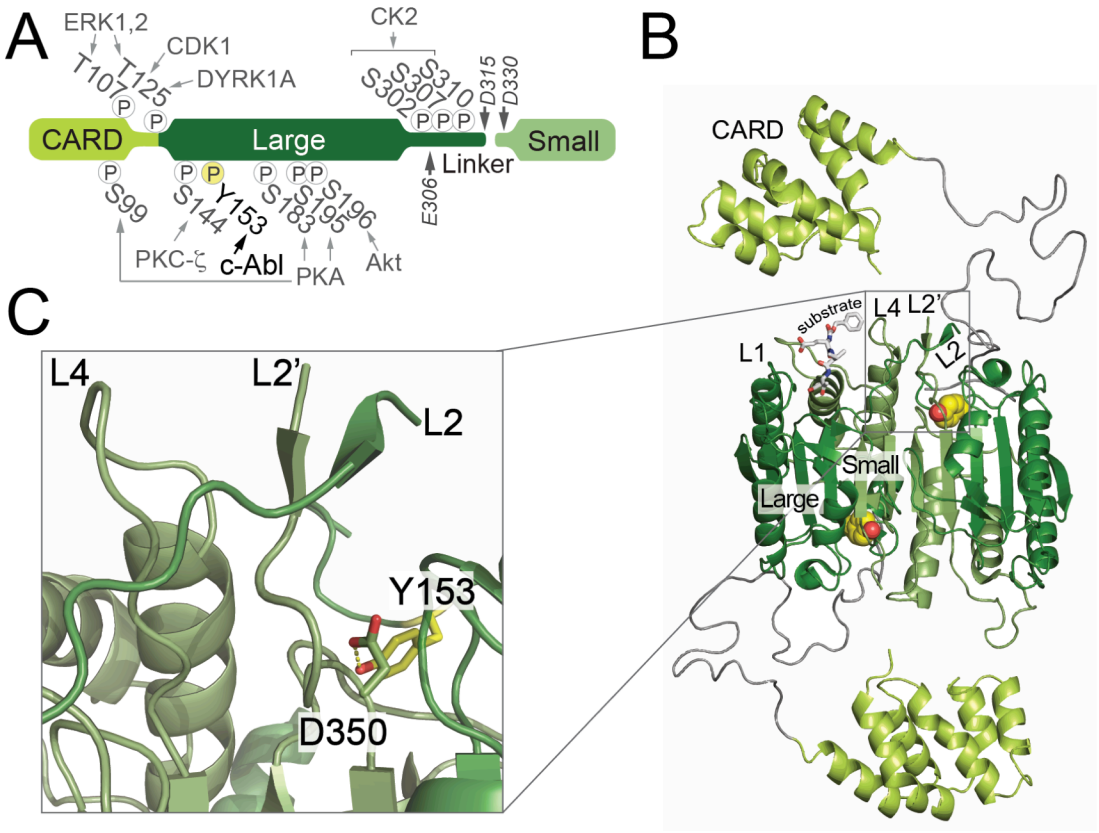

Figure 4.1. Y153 makes critical contacts with active site loop L2'.
(A) Domain architecture of caspase-9 showing the N-terminal caspase activation and recruitment domain (CARD) and the core which is composed of a large (Lg) and a small (Sm) subunit connected by an intersubunit linker. Three cleavage sites in the intersubunit linker are indicated by arrows: E306 (minor, self-cleavage), D315 (major, self-cleavage) and D330 (by caspase-3). Reported phosphorylation sites are indicated by Ⓟ in white; the c-Abl phosphorylation site Y153 in the large subunit is highlighted in yellow. Cognate kinases are indicated with arrows pointing at the phosphorylation site.
(B) Structure of full-length, dimeric caspase-9 showing the phosphorylation site, Y153, as spheres. The structure shown here was modeled from individual structures of the CARD-deleted caspase-9 (aa 138-416; PDB 1JXQ) and the caspase-9 CARD (aa 1-95; PDB 3YGS) from a dimeric complex with Apaf-1 CARD. The region between the CARD and core is not present in either structures and is most likely highly disordered, hence it was modeled as gray coil. The loops forming the substrate binding groove (L2, L3 and L4 from one monomer and L2' from the opposite monomer) are labeled.
(C) Y153 forms an H-bond with D350 in loop L2', supporting the "up" position of L2' in order to properly interact with L2 and L4 and achieve a catalytically competent active site.

Phosphomimetic Y153E has impaired catalytic efficiency compared to WT caspase-9

To probe for the functional consequence of Y153 phosphorylation in caspase-9, we generated the glutamate phosphomimetic Y153E. Following overexpression, Y153E remained in its zymogen (uncleaved) form unlike wild-type (WT) caspase-9, which was expressed as a mature, cleaved enzyme (Figure 4.2A). Caspase-9 zymogen possesses basal activity and hence readily undergoes self-processing; however, it seems that the glutamate substitution blocks function. Unlike the WT zymogen, Y153E lacked the ability to self-process (Figure 4.2B) and did not exhibit any LEHDase activity (Table 4.1) in the zymogen form. To assess whether the

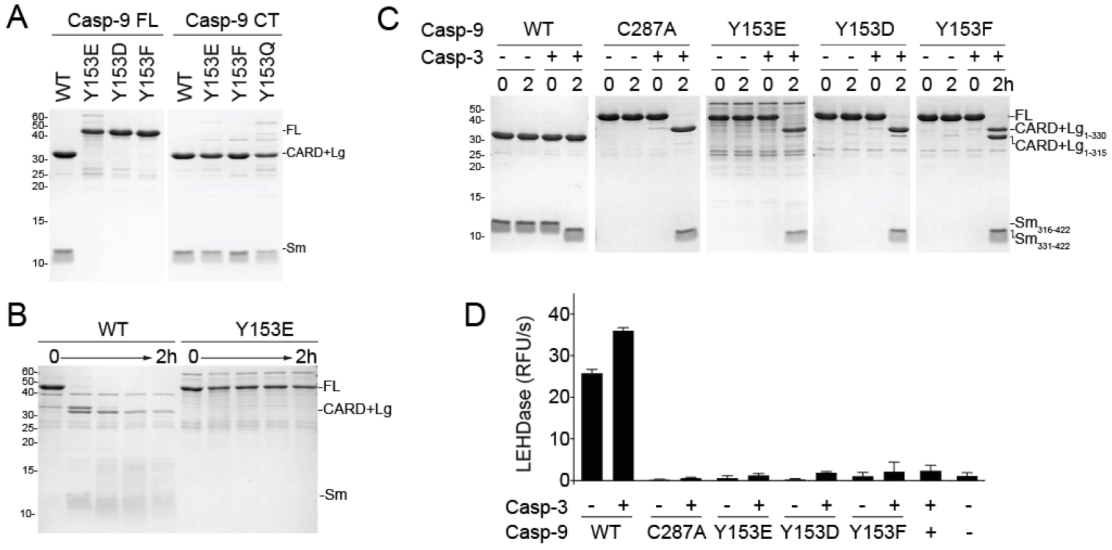

Figure 4.2. Y153 is an inherently sensitive site.
(A) Caspase-9 Y153 variants (phosphomimetics Y153E, Y153D and non-phosphorylatable Y153F) remained in the uncleaved zymogen (full-length) state upon overexpression, whereas WT caspase-9 forms the mature, cleaved state upon overexpression. The constitutively two-chain (CT) versions of caspase-9 are generated by independent translation of the CARD+Large (Lg) and Small (Sm) subunits, thus all caspase-9 CT variants (CT Y153E, CT Y153F and CT Y153Q) are in the "cleaved" state following overexpression.
(B) WT caspase-9 zymogen readily undergoes self-processing into the CARD+Large and small subunits. Full length Y153E is unable to self-process and remains in the zymogen (uncleaved) form, suggesting it is inherently inactive.
(C) Caspase-3 natively cleaves caspase-9 at D330. WT Caspase-9, catalytic-site inactivated variant C287A, phosphomimetic Y153E and variants Y153D and Y153F were incubated alone or with caspase-3. Cleavage at D330 to generate mature proteins only occurred in the presence of caspase-3, except for WT which immediately self-processes.
(D) Caspase-9 full-length variants cleaved by caspase-3 (C) were tested in an LEHDase assay. Y153E, Y153D and Y153F did not gain activity following caspase-3 cleavage.

observed inhibition was due to its zymogen nature and to assess whether these variants are still cleavable by other caspases, full-length Y153E was cleaved by caspase-3 (Figure 4.2C). Even following cleavage to generate the mature form, Y153E remained inactive (Figure 4.2D).

In addition, caspase-9 variants at this position were expressed from a constitutively two-chain (CT) construct, which allows independent translation of the CARD+Large and the small subunits. Even in its fully mature form, CT Y153E remained inactive, suggesting that the glutamate phosphomimetic inherently inhibits caspase-9 activity (Figure 4.2A, Table 4.1). This was in contrast to prior reports, in which phosphorylation at Y153 was suggested to promote caspase-9 self-processing and thereby activation[12]. To validate that the inhibition was a direct consequence of the phosphomimetic, an aspartate substitution (Y153D) was made and showed the same inactivating effect as the glutamate phosphomimetic, while the conservative phenylalanine substitution mutant (Y153F) had a ~150x decrease in catalytic efficiency (Table 4.1). Both Y153D and Y153F were also uncleaved upon overexpression, suggesting impaired self-processing abilities (Figure 4.2A).

Table 4.1. Catalytic parameters[6] of caspase-9 variants.

Caspase-9 variants	K_M (μM)	k_{cat} (s^{-1})	10^3 x k_{cat}/K_M ($\mu M^{-1}s^{-1}$)
Caspase-9 Full-Length (C9 FL)			
Wild-type (WT)	430 ± 35	1.4 ± 0.1	3.3
Y153E	> 3000	< 0.01	< 0.003
Y153D	> 3000	< 0.01	< 0.003
Y153F	2804 ± 829	0.04 ± 0.01	0.02
Y397F	338 ± 18	0.78 ± 0.1	2.7
Caspase-9 Constitutively Two-Chain (C9 CT)			
WT	609 ± 35	1.8 ± 0.03	3.0
Y153E	> 3000	< 0.01	< 0.003
Y153F	> 3000	< 0.01	< 0.003
Y153Q	> 3000	< 0.01	< 0.003
Y397E	961 ± 100	0.57 ± 0.08	0.59

[6] Values are mean (± SEM) of three trials done on three separate days.

Similar to Y153E, caspase-3 was able to cleave Y153D or F to generate mature enzymes; however they remained inactive (Figure 4.2C, 4.2D). Moreover, the CT version of Y153F had no measurable activity, and introducing a polar amide side chain of glutamine (CT Y153Q) did not rescue activity (Table 4.1, Figure 4.2A). These results are in line with prior observations. This region where the L2 and L2' loops interact is extremely sensitive to mutation and post-translational modification. Substitutions that break the L2-L2' interaction disrupt caspase activity[18] and phosphorylation of S257, which is also in this region also inactivates caspase-6[19]. Thus, one might anticipate *a priori* that should Y153 be phosphorylated, it would be inactivating.

Y397 is the major phosphorylation site in caspase-9 by c-Abl

We performed *in vitro* phosphorylation using recombinant c-Abl to interrogate the behavior of the phosphorylated form of caspase-9. Caspase-9 was indeed a substrate of c-Abl, as both the kinase domain only (KD) and the three domain (SH3-SH2-kinase domain) (3D) forms of c-Abl resulted in ^{32}P-labeling of caspase-9 zymogen/full-length (as catalytic site inactivated C287A) in the presence of [γ-^{32}P]-ATP (Figure 4.3). Surprisingly, we did not observe any phosphorylation in the CARD+Large (CARD+Lg) region where Y153 is located, but rather clear phosphorylation of the small subunit (Sm) in cleaved, WT caspase-9 (Figure 4.3B, 4.3D). Upon inspection of all other tyrosine residues in caspase-9 (Y251, Y345, Y363 and Y397), Y397 was the most highly surface-exposed (Figure 4.4A). In addition, the sequence surrounding Y397 contains a consensus sequence for c-Abl recognition (Figure 4.4B, 4.4C).

To pinpoint the phosphorylated residue or residues, Y153 and Y397 were rendered unphosphorylatable by substitution of phenylalanine and incubated with active c-Abl. Y153F substitution did not abolish phosphorylation, as the small subunit was still clearly labeled with ^{32}P (Figure 4.4D). Y397 appears to be more solvent exposed relative to Y153 hence it is possible that the competition for Abl recognition and phosphorylation is heavily weighted towards Y397. However, making Y397 unphosphorylatable (Y397F) did not force phosphorylation of Y153 but almost completely eliminated caspase-9 phosphorylation (Figure 4.4D).

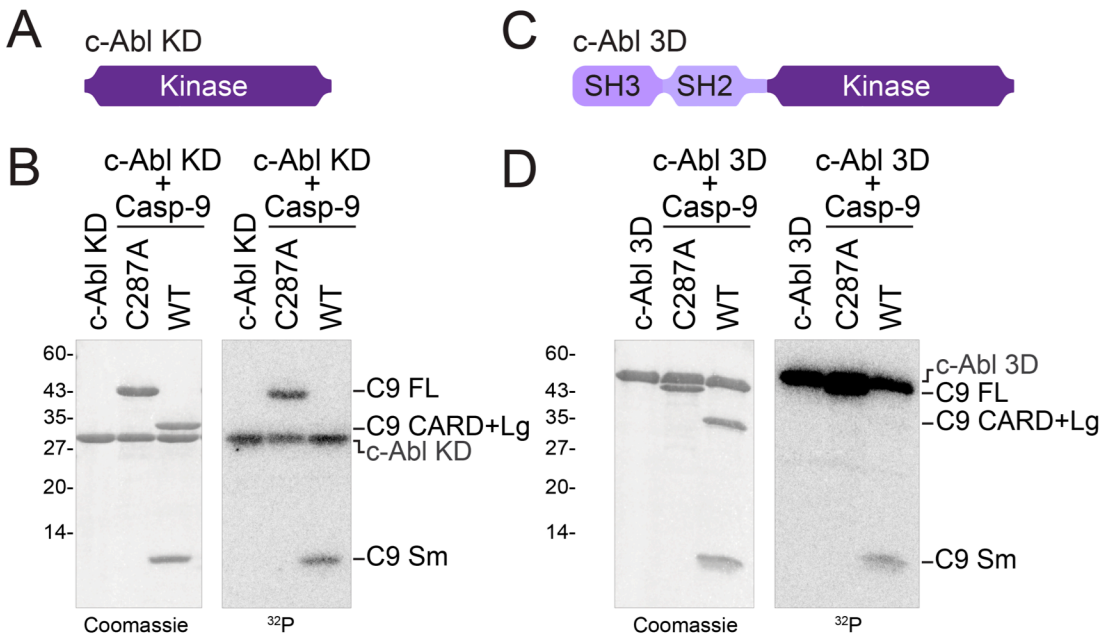

Figure 4.3. c-Abl phosphorylates caspase-9 *in vitro* at the small subunit.
(A) and (C) Recombinant c-Abl constructs used to phosphorylate caspase-9 *in vitro*. The construct c-Abl KD comprises only the kinase domain, while the c-Abl 3D construct contains the SH3-SH2 regulatory/binding domains as well as the kinase domain.
(B) and (D) Caspase-9 catalytic-site inactivated variant C287A (full-length) and WT (cleaved) were subjected to *in vitro* phosphorylation by c-Abl KD or 3D in the presence of ATP + [γ-^{32}P]ATP for 2h. c-Abl undergoes autophosphorylation/autoactivation upon treatment with ATP. Both forms of c-Abl phosphorylated caspase-9 in the zymogen (C287A) and cleaved (WT) forms. No phosphorylation in the CARD+Large region (Y153 site) was detected, but phosphorylation in the small subunit was clearly visible, as shown in the autoradiograph labeled here and in the succeeding figures as ^{32}P.

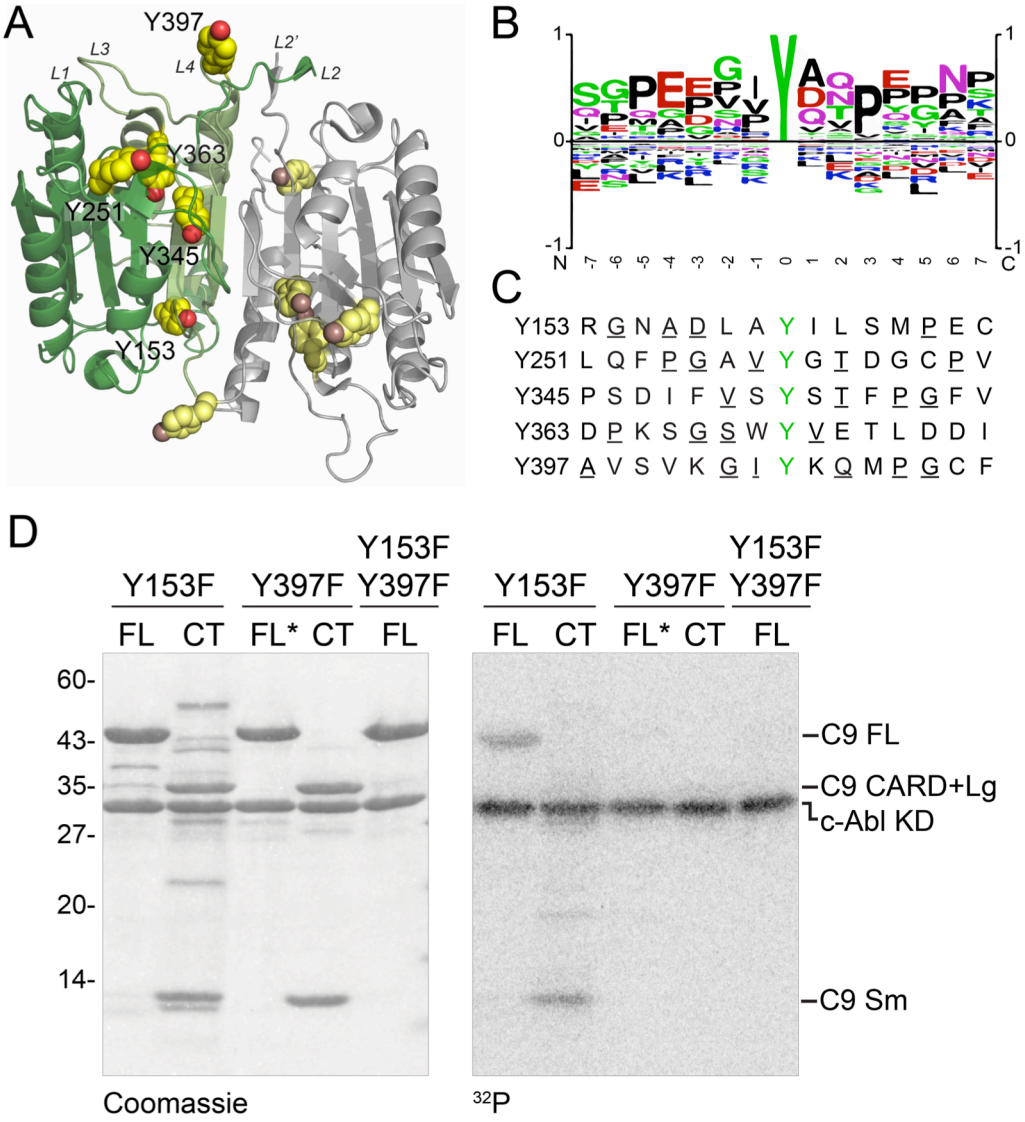

Figure 4.4. Y397 is the predominant site for c-Abl phosphorylation *in vitro*.
(A) Structure of caspase-9 core showing all the tyrosine residues (yellow spheres). Y397 resides in loop L4 and is noticeably solvent-exposed, due to crystal contacts in this structure (PDB ID 1JXQ).
(B) Substrate sequence logo for the consensus recognition sequence of c-Abl (downloaded from PhosphoSitePlus [57])
(C) Sequence of residues surrounding each tyrosine present in caspase-9. Residues in favorable positions are underlined. Sequence surrounding Y397 conforms well to the consensus sequence for c-Abl phosphorylation.
(D) Unphosphorylatable caspase-9 variants (phenylalanine substitutions at putative phosphorylated tyrosines) in both full-length (FL) and CT versions were subjected to *in vitro* phosphorylation by c-Abl for 2h. The * denotes that FL Y397F was constructed in the background of C287A (catalytic cysteine inactivated variant) to prevent self-processing since Y397F is active. FL Y153F caspase-9 was still visibly phosphorylated; the CT version of Y153F revealed that the phosphorylation is in the small subunit. An absence of phosphorylation was observed for Y397F (both FL and CT) and the double mutant Y153F/Y397F.

We also tested CARD-deleted versions of caspase-9 (ΔCARD) to increase Y153 accessibility, as the CARD in the full-length is attached through a highly flexible linker and could potentially block the Y153 site. Even in the absence of the CARD, only phosphorylation at the Sm subunit was observed (Figure 4.5). To unambiguously identify the phosphorylated site, we performed LC-MS/MS on peptide fragments following ArgC proteolysis of c-Abl-phosphorylated WT caspase-9 and observed phosphate labeling at Y397 with high confidence (Figure 4.6A, 4.6B). These results clearly indicate that Y397 is the dominant site for phosphorylation by c-Abl *in vitro*.

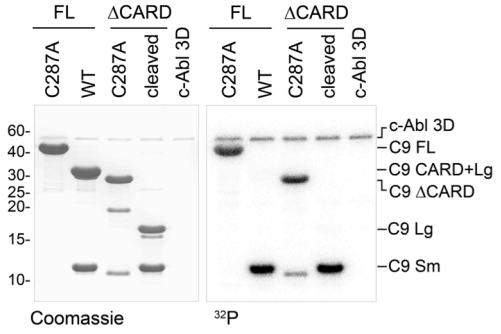

Figure 4.5. Removal of the CARD in caspase-9 (ΔCARD) did not promote Y153 phosphorylation.
No visible phosphorylation in the large subunit was observed in both cleaved versions of WT and ΔCARD caspase-9. Only the small subunit in both cases was robustly phosphorylated. An unidentified non-specific 12 kDa band from ΔCARD C287A was also observed be phosphorylated.

Phosphorylation of Y397 leads to caspase-9 inhibition

This is the first report of a novel site, Y397, being phosphorylated by c-Abl. As such, it is imperative to probe whether this phosphorylation imparts functional or structural perturbations to caspase-9. A modest but statistically significant inhibition of caspase-9 LEHDase activity was observed when WT was phosphorylated at Y397. In contrast, the activity of the unphosphorylatable Y397F variant was unchanged even after treatment with c-Abl (Figure 4.7A, 4.7B). Although full inhibition was not achieved under *in vitro* phosphorylation conditions, a strong correlation between the levels of phosphorylation and caspase-9 inhibition was observed (Figure 4.7C). In fact, phosphocapture experiments resulted in samples with enriched levels of phosphorylated caspase-9 that correspondingly exhibited higher degrees of inhibition (Figure 4.7D), implying that a homogeneous population of phosphorylated caspase-9 would be completely inhibited.

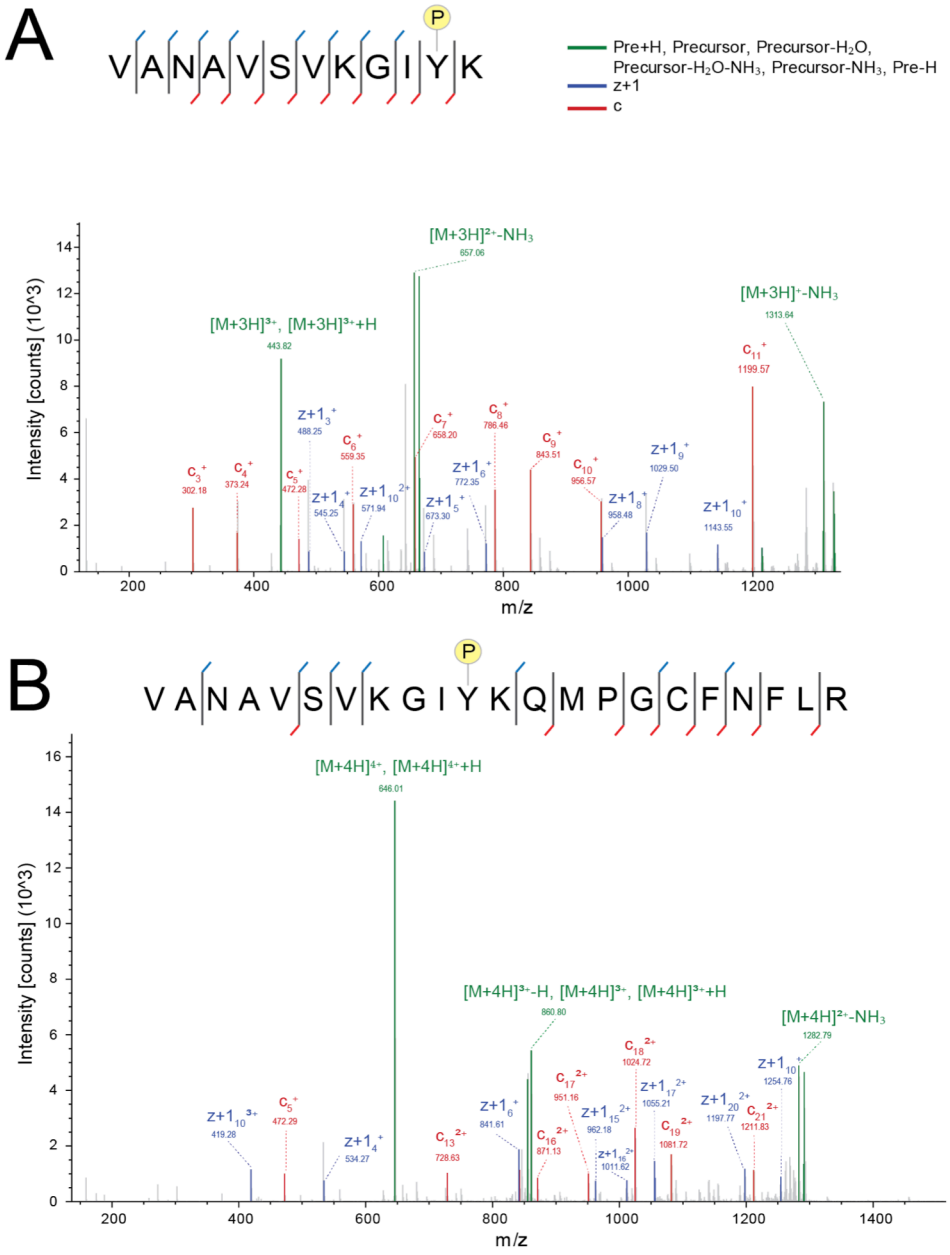

Figure 4.6 MS/MS spectra of peptides of derived from c-Abl-phosphorylated 9.
WT 9 was phosphorylated by c-Abl and was digested with Arg C protease which cleaves on the C-terminal side of arginine and lysine residues. Two peptide fragments showed phosphorylation at Y397 with high confidence. In the same analysis the peptides containing Y153 were only observed with intermediate confidence, nevertheless phosphorylation of Y153 was not indicated by this analysis.

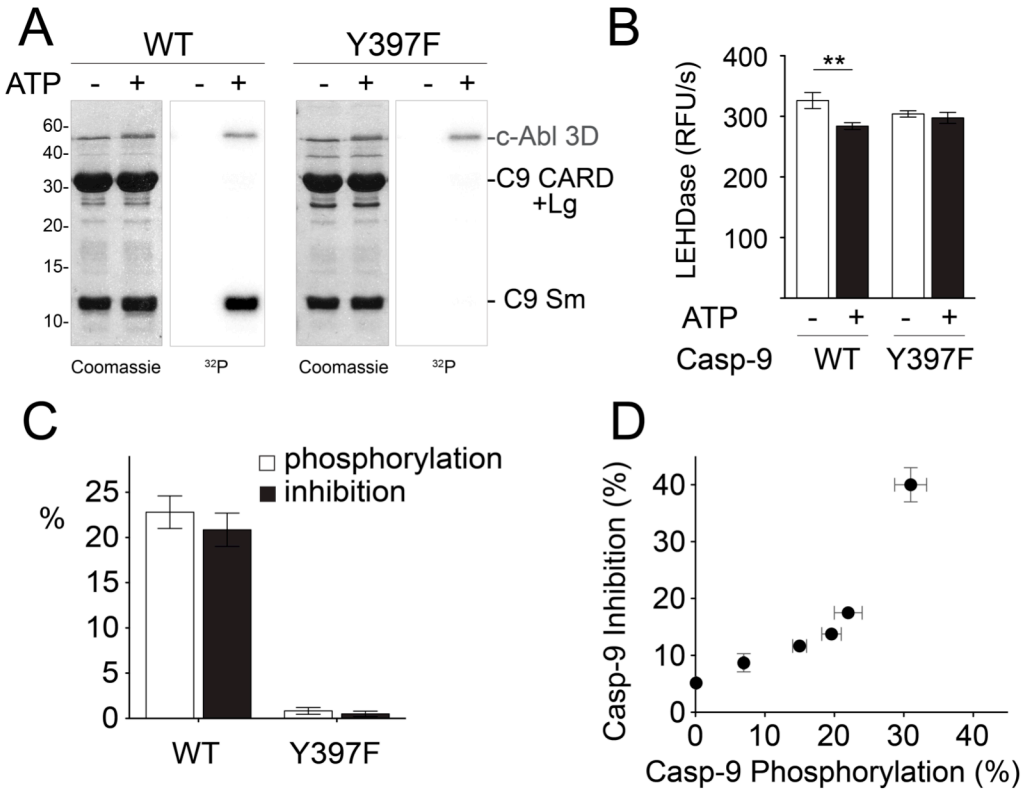

Figure 4.7. Phosphorylation of Y397 leads to caspase-9 inactivation.
(A) WT Caspase-9 and the unphosphorylatable variant Y397F were subjected to *in vitro* phosphorylation by Abl in the presence or absence of ATP for 2h. Phosphorylation of the small subunit was clearly observed in WT caspase-9 but was essentially absent for caspase-9 Y397F. Only background levels of phosphorylation were visible in the CARD+Large region. Gels and corresponding autoradiographs shown are representative of four independent trials performed on four separate days.
(B) Inhibition of WT and Y397F caspase-9 by phosphorylation. The activities of samples in (A) after incubation with c-Abl for 2h were measured using the caspase-9 preferred substrate Ac-LEHD-AFC. WT caspase-9 was moderately inhibited whereas caspase-9 Y397F was insensitive to c-Abl-mediated inhibition. The reduced LEHDase activity for phosphorylated WT caspase-9 (+ ATP) was statistically different from that of unphosphorylated WT (- ATP) (**$P<0.05$) as determined by Student's t-test. Data shown are means ± SEM from four independent experiments performed on four separate days.
(C) The level of caspase-9 phosphorylation correlates with the extent of inhibition. Phosphorylation levels of caspase-9 were determined from [γ-^{32}P]ATP standards exposed on the same autoradiograph as the Coomassie-stained SDS-PAGE gel (see under Methods, Figure 4.18). Percent inhibition for phosphorylated caspase-9 (both c-Abl and ATP present) was normalized against activity in the non-phosphorylated form (with c-Abl but no ATP). Data shown are means ± SEM from four independent experiments performed on four separate days.
(D) Correlation plot between caspase-9 inhibition and caspase-9 phosphorylation. WT caspase-9 was initially phosphorylated *in vitro* by c-Abl and was subjected to phosphoprotein enrichment to capture a greater fraction of phosphorylated caspase-9. Data shown are means ± SD from three independent experiments performed on three separate days.

We also observed that phosphorylation of Y397 is reversible; treatment with CIP (Calf Intestinal Phosphatase) removed phosphorylation with a concomitant rescue in activity (Figure 4.8).

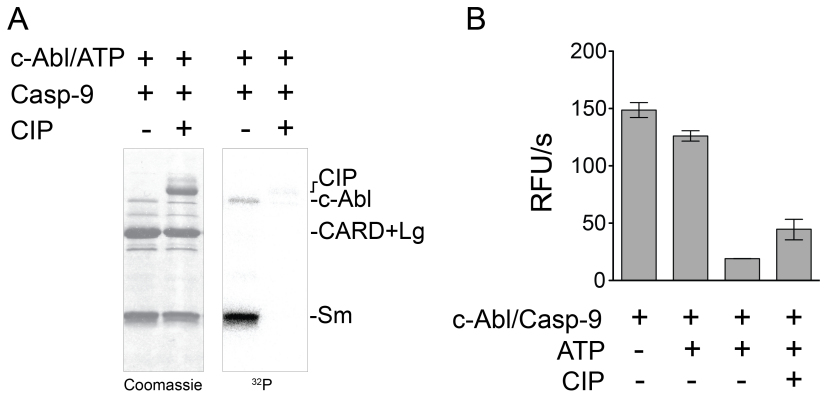

Figure 4.8. Dephosphorylation of caspase-9 relieves inhibition.
(A) c-Abl phosphorylated caspase-9 is dephosphorylated by CIP (Calf Intestinal Phosphatase) for 1h. No visible phosphorylation remains in the CIP-treated caspase-9, suggesting that phosphorylation by c-Abl is reversible.
(B) CIP treatment to dephosphorylate caspase-9 leads to recovery of activity. *Note:* CIP reaction buffer contains 100 μM $ZnCl_2$, which fully inhibits caspase-9 activity. Even when diluted into caspase-9 activity assay buffer, caspase-9 is still partially inhibited, hence the large difference in LEHDase activity before and after CIP treatment.

One of the hallmarks of suppressed apoptosis emanating from caspase-9 inhibition is the attenuation of the cleavage of downstream substrates caspase-3 and caspase-7[20]. WT Caspase-9 phosphorylated by c-Abl cleaved full-length caspase-7 and caspase-3 more slowly than unphosphorylated WT caspase-9 (Figure 4.9A, 4.9E). In contrast, there was no significant difference in caspase-7 or caspase-3 cleavage kinetics by caspase-9 Y397F regardless whether c-Abl was active (+ ATP) or not (no ATP) (Figure 4.9B, 4.9F). This recapitulates the previous finding that Y397F is insensitive to inactivation by c-Abl. Importantly, the degree of caspase-9 phosphorylation also correlates with the decrease of its protein cleavage kinetics (Figure 4.9C, 4.9D for caspase-3 and Figure 4.9G, 4.9H for caspase-7). It is worthwhile to note that Y397F is as active as WT caspase-9 (Table 4.1), therefore the decrease in caspase-9 activity can be unambiguously attributed to phosphorylation and not simply due to inherent sensitivity of this site. Along these lines, we observed a five-fold decrease in catalytic efficiency in the Y397E

phosphomimetic (Table 4.1) and attenuated protein cleavage kinetics (Figure 4.10A, 4.10B). Although Y397E is not a perfect surrogate for phosphorylated Y397, it manifests similar functional outcome to Y397 phosphorylation. Thus one functional effect of Y397 phosphorylation by c-Abl is to diminish caspase-9's activation of executioner caspases.

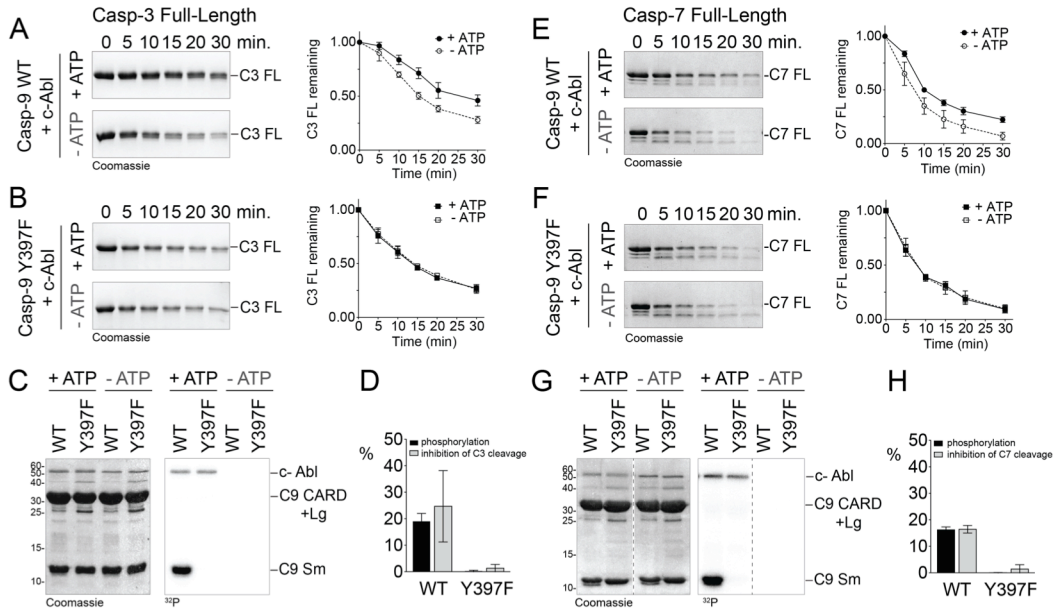

Figure 4.9. Phosphorylated caspase-9 exhibits slower protein cleavage kinetics.
(A) WT or (B) Y397F caspase-9 was incubated with c-Abl in the presence or absence of ATP. 1 μM caspase-9 from the phosphorylation reaction was allowed to cleave 3 μM full-length caspase-3 C163A (catalytic-site inactivated variant) (C3 FL) for 30 min. Cleavage kinetics for each reaction are plotted as a function of the disappearance of the C3 FL band.
(C) Representative Coomassie-stained gels and corresponding autoradiographs of phosphorylation reactions used in (A) and (B). Caspase-9 WT is visibly phosphorylated at Y397.
(D) Correlation between caspase-9 phosphorylation as detected by autoradiography in (C) and inhibition of caspase-3 (C3) cleavage after 30 min. as shown in (A) and (B).
(E) and (F) Caspase-9 WT or Y397F was incubated with c-Abl in the presence or absence of ATP. 1 μM of caspase-9 from the phosphorylation reaction was allowed to cleave 3 μM full-length caspase-7 C186S (catalytic site inactivated variant) (C7 FL) for 30 min. Cleavage kinetics for each reaction are plotted as a function of the disappearance of the C7 FL band.
(G) Representative Coomassie-stained gel and corresponding autoradiograph of phosphorylation reactions used in (E) and (F). Caspase-9 WT is phosphorylated at Y397.
(H) Correlation between caspase-9 phosphorylation as detected by autoradiography in (G) and inhibition of caspase-7 (C7) cleavage after 30 min. as shown in (E) and (F).
Data shown for all of the above experiments are means ± SEM from three independent experiments done on three separate days.

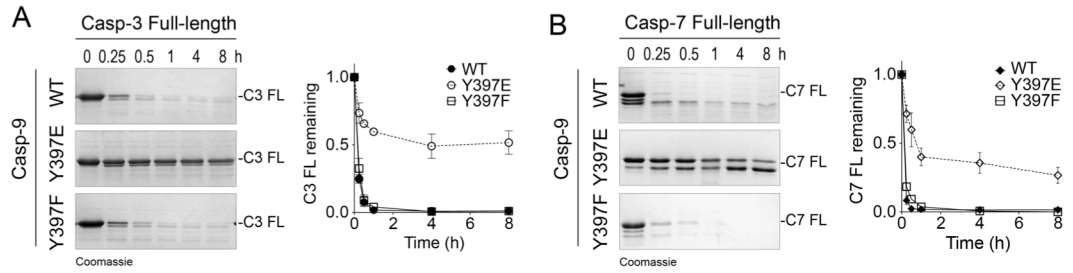

Figure 4.10. Caspase-9 Y397E showed attenuated cleavage kinetics of protein substrates. Cleavage of full-length catalytic site-inactivated variants caspase-3 C163A (A) and caspase-7 C186S (B) by WT caspase-9, Y397E and Y397F, as shown in Coomassie-stained denaturing gels. The intensity of the bands from the cleavage assays were quantified and plotted as a function of amount of full-length substrate protein remaining in the panels on the right. Data shown are means ± SEM of three independent experiments done on three separate days.

Model for caspase-9 inhibition by Y397 phosphorylation

The substrate binding site of active, dimeric caspases consists of highly mobile loops - L2, L3, L4 from one monomer and L2' from the opposite monomer - which, upon substrate binding, assume a properly ordered conformation to perform catalytic cleavage. Y397 is situated in loop L4 of caspase-9 (Figure 4.1A, 4.11B). In the substrate-bound structure, Y397 participates in the hydrophobic network along with I396 and W362 to engage the hydrophobic P4 residue (Figure 4.11A). Modeling a phosphotyrosine in place of Y397, it appears that both the added bulk and charge of phosphoY397 would directly impact substrate binding. Being situated in a highly mobile loop, the phosphotyrosine could be envisioned to reach into the substrate-binding cavity, essentially creating steric and electrostatic clashes with other subsite residues (Figure 4.11B). This would either directly obstruct the incoming substrate from binding, or prevent the loop bundle from assuming an ordered conformation keeping the active site in an unproductive state, or both.

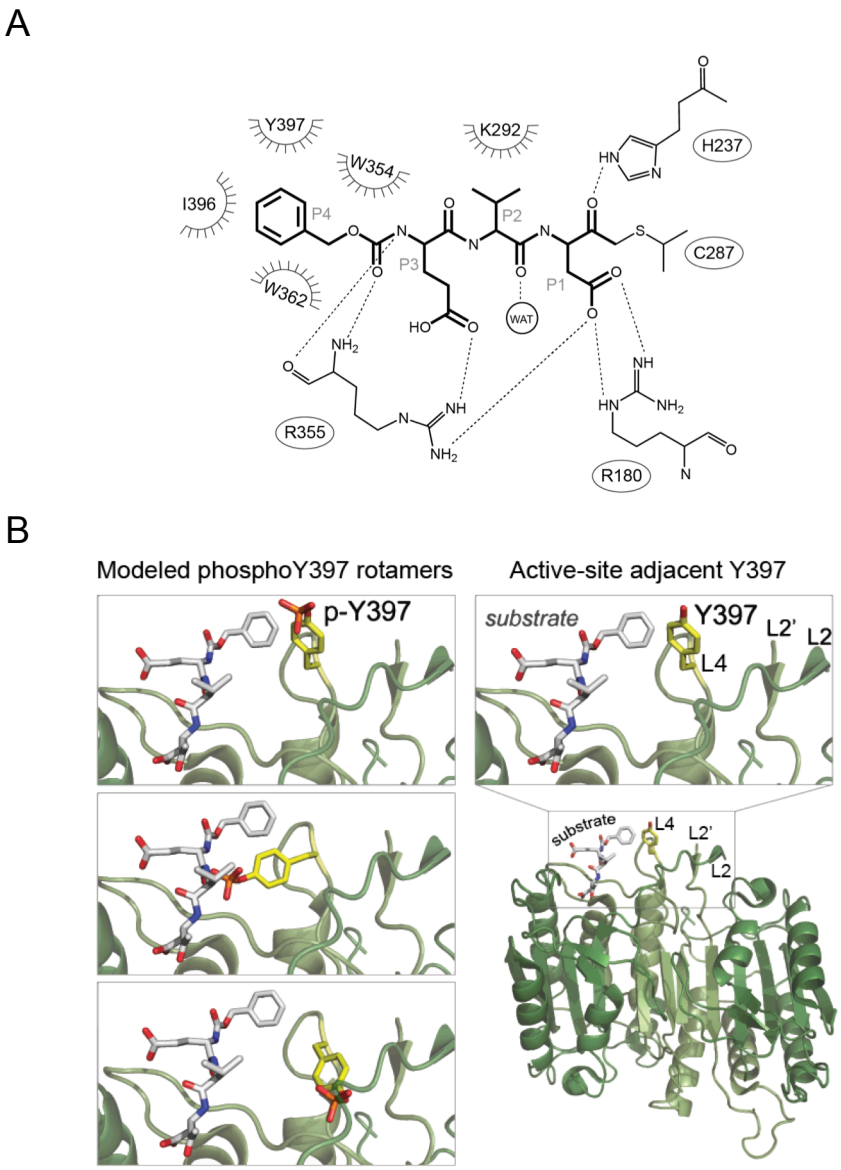

Figure 4.11. Models for 9 inhibition by phosphorylation at Y397.
(A) A diagram of the interactions of 9 residues in the active site with the irreversible peptide inhibitor *Z*-EVD-Dcbmk (benzoxycarbonyl-Glu-Val-Asp-dichlorobenzylmethyl ketone) was generated using Ligplot[58]. The substrate peptide residues are labeled P4, P3, P2 and P1. Broken lines indicate H-bonds. Half-circles ( ) indicate hydrophobic interactions within 5 Å of 9 residues. Y397 takes part in a hydrophobic network to stabilize the side chain in the P4 position in the only extant structure of 9 (PDB ID 1JXQ) bound to a tripeptide capped at the N-terminus with a carboxybenzyl moiety. In the structure the carboxybenzyl occupies the S4 pocket which binds hydrophobic residues in the 9 recognition sites.
(B) Y397 is in the highly mobile L4 loop, in close proximity to the substrate-binding cavity and loops L2 and L2'. A phosphotyrosine in this position (p-Y397) could create steric clashes and potentially prevent substrate binding by blocking access to the active site cavity, or by preventing the active site loops from achieving the catalytically competent conformation. Modeling of the phosphotyrosine was performed in Coot[59] using PDB 1JXQ.

Y397 is phosphorylated in cells upon direct c-Abl activation

In vitro phosphorylation coupled with the use of unphosphorylatable protein variants has allowed identification of putative residues phosphorylated by kinases. However alternative specificity of kinases towards substrates *in vitro* has been reported in isolated cases[21]. The lack of regulatory elements normally present intracellularly has been suggested to contribute to altered phosphorylation. To determine whether Y397 was a *bona fide* cellular site of phosphorylation, recombinant WT caspase-9 was added into HEK 293T lysates supplemented with [γ-^{32}P]ATP and orthovanadate, a phosphatase inhibitor. This resulted in visible phosphorylation of the CARD+Large (Figure 4.12A, Figure 4.13A, no Abl). Given that there are other kinases readily activated by addition of ATP and treatment of orthovanadate, and that caspase-9 has multiple phosphorylation sites in this region[9,11,13–15,22,23], we were not surprised by this observation. Phosphorylation of the small subunit in WT caspase-9 in the absence of c-Abl was not evident, which could either be due to low titers of endogenous c-Abl in HEK 293T, or because c-Abl was not sufficiently activated, or both. Since the activation state of c-Abl was not known, the lysates were supplemented with recombinant c-Abl to allow *in trans* activation of c-Abl. This resulted in distinct phosphorylation of the small subunit in WT caspase-9, whereas Y397F exhibited negligible levels of small subunit phosphorylation (Figure 4.12A, 4.12B, 4.13B). For both WT and Y397F, the CARD+Large region appeared to retain its phosphorylation state. Addition of a c-Abl inhibitor, Imatinib, abrogated the phosphorylation of the small subunit but not that of the CARD+Large (Figure 4.12A). This implies that the phosphorylation observed for the small subunit was predominantly due to c-Abl, while that for the CARD+Large was not, and could be reliant on the action of other kinases.

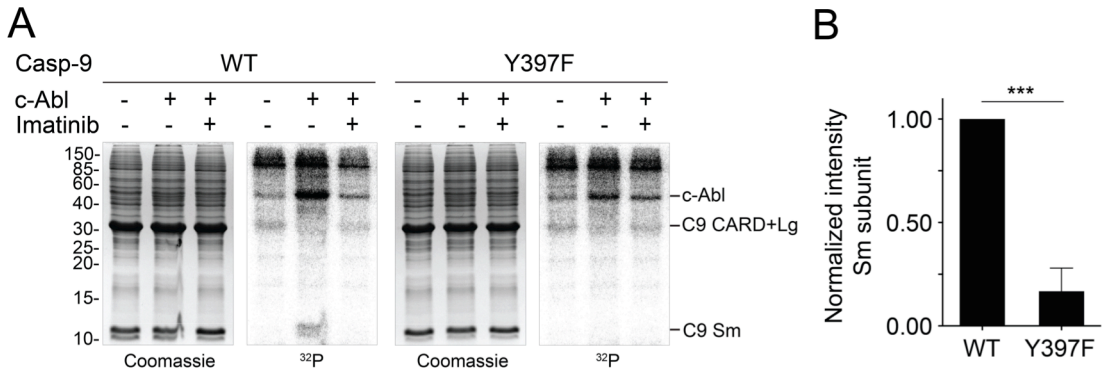

Figure 4.12. Caspase-9 is phosphorylated at Y397 by activated c-Abl in HEK 293T lysates.
(A) Recombinant caspase-9 was phosphorylated in HEK 293T lysates. Lysates were supplemented with 20 nM c-Abl, 200 μM orthovanadate and 1 mM ATP + [γ-^{32}P]ATP to ensure *in trans* activation of c-Abl. Where indicated, lysates were also treated with the c-Abl inhibitor Imatinib (200 μM) 30 min prior to addition of c-Abl. WT or Y397F caspase-9 (30 μg) were added to lysates to allow caspase-9 phosphorylation. WT but not Y397F caspase-9 showed phosphorylation in the small (Sm) subunit, which was not visible with Imatinib-treated lysates. In some trials, the small subunit of Y397F also appears to be labeled albeit at a significantly lower level than that of WT (Supplemental Figure S4.4B). The phosphorylation observed for CARD+Large appeared to be c-Abl-independent, since Imatinib did not eliminate its phosphorylation. The band was confirmed to correspond to ^{32}P-labeled CARD+Lg since it was not present in samples containing only lysates and [γ-^{32}P]ATP (Figure 4.14)
(B) Band intensities corresponding to a phosphorylated small subunit in WT and Y397F show that Y397F is significantly less phosphorylated (student's t-test indicates data is statistically significant ***$P<0.05$ at 99% confidence). Data shown are means ± SEM from three independent experiments performed on three separate days.

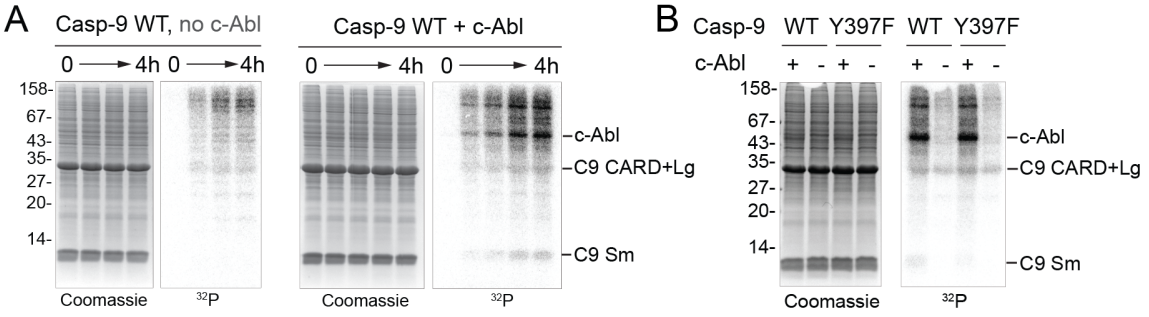

Figure 4.13. **Phosphorylation of recombinant caspase-9 in HEK 293T lysates.**
(A) Recombinant WT caspase-9 was incubated with HEK 293T lysates with and without added c-Abl (20 nM) over the course of 4h. The CARD+Large (CARD+Lg) region of caspase-9 is phosphorylated even without adding c-Abl. Only when c-Abl was added was there visible phosphorylation of the small (Sm) subunit.
(B)Phosphorylation states of WT caspase-9 and Y397F in lysates. The small subunit is clearly phosphorylated in WT and weakly phosphorylated in Y397F.

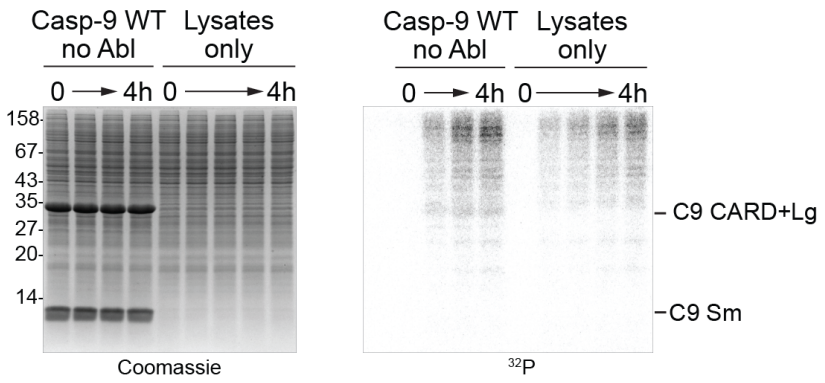

Figure 4.14. Negative control reactions in lysates.
WT caspase-9 is phosphorylated in the CARD+Lg region in the absence of activated c-Abl. The bands were verified to correspond to caspase-9 since a reaction containing only HEK293T lysates and ATP did not show ^{32}P-labeling at the corresponding molecular weight of the caspase-9 CARD+Lg.

We then proceeded to interrogate caspase-9 phosphorylation in cells upon activation of endogenous c-Abl. HEK 293T cells were treated with DPH, a known direct activator of c-Abl[24], along with the phosphatase inhibitor orthovanadate. This led to c-Abl activation, as manifested by phosphorylation of c-Abl at Y412[25]. In addition, CrkII, a well-known physiological substrate of c-Abl[26], was phosphorylated only upon treatment of DPH. The presence of active, phosphorylated c-Abl and phosphorylated CrkII were confirmed by immunoblot against the phosphorylatedresidues p-Y412 (for c-Abl) and p-Y221 (for CrkII) (Figure 4.15A). The c-Abl inhibitor Imatinib abolished these phosphorylation events, demonstrating that c-Abl is indeed activated by DPH and vanadate (Figure 4.15A).

In order to probe caspase-9 phosphorylation by c-Abl, HEK 293T cells were transfected with FLAG-tagged caspase-9 catalytic site-inactivated variant C287A and the unphosphorylatable C287A/Y397F variant. Transfected cells were then treated with DPH/vanadate to induce c-Abl activation (Figures 4.15B, 4.16A, 4.16B, panels labeled Total). Immunoprecipitated caspase-9 C287A was robustly tyrosine-phosphorylated as assessed by phosphotyrosine immunoblot (Figures 4.15B, 4.16A, 4.16B; panels labeled IP:FLAG). Together these data indicate that caspase-9 is a *bona fide* substrate of c-Abl. While phosphorylation was not entirely eliminated in

the unphosphorylatable variant C287A/Y397F, the level of phosphorylation was significantly weaker than in C287A, although the total amount of immunoprecipitated caspase-9 was the same in both transfected conditions (Figure 4.15B, 4.15C). Moreover, transfected cells treated with DMSO showed weak tyrosine phosphorylation of both C287A and C287A/Y397F, the phosphorylation levels of which are comparable to that of C287A/Y397F in DPH/vanadate-treated cells (Figure 4.16A). This strongly supports the model that Y397 is the predominant site for c-Abl phosphorylation upon its activation by DPH and is the dominant site of c-Abl phosphorylation in cells.

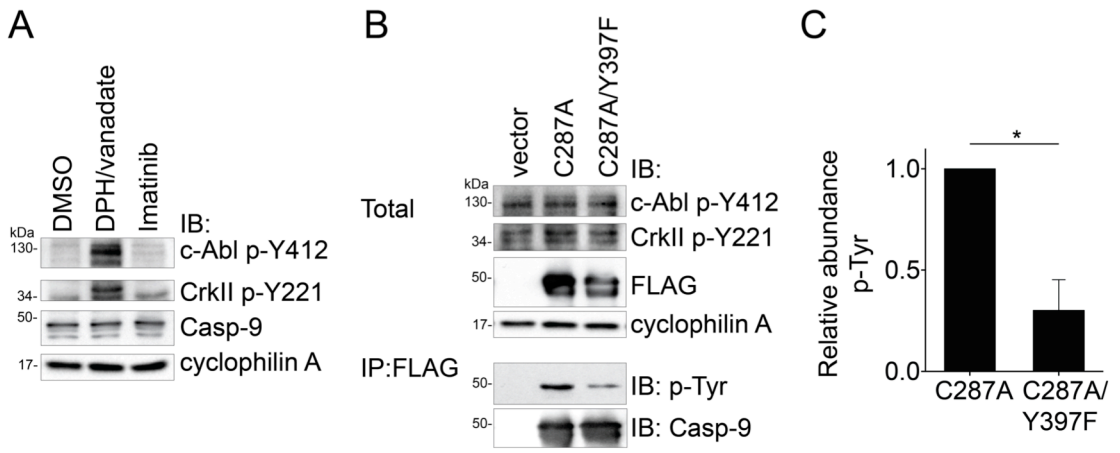

Figure 4.15. Activation of c-Abl leads to caspase-9 phosphorylation at Y397 intracellularly.
(A) c-Abl is activated by 5-(1,3-diaryl-1H-pyrazol-4-yl)hydantoin (DPH) in synergy with orthovanadate treatment. HEK 293T cells were treated with DMSO, the known c-Abl activating compound DPH + orthovandate, or Imatinib for 2h. Lysates were probed for active c-Abl as assessed by immunoblot (IB). Active c-Abl is phosphorylated at Y412. DPH/vanadate treatment clearly resulted in c-Abl activation, as manifested by phosphorylation at Y412 and downstream phosphorylation of a well-known c-Abl substrate, CrkII.
(B) Caspase-9 is phosphorylated at Y397 by active c-Abl intracellularly. HEK 293T cells were transfected with vector alone (p3xFLAG-CMV™-14), catalytic site-inactivated caspase-9 (C9 C287A-3xFLAG or) or the unphosphorylatable variant (C9 C287A/Y397F-3xFLAG). 24h post-transfection, cells were treated with DPH/vanadate for 2h, harvested and lysed. Immunoblot of total proteins confirmed c-Abl activation and caspase-9 expression. Caspase-9 was immunoprecipitated from lysates with an anti-FLAG antibody and probed with anti-phosphotyrosine (p-Tyr) and anti-caspase-9 by immunoblotting. Cells transfected with C287A/Y397F showed significantly lower levels of phosphotyrosine in uncleaved caspase-9 compared with those transfected with C287A, although the levels of immunoprecipitated caspase-9 in both C287A and C287A/Y397F were similar.
(C) Relative abundance of phosphotyrosine (p-Tyr) in caspase-9 C287A and C287A/Y397F. Band intensities of p-Tyr were normalized against corresponding band intensities of caspase-9 in the immunoprecipitates. Student's t-test indicates data is statistically significant *$P<0.05$ at 99% confidence. Data shown are means of three independent experiments done on three separate days.

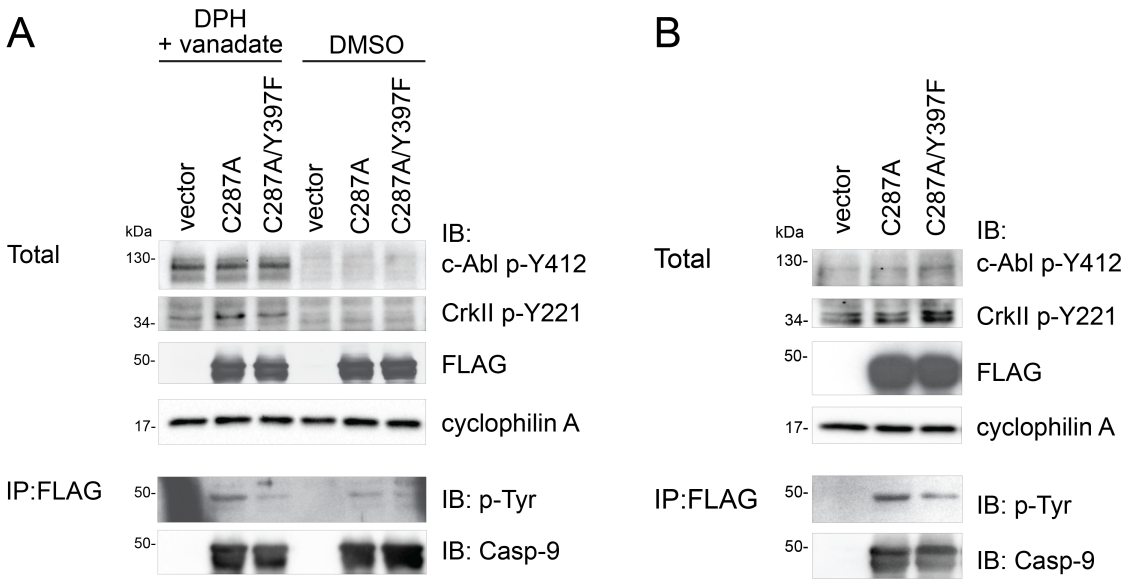

Figure 4.16. Independent trials of caspase-9 phosphorylation in cells by active c-Abl.
(A) Caspase-9 shows basal tyrosine phosphorylation in the absence of active c-Abl. Both caspase-9 C287A and C287A/Y397F in DMSO-treated cells showed weak tyrosine phosphorylation, the levels of which were similar to that of C287A/Y397F in DPH/vanadate-treated cells, suggesting that this basal phosphorylation is independent of c-Abl activity.
(B) Another independent trial showing that cells transfected with C287A/Y397F are less abundant in tyrosine phosphorylated-caspase-9 than those transfected with C287A.

Discussion

It is clear from the data presented here that Y397 is a *bona fide* site of phosphorylation intracellularly, as was predicted by *in vitro* phosphorylation studies using purified proteins. There has been some suggestion in the literature that *in vitro* phosphorylation of kinase substrates sometimes differs from in cellular phosphorylation[21,27,28]. We have not previously observed irregular phosphorylation of caspase substrates by any of the kinases we have studied[19,29,30]. Once again in this work, we found that *in vitro* phosphorylation by c-Abl accurately reflected the intracellular phosphorylation specificity we observed. This fidelity between *in vitro* and cell-based observations is probably due to caspase-9 being a direct substrate of c-Abl. Our data from multiple kinase:caspase pairs suggest that when the appropriate kinase is studied, *in vitro* and cellular phosphorylation patterns are conserved[19,29,30].

While it is clear that Y397 is a *bona fide* site of c-Abl phosphorylation of caspase-9, one of the most surprising aspects of our work is the fact that the reported sites on caspase-9, particularly Y153, was not observed to be phosphorylated by c-Abl either using purified proteins or intracellularly and was not activated by c-Abl as previously reported. This could be for a number of reasons. First, the study that identified Y153 phosphorylation as activating did not investigate the functional impact of substitutions at Y153 on proteolytic activity, but assumed that Y153F caspase-9 was proteolytically active[12]. In this work, we have shown that Y153F is intrinsically inactive. The intrinsic lack of activity led to the interpretation that Y153F transfected cells were less susceptible to cell death due to phosphorylation by c-Abl[12], when in fact, cells should have been rendered less susceptible to cell death due to the lack of proteolytic activity in Y153F caspase-9. Second, it is important to note that Y397 is contained within a much more ideal c-Abl recognition site than Y153 is. Second, c-Abl phosphorylation of caspase-9 at Y153 was reported after induction of DNA damage[12]. c-Abl is known to shuttle between the cytosol and the nucleus[31] and DNA damage activates the nuclear c-Abl[32,33]. It is possible that c-Abl activated by DNA damage has an altered sequence specificity or recognizes caspase-9 in complex with cofactors that direct phosphorylation to Y153, or prefers to phosphorylate Y153 in caspase-9 in a different conformational state. We are only able to speculate on the altered specificity or complex formation, but we have evidence that the conformational state is not likely to contribute significantly to the ability of c-Abl to recognize caspase-9. We found that neither caspase-9 in the zymogen nor in the cleaved state was phosphorylated at Y153 (Figure 4.3B, 4.3D) *in vitro*. Fourth, cases of multisite phosphorylation on proteins resulting in antagonistic effects have been reported[34,35], so it is possible that two sites in caspase-9 are differentially phosphorylated by c-Abl *in vivo*. Finally, and most probably, it is also possible that c-Abl activated by DNA damage activates another kinase that is responsible for Y153 phosphorylation. The fact that Y397 is contained within a more ideal c-Abl recognition site than Y153 may also suggest that Y153

phosphorylation is achieved not by c-Abl directly, but by a different kinase that is activated by c-Abl or by the same stimuli that activate c-Abl.

Y397 is present in the L4 loop, which forms the side of the substrate-binding groove in caspases. This site is a privileged location for regulation in that is adjacent to but does not directly interact with substrate. No phosphorylatable tyrosines are present in the L4 loops of other caspases (Figure 4.17A, 4.17B) so phosphorylation by c-Abl and inhibition by this active-site adjacent mechanism is likely to be unique to caspase-9. Thus Y397 may provide a chemical handle for development of compounds that inhibit caspase-9 specifically. Interestingly, in caspase-6, C264 which is also in the L4 loop, is palmitoylated[36]. The functional impact of this palmitoylation has not been fully uncovered but it is tempting to speculate that like caspase-9 Y397 phosphorylation, caspase-6 C264 palmitoylation may result in loss of activity.

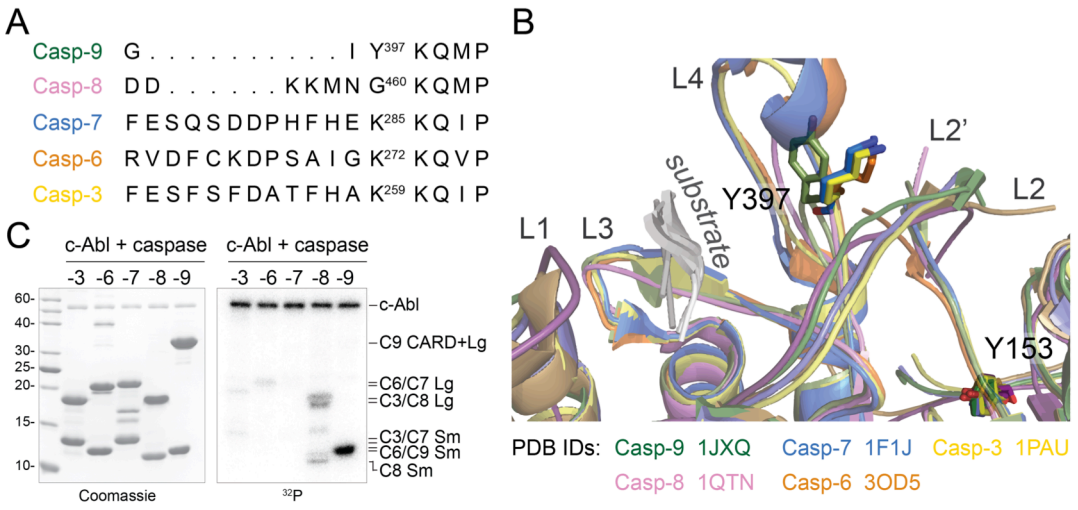

Figure 4.17. Y397 is unique to caspase-9.
(A) Sequence alignment of loop L4 of apoptotic caspases. Only caspase-9 contains the phosphorylatable tyrosine at any position in the L4 loop.
(B) Structure alignment of caspases -3, -6, -7, -8 and -9 highlighting the active site loop bundle. Residues corresponding to sites Y153 and Y397 are shown in sticks. A tyrosine in Y153 site is present in all caspase structures shown, while only caspase-9 has a tyrosine in position Y397.
(C) Other apoptotic caspases were incubated with c-Abl in the presence of ATP + [γ-^{32}P]ATP to assess the ability of c-Abl to phosphorylate them. Caspase-9 clearly appears to be the preferred substrate of c-Abl over other caspases in vitro. Caspase-8 is weakly phosphorylated at both its large and small subunits. The following caspase variants were used: caspase-3 CT C163A, WT caspase-6 CT, caspase-7 CT C186S, caspase-8 ΔDED and WT caspase-9 CT. CT refers to Constitutively Two-Chain caspase construct.

The L4 has the most diverse sequence among the active site loops in the apoptotic caspases thus posttranslational or targeted modification of L4 could be an amenable method of inhibition as it might confer added specificity for each caspase.

While the full impacts of Y397 phosphorylation are not known it is tempting to speculate about the functional impact of this phosphorylation event. A prevalent consequence of phosphorylation is to impact protein-protein interactions. Phosphorylation can either disrupt or promote binding and in some cases even create a new binding interface. The region where Y397 resides, ^{395}GIYK^{398}, in L4 of caspase-9 is involved in crystal contacts[37], which may suggest that this region could potentially be involved in protein-protein binding under native conditions as well. Caspase-9 is activated by recruitment to the apoptosome via CARD-CARD interactions with Apaf-1[38]. Recently, a structure of the human apoptosome revealed that a monomer of caspase-9 core (p20/p10) is "parked" on the apoptosome hub, likely in a dynamic manner, independent of the other caspase-9 dimer/s undergoing activation within the CARD-CARD ring[39]. Monomeric caspase-9 cores were also reported to bind to the apoptosome by forming heterodimer with the Apaf-1 nucleotide oligomerization domain (NOD) via the caspase-9 small (p10) subunit[40]. In addition, the apoptosome of *C. elegans* formed from CED4 and CED3 (homologues of Apaf-1 and caspase-9, respectively) shows that the L2' region of CED3 directly interacts with the oligomerized CED4 and is crucial in the formation of a functional holoenzyme[41]. These observations imply that in addition to the CARD, other regions in caspase-9 interact with the apoptosome and potentially influence its activation. Perhaps the Y397 region of the small subunit is involved in direct interactions with the apoptosome, such that phosphorylation of Y397 would impact these interactions.

c-Abl has been reported to play both pro-apoptotic and anti-apoptotic/pro-survival roles. The fact that caspase-9 is inhibited by c-Abl phosphorylation at Y397 suggests that this molecular event contributes to the pro-survival nature of c-Abl. Whereas c-Abl activation by DNA damage is known to induce cell death, hyperactive cytoplasmic kinase activities of c-Abl and Abl fusion

proteins are recognized for their oncogenic potential[42,43]. Overexpression and activation of c-Abl has been detected in certain breast, colon and lung cancer carcinoma, and in some cases melanoma (review[43]). A prime example is BCR-Abl fusion kinase, whose loss of autoinhibition and increased catalytic activity is highly persistent in chronic myelogenous leukemia (CML) (reviews[44,45]). Besides deregulation and hyperactivity, the expanded diversity of Abl substrates due to altered specificities is thought to be another driving force towards oncogenicity[46,47]. Thus Abl phosphorylation of pro-apoptotic proteins with a loss-of-function consequence is consistent with c-Abl's anti-apoptotic/pro-survival function. Targeting an initiator caspase such as caspase-9 serves as an efficient route to execute an upstream block in apoptosis signaling.

The dynamic crosstalk between caspases and kinases enables their co-regulation, which is essential for cellular homeostasis. In many cases kinases are regulated by proteolysis by the very caspases they phosphorylate (reviews[6,48]). The cellular outcome, whether promotion or suppression of apoptosis, is dictated by which functional impact overcomes or precedes the other: caspase phosphorylation or kinase cleavage. We did not observe any apparent cleavage of c-Abl by caspase-9 *in vitro*. One possibility is that caspase-9 only exhibits basal or much lower levels of activity whereas the kinase activity of c-Abl is heavily favored under *in vitro* phosphorylation conditions. It is also possible that c-Abl is simply not a preferred substrate of caspase-9. However, the case might be different intracellularly since c-Abl was shown to be cleaved by caspase-8 and caspase-3 causing its transformation to an active state[49] and/or its relocation to the nucleus[50]. Given that c-Abl exerts dual yet opposing functions in apoptosis, one could infer that the molecular dialogue between c-Abl and caspase-9 would especially be more relevant in cell death signaling. We also observed that among apoptotic caspases, caspase-9 is the most preferred substrate of c-Abl (Figure 4.15C); we envision that exploiting this interaction could be a suitable approach to specifically control caspase-9 function.

More phosphorylation sites have been reported in caspase-9 than in any other caspase (reviews[6–8]). Perhaps this is simply due to the fact that more effort has focused on caspase-9, or

because there is a need for additional regulation of caspase-9. The latter is more likely, as caspase-9's upstream function requires exquisite control to prevent any inopportune amplification of apoptotic signals. Given the rapid rate of proteomics advancement, we expect more phosphorylation sites to be reported on caspases under different cellular conditions. In the study of the interactions of kinase with their substrates, it is often insufficient to rely solely on cell-based assays, particularly when the intrinsic activity of mutant enzymes has not been assessed. Accurately identifying functionally relevant sites and elucidating the mechanism of phosphoregulation requires complementary cellular, biochemical and structural interrogation, as was done in this case.

Our recent data elucidating Y397 phosphorylation adds to the growing list of caspase phosphoregulation (*see* Chapter V, Table 5.1). Our results clearly demonstrate that Y397 in caspase-9 is a *bona fide* and the dominant site of phosphorylation by c-Abl intracellularly. An active-site adjacent residue, Y397 does not seem to participate in strong molecular interactions with residues within the substrate-binding pocket or with the substrate itself, but phosphorylation transforms this site to one that directly inhibits substrate binding. This is the first report of a novel c-Abl phosphorylation site unique to caspase-9, and targeting Y397 may serve as an alternative approach for the specific control of caspase-9. Our results suggest that phosphorylation of caspase-9 by c-Abl is an important mechanism by which c-Abl fulfills its survival role to escape apoptosis. The next studies prompted by these findings are to determine the level of caspase-9 phosphorylation at Y397 in cancer cells where c-Abl is overexpressed and hyperactive as it may provide possible avenues for caspase-kinase co-therapies in cancer and other proliferative diseases.

Materials and Methods

DNA constructs

The caspase-9 full-length wild-type (C9FL WT) expression construct (gift of Guy Salvesen) consists of the human caspase-9 gene (amino acids 1-416) with C-terminal 6x His tag in pET23b[54]. The caspase-9 constitutively two-chain (C9 CT) construct consists of an *E. coli* codon-optimized synthetic gene (GenScript) built for expression of the CARD+Large subunit (amino acids 1-315) and separate expression of the small subunit (amino acids 316-416 plus 6xHis) which was under the control of a second ribosome binding site. The Caspase-9 ΔCARD expression construct was made by deleting the CARD in the C9FL construct by deletion mutagenesis and inserting a start codon before the first amino acid (Val-139) of the large subunit. Caspase-3 full-length wild-type expression construct (gift of Guy Salvesen) consists of the human caspase-3 gene (amino acids 1-279 plus 6x His) in pET23b [55]. Caspase variants encoding amino acid substitutions were generated by point mutagenesis. Bacterial expression constructs for the c-Abl kinase domain (c-Abl kinase) (residues 229-511) in pET28a, c-Abl SH3-SH2-kinase domains (c-Abl 3D) (residues 46-515) in pET28a and YopH phosphatase in pCDFDuet-1 were gifts from Markus Seeliger[56] (Stony Brook University School of Medicine, NY). Both c-Abl constructs have a TEV protease-cleavable 6xHis tag at the N-termini. For caspase-9 expression in HEK 293T cells, caspase-9 FL C287A or FL C287A/Y397F gene was subcloned between HindIII and BamHI sites of the p3xFLAG-CMV™-14 vector (Sigma), producing a C-terminally 3xFLAG-tagged caspase-9 expression construct.

Expression and Purification of Proteins

Purification of caspase-9 proteins. Caspase-9 (FL, CT and ΔCARD expression constructs) in pET23b were individually transformed into the BL21(DE3) *E. coli* strain. Cells were grown in 2xYT media with 100 μg/mL of Ampicillin at 37˚C with shaking until OD_{600}=1.2. The temperature was lowered to 15˚C and protein expression was induced with 1 mM IPTG for 3

h. Cells were harvested by centrifugation at 4,700 x g for 10 min at 4˚C. Thawed cells were resuspended in a buffer containing 50 mM sodium phosphate pH 7.0, 300 mM NaCl, 2 mM imidazole and lysed by use of a microfluidizer (Microfluidics, Inc.). Cell lysate was clarified by centrifugation at 37,000 x g for 1 h at 4˚C. The supernatant was then loaded onto a HiTrap Ni-affinity column (GE Healthcare). Proteins were eluted using a linear imidazole gradient from 2-100 mM. Fractions containing caspase-9 were pooled, diluted eight-fold in 20 mM Tris pH 8.5, 5 mM DTT and loaded onto a HiTrap Q-column (GE Healthcare). Proteins were eluted using a linear NaCl gradient from 0-275 mM. Caspase-9 eluted in buffer with 180 mM NaCl. Peak fractions were analyzed by SDS-PAGE for purity and stored in -80˚C until further use.

Purification of caspase-3. Full-length caspase-3 (wild-type or the catalytic site inactivated variant C163S expression constructs) in pET23b were individually transformed into the BL21(DE3) strain of *E. coli*. Cultures were grown in 2xYT media supplemented with 100 µg/mL ampicillin at 37˚C with shaking until OD_{600}=0.8. The temperature was lowered to 30˚C and protein expression as induced by 1 mM IPTG for 3 h. Cells were harvested by centrifugation at 4,700 x g for 10 min at 4˚C. Cells were freeze-thawed, resuspended in lysis buffer (50 mM sodium phosphate pH 8,300 mM NaCl, 2 mM imidazole) and lysed by use of a microfluidizer. Lysed cells were centrifuged at 30,600 x g for 50 min at 4˚C to remove cellular debris. The supernatant was loaded onto a HiTrap Ni-NTA column. The column was then washed with 50 mM imidazole in lysis buffer and proteins were eluted with 250 mM in lysis buffer. The eluent was diluted six-fold with buffer A (20 mM Tris pH 8.0, 3 mM DTT) and loaded onto a HiTrap Q-column. Proteins were eluted using a linear gradient from 0 – 500 mM NaCl. Caspase-3 eluted in buffer A with 250 mM NaCl. Peak fractions were analyzed by SDS-PAGE for purity and stored in -80˚C until use.

Purification of c-Abl kinase. c-Abl kinase was purified according to a method developed by Seeliger, et al[56]. Briefly, the expression constructs for c-Abl in pET28a and for YopH in pCDFDuet were co-transformed in BL21(DE3) *E. coli* cells. Cells were grown in 2xYT media

supplemented with kanamycin (50 μg/mL) and streptomycin (50 μg/mL) at 37˚C with shaking until OD_{600}=1.2. The temperature was lowered to 18˚C and protein expression was induced with 0.2 mM IPTG for 16h. Cells were harvested by centrifugation at 4,700 x g at 4˚C and stored in -80˚C until use. Thawed cells were resuspended in lysis buffer (50 mM Tris pH 8.0, 500 mM NaCl, 5% glycerol, 25 mM imidazole), lysed by passing through a microfluidizer and centrifuged at 37,000 x g for 1h at 4˚C. The supernatant was loaded onto a 5-mL HiTrap Ni-affinity column. Proteins were eluted using a linear gradient of 25 – 250 mM imidazole in lysis buffer. Fractions containing c-Abl were pooled and treated with TEV protease to cleave the His-tag (1 mg of TEV per 25 mg of crude kinase). Cleavage proceeded at 4˚C for 16 h while dialyzing against 20 volumes of buffer A (20 mM Tris pH 8.0, 100 mM NaCl, 5% glycerol and 1 mM DTT). The dialysate was diluted two-fold with buffer A and loaded onto a HiTrap Q column. The column was developed using a linear gradient of 100-350 mM NaCl in buffer A. c-Abl eluted in buffer A with 200 mM NaCl. Peak fractions were analyzed by SDS-PAGE for purity and stored in -80˚C until use.

***In vitro* phosphorylation and dephosphorylation of caspase-9**

Autophosphorylation of c-Abl. c-Abl (20 μM) was incubated in kinase activity buffer (50 mM Tris-Cl pH 7.5, 20 mM $MgCl_2$, 0.1 mM EDTA, 0.5 mM EGTA, 5 mM β-glycerophosphate, 1 mM Na_3VO_4) and allowed to autoactivate in the presence of 250 μM ATP spiked with [γ-^{32}P]ATP (10 μCi/μL, Perkin Elmer) for 2 h at 30˚C.

Phosphorylation of caspase-9. Caspase-9 (50 μM) was incubated with 1 μM of autoactivated c-Abl in kinase activity buffer with 1 mM ATP with [γ-^{32}P]ATP for 4 h at 30˚C. For phosphorylation of caspase-9 in HEK 293T lysates, 20 nM of c-Abl was incubated first with the lysates (150 μg total protein) with or without Imatinib (200 μM, Sigma) for 30 min. Caspase-9, WT or Y397F, (30 μg) was then added and the reaction was allowed to proceed for 4h at 30˚C.

Dephosphorylation of caspase-9. Phosphorylation reactions were treated with calf intestinal alkaline phosphatase (CIP)(NEB) (10 U for every 10 µg of incorporated phosphate). The reaction was incubated at 30˚C for 1 h. Removal of phosphates was confirmed by the loss of band intensity in the phosphorimage.

Phosphoenrichment. c-Abl-phosphorylated caspase-9 WT (100 µM) was buffer-exchanged into a loading buffer (TALON® PMAC kit, Clontech) using a NAP™5 desalting column (GE Healthcare). The buffer-exchanged protein solution was then mixed with TALON® PMAC magnetic beads (Clontech) for 1 h at 4˚C. The beads were washed twice with loading buffer and phosphorylated proteins were eluted stepwise from the beads using 250 mM sodium phosphate pH 7.2, 0.5 M NaCl. Protein concentrations of eluted fractions were estimated using a BCA (bicinchoninic acid) assay kit (Pierce™, Thermo Scientific).

All reactions were stopped by addition of SDS-PAGE sample dye and boiling for 10 min. Proteins were resolved by denaturing SDS-PAGE. Phosphorimages were obtained using Typhoon FLA 7000 (GE Healthcare) and bands were quantified using ImageQuant TL software (GE Healthcare). Amount of phosphate incorporated was quantified from an ATP standard curve on the same phosphorimage (Figure 4.18).

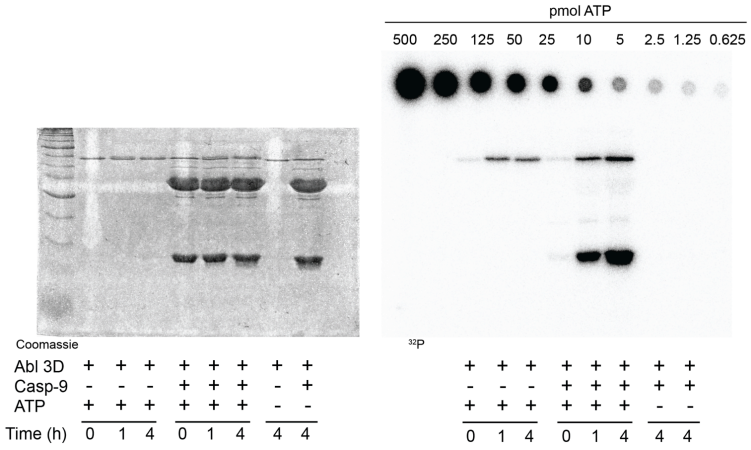

Figure 4.18. [γ-^{32}P]ATP standards allow quantification of phosphorylation levels in caspase-9.
Representative Coomassie-stained gel and corresponding phosphorimage of casp-9 phosphorylation by the three domain (3D) c-Abl kinase in the presence of [γ-^{32}P]ATP with ATP standards on the same phosphorimage. The intensity of the standards allowed phosphorylation levels in casp-9 and c-Abl to be accurately quantified.

Caspase-9 activity assay

Caspase-9 was diluted in caspase-9 activity assay buffer (100 mM MES pH 6.5, 10% PEG 8000, 5 mM DTT) to a final concentration of 800 nM. For determination of catalytic parameters, a substrate titration was performed in the range of 0 - 3 mM fluorogenic substrate Ac-LEHD-AFC (Ex 365 / Em 495) (Enzo Life Sciences). Enzyme concentrations were determined by active-site titration using a quantitative inhibitor z-VAD-FMK (Enzo Life Sciences). The rate of LEHD cleavage (LEHDase) was measured using a Spectramax M5 fluorescence plate reader (Molecular Devices). For caspase-9 activity assays after phosphorylation, 1.5 μM of caspase-9 and 1 mM substrate were used.

Protein Cleavage assays

Self-cleavage. Zymogen forms of caspase-9 (WT, Y153E, Y153D and Y153F) (3 μM) were allowed to undergo self-cleavage in a minimal activity assay buffer (100 mM MES pH 6.5, 20% PEG 400, 5 mM DTT) at 37˚C over the course of 2 h.

Cleavage by caspase-3. Caspase-3 WT (20 nM) was prepared in caspase-3 activity assay buffer (20 mM HEPES pH 7.5, 150 mM NaCl, 5 mM $CaCl_2$, 10% PEG 400, 2 mM DTT). Full-length, uncleaved caspase-9 (catalytic site inactivated variant C287A or phosphomimetics Y153E and Y153D, or Y153F) (5 μM) was added and the reaction was incubated at 37˚C for times indicated.

Cleavage of caspase-3 and caspase-7 by caspase-9. Caspase-9 WT or Y397F (50 μM) was initially phosphorylated by c-Abl. Phosphorylated (WT) and unphosphorylated (Y397F) caspase-9 was then diluted to 1 μM in caspase-9 minimal activity buffer after which each of the catalytic site inactivated variants of caspase-3 C163S or caspase-7 C186A were added to a final concentration of 3 μM and incubated at 32˚C. Aliquots were taken at different time points within 30 min.

All cleavage reactions were stopped by addition of SDS-PAGE sample buffer and boiling for 10 min. Bands were quantified by densitometry using ImageLab software (BioRad).

Mammalian Cell culture, transfections and preparation of extracts

HEK 293T cells were grown in RPMI media supplemented with 10% fetal bovine serum, 2 mM glutamine, 50 I.U. penicillin, 50 µg/mL streptomycin and 2 mM sodium pyruvate. Cells were incubated at 37°C in a humidified atmosphere maintained at 5% CO_2. Cells were transiently transfected with either empty vector (p3xFLAG-CMV-14) or caspase-9 (C9 C287A-3xFLAG or C9 C287A/Y397F-3xFLAG) using the X-tremeGENE HP DNA transfection reagent (Roche) according to manufacturer instructions.

After 24 h of expression, transfected cells were washed with 1x PBS and lysed with 1x Modified Barth's Saline (MBS)-TritonX pH 7.8 containing 5 mM HEPES pH 7.8, 176 mM NaCl, 1 mM KCl, 1mM $MgSO_4$, 2.5 mM $NaHCO_3$, 1% Triton-X100 and supplemented with Halt™ protease and phosphatase inhibitor cocktail (Thermo Scientific). Lysates were clarified by centrifugation for 30 min at 16,100 x g at 4˚C.

Activation of c-Abl in HEK 293T

Transfected HEK 293T cultures grown to ~90% confluency were treated with 20 µM 5-(1,3-diaryl-1H-pyrazol-4-yl)hydantoin (DPH) (Sigma) and 100 µM sodium orthovanadate (Sigma) for 2 h. For untreated cells, DMSO was added in place of DPH. To determine the inhibition of endogenous c-Abl, HEK 293T cells were initially treated with 20 µM of Imatinib mesylate (Sigma) for 16h prior to DPH treatment. Activation was assessed by monitoring autophosphorylation of c-Abl at Y412 and phosphorylation of known c-Abl substrate CrkII by immunoblot.

Immunoprecipitation and Immunoblotting

3xFLAG-tagged caspase-9 from lysates of transfected cells were immunoprecipitated using anti-FLAG® M2 Affinity Gel (Sigma). The beads with covalently linked antibody were incubated with the lysates for 16 h at 4˚C using an end-to-end rotator. Beads were washed three times with 1x MBS-TritonX buffer with Halt™ protease and phosphatase inhibitor cocktail (Thermo Scientific). Immunoprecipitates were eluted with non-denaturing Laemmli buffer, after

which 5 mM DTT (final concentration) was added and the solution was boiled for 5 min. Total lysates and immunoprecipitates were loaded onto a 5-22 % SDS-PAGE and electroblotted to a PVDF membrane. Total lysates were probed with antibodies against the following: FLAG (mouse, clone M2, Millipore), phosphoY412 c-Abl (rabbit, Cell Signaling Technologies (CST)), phosphoY221 CrkII (rabbit, CST), caspase-9 (rabbit, CST) and cyclophilin A (rabbit, CST) which served as a loading control. Antibody-antigen complexes were probed with anti-phosphotyrosine (mouse, 4G10 Platinum, Millipore) and anti-caspase-9 (mouse, Proteintech). All primary antibodies were used at 1:1000 dilution. Prior to immunoblotting with anti-caspase-9, the membrane was stripped using a stripping buffer pH 2.2 (20 mM glycine, 0.1% (w/v) SDS, 1% Tween) for 1h then washed sequentially with 1x PBS and 1xTBST. Stripping was confirmed by probing with a secondary antibody and visualizing no bands after substrate incubation. The following HRP-conjugated secondary antibodies were used (all from Jackson Immunoresearch): goat anti-mouse IgG, goat anti-mouse IgG light chain-specific, goat anti-rabbit IgG. Immunoreactive bands were were detected by enhanced chemiluminescence using an X-ray film and by visualizing in ChemiDoc XRS+ (BioRad). For detection by X-ray fil, secondary antibodies were diluted 1:5000; for detection by ChemiDoc XRS+, secondary antibodies were diluted 1:50,000.

Protein Digestion and LC-MS/MS

In-solution digestion. Caspase-9 (50 μM) was phosphorylated by c-Abl (1 μM) with 1 mM ATP for 4h at 30˚C. After phosphorylation, 5 mM DTT (final concentration) was added and incubated at 30˚C for 20 min. Cysteine alkylation was then performed by treatment of the sample with 8 mM iodoacetamide (Sigma). The tube was covered with foil to prevent light-mediated reactions and the reaction was agitated using an end-to-end rotator for 15 min at RT. Unreacted iodoacetamide was quenched by adding 5 mM DTT for 15 min at RT. Half of this reaction (~100 μg caspase-9) was diluted in the same volume of Arg-C incubation buffer (50 mM Tris pH 7.7, 5 mM $CaCl_2$ and 2 mM EDTA). 1 μg of Arg-C protease (sequencing grade, Promega) in 50 μL

activation buffer (5 mM Tris-Cl pH 7.7, 5 mM DTT, 200 µM EDTA) was then added to the reaction. Digestion was allowed to proceed for 16h at 37˚C. The reaction was stopped by adding 10% formic acid to a final concentration of 0.5%. Final pH was confirmed to be ≤ 2.0. Arg-C was removed using a Microcon® spin filter column MWCO 10K (Millipore) centrifuged at 16,100 x g for 15 min. Peptide concentration was estimated by absorbance at 280 nm using a NanoDrop™ 2000c spectrophotometer (Thermo Scientific). Digested proteins were diluted with 1% formic acid to contain 2 µg of peptides.

LC-MS/MS. Protein digests were diluted in 0.1% formic acid in water (solvent A) and were analyzed on an Orbitrap Fusion™ mass spectrometer (Thermo Scientific) coupled to an Easy-nLC 1000 (Thermo Scientific) ultra high-pressure liquid chromatography (UHPLC) pump. Analytical LC separations were performed on a FortisBIO C18 nano-flow column (150 mm x 75 µm, 1.7 µm (Fortis Technologies Ltd.)) at a flow rate of 225 nL/min. The following step gradient was used: 0-40% solvent B (0.1% formic acid in acetonitrile) for the first 90 min then 40-85% B for 90-95 min. Total run time was set to 130 min. MS1 spectra were collected on a positive polarity mode with a scan range from m/z 350-1500 at a resolution of 120,000 with an automated gain control (AGC) target of 400,000 and a maximum injection time of 50 ms. The most intense ions were selected for MS/MS. A dynamic exclusion window of 60 s with a mass tolerance of ±10 ppm was used to exclude precursors. MS2 precursors were isolated with a quadrupole mass filter, fragmented by electron transfer dissociation (ETD) and detected by an ion trap mass analyzer. MS2 was operated with an AGC target of 50,000 and a maximum injection time of 100 ms. MS/MS analysis workflow was created with Proteome Discoverer v1.4 (Thermo Scientific). Assignment of MS/MS spectra was performed using the SEQUEST algorithm utilizing the FASTA sequence for human caspase-9 (UniProt ID P55211). SEQUEST searches were performed with a 10 ppm precursor mass tolerance and 0.5 Da fragment mass tolerance while requiring peptide termini to have ArgC protease specificity and allowing up to three missed

cleavages. Carbamidomethylation of cysteine residues (+57.021 Da) and phosphorylation of tyrosine residues (+79.966) were set as dynamic modifications.

Acknowledgments

This work was supported by the National Institutes of Health (GM 080532) to JAH. BS was supported in part by the UMass Chemistry-Biology Interface Training Program (National Research Service Award T32 GM 08515 from the National Institutes of Health). We thank Stephen Eyles, Director of the UMass Mass Spectrometry facility for assistance with mass spectrometric analysis.

Author Contributions

BS designed, initiated and performed all experiments and data analysis, prepared all figures and is the principal author of the manuscript. HS performed some of the cell culture experiments. DA designed cell culture experiments and edited the manuscript. JH conceptualized and directed the research project, secured funding, analyzed and interpreted data, wrote and edited parts of the manuscript.

References

1. Alnemri, E. S. *et al.* Human ICE/CED-3 Protease Nomenclature. *Cell* **87,** 171 (1996).
2. Chęcińska, A., Giaccone, G., Rodriguez, J. A., Kruyt, F. A. E. & Jimenez, C. R. Comparative proteomics analysis of caspase-9-protein complexes in untreated and cytochrome c/dATP stimulated lysates of NSCLC cells. *J. Proteomics* **72,** 575–585 (2009).
3. Seaman, J. E. *et al.* Cacidases: caspases can cleave after aspartate, glutamate and phosphoserine residues. *Cell Death Differ.* (2016). doi:10.1038/cdd.2016.62
4. Franklin, R. A. & McCubrey, J. A. Kinases: positive and negative regulators of apoptosis. *Leukemia* **14,** 2019–2034 (2000).
5. López-Otín, C. & Hunter, T. The regulatory crosstalk between kinases and proteases in cancer. *Nat. Rev. Cancer* **10,** 278–92 (2010).
6. Kurokawa, M. & Kornbluth, S. Caspases and kinases in a death grip. *Cell* **138,** 838–54 (2009).

7. Dagbay, K. *et al.* A multipronged approach for compiling a global map of allosteric regulation in the apoptotic caspases. *Methods Enzymol.* (2014). doi:10.1016/B978-0-12-417158-9.00009-1

8. Zamaraev, A. V., Kopeina, G. S., Prokhorova, E. A., Zhivotovsky, B. & Lavrik, I. N. Post-translational Modification of Caspases: The Other Side of Apoptosis Regulation. *Trends Cell Biol.* **27,** 322–339 (2017).

9. Allan, L. A. & Clarke, P. R. Phosphorylation of caspase-9 by CDK1/cyclin B1 protects mitotic cells against apoptosis. *Mol. Cell* **26,** 301–10 (2007).

10. McDonnell, M. A. *et al.* Phosphorylation of murine caspase-9 by the protein kinase casein kinase 2 regulates its cleavage by caspase-8. *J. Biol. Chem.* **283,** 20149–58 (2008).

11. Brady, S. C., Allan, L. A. & Clarke, P. R. Regulation of Caspase 9 through Phosphorylation by Protein Kinase C Zeta in Response to Hyperosmotic Stress. *Mol. Cell. Biol.* **25,** 10543–10555 (2005).

12. Raina, D. *et al.* c-Abl tyrosine kinase regulates caspase-9 autocleavage in the apoptotic response to DNA damage. *J. Biol. Chem.* **280,** 11147–51 (2005).

13. Cardone, M. H. *et al.* Regulation of Cell Death Protease Caspase-9 by Phosphorylation. *Science (80-.).* **282,** 1318–1321 (1998).

14. Allan, L. A. *et al.* Inhibition of caspase-9 through phosphorylation at Thr 125 by ERK MAPK. *Nat. Cell Biol.* **5,** 647–54 (2003).

15. Seifert, A., Allan, L. A. & Clarke, P. R. DYRK1A phosphorylates caspase 9 at an inhibitory site and is potently inhibited in human cells by harmine. *FEBS J.* **275,** 6268–80 (2008).

16. Allan, L. A. & Clarke, P. R. Apoptosis and autophagy: Regulation of caspase-9 by phosphorylation. *FEBS J.* **276,** 6063–73 (2009).

17. Wang, J. Y. J. The Capable ABL: What Is Its Biological Function? *Mol. Cell. Biol.* **34,** 1188–1197 (2014).

18. Witkowski, W. A. & Hardy, J. A. L2' loop is critical for caspase-7 active site formation. *Protein Sci.* **18,** 1459–68 (2009).

19. Velázquez-Delgado, E. M. & Hardy, J. A. Phosphorylation regulates assembly of the caspase-6 substrate-binding groove. *Structure* **20,** 742–51 (2012).

20. Slee, E. A. *et al.* Ordering the cytochrome c-initiated caspase cascade: Hierarchical activation of caspases-2, -3, -6, -7, -8 and -10 in a caspase-9-dependent manner. *Mol. Cell* **144,** 281–292 (1999).

21. Manning, B. D. & Cantley, L. C. Hitting the Target: Emerging Technologies in the Search for Kinase Substrates. *Sci. Signal.* **2002,** (2002).

22. Martin, M. C. *et al.* Protein kinase A regulates caspase-9 activation by Apaf-1 downstream of cytochrome c. *J. Biol. Chem.* **280,** 15449–55 (2005).

23. Laguna, A. *et al.* The protein kinase DYRK1A regulates caspase-9-mediated apoptosis during retina development. *Dev. Cell* **15,** 841–53 (2008).

24. Yang, J. *et al.* Discovery and Characterization of a Cell-Permeable, Small-Molecule c-Abl Kinase Activator that Binds to the Myristoyl Binding Site. *Chem. Biol.* **18,** 177–186 (2011).

25. Brasher, B. B. & Van Etten, R. a. c-Abl has high intrinsic tyrosine kinase activity that is stimulated by mutation of the Src homology 3 domain and by autophosphorylation at two distinct regulatory tyrosines. *J. Biol. Chem.* **275,** 35631–7 (2000).

26. Feller, S. M., Knudsen, B. & Hanafusa, H. c-Abl kinase regulates the protein binding activity of c-Crk. *EMBO J.* **13,** 2341–51 (1994).

27. Cheng, H.-C., Matsuura, I. & Wang, J. H. in *Reversible Protein Phosphorylation in Cell Regulation* 103–112 (Springer US, 1993). doi:10.1007/978-1-4615-2600-1_9

28. Johnson, S. A. & Hunter, T. Kinomics: methods for deciphering the kinome. *Nat. Methods* **2,** 17–25 (2005).

29. Eron, S. J., Raghupathi, K. & Hardy, J. A. Dual Site Phosphorylation of Caspase-7 by PAK2 Blocks Apoptotic Activity by Two Distinct Mechanisms. *Structure* **0,** 1913–1918 (2016).

30. Serrano, B. P. & Hardy, J. A. Phosphorylation by Protein Kinase A Disassembles the Caspase-9 Core. *Cell Death Differ.* (2017).

31. Taagepera, S. *et al.* Nuclear-cytoplasmic shuttling of C-ABL tyrosine kinase. *Proc. Natl. Acad. Sci.* **95,** 7457–7462 (1998).

32. Kharbanda, S. *et al.* Activation of the c-Abl tyrosine kinase in the stress response to DNA-damaging agents. *Nature* **376,** 785–788 (1995).

33. Shaul, Y. c-Abl: activation and nuclear targets. *Cell Death Differ.* **7,** 10–6 (2000).

34. Mylona, A. *et al.* Opposing effects of Elk-1 multisite phosphorylation shape its response to ERK activation. *Science* **354,** 233–237 (2016).

35. Vanselow, K. *et al.* Differential effects of PER2 phosphorylation: molecular basis for the human familial advanced sleep phase syndrome (FASPS). *Genes Dev.* **20,** 2660–72 (2006).

36. Skotte, N. H. *et al.* Palmitoylation of caspase-6 by HIP14 regulates its activation. *Cell Death Differ.* **24,** 433–444 (2017).

37. Renatus, M., Stennicke, H. R., Scott, F. L., Liddington, R. C. & Salvesen, G. S. Dimer formation drives the activation of the cell death protease caspase-9. *Proc. Natl. Acad. Sci. U. S. A.* **98,** 14250–5 (2001).

38. Qin, H. *et al.* Structural basis of procaspase-9 recruitment by the apoptotic protease-activating factor 1. *Nature* **399,** 549–57 (1999).

39. Cheng, T. C., Hong, C., Akey, I. V., Yuan, S. & Akey, C. W. A near atomic structure of the active human apoptosome. *Elife* **5,** 1–28 (2016).

40. Wu, C.-C. *et al.* The Apaf-1 apoptosome induces formation of caspase-9 homo- and heterodimers with distinct activities. *Nat. Commun.* **7,** 13565 (2016).

41. Huang, W. *et al.* Mechanistic insights into CED-4-mediated activation of CED-3. *Genes Dev.* **27,** 2039–48 (2013).

42. Sirvent, A., Benistant, C. & Roche, S. Cytoplasmic signalling by the c-Abl tyrosine kinase in normal and cancer cells. *Biol. Cell* **100,** 617–631 (2008).

43. Greuber, E. K., Smith-Pearson, P., Wang, J. & Pendergast, A. M. Role of ABL family kinases in cancer: from leukaemia to solid tumours. *Nat. Rev. Cancer* **13,** 559–571 (2013).

44. Wong, S. & Witte, O. N. The BCR-ABL Story: Bench to Bedside and Back. *Annu. Rev. Immunol.* **22,** 247–306 (2004).

45. Hantschel, O. & Superti-Furga, G. Regulation of the c-Abl and Bcr-Abl tyrosine kinases. *Nat. Rev. Mol. Cell Biol.* **5,** 33–44 (2004).

46. Wu, J. J., Phan, H. & Lam, K. S. Comparison of the intrinsic kinase activity and substrate specificity of c-Abl and Bcr-Abl. *Bioorg. Med. Chem. Lett.* **8,** 2279–84 (1998).

47. Voss, J. *et al.* The leukaemic oncoproteins Bcr-Abl and Tel-Abl (ETV6/Abl) have altered substrate preferences and activate similar intracellular signalling pathways. *Oncogene* **19,** 1684–1690 (2000).

48. Dix, M. M. *et al.* Functional interplay between caspase cleavage and phosphorylation sculpts the apoptotic proteome. *Cell* **150,** 426–40 (2012).

49. Machuy, N., Rajalingam, K. & Rudel, T. Requirement of caspase-mediated cleavage of c-Abl during stress-induced apoptosis. *Cell Death Differ.* **11,** 290–300 (2004).

50. Barilà, D. *et al.* Caspase-Dependent Cleavage of c-Abl Contributes to Apoptosis Caspase-Dependent Cleavage of c-Abl Contributes to Apoptosis. *Mol. Cell. Biol.* **23,** 2790–2799 (2003).

51. Duncan, J. S. *et al.* A peptide-based target screen implicates the protein kinase CK2 in the global regulation of caspase signaling. *Sci. Signal.* **4,** ra30 (2011).

52. Tsang, J. L. *et al.* Tyrosine Phosphorylation of Caspase-8 Abrogates Its Apoptotic Activity and Promotes Activation of c-Src. *PLoS One* **11,** e0153946 (2016).

53. Powley, I. R., Hughes, M. A., Cain, K. & MacFarlane, M. Caspase-8 tyrosine-380 phosphorylation inhibits CD95 DISC function by preventing procaspase-8 maturation and cycling within the complex. *Oncogene* **35,** 5629–5640 (2016).

54. Stennicke, H. R. *et al.* Caspase-9 can be activated without proteolytic processing. *J. Biol. Chem.* **274,** 8359–62 (1999).

55. Zhou, Q. *et al.* Target Protease Specificity of the Viral Serpin CrmA: ANALYSIS OF FIVE CASPASES. *J. Biol. Chem.* **272,** 7797–7800 (1997).

56. Seeliger, M. A. *et al.* High yield bacterial expression of active c-Abl and c-Src tyrosine kinases. 3135–3139 (2005). doi:10.1110/ps.051750905.kemia

57. Hornbeck, P. V. *et al.* PhosphoSitePlus, 2014: mutations, PTMs and recalibrations. *Nucleic Acids Res.* **43,** D512–D520 (2015).

58. Laskowski, R. A. & Swindells, M. B. LigPlot+: Multiple Ligand-Protein Interaction Diagrams for Drug Discovery. *J. Chem. Inf. Model.* **51,** 2778–2786 (2011).

59. Emsley, P., Lohkamp, B., Scott, W. G. & Cowtan, K. Features and development of Coot. *Acta Crystallogr. Sect. D Biol. Crystallogr.* **66,** 486–501 (2010).

CHAPTER V

CASPASE-9 PHOSPHORYLATION BY PKA AND c-ABL: BLOCKING THE APOPTOTIC CASCADE

The power to control cellular signaling pathways has been one of the driving concepts in therapeutic intervention and drug development aimed at finding cures for deadly and severely debilitating human diseases. A retrospective examination of the basis of the pathogenesis of these diseases would reveal a fundamental signaling pathway that almost always contributes to the progression, or even accounts for that disease. A prominent critical pathway is apoptosis or programmed cell death, a mechanism utilized by multicellular organisms to achieve tissue homeostasis and ensure survival by safely disposing unwanted, harmful or unneeded cells. Diseases associated with defective apoptosis include cancer, neurodegeneration, cardiovascular diseases and autoimmune disorders. The past few decades have seen continuous efforts to unravel the many layers of how the cell expertly controls this very complex pathway, resulting in a breathtaking wealth of knowledge about apoptotic signaling. The attractive idea that one would be able to control cell death as a means to treat cancer or neurodegeneration has prompted numerous studies involving core apoptotic components that can either serve as targets or, those that could potentially be elevated to the clinic as biological therapeutics.

Many elements coordinate to ensure the faithful execution of apoptosis, but caspases have solicited much interest as appealing therapeutic targets not only because of the great extent of their killing potential, but also the distinctive property of possessing various switches that allow them to be turned on or off. One particular molecular switch that controls caspase function is phosphorylation. While the functional phenotype (suppression or induction of apoptosis) resulting from phosphorylation of caspases has been known in most cases, key molecular details that would explain the functional consequences of phosphorylation have been nearly completely lacking. This dissertation presented detailed structural and mechanistic investigations of caspase-

9 regulation by phosphorylation in order to provide information that will aid in designing therapeutic strategies for apoptosis-associated diseases.

Phosphorylation at S183 and Y397 Directly Inhibits Caspase-9

In Chapter I, we put forth the many aspects in caspase-9 phosphorylation that needs to be addressed in order to fully harness the mechanism of phosphoregulation for therapeutic purposes. One of the major findings of this work is that phosphorylation of caspase-9 at two dominant sites, S183 and Y397, abides by the common theme of phosphorylation, directly inhibiting a caspase's catalytic function. S183 is phosphorylated by PKA, while Y397 is acted upon by c-Abl kinase. Two previous findings prompted us to investigate caspase-9 phosphorylation by PKA and c-Abl. One was the prior report and conclusion that phosphorylation of three sites (S99, S183 and S95) in caspase-9 was redundant and nonessential to caspase-9 inhibition[1]. The second was that among the many reported phosphorylation of caspase-9, only phosphosphorylation by c-Abl at Y153 apparently leads to self-activation and promotes apoptosis[2]. Our experience with studying multiple caspase:kinase[3,4] pairs led us to hypothesize that contrary to what was reported, phosphorylation by PKA and c-Abl would directly inhibit caspase-9 function. The data in this dissertation have shown that assertion to be true.

Chapter II presents comprehensive studies to elucidate the molecular mechanism of caspase-9 inhibition by PKA. One crucial detail that emerged was that caspase-9 was directly inhibited by PKA phosphorylation. Using phosphomimetics, *in vitro* phosphorylation and site-specific phosphoincorporation, we identified S183 as the predominant site of caspase-9 phosphorylation leading to inhibition. This finding is noteworthy because it contradicts the prior conclusion of Martin et al.[1] about the non-functional or silent effect of PKA phosphorylation in caspase-9 inhibition. We are able to explain why Martin et al. misinterpreted their data leading to an erroneous conclusion. Specifically, as is common in many cell-biological studies, they neglected to biochemically assess the catalytic function of the mutants they used in their studies. Because the variants they used were inherently inactive, but were assumed to be active, the

conclusions drawn by their paper were faulty. Our results clearly showed that a phosphorylation of S183 was enough to render caspase-9 catalytically inactive. In Chapter IV, we employed the same strategies from Chapter II to explore the activating effect of c-Abl phosphorylation on caspase-9 as previously reported[2]. While we were thrilled with the prospect of exploiting a unique activating mechanism in caspase-9, our results pointed two major findings, both of which were contrary to what was previously reported. First, we uncovered that Y153 is not the major site of phosphorylation by c-Abl, rather we discovered a novel site of phosphorylation in caspase-9, Y397, which was observed to be robustly phosphorylated both *in vitro* and intracellularly. Second, phosphorylation of Y397 by c-Abl does not activate but inhibits caspase-9 activity. In the paper by Raina et al.[2], the conclusion that phosphorylation by c-Abl activates caspase-9 was again based on the erroneous assumption that the unphosphorylatable mutant Y153F was active. They attributed the observed suppression of apoptosis to the absence of phosphorylation in Y153. In fact, our biochemical assays clearly show that Y153F has severely impaired catalytic activity, and would explain the attenuated apoptosis in cells expressing Y153F.

It was evident that our results were not in total agreement with what was previously reported. We provided an updated interpretation of the previous results, citing the importance of performing structural and biochemical analyses to complement cell-based assays. While cell-based assays are essential in discerning the biological relevance of phosphorylation, conclusions derived from these assays can be misleading, most especially when the intrinsic activities of caspase-9 variants were not assessed and taken into account. Such was the case for both papers on PKA and c-Abl phosphorylation. In addition, structural analysis of caspase-9 S183 and Y153 would have instantly provided a snapshot of the possible functional effect of phosphorylation. S183 is involved in critical interactions within conserved residues in the active site, while Y153 contacts with the L2 loop to support the active site loop bundle. Based on these, one would have predicted that phosphorylation of S183 and Y153 would be inactivating, and not silent or activating, respectively. Based on this theme, we recommend to other investigators probing

capsase or caspase-kinase interaction that in the future, the phosphomimetic and unphosphorylatable versions of all caspases be functionally assessed before any cell-based assays with mutant proteins are undertaken.

Structural analyses allowed us to expound on the molecular details of how phosphorylation of S183 and Y397 directly inhibits caspase-9 activity. One detail that particularly stood out is the proximity of these two residues to the substrate-binding groove (Figure 2.1B, 4.11B), which seems to be a hotspot for phosphorylation in other caspases as well[3,4]. We have presented models that would explain the mechanism of inhibition by phosphorylation at S183 and Y397. Both models suggest that phosphorylation of these sites prevent substrate binding through different but related mechanisms. S183 phosphorylation disorients the active site loop bundle, while Y397 phosphorylation reaches into and blocks the substrate-binding pocket.

Our results that phosphorylation by PKA and c-Abl leads to caspase-9 inhibition suggest an anti-apoptotic/prosurvival role of these kinases. This is particularly relevant in deciphering the relationship between c-Abl and caspase-9. c-Abl has been reported to play dual yet opposing roles in apoptotic signaling, depending on its cellular localization. Our observation that caspase-9 is inhibited by c-Abl phosphorylation suggests that this molecular event contributes to the prosurvival nature of c-Abl, which is consistent with c-Abl's anti-apoptotic function in the cytosol where majority of caspase-9 cellular pool are found. Phosphorylation of caspase-9 by PKA and c-Abl therefore act as upstream block in the apoptotic cascade.

Structural Impacts of Phosphorylation on Caspase-9

A significant finding in Chapter II was that S183 phosphorylation by PKA appears to utilize two different mechanisms of inhibiting caspase-9, depending on its conformational state. Phosphorylation of S183 while caspase-9 is in its latent/zymogen state directly prevents substrate binding, but in its mature/fully cleaved state, S183 phosphorylation triggers the disassembly of caspase-9 by unfolding its catalytic core. This supports our previous assertion that phosphorylation can differentially exert its influence throughout the different stages in caspase-

9's life cycle. Another fascinating observation was that S183 is distal from the caspase-9 large:small interface, thus the unfolding and disassembly likely proceeds through allosteric mechanism. To our knowledge this is the first report of such allosteric mechanism of inhibition in caspases. The most intriguing detail in S183 phosphorylation is our observation that upon phosphorylation-induced unfolding, caspase-9 formed ordered aggregates, the morphology of which were visualized through electron microscopy (Figure 2.9, 2.10). While the existence and possible function of caspase-9 ordered aggregates *in vivo* remain in question, we offered two possible scenarios that would explain why phosphorylated caspase-9 might engage such a mechanism (see Discussion in Chapter II). One is the possibility that the disassembly of the catalytic core is a surefire way to completely block the apoptotic cascade. Our results point to the idea that phosphorylated S183 is completely inhibited and more importantly, non-activatable, even as caspase-9 was directed to the apoptosome. Within the apoptosome, activation by cleavage of caspase-9 occurs. Cleaved caspase-9 phosphorylated at S183E is severely unstable. This leads to its unfolding and eventually being disengaged from the apoptosome because it is no longer structurally intact, and possibly gets directed to proteasomal degradation. The second scenario involves these ordered aggregates as a mechanism to hold caspase-9 in its latent/inactive state until caspase-9 gets dephosphorylated and reactivated, a mechanism analogous to that of functional aggregates. Both scenarios are appealing from a therapeutic and a mechanistic viewpoint. Phosphorylation-mediated unfolding and degradation suggests crosstalk between phosphorylation and ubiquitination pathways, thus providing an additional node of possible therapeutic intervention to control apoptosis. The notion that caspase-9 forms higher order structures apart from the apoptosome and more importantly, with an opposite function, i.e. deactivating, adds another layer in the hierarchical nature of caspase-9 structure and function.

In our experiments, ordered aggregates were derived from the phosphomimetic S183E. What would aid in thorough investigations of the mechanism of formation of these ordered aggregates is to use a phosphorylated version of S183. While we have successfully generated

phosphoS183 using site-specific phosphoincorporation in *E. coli*, the extremely low expression levels of the phosphocaspase has limited the amount of material to perform aggregation and subsequent experiments. We recently constructed an MBP-fused phosphocaspase-9, which was observed to significantly boost caspase-9 expression. It would then be interesting to take S183-phosphorylated caspase-9, subject it to aggregation and test whether dephosphorylation would resolubilize and reactivate caspase-9. If so, then it would strengthen our hypothesis of the nature and function of these ordered aggregates. The next phase would be to determine the structure of caspase-9 aggregates by cryo-EM to identify critical interactions within caspase-9 domains or among caspase-9 molecules.

We also probed and characterized the interaction between the caspase-9 CARD and catalytic core. This physical interaction influences the stability and activity of caspase-9, but is dictated by the geometry of the active site and the conformational states of the enzyme. The region of binding between the CARD and core is still unknown, but would greatly benefit from structural studies such as X-ray crystallography and small-angle X-ray scattering. While numerous structures are available for other apoptotic caspases, to date there are only six structures of non-apoptosome-bound caspase-9 in the PDB. In addition, there is no available structure of the full-length caspase-9, only that of the catalytic core (ΔCARD)[5–8] or the CARD[9,10], alone or in complex with other proteins or domains. It would be helpful to obtain a crystal structure of the full-length caspase-9. Since in almost all crystal structures, the caspase-9 core is a homodimer, we envision that full-length caspase-9 will crystallize as a dimer as well. What would be most interesting is whether the interaction between the CARD and catalytic core would be present in the structure of the full-length caspase-9 with an active-site ligand bound.

Caspase-9-Kinase Interplay

Crosstalk between caspases and kinases is important in their co-regulation, and the cellular outcome of either promotion or suppression of apoptosis is dictated by whether caspase phosphorylation or kinase cleavage takes precedence over the other. Typically caspases cleave

the very kinase that phosphorylates them; such cases were observed in caspase-7 with PAK2[4] and caspase-8 with Src[11]. In our studies on caspase-9 phosphorylation by PKA and c-Abl, we did not observe any cleavage of either kinase by caspase-9. This observation could be explained by the relatively low activity of caspase-9 in *in vitro* conditions. A good model to test whether caspase-9 would cleave PKA and c-Abl is monitor kinase cleavage using caspase-9 in the presence of Apaf-1, cytochrome c and dATP, which may accurately reflect an active caspase-9 in the apoptosome. Should kinase cleavage be observed, the next study would be to determine whether PKA and c-Abl prefers to phosphorylate caspase-9 in a specific conformational state, i.e, apoptosome-bound and cleaved caspase-9 or free caspase-9 in zymogen state.

Alternatively, it is also likely is that the cross talk between caspase-9 and its cognate kinases is heavily weighted towards phosphorylation. A reason for this assumption is that unlike other caspase:kinase pairs (review[12]), no cognate kinase has been reported to be a substrate of caspase-9. In fact, sequence analyses predicted no caspase-9 cleavage site in PKA. c-Abl is cleaved by both caspase-3[13,14] and caspase-8[14], and while it may be feasible caspase-9 likewise cleaves c-Abl intracellularly, the caspase cleavage sequences present in c-Abl are not preferred by caspase-9. Thus it appears that for both PKA and c-Abl (and possibly all other cognate kinases of caspase-9), phosphorylation-mediated inhibition of caspase-9 would always prevail over kinase cleavage. A complete understanding of this relationship would be critical in the development of caspase-kinase co-therapies. For example, in cancer and tumor applications, turning on an upstream apoptotic caspase like caspase-9 while turning off any inhibition coming from a specific kinase could potentially result in maximum killing of targeted cells.

Specificity of Phosphorylation by PKA and c-Abl among Apoptotic Caspases

A notable observation in Chapter IV was that caspase-9 is the most preferred caspase substrate of c-Abl. In addition, the phosphorylated residue, Y397 is a site that is only present in caspase-9 and not in other apoptotic caspases. This provides multiple potential strategies for the specific control of caspase-9, either by targeting c-Abl or by exploiting the Y397 site to develop

inhibitors that will specifically target caspase-9. In contrast to the specificity displayed by c-Abl towards caspase-9, other apoptotic caspases including caspase-8, -10, -3, -6, and -7 contain the PKA phosphorylation motif surrounding the S183 site. Surprisingly, caspase-9 is the only reported caspase substrate of PKA. It would be interesting to explore if these caspases are also phosphorylated by PKA and whether they are similarly inhibited by the same the mechanisms as those observed in caspase-9. If other caspases were found to be PKA substrates, this suggests that PKA could have the upper hand in putting a break in the apoptotic pathways by phosphorylating and inhibiting multiple caspases, a mechanism which may be exploited by cells in many cancers and tumor types where PKA is overexpressed[15,16].

Other Sites of Phosphorylation in Caspase-9

Caspase-9 contains the greatest number of phosphorylation sites among caspases, highlighting the need for additional regulation of caspase-9. In the major chapters of this dissertation, we only focused on two sites of phosphorylation, S183 and Y397, and already uncovered many layers that govern phosphoregulation of caspase-9. In the Appendix, we present initial studies on other phosphorylation sites within the CARD and core (S99, T125, S144, S195) and intersubunit linker (S302, S307 and S310) using phosphomimetics in an attempt to identify which sites would also inhibit caspase-9 function. We found that in most cases, phosphomimetics did not directly inhibit catalytic activity, which strongly suggests that phosphorylation of these residues affect caspase-9 function at a different level. Two particular phosphorylation sites are of interest – S307 and T125. Our results showed that phosphomimetic S307E is ~40x less active than WT, although it is capable of self-processing/autoactivation. In this case, phosphorylation appears to permit zymogen activation of caspase-9, but prevents it from achieving a fully active state. T125 is the site that is targeted by multiple kinases[17–19] to inhibit caspase-9 intracellularly. In our phosphomimetic studies, T125E is as active as WT and binding assays showed that it does not prevent caspase-9 from being recruited by Apaf-1. The exact mechanism of how T125 phosphorylation inhibit caspase-9 function remains to be seen. T125 sits in the potentially flexible

region between the CARD and the large subunit. Reported exosites in caspases seem to cluster in the prodomain-adjacent region, such as the ^{38}KKKK^{41} patch[20] and S30[4] in caspase-7 and a putative hydrophobic exosite patch in caspase-6 composed of ^{55}FFW^{57} [21]. In light of these observations, one might wonder if there are also exosites in caspase-9 that reside in the prodomain-adjacent region (such as T125 and S99) and whether phosphorylation would influence exosite binding. Assessing the ability of T125E and S99E to cleave caspase-9 substrates and comparing it with that of WT is a good place to start exploring this exosite concept.

Diverse Molecular Mechanisms of Phosphorylation-Mediated Caspase Inhibition

Prior to this work, only one mechanism of caspase-9 phosphoregulation (mediated by CK2) has been elucidated. The work presented in this dissertation now adds three distinct mechanisms of caspase-9 phosphoregulation to the growing list of molecular mechanisms of phosphorylation-mediated caspase inhibition (Table 5.1). Some of these mechanisms operate by inhibiting the early stages of caspase activation, particularly zymogen activation. The conversion of caspases from a zymogen to a cleaved (mature) state to gain maximal activity is achieved by cleavage at the intersubunit linker, either by the self-processing or by the action of another caspase. Phosphorylation of residues adjacent or within the cleavage site(s) in the intersubunit linker has been shown to block linker cleavage, as observed in casp-3[22], -8[11,23] and -9[24]. Recently, phosphorylation of casp-7 at a prodomain-adjacent S30 was observed to block interaction with caspase-9, leading to failure of casp-7 cleavage and activation[4]. Phosphorylation also impacts the catalytic activity of mature caspases. The mobile nature of the active site loops allows the kinase facile access to phosphorylation sites that are in close proximity to or within the substrate-binding pocket. Phosphorylation of these residues appears to be a robust way to directly inhibit catalytic function either by blocking substrate binding through steric clash, as observed in casp-7 S239[4], or by disorienting the substrate-binding loops, thus making them incompetent to bind substrate, as in casp-6 S257 and caspase-9 S183[3,25]. Another is through an active site-adjacent mechanism, as in Y397 in caspase-9, in which a residue in close proximity to the active site is able to reach into the

susbtrate binding pocket to block substrate binding[26]. We also observed an intriguing allosteric mechanism of phosphoregulation in caspase-9 wherein phosphorylation of S183 in the mature form is sufficient to disassemble the caspase-9 core despite S183 being distal from the large:small interface[25]. We expect that more distinct mechanisms will be added in this growing list.

Table 5.1 Molecular mechanisms of phosphorylation-mediated caspase inhibition.

Molecular Mechanism	Caspase	Site	Kinase
Preventing zymogen activation	Caspase-3	T174, S176	CK2[22]
	Caspase-8	Y380	Src[11,23]
	Caspase-9	S310 (S348 murine)	CK2[24]
Blocking protein-protein interactions	Caspase-7	S30	PAK2[4]
Disorienting substrate-binding loops	Caspase-9	S183	PKA[25]
	Caspase-6	S257	Ark5[3]
Directly blocking substrate binding	Caspase-7	S239	PAK2[4]
Core disruption & formation of ordered aggregates	Caspase-9	S183	PKA[25]
Active-site adjacent	Caspase-9	Y397	c-Abl[26]

Many molecular questions still abound concerning caspase phosphoregulation. Of these, we consider two important questions, which when addressed, will greatly aid in our understanding about caspase phosphorylation and how it influences the apoptotic pathways. First, what degree of phosphorylation of caspases is sufficient to switch on or off their function, and is there a threshold of phosphorylation level that would lead to either suppression or induction of apoptosis? And second, what phosphatases are associated with these phosphorylation events that will ensure reversibility of phosphorylation in order to regain balance between cell death and survival?

References

1. Martin, M. C. *et al.* Protein kinase A regulates caspase-9 activation by Apaf-1 downstream of cytochrome c. *J. Biol. Chem.* **280,** 15449–55 (2005).
2. Raina, D. *et al.* c-Abl tyrosine kinase regulates caspase-9 autocleavage in the apoptotic response to DNA damage. *J. Biol. Chem.* **280,** 11147–51 (2005).
3. Velázquez-Delgado, E. M. & Hardy, J. A. Phosphorylation regulates assembly of the caspase-6 substrate-binding groove. *Structure* **20,** 742–51 (2012).
4. Eron, S. J., Raghupathi, K. & Hardy, J. A. Dual Site Phosphorylation of Caspase-7 by PAK2 Blocks Apoptotic Activity by Two Distinct Mechanisms. *Structure* **25,** 27–39 (2017).
5. Renatus, M., Stennicke, H. R., Scott, F. L., Liddington, R. C. & Salvesen, G. S. Dimer formation drives the activation of the cell death protease caspase-9. *Proc. Natl. Acad. Sci. U. S. A.* **98,** 14250–5 (2001).
6. Shiozaki, E. N. *et al.* Mechanism of XIAP-mediated inhibition of caspase-9. *Mol. Cell* **11,** 519–27 (2003).
7. Chao, Y. *et al.* Engineering a dimeric caspase-9: a re-evaluation of the induced proximity model for caspase activation. *PLoS Biol.* **3,** e183 (2005).
8. Steuber, H. *et al.* The E . coli Effector Protein NleF Is a Caspase Inhibitor. *PLoS One* **8,** e58937 (2013).
9. Zhou, P., Chou, J., Olea, R. S., Yuan, J. & Wagner, G. Solution structure of Apaf-1 CARD and its interaction with caspase-9 CARD: a structural basis for specific adaptor/caspase interaction. *Proc. Natl. Acad. Sci. U. S. A.* **96,** 11265–70 (1999).
10. Shiozaki, E. N., Chai, J. & Shi, Y. Oligomerization and activation of caspase-9, induced by Apaf-1 CARD. *Proc. Natl. Acad. Sci. U. S. A.* **99,** 4197–202 (2002).
11. Tsang, J. L. *et al.* Tyrosine Phosphorylation of Caspase-8 Abrogates Its Apoptotic Activity and Promotes Activation of c-Src. *PLoS One* **11,** e0153946 (2016).
12. Kurokawa, M. & Kornbluth, S. Caspases and kinases in a death grip. *Cell* **138,** 838–54 (2009).
13. Machuy, N., Rajalingam, K. & Rudel, T. Requirement of caspase-mediated cleavage of c-Abl during stress-induced apoptosis. *Cell Death Differ.* **11,** 290–300 (2004).
14. Barilà, D. *et al.* Caspase-Dependent Cleavage of c-Abl Contributes to Apoptosis Caspase-Dependent Cleavage of c-Abl Contributes to Apoptosis. *Mol. Cell. Biol.* **23,** 2790–2799 (2003).
15. Caretta, A. & Mucignat-Caretta, C. Protein kinase a in cancer. *Cancers (Basel).* **3,** 913–26 (2011).
16. Sapio, L. *et al.* Targeting protein kinase A in cancer therapy: an update. *EXCLI J.* **13,** 843–55 (2014).
17. Allan, L. A. *et al.* Inhibition of caspase-9 through phosphorylation at Thr 125 by ERK MAPK. *Nat. Cell Biol.* **5,** 647–54 (2003).
18. Laguna, A. *et al.* The protein kinase DYRK1A regulates caspase-9-mediated apoptosis during retina development. *Dev. Cell* **15,** 841–53 (2008).

19. Allan, L. A. & Clarke, P. R. Phosphorylation of caspase-9 by CDK1/cyclin B1 protects mitotic cells against apoptosis. *Mol. Cell* **26,** 301–10 (2007).

20. Boucher, D., Blais, V. & Denault, J.-B. Caspase-7 uses an exosite to promote poly(ADP ribose) polymerase 1 proteolysis. *Proc. Natl. Acad. Sci. U. S. A.* **109,** 5669–74 (2012).

21. Dagbay, K. B., Bolik-Coulon, N., Savinov, S. N. & Hardy, J. A. Caspase-6 Undergoes a Distinct Helix-Strand Interconversion upon Substrate Binding. *J. Biol. Chem.* **292,** 4885–4897 (2017).

22. Duncan, J. S. *et al.* A peptide-based target screen implicates the protein kinase CK2 in the global regulation of caspase signaling. *Sci. Signal.* **4,** ra30 (2011).

23. Powley, I. R., Hughes, M. A., Cain, K. & MacFarlane, M. Caspase-8 tyrosine-380 phosphorylation inhibits CD95 DISC function by preventing procaspase-8 maturation and cycling within the complex. *Oncogene* **35,** 5629–5640 (2016).

24. McDonnell, M. A. *et al.* Phosphorylation of murine caspase-9 by the protein kinase casein kinase 2 regulates its cleavage by caspase-8. *J. Biol. Chem.* **283,** 20149–58 (2008).

25. Serrano, B. P. & Hardy, J. A. Phosphorylation by Protein Kinase A Disassembles the Caspase-9 Core. *Cell Death Differ.* (2017).

26. Serrano, B. P., Szydlo, H. S., Alfandari, D. R. & Hardy, J. A. Active-site adjacent phosphorylation at Tyr-397 by c-Abl kinase inactivates caspase-9. *J. Biol. Chem.* **292,** 21352–21365 (2017).

APPENDIX

INTERROGATION OF OTHER PHOSPHORYLATION SITES IN CASPASE-9

The use of glutamate as a phosphomimetic has allowed us to widely investigate functional effects arising from phosphorylation. Glutamate is typically an acceptable surrogate for a phosphoSer and phosphoThr, imparting both the bulk and negative charge similar to a phosphate moiety. Besides the ease by which it can be constructed by site-directed mutagenesis, one particular advantage of using a phosphomimetic is the ability to obtain homogeneously "labeled" samples, whereas *in vitro* reactions typically do not achieve 100% phosphorylation. Thus the intrinsic functional effect of phosphorylation can readily be examined and explicitly attributed to that modification. In this section, we employed phosphomimetics to interrogate residues that were not directly inactivating upon phosphorylation, but could influence other aspects of caspase-9 structure and function such as oligomerization, protein-protein interactions and cleavage.

Phosphorylation in CARD and Catalytic Core Domains

The CARD and catalytic core of caspase-9 contain the greatest number of phosphorylation sites (Figure 1.5, 1.6). In Chapter II, we identified S183 as the predominant site of phosphorylation that leads to inactivation of caspase-9 by PKA via allosteric mechanisms. In Chapter IV, Y397 was determined to be a novel site of inactivation upon c-Abl phosphorylation. Along with S183, two other sites were phosphorylated by PKA – S99 and S195, however phosphorylation of these sites was reported to be dispensable to caspase-9 inhibition[1], and we make the same observation (Chapter II, Figure 2.2F) . Other sites that reside in the CARD and core regions are S144, which was observed to be phosphorylated by the atypical PKC ζ under hyperosmotic stress, and T125, a site phosphorylated by multiple kinases including ERK1,2[2], DYRK1A[3] and CDK1[4]. In some cases, T107 is reported to be phosphorylated along with T125, albeit in low levels[2,4]. Caspase-9 in cell extracts that were phosphorylated on either S144 or T125

showed diminished self-processing upon incubation with Apaf-1 and cytochrome c. In addition, a decrease in both casp-3 cleavage and DEVDase activity in these cell extracts were observed, suggesting that S144- or T125-phosphorylated caspase-9 failed to cleave and activate downstream caspases. These results initially point towards a direct inactivation of caspase-9 activity upon phosphorylation.

Phosphomimetic versions S99E, S195E, S144E, and T125E were constructed, overexpressed and purified from *E. coli*. In contrast to previous reports where phosphorylation was inhibitory to caspase-9 activity, all phosphomimetic variants (S99E, S195E, S144E and T125E) displayed LEHDase activity. Following overexpression, these variants were in fully mature/cleaved forms (Figure A.1), indicating that the variants were capable of self-activation/cleavage. Moreover, their catalytic parameters against caspase-9 substrate LEHD showed that they were active (Table A.1).

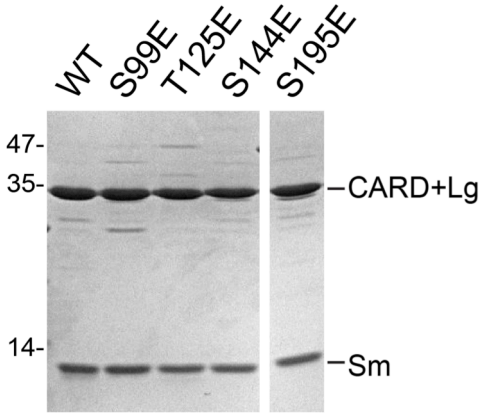

Figure A.1. WT and phosphomimetic versions of caspase-9. Following overexpression all variants were in the fully mature/cleaved state.

Table A.1. Catalytic parameters[9] of WT caspase-9 and phosphomimetic variants using substrate Ac-LEHD-AFC.

Caspase-9 variant	K_M (μM)	k_{cat} (s^{-1})	10^3 x k_{cat} / K_M ($\mu M^{-1}s^{-1}$)
WT	430 ± 35	1.4 ± 0.10	3.3
S99E	1280 ± 295	0.97 ± 0.10	0.80
T125E	509 ± 47	1.38 ± 0.40	2.7
S144E	280 ± 85	0.72 ± 0.15	2.6
S195E	440 ± 85	0.90 ± 0.10	2.1

[9]Values are mean (± SEM) of three trials done on three separate days.

The observation that there was no direct hit to the catalytic activity of these caspase-9 variants could simply imply non-functional or silent phosphorylation, an idea that has been

debated in the phosphorylation field[5,6]. Although it is appealing to assign these sites as non-functional, knowing the multifaceted nature of caspase-9 regulation led us to further probe how phosphorylation of these sites, besides affecting catalytic activity, could influence caspase-9 activation. Prior work in our group has clearly shown that phosphorylation of one site does not necessarily alter catalytic activity, yet impacts a different aspect of caspase function. This was evident in casp-7 phosphorylation by PAK2, where phosphorylation of S30 and phosphomimetic S30E had no effect in activity but was found to significantly attenuate procasp-7 cleavage and activation by caspase-9[7].

Exploring Apaf-1 CARD:caspase-9 CARD Interactions

From Chapter III it was clear that S99E and T125E did not abolish the interactions between the CARD and catalytic core of caspase-9 (Chapter II, Figure 3.10). We then explored whether S99E and T125E could disrupt the interaction between caspase-9 CARD and Apaf-1 CARD. This CARD:CARD interaction is paramount to the initial step of caspase-9 activation in the apoptosome; any event that breaks this interaction will be an upstream block in the caspase-9 activation cascade. S99 and T125 are located in the potentially flexible linker preceding the large subunit (Chapter I, Figure 1.6). These residues do not appear to directly participate in Apaf-1 CARD:caspase-9 CARD interactions, based on the available structures of the CARD:CARD complex, both in isolation[8,9] and in the apoptosome[10–14]. However, we reasoned that the flexible nature of the S99 and T125 and the altered properties of the residues due to the glutamate substitution could prevent interaction with Apaf-1 CARD since CARD:CARD interactions are driven by electrostatics. In addition, there are other charged surfaces outside of CARD:CARD binding interface that remain exposed[9] which could potentially interact with E99 or E125. Gel mobility shift assays show that the migration of S99E and T125E clearly shifted upon incubation with Apaf-1 CARD, suggesting that the CARD:CARD interactions are still intact in these caspase-9 variants (Figure A.2A). In the presence of Apaf-1 CARD, full-length caspase-9 has been observed to form two species – a heterotetramer composed of a homodimer of caspase-9

with two Apaf-1 CARD bound, and a high molecular weight oligomer/complex (~300-400 kDa)[9]. It was suggested that the high molecular weight complex is formed due to additional interactions outside of the CARD:CARD binding interface, possibly between the caspase-9 catalytic core and the CARD:CARD platform. Along with the formation of these oligomers was a marked elevation in caspase-9 activity. A similar increase in activity was observed with WT caspase-9 and T125E when bound to Apaf-1 CARD. Strikingly, S99E failed to exhibit this increase in activity (Figure A.2B). S99E itself was less active than WT (Table A.1), and a similar diminished activity was also observed with the phosphorylated version, phosphoS99 (Chapter II, Figure 2.3B). Thus it seems that S99E has enough intrinsic activity to undergo self-processing but is resistant to enhancement even in the presence of an activating scaffold. Studies such as testing the activities of S99E and T125E or the phosphorylated versions (using site-specific phosphoincorporation) in the presence of a reconstituted apoptosome will provide additional insights into how phosphorylation of S99 and T125 inhibits caspase-9 activity as reported.

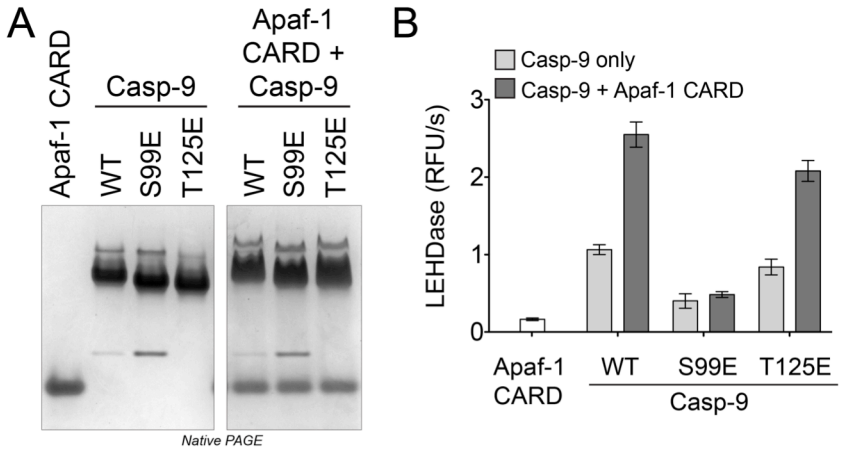

Figure A.2. S99E and T125E are able to interact with Apaf-1 CARD.
(A) Gel mobility shift assay of WT caspase-9, and phosphomimetic variants S99E and T125E in the presence of two-fold excess Apaf-1 CARD. Clear migration shifts were observed for all caspase-9 variants, suggesting an interaction with Apaf-1 CARD.
(B) Change in caspase-9 activity after incubation with Apaf-1 CARD. Elevated LEHDase activity was observed in WT caspase-9 and T125E while S99E did not display any change in activity.

Utilizing Phosphomimetics to Explore Potential Exosites

One recently explored mechanism that dictates caspase function is that caspases possess exosites critical to substrate recognition and binding. Due the negative charge that the phosphate moiety imparts on a residue, phosphorylation can alter binding interfaces, either promoting interactions by creating a new interface, or abrogating interactions by introducing charge repulsion. Thus one strategy to explore the presence of exosites in caspases is through phosphorylation. In casp-7, S30 was uncovered to be an exosite for binding with caspase-9. Phosphorylation of S30 abrogated binding of caspase-9 to procasp-7, leading to an attenuation of procasp-7 cleavage by caspase-9. This cleavage is paramount to casp-7 activation. However S30E had no direct effect on the DEVDase activity of the fully mature/cleaved casp-7[7]. In light of these observations, we examined whether S144 and S195 sites in caspase-9 also serve as exosites that are utilized by caspase-9 to bind and turnover protein substrates.

Both S144 and S195 are on the surface of helices in the catalytic core that could potentially be binding surfaces in caspase-9 (Figure 1.6B, A.3). Both sites are adjacent to charged patches in the catalytic core and substitution of both S144 and S195 to glutamate increases the surface area of these charged patches (Figure A.3).

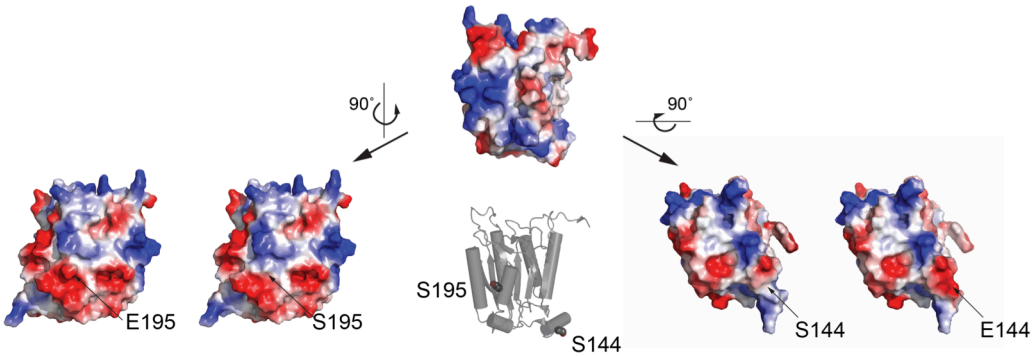

Figure A.3. Electrostatic potential map of catalytic core of caspase-9 monomer.
Surface representation of caspase-9 highlighting the changes in electrostatic potential in S195E (left) and S144E (right) when substituted with glutamate (E195 and E144, respectively). Cartoon representation in the middle shows the location of S144 and S195 in the caspase-9 monomer. Electrostatic potential maps were created using Pymol.

Caspase-9 phosphomimetic variants S144E and S195E exhibited WT-like LEHDase activities (Table A.1). We assessed whether S144E and S195E would impact the cleavage of protein substrates. Being an initiator caspase, it is extremely important that caspase-9 fulfills its function of cleaving downstream executioner caspases. Caspase-9 should also be able to undergo self-processing in the apoptosome, as it has emerged that uncleavable versions of caspase-9 could not be efficiently activated in the apoptosome[15].

S144E, S195E and the double glutamate variant S144E/S195E were tested in their ability to cleave the zymogen caspase-9 variant C287A (Figure A.4) to represent the ability of caspase-9 to perform *in trans* cleavage of other procaspase-9 enzymes. The rate of cleavage of caspase-9 C287A was similar for WT and S144E. S195E cleaved C287A slightly faster than WT, while the double mutant S144E/S195E displayed similar cleavage kinetics to WT. These data suggest that the phosphomimetic variants tested were capable of *in trans* caspase-9 processing.

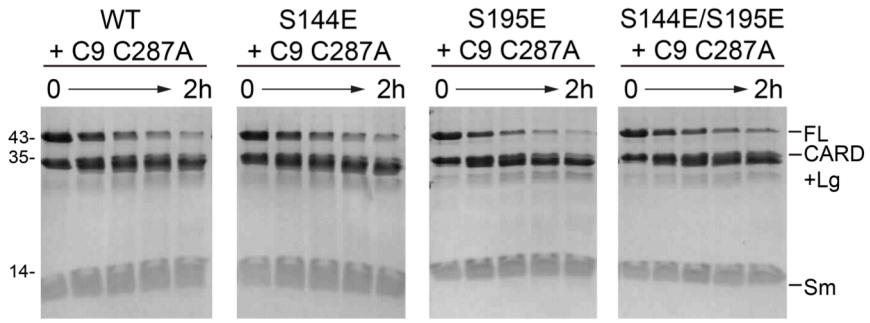

Figure A.4. Phosphomimetic S144E, S195E and S144E/S195E do not block *in trans* caspase-9 processing.
Full-length, zymogen caspase-9 C287A (catalytic site-inactivated) was cleaved with S144E, S195E and S144E/S195E variants for 2h. All variants cleaved C287A with comparable kinetics.

S195E was further tested in cleaving of executioner caspases casp-3 and -7. If caspase-9 utilizes S195 to bind and cleave casp-3 or casp-7, then the glutamate phosphomimetic S195E would display either faster or slower protein cleavage kinetics. However, there was no significant difference in its cleavage kinetics compared to WT caspase-9 (Figure A.5).

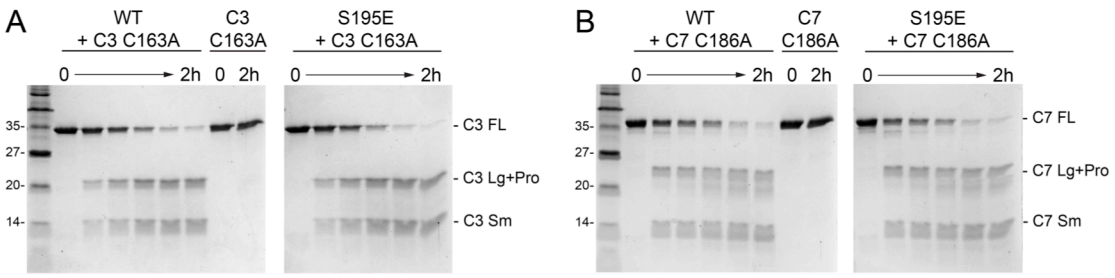

Figure A.5. Cleavage of procasp-3 and procasp-7 by caspase-9 S195E.
(A) Full-length, zymogen casp-3 (catalytic site-inactivated C163S), or (B) full-length zymogen casp-7 (catalytic site-inactivated C186A) was cleaved by WT caspase-9 or S195E for 2h. No significant difference in cleavage kinetics was observed between WT and S195E.

While phosphorylation of S144 and S195 reportedly led to caspase-9 inhibition in cell extracts, our assays showed no difference in protein cleavage activities between WT and the phosphomimetics. The mechanism for the reported inhibition of caspase-9 upon phosphorylation of these residues remains to be explained.

Phosphorylation of the Intersubunit Linker

Procaspase-9 is cleaved at three sites in the intersubunit linker. The major site for self-processing and cleavage by casp-8 is D315 in caspase-9 while minor processing occurs at E306. Caspase-9 D330 is the recognition and cleavage site for casp-3. Cleavage of the linker is an activating event for all caspases because it allows the critical L2 and L2' loops to sample the "up" conformation to stabilize the active site loop bundle. As an initiator caspase, no upstream caspase in the intrinsic pathway cleaves the caspase-9 linker, hence it undergoes processing and activation once incorporated in the apoptosome. Although it has been observed that cleavage of procaspase-9 is not necessary for catalytic activity, cleavage plays an integral part of caspase-9 regulation in various ways. First, the initial cleavage at D315 yields the p35 CARD+Large subunit and the p12 small subunit. The neo-N-terminal of the p12 subunit generates the IAP binding motif (^{316}ATPF^{319}) that is recognized by the BIR3 domain of XIAP, the apoptotic suppressor that traps caspase-9 in its monomeric state by binding to this epitope and blocking the dimerization interface, preventing caspase-9 activation. However, the second cleavage at D330 removes the IAP binding motif and partially relieves XIAP inhibition and allow caspase-9 activation. Second,

it was reported that cleaved caspase-9 has a weaker affinity for the apoptosome than procaspase-9/zymogen, causing procaspase-9 to displace any auto-activated/cleaved caspase-9 from the apoptosome. This process of recruitment-activation-displacement of caspase-9 in the apoptosome is hypothesized to function as a molecular timer, with the intracellular concentration of procaspase-9 setting the duration of the timer to process executioner caspases as caspase-9 substrates[16]. If this model is accurate, then cleavage of the intersubunit linker is critical, since without cleavage, procaspase-9 might remain bound to the apoptosome and cause the molecular timer to be suspended. Third, uncleavable versions of caspase-9 (E306A/D315A/D330A) were observed to be inefficiently activated by the apoptosome, attributing the drastic reduction in activity to the reduced ability of uncleavable caspase-9 to form homodimers[15]. Fourth, although the form in which caspase-9 functions outside of the apoptosome is still unknown, activated caspase-9 has been observed to be cleaved[17].

Phosphorylation of caspase substrates has been reported to alter their tendency to undergo cleavage by caspases (reviews[18,19]). This effect, whether promotion or protection against cleavage is commonly observed when phosphorylation is very near the caspase cleavage site. Caspase-9 has three phosphorylation sites in the intersubunit linker (Figure A.6A). These three sites are both adjacent to each other and neighbors the natural cleavage sites E306 and D315 (Figure A.6B). All three sites – S302, S307 and S310 – are reported to be phosphorylated by the kinase CK2 (casein kinase 2[20,21]). CK2 recognizes the minimal consensus sequence S-X-X-D/E/pS/pT (where pS and pT are phosphoSer and phosphoThr, respectively). Close inspection of these three sites revealed that the sequences surrounding these sites conform to the CK2 recognition sequence. Since these sites are adjacent to the linker cleavage sites in caspase-9, phosphorylation could prevent or promote self-cleavage of caspase-9. Phosphomimetic versions (S302E, S307E and S310E) were expressed in the full-length construct. Following overexpression, we observed that all phosphomimetic variants were in the fully mature/cleaved form, indicating that phosphomimicry most likely does not block caspase-9 self-cleavage. One interesting observation was the cleavage

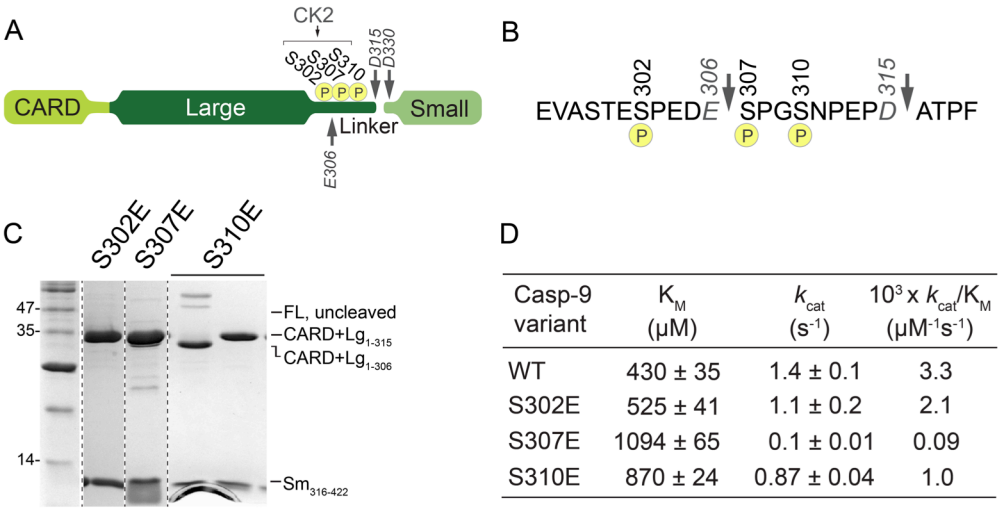

Casp-9 variant	K_M (μM)	k_{cat} (s^{-1})	$10^3 \times k_{cat}/K_M$ ($\mu M^{-1}s^{-1}$)
WT	430 ± 35	1.4 ± 0.1	3.3
S302E	525 ± 41	1.1 ± 0.2	2.1
S307E	1094 ± 65	0.1 ± 0.01	0.09
S310E	870 ± 24	0.87 ± 0.04	1.0

Figure A.6. Caspase-9 intersubunit linker phosphomimetic variants.
(A) Caspase-9 domains showing phosphorylation sites at intersubunit linker by CK2.
(B) The phosphorylation sites are adjacent to self-cleavage sites (E306 and D315, indicated by arrows) of caspase-9.
(C) Following overexpression, all phosphomimetic variants are in fully cleaved/mature form. S310E shows a distribution of two cleavage fragments.
(D) Catalytic parameters of linker variants using substrate LEHD-AFC. The catalytic efficiency of S307E is drastically reduced.

pattern of S310E. The predominant cleavage happens at D315, with a little (< 5%) processing observed at E306, and both fragments co-elute over the course of an ion exchange gradient. This fraction and co-elution were consistently observed in all our preparations of active caspase-9 variants. Intriguingly, S310E appears to promote cleavage at E306 (Figure A.6C, first lane in S310E), generating the E306 cleavage fragment greater than 5% that can be separated from the D315 fragment on an ion exchange gradient. The relevance of this cleavage pattern is still unknown but there was a moderate decrease in LEHDase activity observed for S310E (Figure A.6D).

The most striking observation among the linker variants was the dramatically reduced activity of S307E. It was able to auto-/self-process yet its catalytic efficiency is ~ 40x less than WT (Figure A.6C, A.6D). The fact that S307E was able to self-process yet exhibits a diminished catalytic activity suggests that phosphorylation affects the mature/cleaved form more severely

than the zymogen. We have yet to explore the mechanism by which S307E is inactivating, but we surmise that the long linker of caspase-9 can reach into its substrate-binding groove, and a phosphorylated S307 could either destabilize the active site loop bundle or occlude the substrate from binding, or both. The linker region of caspases have been shown to perform conformational acrobatics that contribute to the activation and catalytic function of caspases[22,23]. Casp-6 has a relatively long linker compared to other executioner caspases which allows for intramolecular cleavage[24]. In the structure of procasp-8 obtained by NMR, it was observed that the intact linker sits within the vicinity of the active site and forms intramolecular contacts with residues in the active site loop bundle[23]. Thus is it conceivable that the longer linker of caspase-9 would similarly be able to form these interactions with the active site loops and that phosphorylation of S307 would perturb critical interactions within the active site necessary for catalytic activity.

Phosphorylation of the intersubunit linker near cleavage sites in caspases has been reported to prevent zymogen activation, either by self-processing or by cleavage by other caspases. Casp-3 is phosphorylated by CK2 at T174 and S176, blocking linker cleavage by casp-8 and caspase-9[20]. Casp-8 is phosphorylated by Src kinase at Y380, preventing its maturation and activation in the DISC[25,26]. In murine caspase-9, phosphorylation of S348, which corresponds to S310 in human, also prevents auto/self-processing. However, our results showed that the corresponding phosphomimetics for the phosphorylation sites in the linker were still capable of self-processing since they were in the fully cleaved/mature form following overexpression (Figure A.6C). It would be worthwhile to study whether these phosphomimetics block cleavage of caspase-9 by other caspases including casp-3 and casp-8, which naturally cleave caspase-9. In addition, the phosphate moiety is in itself a glutamate mimic[19,27,28], thus it could potentially create new cleavage sites in caspase-9 that can be recognized by other caspases.

References

1. Martin, M. C. *et al.* Protein kinase A regulates caspase-9 activation by Apaf-1 downstream of cytochrome c. *J. Biol. Chem.* **280,** 15449–55 (2005).

2. Allan, L. A. *et al.* Inhibition of caspase-9 through phosphorylation at Thr 125 by ERK MAPK. *Nat. Cell Biol.* **5,** 647–54 (2003).

3. Seifert, A., Allan, L. A. & Clarke, P. R. DYRK1A phosphorylates caspase 9 at an inhibitory site and is potently inhibited in human cells by harmine. *FEBS J.* **275,** 6268–80 (2008).

4. Allan, L. A. & Clarke, P. R. Phosphorylation of caspase-9 by CDK1/cyclin B1 protects mitotic cells against apoptosis. *Mol. Cell* **26,** 301–10 (2007).

5. Lienhard, G. E. Non-functional phosphorylations? *Trends in Biochemical Sciences* **33,** 351–352 (2008).

6. Landry, C. R., Levy, E. D. & Michnick, S. W. Weak functional constraints on phosphoproteomes. *Trends Genet.* **25,** 193–197 (2009).

7. Eron, S. J., Raghupathi, K. & Hardy, J. A. Dual Site Phosphorylation of Caspase-7 by PAK2 Blocks Apoptotic Activity by Two Distinct Mechanisms. *Structure* **0,** 1913–1918 (2016).

8. Zhou, P., Chou, J., Olea, R. S., Yuan, J. & Wagner, G. Solution structure of Apaf-1 CARD and its interaction with caspase-9 CARD: a structural basis for specific adaptor/caspase interaction. *Proc. Natl. Acad. Sci. U. S. A.* **96,** 11265–70 (1999).

9. Shiozaki, E. N., Chai, J. & Shi, Y. Oligomerization and activation of caspase-9, induced by Apaf-1 CARD. *Proc. Natl. Acad. Sci. U. S. A.* **99,** 4197–202 (2002).

10. Acehan, D. *et al.* Three-Dimensional Structure of the Apoptosome : Implications for Assembly, Procaspase-9 Binding, and Activation. *Mol. Cell* **9,** 423–432 (2002).

11. Yuan, S., Yu, X., Asara, J. & Heuser, J. The holo-apoptosome: activation of procaspase-9 and interactions with caspase-3. *Structure* **19,** 1084–1096 (2011).

12. Li, Y. *et al.* Mechanistic insights into caspase-9 activation by the structure of the apoptosome holoenzyme. *Proc. Natl. Acad. Sci. U. S. A.* **114,** 1542–1547 (2017).

13. Hu, Q. *et al.* Molecular determinants of caspase-9 activation by the Apaf-1 apoptosome. *Proc. Natl. Acad. Sci. U. S. A.* **111,** 16254–61 (2014).

14. Cheng, T. C., Hong, C., Akey, I. V., Yuan, S. & Akey, C. W. A near atomic structure of the active human apoptosome. *Elife* **5,** 1–28 (2016).

15. Hu, Q., Wu, D., Chen, W., Yan, Z. & Shi, Y. Proteolytic Processing of Caspase-9 Zymogen Is Required for Apoptosome-mediated Activation of Caspase-9. *J. Biol. Chem.* 1–12 (2013). doi:10.1074/jbc.M112.441568

16. Malladi, S., Challa-Malladi, M., Fearnhead, H. O. & Bratton, S. B. The Apaf-1-procaspase-9 apoptosome complex functions as a proteolytic-based molecular timer. *EMBO J.* **28,** 1916–25 (2009).

17. Bitzer, M. *et al.* Caspase-8 and Apaf-1-independent Caspase-9 Activation in Sendai Virus-infected Cells. *J. Biol. Chem.* **277,** 29817–29824 (2002).

18. Kurokawa, M. & Kornbluth, S. Caspases and kinases in a death grip. *Cell* **138,** 838–54 (2009).

19. Dix, M. M. *et al.* Functional interplay between caspase cleavage and phosphorylation sculpts the apoptotic proteome. *Cell* **150,** 426–40 (2012).

20. Duncan, J. S. *et al.* A peptide-based target screen implicates the protein kinase CK2 in the global regulation of caspase signaling. *Sci. Signal.* **4,** ra30 (2011).

21. McDonnell, M. A. *et al.* Phosphorylation of murine caspase-9 by the protein kinase casein kinase 2 regulates its cleavage by caspase-8. *J. Biol. Chem.* **283,** 20149–58 (2008).

22. Dagbay, K. B. & Hardy, J. A. Multiple proteolytic events in caspase-6 self-activation impact conformations of discrete structural regions. *Proc. Natl. Acad. Sci. U. S. A.* 201704640 (2017). doi:10.1073/pnas.1704640114

23. Keller, N., Mares, J., Zerbe, O. & Grütter, M. G. Structural and biochemical studies on procaspase-8: new insights on initiator caspase activation. *Structure* **17,** 438–448 (2009).

24. Wang, X.-J. *et al.* Crystal structures of human caspase 6 reveal a new mechanism for intramolecular cleavage self-activation. *EMBO Rep.* **11,** 841–7 (2010).

25. Tsang, J. L. *et al.* Tyrosine Phosphorylation of Caspase-8 Abrogates Its Apoptotic Activity and Promotes Activation of c-Src. *PLoS One* **11,** e0153946 (2016).

26. Powley, I. R., Hughes, M. A., Cain, K. & MacFarlane, M. Caspase-8 tyrosine-380 phosphorylation inhibits CD95 DISC function by preventing procaspase-8 maturation and cycling within the complex. *Oncogene* **35,** 5629–5640 (2016).

27. Duncan, J. S. *et al.* Regulation of cell proliferation and survival: convergence of protein kinases and caspases. *Biochim. Biophys. Acta* **1804,** 505–10 (2010).

28. Seaman, J. E. *et al.* Cacidases: caspases can cleave after aspartate, glutamate and phosphoserine residues. *Cell Death Differ.* (2016). doi:10.1038/cdd.2016.62

BIBLIOGRAPHY

Acehan, D., Jiang, X., Morgan, D.G., Heuser, J.E., Wang, X., and Akey, C.W. (2002). Three-Dimensional Structure of the Apoptosome : Implications for Assembly, Procaspase-9 Binding, and Activation. Mol. Cell *9*, 423–432.

Aguzzi, A., and O'Connor, T. (2010). Protein aggregation diseases: pathogenicity and therapeutic perspectives. Nat. Rev. Drug Discov. *9*, 237–248.

Allan, L.A., and Clarke, P.R. (2007). Phosphorylation of caspase-9 by CDK1/cyclin B1 protects mitotic cells against apoptosis. Mol. Cell *26*, 301–310.

Allan, L.A., and Clarke, P.R. (2009). Apoptosis and autophagy: Regulation of caspase-9 by phosphorylation. FEBS J. *276*, 6063–6073.

Allan, L.A., Morrice, N., Brady, S., Magee, G., Pathak, S., and Clarke, P.R. (2003). Inhibition of caspase-9 through phosphorylation at Thr 125 by ERK MAPK. Nat. Cell Biol. *5*, 647–654.

Alnemri, E.S., Livingston, D.J., Nicholson, D.W., Salvesen, G., Thornberry, N.A., Wong, W.W., and Yuan, J. (1996). Human ICE/CED-3 Protease Nomenclature. Cell *87*, 171.

Bah, A., Vernon, R.M., Siddiqui, Z., Krzeminski, M., Muhandiram, R., Zhao, C., Sonenberg, N., Kay, L.E., and Forman-Kay, J.D. (2014). Folding of an intrinsically disordered protein by phosphorylation as a regulatory switch. Nature *519*, 106–109.

Barilà, D., Rufini, A., Condò, I., Dorey, K., Superti-furga, G., Barila, D., Condo, I., Ventura, N., and Testi, R. (2003). Caspase-Dependent Cleavage of c-Abl Contributes to Apoptosis Caspase-Dependent Cleavage of c-Abl Contributes to Apoptosis. Mol. Cell. Biol. *23*, 2790–2799.

Berson, J.F., Harper, D.C., Tenza, D., Raposo, G., and Marks, M.S. (2001). Pmel17 initiates premelanosome morphogenesis within multivesicular bodies. Mol. Biol. Cell *12*, 3451–3464.

Biancalana, M., and Koide, S. (2010). Molecular mechanism of Thioflavin-T binding to amyloid fibrils. Biochim Biophys Acta *1804*, 1405–1412.

Bitzer, M., Armeanu, S., Prinz, F., Ungerechts, G., Wybranietz, W., Spiegel, M., Bernlohr, C., Cecconi, F., Gregor, M., Neubert, W.J., et al. (2002). Caspase-8 and Apaf-1-independent Caspase-9 Activation in Sendai Virus-infected Cells. J. Biol. Chem. *277*, 29817–29824.

Boatright, K.M., Renatus, M., Scott, F.L., Sperandio, S., Shin, H., Pedersen, I.M., Ricci, J.-E., Edris, W.A., Sutherlin, D.P., Green, D.R., et al. (2003). A Unified Model for Apical Caspase Activation. Mol. Cell *11*, 529–541.

Boucher, D., Blais, V., and Denault, J.-B. (2012). Caspase-7 uses an exosite to promote poly(ADP ribose) polymerase 1 proteolysis. Proc. Natl. Acad. Sci. U. S. A. *109*, 5669–5674.

Brady, S.C., Allan, L.A., and Clarke, P.R. (2005). Regulation of Caspase 9 through Phosphorylation by Protein Kinase C Zeta in Response to Hyperosmotic Stress. Mol. Cell. Biol. *25*, 10543–10555.

Brasher, B.B., and Van Etten, R. a (2000). c-Abl has high intrinsic tyrosine kinase activity that is stimulated by mutation of the Src homology 3 domain and by autophosphorylation at two distinct regulatory tyrosines. J. Biol. Chem. *275*, 35631–35637.

Bratton, S.B., Walker, G., Srinivasula, S.M., Sun, X.M., Butterworth, M., Alnemri, E.S., and Cohen, G.M. (2001). Recruitment, activation and retention of caspases-9 and -3 by Apaf-1 apoptosome and associated XIAP complexes. EMBO J. *20*, 998–1009.

Bredesen, D.E. (2009). Neurodegeneration in Alzheimer's disease: caspases and synaptic element interdependence. Mol. Neurodegener. *4*, 27.

Cain, K., Brown, D.G., Langlais, C., and Cohen, G.M. (1999). Caspase activation involves the formation of the apoptosome, a large (approximately 700 kDa) caspase-activating complex. J. Biol. Chem. *274*, 22686–22692.

Cao, Q., Wang, X.J., Liu, C.W., Liu, D.F., Li, L.F., Gao, Y.Q., and Su, X.D. (2012). Inhibitory mechanism of caspase-6 phosphorylation revealed by crystal structures, molecular dynamics simulations, and biochemical assays. J. Biol. Chem. *287*, 15371–15379.

Cardone, M.H., Roy, N., Stennicke, H.R., Salvese, G.S., Franke, T.F., Stanbridge, E., Frisch, S., and Reed, J.C. (1998). Regulation of Cell Death Protease Caspase-9 by Phosphorylation. Science (80-.). *282*, 1318–1321.

Caretta, A., and Mucignat-Caretta, C. (2011). Protein kinase a in cancer. Cancers (Basel). *3*, 913–926.

Chao, Y., Shiozaki, E.N., Srinivasula, S.M., Rigotti, D.J., Fairman, R., and Shi, Y. (2005). Engineering a dimeric caspase-9: a re-evaluation of the induced proximity model for caspase activation. PLoS Biol. *3*, e183.

Chęcińska, A., Giaccone, G., Rodriguez, J.A., Kruyt, F.A.E., and Jimenez, C.R. (2009). Comparative proteomics analysis of caspase-9-protein complexes in untreated and cytochrome c/dATP stimulated lysates of NSCLC cells. J. Proteomics *72*, 575–585.

Cheng, H.C., Matsuura, I., and Wang, J.H. (1993). In vitro substrate specificity of protein tyrosine kinases. In Reversible Protein Phosphorylation in Cell Regulation, (Boston, MA: Springer US), pp. 103–112.

Cheng, T.C., Hong, C., Akey, I. V., Yuan, S., and Akey, C.W. (2016). A near atomic structure of the active human apoptosome. Elife *5*, 1–28.

Chijiwa, T., Mishima, A., Hagiwara, M., Sano$, M., Hayash&, K., Inouev, T., Naitoy, K., Toshiokall, T., and Hidakall, H. (1990). Inhibition of Forskolin-induced Neurite Outgrowth and Protein Phosphorylation by a Newly Synthesized Selective Inhibitor of Cyclic AMP-dependent Protein Kinase, N-[2-(p-Bromocinnamylamino)ethyl]-54soquinolinesulfonamide (H-89), of PC12D Pheochromocytoma Cells*. J. Biol. Chem. *265*, 5267–5.

Chimienti, F., Seve, M., Richard, S., Mathieu, J., and Favier, A. (2001). Role of cellular zinc in programmed cell death: temporal relationship between zinc depletion, activation of caspases, and cleavage of Sp family transcription factors. Biochem. Pharmacol. *62*, 51–62.

Chiti, F., and Dobson, C.M. (2006). Protein Misfolding, Functional Amyloid, and Human Disease. Annu. Rev. Biochem. *75*, 333–366.

Clerici, M., Luna-Vargas, M.P.A., Faesen, A.C., and Sixma, T.K. (2014). The DUSP–Ubl domain of USP4 enhances its catalytic efficiency by promoting ubiquitin exchange. Nat. Commun. *5*.

Cohen, P. (2000). The regulation of protein function by multisite phosphorylation – a 25 year update. Trends Biochem. Sci. *25*, 596–601.

Dagbay, K.B., and Hardy, J.A. (2017). Multiple proteolytic events in caspase-6 self-activation impact conformations of discrete structural regions. Proc. Natl. Acad. Sci. U. S. A. 201704640.

Dagbay, K., Eron, S.J., Serrano, B.P., Velázquez-Delgado, E.M., Zhao, Y., Lin, D., Vaidya, S., and Hardy, J.A. (2014). A multipronged approach for compiling a global map of allosteric regulation in the apoptotic caspases. Methods Enzymol.

Dagbay, K.B., Bolik-Coulon, N., Savinov, S.N., and Hardy, J.A. (2017). Caspase-6 Undergoes a Distinct Helix-Strand Interconversion upon Substrate Binding. J. Biol. Chem. *292*, 4885–4897.

Denault, J.-B., and Salvesen, G.S. (2003). Human caspase-7 activity and regulation by its N-terminal peptide. J. Biol. Chem. *278*, 34042–34050.

Dix, M.M., Simon, G.M., Wang, C., Okerberg, E., Patricelli, M.P., and Cravatt, B.F. (2012). Functional interplay between caspase cleavage and phosphorylation sculpts the apoptotic proteome. Cell *150*, 426–440.

Duncan, J.S., Turowec, J.P., Vilk, G., Li, S.S.C., Gloor, G.B., and Litchfield, D.W. (2010). Regulation of cell proliferation and survival: convergence of protein kinases and caspases. Biochim. Biophys. Acta *1804*, 505–510.

Duncan, J.S., Turowec, J.P., Duncan, K.E., Vilk, G., Wu, C., Lüscher, B., Li, S.S.-C., Gloor, G.B., and Litchfield, D.W. (2011). A peptide-based target screen implicates the protein kinase CK2 in the global regulation of caspase signaling. Sci. Signal. *4*, ra30.

Eguchi, K. (2001). Apoptosis in Autoimmune Diseases. Intern. Med. *40*, 275–284.

Elmore, S. (2007). Apoptosis: a review of programmed cell death. Toxicol. Pathol. *35*, 495–516.

Emsley, P., Lohkamp, B., Scott, W.G., and Cowtan, K. (2010). Features and development of Coot. Acta Crystallogr. Sect. D Biol. Crystallogr. *66*, 486–501.

Eron, S.J., Raghupathi, K., and Hardy, J.A. (2017). Dual Site Phosphorylation of Caspase-7 by PAK2 Blocks Apoptotic Activity by Two Distinct Mechanisms. Structure *25*, 27–39.

Fatemi, M., Hermann, A., Pradhan, S., and Jeltsch, A. (2001). The activity of the murine DNA methyltransferase Dnmt1 is controlled by interaction of the catalytic domain with the N-terminal part of the enzyme leading to an allosteric activation of the enzyme after binding to methylated DNA. J. Mol. Biol. *309*, 1189–1199.

Fava, L.L., Bock, F.J., Geley, S., and Villunger, A. (2013). Caspase-2 at a glance. J. Cell Sci. *125*.

Favaloro, B., Allocati, N., Graziano, V., Di Ilio, C., and De Laurenzi, V. (2012). Role of apoptosis in disease. Aging (Albany. NY). *4*, 330–349.

Feller, S.M., Knudsen, B., and Hanafusa, H. (1994). c-Abl kinase regulates the protein binding activity of c-Crk. EMBO J. *13*, 2341–2351.

Fischer, U., Jänicke, R.U., and Schulze-Osthoff, K. (2003). Many cuts to ruin: a comprehensive update of caspase substrates. Cell Death Differ. *10*, 76–100.

Fombonne, J., Bissey, P.-A., Guix, C., Sadoul, R., Thibert, C., and Mehlen, P. (2012). Patched dependence receptor triggers apoptosis through ubiquitination of caspase-9. Proc. Natl. Acad. Sci. U. S. A. *109*, 10510–10515.

Fowler, D.M., Koulov, A. V, Balch, W.E., and Kelly, J.W. Functional amyloid – from bacteria to humans.

Fowler, D.M., Koulov, A. V, Alory-Jost, C., Marks, M.S., Balch, W.E., and Kelly, J.W. Functional Amyloid Formation within Mammalian Tissue.

Franklin, R.A., and McCubrey, J.A. (2000). Kinases: positive and negative regulators of apoptosis. Leukemia *14*, 2019–2034.

Friedlander, R.M. (2003). Apoptosis and Caspases in Neurodegenerative Diseases. N. Engl. J. Med. *348*, 1365–1375.

Fuentes-Prior, P., and Salvesen, G.S. (2004). The protein structures that shape caspase activity, specificity, activation and inhibition. Biochem. J. *384*, 201–232.

Fujita, E., Egashira, J., Urase, K., Kuida, K., and Momoi, T. (2001). Caspase-9 processing by caspase-3 via a feedback amplification loop in vivo. Cell Death Differ. *8*, 335–344.

Garrido, C., Bruey, J.-M., Fromentin, A., Hammann, A., Arrigo, A.P., and Solary, E. (1999). HSP27 inhibits cytochrome c-dependent activation of procaspase-9. FASEB J. *13*, 2061–2070.

Garza, A.M.S., Khan, S.H., and Kumar, R. (2010). Site-Specific Phosphorylation Induces Functionally Active Conformation in the Intrinsically Disordered N-Terminal Activation Function (AF1) Domain of the Glucocorticoid Receptor. Mol. Cell. Biol. *30*, 220–230.

Gasteiger, E., Hoogland, C., Gattiker, A., Duvaud, S., Wilkins, M.R., Appel, R.D., and Bairoch, A. (2005). Protein Identification and Analysis Tools on the ExPASy Server. In The Proteomics Protocols Handbook, John M. Walker, ed. (Totowa, NJ: Humana Press Inc), pp. 571–607.

Ghavami, S., Hashemi, M., Ande, S.R., Yeganeh, B., Xiao, W., Eshraghi, M., Bus, C.J., Kadkhoda, K., Wiechec, E., Halayko, A.J., et al. (2009). Apoptosis and cancer: mutations within caspase genes. J. Med. Genet. *46*, 497–510.

Green, D.R., Beere, H.M., Wolf, B.B., Cain, K., Mosser, D.D., Mahboubi, A., Kuwana, T., Tailor, P., Morimoto, R.I., and Cohen, G.M. (2000). Heat-shock protein 70 inhibits apoptosis by preventing recruitment of procaspase-9 to the Apaf-1 apoptosome. Nat. Cell Biol. *2*, 469–475.

Greuber, E.K., Smith-Pearson, P., Wang, J., and Pendergast, A.M. (2013). Role of ABL family kinases in cancer: from leukaemia to solid tumours. Nat. Rev. Cancer *13*, 559–571.

Groenning, M. (2010). Binding mode of Thioflavin T and other molecular probes in the context of amyloid fibrils-current status. J. Chem. Biol. *3*, 1–18.

Gyrd-Hansen, M., Farkas, T., Fehrenbacher, N., Bastholm, L., Hoyer-Hansen, M., Elling, F., Wallach, D., Flavell, R., Kroemer, G., Nylandsted, J., et al. (2006). Apoptosome-Independent Activation of the Lysosomal Cell Death Pathway by Caspase-9. Mol. Cell. Biol. *26*, 7880–7891.

Hantschel, O., and Superti-Furga, G. (2004). Regulation of the c-Abl and Bcr-Abl tyrosine kinases. Nat. Rev. Mol. Cell Biol. *5*, 33–44.

Hardy, J.A., and Wells, J.A. (2009). Dissecting an allosteric switch in caspase-7 using chemical and mutational probes. J. Biol. Chem. *284*, 26063–26069.

Hengartner, M. (2000). The biochemistry of apoptosis. Nature *407*, 770–776.

Hornbeck, P. V., Zhang, B., Murray, B., Kornhauser, J.M., Latham, V., and Skrzypek, E. (2015). PhosphoSitePlus, 2014: mutations, PTMs and recalibrations. Nucleic Acids Res. *43*, D512–D520.

Hou, F., Sun, L., Zheng, H., Skaug, B., Jiang, Q.-X., and Chen, Z.J. (2011). MAVS Forms Functional Prion-like Aggregates to Activate and Propagate Antiviral Innate Immune Response. Cell *146*, 448–461.

Howley, B., and Fearnhead, H.O. (2008). Caspases as therapeutic targets. J. Cell. Mol. Med. *12*, 1502–1516.

Hu, Q., Wu, D., Chen, W., Yan, Z., and Shi, Y. (2013). Proteolytic Processing of Caspase-9 Zymogen Is Required for Apoptosome-mediated Activation of Caspase-9. J. Biol. Chem. 1–12.

Hu, Q., Wu, D., Chen, W., Yan, Z., Yan, C., He, T., Liang, Q., and Shi, Y. (2014). Molecular determinants of caspase-9 activation by the Apaf-1 apoptosome. Proc. Natl. Acad. Sci. U. S. A. *111*, 16254–16261.

Huang, W., Jiang, T., Choi, W., Qi, S., Pang, Y., Hu, Q., Xu, Y., Gong, X., Jeffrey, P.D., Wang, J., et al. (2013). Mechanistic insights into CED-4-mediated activation of CED-3. Genes Dev. *27*, 2039–2048.

Huber, K.L., and Hardy, J.A. (2012a). Mechanism of zinc-mediated inhibition of caspase-9. Protein Sci. *21*, 1056–1065.

Inoue, H., Tsukita, K., Iwasato, T., Suzuki, Y., Tomioka, M., Tateno, M., Nagao, M., Kawata, A., Saido, T.C., Miura, M., et al. (2003). The crucial role of caspase-9 in the disease progression of a transgenic ALS mouse model. EMBO J. *22*, 6665–6674.

Insel, P.A., Zhang, L., Murray, F., Yokouchi, H., and Zambon, A.C. (2012). Cyclic AMP is both a pro-apoptotic and anti-apoptotic second messenger. Acta Physiol. *204*, 277–287.

Johnson, S.A., and Hunter, T. (2005). Kinomics: methods for deciphering the kinome. Nat. Methods *2*, 17–25.

Kashiwagi, M., Enghild, J.J., Gendron, C., Hughes, C., Caterson, B., Itoh, Y., and Nagase, H. (2004). Altered proteolytic activities of ADAMTS-4 expressed by C-terminal processing. J. Biol. Chem. *279*, 10109–10119.

Keller, N., Mares, J., Zerbe, O., and Grütter, M.G. (2009). Structural and biochemical studies on procaspase-8: new insights on initiator caspase activation. Structure *17*, 438–448.

Kharbanda, S., Ren, R., Pandey, P., Shafman, T.D., Feller, S.M., Weichselbaum, R.R., and Kufe, D.W. (1995). Activation of the c-Abl tyrosine kinase in the stress response to DNA-damaging agents. Nature *376*, 785–788.

Kim, J.-E., and Tannenbaum, S.R. (2004). S-Nitrosation regulates the activation of endogenous procaspase-9 in HT-29 human colon carcinoma cells. J. Biol. Chem. *279*, 9758–9764.

Kim, I.R., Murakami, K., Chen, N.-J., Saibil, S.D., Matysiak-Zablocki, E., Elford, A.R., Bonnard, M., Benchimol, S., Jurisicova, A., Yeh, W.-C., et al. (2009). DNA damage- and stress-induced apoptosis occurs independently of PIDD. Apoptosis *14*, 1039–1049.

Klaiman, G., Champagne, N., and LeBlanc, A.C. (2009). Self-activation of Caspase-6 in vitro and in vivo: Caspase-6 activation does not induce cell death in HEK293T cells. Biochim. Biophys. Acta - Mol. Cell Res. *1793*, 592–601.

Kobe, B., Jennings, I.G., House, C.M., Michell, B.J., Goodwill, K.E., Santarsiero, B.D., Stevens, R.C., Cotton, R.G.H., and Kemp, B.E. (1999). Structural basis of autoregulation of phenylalanine hydroxylase. Nat. Struct. Biol. *6*, 442–448.

Kumar, S., and Walter, J. (2011). Phosphorylation of amyloid beta peptides- A trigger for formation of toxic aggregates in Alzheimer's disease. Aging (Albany. NY). *3*, 803–812.

Kurokawa, M., and Kornbluth, S. (2009). Caspases and kinases in a death grip. Cell *138*, 838–854.

Laguna, A., Aranda, S., Barallobre, M.J., Barhoum, R., Fernández, E., Fotaki, V., Delabar, J.M., de la Luna, S., de la Villa, P., and Arbonés, M.L. (2008). The protein kinase DYRK1A regulates caspase-9-mediated apoptosis during retina development. Dev. Cell *15*, 841–853.

Landry, C.R., Levy, E.D., and Michnick, S.W. (2009). Weak functional constraints on phosphoproteomes. Trends Genet. *25*, 193–197.

Lanneau, D., Brunet, M., Frisan, E., Solary, E., Fontenay, M., and Garrido, C. (2008). Heat shock proteins: essential proteins for apoptosis regulation. J. Cell. Mol. Med. *12*, 743–761.

Laskowski, R.A., and Swindells, M.B. (2011). LigPlot+: Multiple Ligand-Protein Interaction Diagrams for Drug Discovery. J. Chem. Inf. Model. *51*, 2778–2786.

LeBlanc, A.C. (2003). Natural cellular inhibitors of caspases. Prog. Neuro-Psychopharmacology Biol. Psychiatry *27*, 215–229.

Li, J., and Yuan, J. (2008). Caspases in apoptosis and beyond. Oncogene *27*, 6194–6206.

Li, J., McQuade, T., Siemer, A.B., Napetschnig, J., Moriwaki, K., Hsiao, Y.-S., Damko, E., Moquin, D., Walz, T., McDermott, A., et al. (2012). The RIP1/RIP3 Necrosome Forms a Functional Amyloid Signaling Complex Required for Programmed Necrosis. Cell *150*, 339–350.

Li, Y., Zhou, M., Hu, Q., Bai, X.-C., Huang, W., Scheres, S.H.W., and Shi, Y. (2017). Mechanistic insights into caspase-9 activation by the structure of the apoptosome holoenzyme. Proc. Natl. Acad. Sci. U. S. A. *114*, 1542–1547.

Lienhard, G.E. (2008). Non-functional phosphorylations? Trends Biochem. Sci. *33*, 351–352.

Lin, S.C., Lo, Y.C., and Wu, H. (2010). Helical assembly in the MyD88-IRAK4-IRAK2 complex in TLR/IL-1R signalling. Nature *465*, 885–890.

López-Otín, C., and Hunter, T. (2010). The regulatory crosstalk between kinases and proteases in cancer. Nat. Rev. Cancer *10*, 278–292.

Lu, A., Li, Y., Schmidt, F.I., Yin, Q., Chen, S., Fu, T.-M., Tong, A.B., Ploegh, H.L., Mao, Y., and Wu, H. (2016). Molecular basis of caspase-1 polymerization and its inhibition by a new capping mechanism. Nat. Struct. Mol. Biol. *23*, 1–12.

Lyskov, S., and Gray, J.J. (2008). The RosettaDock server for local protein-protein docking. Nucleic Acids Res. *36*, W233–W238.

Machuy, N., Rajalingam, K., and Rudel, T. (2004). Requirement of caspase-mediated cleavage of c-Abl during stress-induced apoptosis. Cell Death Differ. *11*, 290–300.

MacKenzie, S.H., and Clark, A.C. (2012). Death by caspase dimerization. Adv. Exp. Med. Biol. *747*, 55–73.

Malladi, S., Challa-Malladi, M., Fearnhead, H.O., and Bratton, S.B. (2009). The Apaf-1-procaspase-9 apoptosome complex functions as a proteolytic-based molecular timer. EMBO J. *28*, 1916–1925.

Mannick, J.B. (2007). Regulation of apoptosis by protein S-nitrosylation. Amino Acids *32*, 523–526.

Mannick, J.B., Schonhoff, C., Papeta, N., Ghafourifar, P., Szibor, M., Fang, K., and Gaston, B. (2001). S-Nitrosylation of mitochondrial caspases. J. Cell Biol. *154*, 1111–1116.

Manning, B.D., and Cantley, L.C. (2002). Hitting the Target: Emerging Technologies in the Search for Kinase Substrates. Sci. Signal. *2002*.

Manns, J., Daubrawa, M., Driessen, S., Paasch, F., Hoffmann, N., Löffler, A., Lauber, K., Dieterle, A., Alers, S., Iftner, T., et al. (2011). Triggering of a novel intrinsic apoptosis pathway by the kinase inhibitor staurosporine: activation of caspase-9 in the absence of Apaf-1. FASEB J. *25*, 3250–3261.

Manzl, C., Peintner, L., Krumschnabel, G., Bock, F., Labi, V., Drach, M., Newbold, A., Johnstone, R., and Villunger, A. (2012). PIDDosome-independent tumor suppression by Caspase-2. Cell Death Differ. *19*, 1722–1732.

Martin, M.C., Dransfield, I., Haslett, C., and Rossi, A.G. (2001). Cyclic AMP regulation of neutrophil apoptosis occurs via a novel protein kinase A-independent signaling pathway. J. Biol. Chem. *276*, 45041–45050.

Martin, M.C., Allan, L.A., Lickrish, M., Sampson, C., Morrice, N., and Clarke, P.R. (2005). Protein kinase A regulates caspase-9 activation by Apaf-1 downstream of cytochrome c. J. Biol. Chem. *280*, 15449–15455.

Masumoto, J., Taniguchi, S., Ayukawa, K., Sarvotham, H., Kishino, T., Niikawa, N., Hidaka, E., Katsuyama, T., Higuchi, T., and Sagara, J. (1999). ASC, a Novel 22-kDa Protein, Aggregates during Apoptosis of Human Promyelocytic Leukemia HL-60 Cells. J. Biol. Chem. *274*, 33835–33838.

McDonnell, M.A., Wang, D., Khan, S.M., Vander Heiden, M.G., and Kelekar, A. (2003). Caspase-9 is activated in a cytochrome c-independent manner early during TNFα-induced apoptosis in murine cells. Cell Death Differ. *10*, 1005–1015.

McDonnell, M.A., Abedin, M.J., Melendez, M., Platikanova, T.N., Ecklund, J.R., Ahmed, K., and Kelekar, A. (2008). Phosphorylation of murine caspase-9 by the protein kinase casein kinase 2 regulates its cleavage by caspase-8. J. Biol. Chem. *283*, 20149–20158.

McIlwain, D.R., Berger, T., and Mak, T.W. (2013). Caspase functions in cell death and disease. Cold Spring Harb. Perspect. Biol. *5*, 1–27.

McStay, G.P., Salvesen, G.S., and Green, D.R. (2008). Overlapping cleavage motif selectivity of caspases: implications for analysis of apoptotic pathways. Cell Death Differ. *15*, 322–331.

Meergans, T., Hildebrandt, A.-K., Horak, D., Haenisch, C., and Wendel, A. (2000). The short prodomain influences caspase-3 activation in HeLa cells. Biochem. J *349*, 135–140.

Metcalfe, E.E., Traaseth, N.J., and Veglia, G. (2005). Serine 16 phosphorylation induces an order-to-disorder transition in monomeric phospholamban. Biochemistry *44*, 4386–4396.

Micsonai, A., Wien, F., Kernya, L., Lee, Y.-H., Goto, Y., Réfrégiers, M., and Kardos, J. (2015). Accurate secondary structure prediction and fold recognition for circular dichroism spectroscopy. Proc. Natl. Acad. Sci. U. S. A. *112*, E3095-103.

Mille, F., Thibert, C., Fombonne, J., Rama, N., Guix, C., Hayashi, H., Corset, V., Reed, J.C., and Mehlen, P. (2009). The Patched dependence receptor triggers apoptosis through a DRAL–caspase-9 complex. Nat. Cell Biol. *11*, 739–746.

Mitrea, D.M., and Kriwacki, R.W. (2013). Regulated unfolding of proteins in signaling. FEBS Lett. *587*, 1081–1088.

Mueller, T., Voigt, W., Simon, H., Fruehauf, A., Bulankin, A., Grothey, A., and Schmoll, H.-J. (2003). Failure of Activation of Caspase-9 Induces a Higher Threshold for Apoptosis and Cisplatin Resistance in Testicular Cancer. Cancer Res. *63*, 513–521.

Murray, T.V.A., McMahon, J.M., Howley, B.A., Stanley, A., Ritter, T., Mohr, A., Zwacka, R., and Fearnhead, H.O. (2008). A non-apoptotic role for caspase-9 in muscle differentiation. J. Cell Sci. *121*, 3786–3793.

Muzio, M., Chinnaiyan, A.M., Kischkel, F.C., O'Rourke, K., Shevchenko, A., Ni, J., Scaffidi, C., Bretz, J.D., Zhang, M., Gentz, R., et al. (1996). FLICE, A Novel FADD-Homologous ICE/CED-3–like Protease, Is Recruited to the CD95 (Fas/APO-1) Death-Inducing Signaling Complex. Cell *85*, 817–827.

Mylona, A., Theillet, F.-X., Foster, C., Cheng, T.M., Miralles, F., Bates, P.A., Selenko, P., and Treisman, R. (2016). Opposing effects of Elk-1 multisite phosphorylation shape its response to ERK activation. Science *354*, 233–237.

Narayana, N., Cox, S., Shaltiel, S., Taylor, S.S., and Xuong, N. (1997). Crystal structure of a polyhistidine-tagged recombinant catalytic subunit of cAMP-dependent protein kinase complexed with the peptide inhibitor PKI(5-24) and adenosine. Biochemistry *36*, 4438–4448.

Nesterova, M. V., and Cho-Chung, Y.S. (2006). Significance of Protein Kinase A in Cancer. In Apoptosis, Cell Signaling, and Human Diseases, (Totowa, NJ: Humana Press), pp. 3–30.

Nishi, H., Hashimoto, K., and Panchenko, A.R. (2011). Phosphorylation in Protein-Protein Binding: Effect on Stability and Function. Structure *19*, 1807–1815.

Nishi, H., Fong, J.H., Chang, C., Teichmann, S.A., and Panchenko, A.R. (2013). Regulation of protein–protein binding by coupling between phosphorylation and intrinsic disorder: analysis of human protein complexes. Mol. Biosyst. *9*, 1620.

Nishi, H., Shaytan, A., and Panchenko, A.R. (2014). Physicochemical mechanisms of protein regulation by phosphorylation. Front. Genet. *5*, 270.

Olsson, M., and Zhivotovsky, B. (2011). Caspases and cancer. Cell Death Differ. *18*, 1441–1449.

Orlov, S.N., Thorin-Trescases, N., Dulin, N.O., Dam, T.-V., Fortuno, M.A., Tremblay, J., and Hamet, P. (1999). Activation of cAMP signaling transiently inhibits apoptosis in vascular smooth muscle cells in a site upstream of caspase-3. Cell Death Differ. *6*, 661–672.

Öztaş, P., Lortlar, N., Polat, M., Allı, N., Ömeroğlu, S., and Basman, A. (2007). Caspase-9 expression is increased in endothelial cells of active Behçet's disease patients. Int. J. Dermatol. *46*, 172–176.

Palmerini, F., Devilard, E., Jarry, A., Birg, F., and Xerri, L. (2001). Caspase-7 downregulation as an immunohistochemical marker of colonic carcinoma. Hum. Pathol. *32*, 461–467.

Park, H.H., Lo, Y.-C., Lin, S.-C., Wang, L., Yang, J.K., and Wu, H. (2007). The death domain superfamily in intracellular signaling of apoptosis and inflammation. Annu. Rev. Immunol. *25*, 561–586.

Parrish, A.B., Freel, C.D., and Kornbluth, S. (2013). Cellular Mechanisms Controlling Caspase Activation and Function. Cold Spring Harb Perspect Biol *5*, 1–24.

Pathan, N., Marusawa, H., Krajewska, M., Matsuzawa, S., Kim, H., Okada, K., Torii, S., Kitada, S., Krajewski, S., Welsh, K., et al. (2001). TUCAN, an antiapoptotic caspase-associated recruitment domain family protein overexpressed in cancer. J. Biol. Chem. *276*, 32220–32229.

Pirman, N.L., Barber, K.W., Aerni, H.R., Ma, N.J., Haimovich, A.D., Rogulina, S., Isaacs, F.J., and Rinehart, J. (2015). A flexible codon in genomically recoded Escherichia coli permits programmable protein phosphorylation. Nat. Commun. *6*, 8130.

Pop, C., and Salvesen, G.S. (2009). Human caspases: activation, specificity, and regulation. J. Biol. Chem. *284*, 21777–21781.

Pop, C., Timmer, J., Sperandio, S., and Salvesen, G.S. (2006). The apoptosome activates caspase-9 by dimerization. Mol. Cell *22*, 269–275.

Powley, I.R., Hughes, M.A., Cain, K., and MacFarlane, M. (2016). Caspase-8 tyrosine-380 phosphorylation inhibits CD95 DISC function by preventing procaspase-8 maturation and cycling within the complex. Oncogene *35*, 5629–5640.

Qiao, Q., Yang, C., Zheng, C., Fontá, L., David, L., Yu, X., Bracken, C., Rosen, M., Melnick, A., Egelman, E.H., et al. (2013). Structural Architecture of the CARMA1/Bcl10/MALT1 Signalosome: Nucleation-Induced Filamentous Assembly. Mol. Cell *51*, 766–779.

Qin, H., Srinivasula, S.M., Wu, G., Fernandes-Alnemri, T., Alnemri, E.S., and Shi, Y. (1999). Structural basis of procaspase-9 recruitment by the apoptotic protease-activating factor 1. Nature *399*, 549–557.

Raina, D., Pandey, P., Ahmad, R., Bharti, A., Ren, J., Kharbanda, S., Weichselbaum, R., and Kufe, D. (2005). c-Abl tyrosine kinase regulates caspase-9 autocleavage in the apoptotic response to DNA damage. J. Biol. Chem. *280*, 11147–11151.

Renatus, M., Stennicke, H.R., Scott, F.L., Liddington, R.C., and Salvesen, G.S. (2001). Dimer formation drives the activation of the cell death protease caspase-9. Proc. Natl. Acad. Sci. U. S. A. *98*, 14250–14255.

Rodriguez, J., and Lazebnik, Y. (1999). Caspase-9 and Apaf-1 form an active holoenzyme. Genes Dev. *13*, 3179–3184.

Ross, C.A., and Poirier, M.A. (2004). Protein aggregation and neurodegenerative disease. Nat. Med. *10*, S10–S17.

Rossi, A.G., Cousin, J.M., Dransfield, I., Lawson, M.F., Chilvers, E.R., and Haslett, C. (1995). Agents That Elevate cAMP Inhibit Human Neutrophil Apoptosis. Biochem. Biophys. Res. Commun. *217*, 892–899.

Rutter, J., Michnoff, C.H., Harper, S.M., Gardner, K.H., and McKnight, S.L. (2001). PAS kinase: an evolutionarily conserved PAS domain-regulated serine/threonine kinase. Proc. Natl. Acad. Sci. U. S. A. *98*, 8991–8996.

Salazar, C., and Höfer, T. (2009). Multisite protein phosphorylation - from molecular mechanisms to kinetic models. FEBS J. *276*, 3177–3198.

Salvesen, G., and Dixit, V. (1999). Caspase activation: the induced-proximity model. Proc. Natl. Acad. Sci. U. S. A. *96*, 10964–10967.

Samraj, A.K., Keil, E., Ueffing, N., Schulze-Osthoff, K., and Schmitz, I. (2006). Loss of caspase-9 provides genetic evidence for the type I/II concept of CD95-mediated apoptosis. J. Biol. Chem. *281*, 29652–29659.

Samraj, A.K., Sohn, D., Schulze-Osthoff, K., and Schmitz, I. (2007). Loss of caspase-9 reveals its essential role for caspase-2 activation and mitochondrial membrane depolarization. Mol. Biol. Cell *18*, 84–93.

Samuel, F., Flavin, W.P., Iqbal, S., Pacelli, C., Sri Renganathan, S.D., Trudeau, L.-E., Campbell, E.M., Fraser, P.E., and Tandon, A. (2016). Effects of Serine 129 Phosphorylation on α-Synuclein Aggregation, Membrane Association, and Internalization. J. Biol. Chem. *291*, 4374–4385.

Sapio, L., Di Maiolo, F., Illiano, M., Esposito, A., Chiosi, E., Spina, A., and Naviglio, S. (2014). Targeting protein kinase A in cancer therapy: an update. EXCLI J. *13*, 843–855.

Sato, H., Kato, T., and Arawaka, S. (2013). The role of Ser129 phosphorylation of α-synuclein in neurodegeneration of Parkinson's disease: a review of in vivo models. Rev. Neurosci. *24*, 115–123.

Schultz, J.E., and Natarajan, J. (2013). Regulated unfolding: a basic principle of intraprotein signaling in modular proteins. Trends Biochem. Sci. *38*, 538–545.

Schwerk, C., and Schulze-Osthoff, K. (2005). Regulation of Apoptosis by Alternative Pre-mRNA Splicing. Mol. Cell *19*, 1–13.

Seaman, J.E., Julien, O., Lee, P.S., Rettenmaier, T.J., Thomsen, N.D., and Wells, J.A. (2016). Cacidases: caspases can cleave after aspartate, glutamate and phosphoserine residues. Cell Death Differ.

Seeliger, M.A., Young, M., Henderson, M.N., Pellicena, P., King, D.S., Falick, A.M., and Kuriyan, J. (2005). High yield bacterial expression of active c-Abl and c-Src tyrosine kinases. 3135–3139.

Seifert, A., Allan, L.A., and Clarke, P.R. (2008). DYRK1A phosphorylates caspase 9 at an inhibitory site and is potently inhibited in human cells by harmine. FEBS J. *275*, 6268–6280.

Sekimura, A., Konishi, A., Mizuno, K., Kobayashi, Y., Sasaki, H., Yano, M., Fukai, I., and Fujii, Y. (2004). Expression of Smac/DIABLO is a novel prognostic marker in lung cancer. Oncol. Rep. *11*, 797–802.

Serrano, B.P., and Hardy, J.A. (2017). Phosphorylation by Protein Kinase A Disassembles the Caspase-9 Core. Cell Death Differ.

Serrano, B.P., Szydlo, H.S., Alfandari, D.R., and Hardy, J.A. (2017). Active-site adjacent phosphorylation at Tyr-397 by c-Abl kinase inactivates caspase-9. J. Biol. Chem. *292*, 21352–21365.

Shaul, Y. (2000). c-Abl: activation and nuclear targets. Cell Death Differ. *7*, 10–16.

Shi, Y. (2002). Mechanisms of Caspase Activation and Inhibition during Apoptosis Caspases are central components of the machinery. Mol. Cell *9*, 459–470.

Shi, Y. (2004). Caspase activation: revisiting the induced proximity model. Cell *117*, 855–858.

Shi, Y. (2005). Activation of Initiator Caspases : History, Hypotheses, and Perspectives. J. Cancer Mol. *1*, 9–18.

Shiozaki, E.N., Chai, J., and Shi, Y. (2002). Oligomerization and activation of caspase-9, induced by Apaf-1 CARD. Proc. Natl. Acad. Sci. U. S. A. *99*, 4197–4202.

Shiozaki, E.N., Chai, J., Rigotti, D.J., Riedl, S.J., Li, P., Srinivasula, S.M., Alnemri, E.S., Fairman, R., and Shi, Y. (2003). Mechanism of XIAP-mediated inhibition of caspase-9. Mol. Cell *11*, 519–527.

Siegel, R.M., Martin, D.A., Zheng, L., Ng, S.Y., Bertin, J., Cohen, J., and Lenardo, M.J. (1998). Death-effector filaments: novel cytoplasmic structures that recruit caspases and trigger apoptosis. J. Cell Biol. *141*, 1243–1253.

Sirvent, A., Benistant, C., and Roche, S. (2008). Cytoplasmic signalling by the c-Abl tyrosine kinase in normal and cancer cells. Biol. Cell *100*, 617–631.

Skotte, N.H., Sanders, S.S., Singaraja, R.R., Ehrnhoefer, D.E., Vaid, K., Qiu, X., Kannan, S., Verma, C., and Hayden, M.R. (2017). Palmitoylation of caspase-6 by HIP14 regulates its activation. Cell Death Differ. *24*, 433–444.

Slee, E.A., Harte, M.T., Kluck, R.M., Wolf, B.B., Casiano, C.A., Newmeyer, D.D., Wang, H., Reed, J.C., Nicholson, D.W., Alnemri, E.S., et al. (1999a). Ordering the cytochrome c-initiated caspase cascade: Hierarchical activation of caspases-2, -3, -6, -7, -8 and -10 in a caspase-9-dependent manner. Mol. Cell *144*, 281–292.

Slee, E.A., Harte, M.T., Kluck, R.M., Wolf, B.B., Casiano, C.A., Newmeyer, D.D., Wang, H.G., Reed, J.C., Nicholson, D.W., Alnemri, E.S., et al. (1999b). Ordering the cytochrome c-initiated caspase cascade: Hierarchical activation of caspases-2,-3,-6,-7,-8, and -10 in a caspase-9-dependent manner. J. Cell Biol. *144*, 281–292.

Slice, L.W., and Taylor, S.S. (1989). Expression of the Catalytic Subunit of CAMP-dependent Protein Kinase in. J. Biol. Chem. *264*, 20940–20946.

Srinivasula, S.M., Ahmad, M., Fernandes-Alnemri, T., and Alnemri, E.S. (1998). Autoactivation of Procaspase-9 by Apaf-1-Mediated Oligomerization. Mol. Cell *1*, 949–957.

Srinivasula, S.M., Ahmad, M., Guo, Y., Zhan, Y., Lazebnik, Y., Fernandes-Alnemri, T., and Alnemri, E.S. (1999). Identification of an endogenous dominant-negative short isoform of caspase-9 that can regulate apoptosis. Cancer Res. *59*, 999–1002.

Srinivasula, S.M., Hegde, R., Saleh, A., Datta, P., Shiozaki, E., Chai, J., Lee, R.-A., Robbins, P.D., Fernandes-Alnemri, T., Shi, Y., et al. (2001). A conserved XIAP-interaction motif in caspase-9 and Smac/DIABLO regulates caspase activity and apoptosis. Nature *410*, 112–116.

Stamogiannos, A., Maben, Z., Papakyriakou, A., Mpakali, A., Kokkala, P., Georgiadis, D., Stern, L.J., and Stratikos, E. (2017). Critical Role of Interdomain Interactions in the Conformational Change and Catalytic Mechanism of Endoplasmic Reticulum Aminopeptidase 1. Biochemistry *56*, 1546–1558.

Stanger, K., Steffek, M., Zhou, L., Pozniak, C.D., Quan, C., Franke, Y., Tom, J., Tam, C., Elliott, J.M., Lewcock, J.W., et al. (2012). Allosteric peptides bind a caspase zymogen and mediate caspase tetramerization. Nat. Chem. Biol. *8*, 655–660.

Steinmetz, M.O., Jahnke, W., Towbin, H., Garcia-Echeverria, C., Voshol, H., Muller, D., and van Oostrum, J. (2001). Phosphorylation disrupts the central helix in Op18/stathmin and suppresses binding to tubulin. EMBO Rep. *2*, 505–510.

Stennicke, H.R., and Salvesen, G.S. (1999). Caspases: Preparation and Characterization. Methods *17*, 313–319.

Stennicke, H.R., Deveraux, Q.L., Humke, E.W., Reed, J.C., Dixit, V.M., and Salvesen, G.S. (1999). Caspase-9 can be activated without proteolytic processing. J. Biol. Chem. *274*, 8359–8362.

Steuber, H., Siszler, G., Nisa, S., Schwarz, F., Blasche, S., Mo, M., Lavrik, I., Gronewold, T.M.A., Maskos, K., Donnenberg, M.S., et al. (2013). The E . coli Effector Protein NleF Is a Caspase Inhibitor. PLoS One *8*, e58937.

Sträter, J., Herter, I., Merkel, G., Hinz, U., Weitz, J., and Möller, P. (2010). Expression and prognostic significance of APAF-1, caspase-8 and caspase-9 in stage II/III colon carcinoma: caspase-8 and caspase-9 is associated with poor prognosis. Int. J. Cancer *127*, 873–880.

Taagepera, S., McDonald, D., Loeb, J.E., Whitaker, L.L., McElroy, A.K., Wang, J.Y.J., and Hope, T.J. (1998). Nuclear-cytoplasmic shuttling of C-ABL tyrosine kinase. Proc. Natl. Acad. Sci. *95*, 7457–7462.

Takayama, S., Reed, J.C., and Homma, S. (2003). Heat-shock proteins as regulators of apoptosis. Oncogene *22*, 9041–9047.

Tashker, J.S., Olson, M., and Kornbluth, S. (2002). Post–cytochrome c protection from apoptosis conferred by a MAPK pathway in Xenopus egg extracts. Mol. Biol. Cell *13*, 393–401.

Tenreiro, S., Eckermann, K., and Outeiro, T.F. (2014). Protein phosphorylation in neurodegeneration: friend or foe? Front. Mol. Neurosci. *7*, 42.

Timmer, J.C., and Salvesen, G.S. (2007). Caspase substrates. Cell Death Differ. *14*, 66–72.

Tinel, A., and Tschopp, J. (2004). The PIDDosome, a Protein Complex Implicated in Activation of Caspase-2 in Response to Genotoxic Stress. Science (80-.). *304*.

Tsang, J.L., Jia, S.H., Parodo, J., Plant, P., Lodyga, M., Charbonney, E., Szaszi, K., Kapus, A., and Marshall, J.C. (2016). Tyrosine Phosphorylation of Caspase-8 Abrogates Its Apoptotic Activity and Promotes Activation of c-Src. PLoS One *11*, e0153946.

Twiddy, D., and Cain, K. (2007). Caspase-9 cleavage, do you need it? Biochem. J. *405*, e1-2.

Vaidya, S., and Hardy, J.A. (2011). Caspase-6 Latent State Stability Relies on Helical Propensity. Biochemistry *50*, 3282–3287.

Vaidya, S., Velázquez-Delgado, E.M., Abbruzzese, G., and Hardy, J.A. (2011). Substrate-induced conformational changes occur in all cleaved forms of caspase-6. J. Mol. Biol. *406*, 75–91.

Vanselow, K., Vanselow, J.T., Westermark, P.O., Reischl, S., Maier, B., Korte, T., Herrmann, A., Herzel, H., Schlosser, A., and Kramer, A. (2006). Differential effects of PER2 phosphorylation: molecular basis for the human familial advanced sleep phase syndrome (FASPS). Genes Dev. *20*, 2660–2672.

Velázquez-Delgado, E.M., and Hardy, J.A. (2012a). Zinc-mediated allosteric inhibition of caspase-6. J. Biol. Chem. *287*, 36000–36011.

Voss, J., Posern, G., Hannemann, J.R., Wiedemann, L.M., Turhan, a G., Poirel, H., Bernard, O. a, Adermann, K., Kardinal, C., and Feller, S.M. (2000). The leukaemic oncoproteins Bcr-Abl and Tel-Abl (ETV6/Abl) have altered substrate preferences and activate similar intracellular signalling pathways. Oncogene *19*, 1684–1690.

Voss, O.H., Batra, S., Kolattukudy, S.J., Gonzalez-Mejia, M.E., Smith, J.B., and Doseff, A.I. (2007). Binding of caspase-3 prodomain to heat shock protein 27 regulates monocyte apoptosis by inhibiting caspase-3 proteolytic activation. J. Biol. Chem. *282*, 25088–25099.

Wang, J.Y.J. (2014). The Capable ABL: What Is Its Biological Function? Mol. Cell. Biol. *34*, 1188–1197.

Wang, X.-J., Cao, Q., Liu, X., Wang, K.-T., Mi, W., Zhang, Y., Li, L.-F., LeBlanc, A.C., and Su, X.-D. (2010). Crystal structures of human caspase 6 reveal a new mechanism for intramolecular cleavage self-activation. EMBO Rep. *11*, 841–847.

Westphal, D., Kluck, R.M., and Dewson, G. (2014). Building blocks of the apoptotic pore: how Bax and Bak are activated and oligomerize during apoptosis. Cell Death Differ. *21*, 196–205.

Witkowski, W.A., and Hardy, J.A. (2009). L2' loop is critical for caspase-7 active site formation. Protein Sci. *18*, 1459–1468.

Wong, R.S.Y. (2011). Apoptosis in cancer: from pathogenesis to treatment. J. Exp. Clin. Cancer Res. *30*, 87.

Wong, S., and Witte, O.N. (2004). The BCR-ABL Story: Bench to Bedside and Back. Annu. Rev. Immunol. *22*, 247–306.

Wu, C.-C., Lee, S., Malladi, S., Chen, M.-D., Mastrandrea, N.J., Zhang, Z., and Bratton, S.B. (2016). The Apaf-1 apoptosome induces formation of caspase-9 homo- and heterodimers with distinct activities. Nat. Commun. *7*, 13565.

Wu, J.J., Phan, H., and Lam, K.S. (1998). Comparison of the intrinsic kinase activity and substrate specificity of c-Abl and Bcr-Abl. Bioorg. Med. Chem. Lett. *8*, 2279–2284.

Yamamoto, M., Torigoe, T., Kamiguchi, K., Hirohashi, Y., Nakanishi, K., Nabeta, C., Asanuma, H., Tsuruma, T., Sato, T., Hata, F., et al. (2005). A Novel Isoform of TUCAN Is Overexpressed in Human Cancer Tissues and Suppresses Both Caspase-8– and Caspase-9–Mediated Apoptosis. Cancer Res. *65*.

Yang, J., Campobasso, N., Biju, M.P., Fisher, K., Pan, X.-Q., Cottom, J., Galbraith, S., Ho, T., Zhang, H., Hong, X., et al. (2011). Discovery and Characterization of a Cell-Permeable, Small-Molecule c-Abl Kinase Activator that Binds to the Myristoyl Binding Site. Chem. Biol. *18*, 177–186.

Yonemoto, W., McGlone, M.L., Grant, B., and Taylor, S.S. (1997). Autophosphorylation of the catalytic subunit of cAMP-dependent protein kinase in Escherichia coli. Protein Eng. *10*, 915–925.

Yoo, N., Lee, S., and Jeong, E. (2007). Expression of phosphorylated caspase-9 in gastric carcinomas. APMIS 354–359.

Yuan, S., Yu, X., Asara, J.M., Heuser, J.E., Ludtke, S.J., and Akey, C.W. (2011a). The Holo-Apoptosome: Activation of Procaspase-9 and Interactions with Caspase-3. Structure *19*, 1084–1096.

Yuan, S., Yu, X., Asara, J., and Heuser, J. (2011b). The holo-apoptosome: activation of procaspase-9 and interactions with caspase-3. Structure *19*, 1084–1096.

Zamaraev, A. V., Kopeina, G.S., Prokhorova, E.A., Zhivotovsky, B., and Lavrik, I.N. (2017). Post-translational Modification of Caspases: The Other Side of Apoptosis Regulation. Trends Cell Biol. *27*, 322–339.

Zhai, D., Yu, E., Jin, C., Welsh, K., Shiau, C., Chen, L., Salvesen, G.S., Liddington, R., and Reed, J.C. (2010). Vaccinia virus protein F1L is a caspase-9 inhibitor. J. Biol. Chem. *285*, 5569–5580.

Zhou, P., Chou, J., Olea, R.S., Yuan, J., and Wagner, G. (1999). Solution structure of Apaf-1 CARD and its interaction with caspase-9 CARD: a structural basis for specific adaptor/caspase interaction. Proc. Natl. Acad. Sci. U. S. A. *96*, 11265–11270.

Zhou, Q., Snipas, S., Orth, K., Muzio, M., Dixit, V.M., and Salvesen, G.S. (1997). Target Protease Specificity of the Viral Serpin CrmA: ANALYSIS OF FIVE CASPASES. J. Biol. Chem. *272*, 7797–7800.

Zou, H., Li, Y., Liu, X., and Wang, X. (1999). An Apaf-1-cytochrome c multimeric complex is a functional apoptosome that activates procaspase-9. J. Biol. Chem. *274*, 11549–11556.